Functional role of microRNAs in breast morphogenesis and epithelial to mesenchymal transition

Eiríkur Briem

Thesis for the degree of Philosophiae Doctor

Supervised by:
Þórarinn Guðjónsson

Co-supervised by:
Magnús Karl Magnússon

Doctoral committee:
Erna Magnúsdóttir
Hans Tómas Björnsson
Þórunn Rafnar

April 2018

UNIVERSITY OF ICELAND
SCHOOL OF HEALTH SCIENCES
FACULTY OF MEDICINE

Hlutverk microRNA í formgerð brjóstkirtils og bandvefsumbreytingu þekjuvefjar

Eiríkur Briem

Ritgerð til doktorsgráðu

Leiðbeinandi:
Þórarinn Guðjónsson

Meðleiðbeiðandi:
Magnús Karl Magnússon

Doktorsnefnd:
Erna Magnúsdóttir
Hans Tómas Björnsson
Þórunn Rafnar

Apríl 2018

UNIVERSITY OF ICELAND
SCHOOL OF HEALTH SCIENCES
FACULTY OF MEDICINE

ISBN 978-9935-9421-0-4

ORCID 0000-0001-7383-3570

Printing by Háskólaprent ehf.

Reykjavík, Iceland 2018

Ágrip

Brjóstkirtillinn er myndaður af greinóttum kirtilgöngum sem umluktir eru æðaþelsríkum bandvef. Brjóstakrabbamein á upptök í kirtilþekjufrumum í endum kirtilganga. Brjóstakrabbameinsfrumur nýta sér ferli sem kallast bandvefsumbreyting þekjuvefjar til að skríða í gegnum aðliggjandi bandvef. Í doktorsverkefni mínu rannsakaði ég genatjáningarmynstur brjóstastofnfrumulínunnar D492 í myndun greinóttrar formgerðar og bandvefsumbreytingu þekjuvefjar. D492 myndar kirtilganga og kirtilber í þrívíðri frumurækt sem líkjast því sem sést í brjóstkirtli. Þegar D492 er ræktuð í þrívíðri samrækt með æðaþelsfrumum þá eykst geta hennar til greinóttrar formmyndunar sem einnig getur leitt til óafturkræfrar bandvefsumbreytingar þekjuvefjar sem einkennist af breyttri formgerð, tapi á E-cadherin og keratín tjáningu samhliða aukinni tjáningu á N-cadherin. Búið er að einangra og rækta bandvefslíka dótturfrumulínu úr þrívíðum samræktum D492 og æðaþelsfruma sem við köllum D492M og sýnt hefur verið fram á að er upprunnin frá bandvefsumbreytingu þekjuvefjar. Í verkefninu notaði ég D492 og D492M frumulínurnar til að rannsaka genatjáningu á mismunandi stigum greinóttrar formgerðar og í bandvefsumbreytingu þekjuvefjar.

Í fyrstu greininni sýndum við fram á mikinn mun í genatjáningu smásærra RNA sameinda (miRNA) milli D492 og D492M. Genatjáning sem einkennir þekjuvef er ríkjandi í D492 en genatjáning bandvefs er ríkjandi í D492M. Við greiningu miRNA tjáningar kom í ljós að mest minnkun í D492M var á tjáningu miRNA sem tilheyra miRNA-200 fjölskyldunni ásamt miR-203a og miR-205. Þessi miRNA gegna mikilvægu hlutverki í viðhaldi þekjuvefsformgerðar og minnkuð tjáning þeirra hefur verið tengd bandvefsumbreytingu þekjuvefjar. Þegar við yfirtjáðum miR-200c-141 í D492M (D492M$^{miR\text{-}200c\text{-}141}$) olli það umbreytingu frá bandvefsformgerð yfir í þekjuvefsformgerð. Þegar genatjáningarmynstur D492M$^{miR\text{-}200c\text{-}141}$ var skoðað kom í ljós að vöðvaþekjuvefs umritunarþátturinn ΔNp63 var ekki tjáður í D492M$^{miR\text{-}200c\text{-}141}$. Þegar við yfirtjáðum ΔNp63 í D492M$^{miR\text{-}200c\text{-}141}$ voru stofnfrumueiginleikar frumulínunnar endurheimtir, þ.e. frumulínan gat myndað bæði vöðvaþekjufrumur og kirtilber í þrívíðri frumurækt.

Í megin grein doktorsverkefnisins var hlutverk miR-203a í greinóttri formgerð og bandvefsumbreytingu þekjuvefjar rannsakað. Í ljós kom að tjáning miR-203a í D492 eykst milli tímapunkta í þrívíðri rækt, þ.e. við

myndun kirtilberjanna eykst tjáning miR-203a samhliða aukinni þroskun og sérhæfingu. Einnig var sýnt fram á að tjáning miR-203a er hverfandi í D492M í þrívíðri rækt og þegar miR-203a var yfirtjáð í D492M (D492M$^{miR\text{-}203a}$) breytist svipgerð að hluta til í átt til þekjuvefsfrumugerðar. Yfirtjáning á miR-203a í D492M leiddi til hægari frumufjölgunar, minnkaðrar getu til vaxtar í rækt án viðloðunar við fast yfirborð, hægara frumuskriðs og minni getu til ífarandi vaxtar. Niðurstöður á samanburði genatjáningar milli D492M og D492M$^{miR\text{-}203a}$ leiddu til uppgötvunar á peroxidasin (*PXDN*) sem markgens miR-203a. PXDN getur myndað krosstengi í kollagen IV (COL4A1) sem er mikilvægt fyrir stöðugleika grunnhimnunar. *PXDN* hefur þrjá bindistaði fyrir miR-203a á 3‘-UTR svæðinu og var það staðfest með Lúsíferasa prófi.

Í þriðju greininni sýndum við fram á mismikið næmi D492 og D492M við hindrun á prótín týrósín fosfatasa 1B (PTP1B). Hindrun á PTP1B truflaði millifrumutengi og olli frumudauða í D492 frumum. Athyglisvert er að D492M frumur voru næmari fyrir hindrun á PTP1B heldur en D492 og að þegar miR-200c-141 var yfirtjáð í D492M minnkaði næmi frumanna fyrir PTP1B hindrun. Tilgáta okkar var að PTP1B hindrun gæti mögulega komið að notum í meðferð við krabbameinum þar sem bandvefsumbreyting þekjuvefjar á sér stað.

Samantekið þá notaði ég brjóstastofnfrumulínuna D492 og bandvefslíka dótturfrumulínu hennar D492M til að rannsaka tjáningu og hlutverk smásærra RNA sameinda (miRNA) í greinóttri formmyndun og EMT. Ég varpaði ljósi á hlutverk miR-200c-141 og miR-203a í þessum ferlum og uppgötvað *PXDN* sem nýtt markgen fyrir miR-203a. Einnig var sýnt fram á að hindrun á PTP1B hefur áhrif á millifrumutengi og veldur frumudauða í D492 og D492M frumum.

Lykilorð:

Greinótt formgerð, brjóstastofnfrumur, miRNA, EMT, MET.

Abstract

In this thesis, I investigated gene expression in branching morphogenesis and epithelial to mesenchymal transition (EMT) in D492, a breast epithelial progenitor cell line. D492 generates luminal- and myoepithelial cells and in three-dimensional reconstituted basement membrane matrix (3D-rBM) it generates structures reminiscent of the terminal duct lobular units (TDLUs) of the breast. When co-cultured with endothelial cells, subset of D492 cells undergo EMT, as is evidenced by a spindle shape morphology, E- to N-cadherin switch and a loss of keratin expression. We have established an endothelial-induced mesenchymal subline from D492 referred to as D492M. In my work, I used D492 and D492M cultivated in 3D-rBM as a model to investigate gene expression of noncoding RNAs (mainly miRNAs) and protein coding genes during different stages of branching morphogenesis and in EMT.

MiRNAs expression analysis, between D492 and D492M, were done on cells from monolayer cultures and were performed using microarrays. Of the most downregulated miRNAs in D492M were members of the miR-200 family and miR-203a. I participated in elucidating the role of miR-200c-141 in branching and EMT by overexpressing these miRNAs in D492M. Characterization of D492M$^{miR\text{-}200c\text{-}141}$ demonstrated reversion towards the epithelial phenotype, albeit only to the luminal epithelial phenotype. It was further shown that the myoepithelial transcription factor ΔNp63 was missing from D492M$^{miR\text{-}200c\text{-}141}$. When ΔNp63 was overexpressed in D492M$^{miR\text{-}200c\text{-}141}$ the full progenitor cell phenotype of D492 was restored, meaning that these cells could generate both luminal and myoepithelial cells and form TDLU-like structures in 3D-rBM culture.

The main paper in my thesis focused on miRNA-203a, its expression during branching and EMT, and the identification of potential novel targets of miR-203a. In this paper, I repeated the miRNA expression analysis, which was done between D492 and D492M, and instead of using microarrays, I used next generation sequencing (NGS). I focused on differences in gene expression from 3D-rBM cultures at different stages of branching (D492) and also compared to the mesenchymal phenotype generated by D492M. The expression patterns from NGS were surprisingly similar to previous analysis done on monolayer cultures using microarrays. It was interesting to see that

miR-203a showed a gradual increase in expression accompanied by increased complexity of the branching structures. MiR-203a was not detected in D492M and when it was overexpressed in D492M, cells partially changed phenotype towards the epithelial phenotype, but not as prominently as was previously seen in D492M$^{miR\text{-}200c\text{-}141}$. D492M$^{miR\text{-}203a}$ cells showed reduced cell proliferation, less ability to form colonies in low attachment cultures, less ability to migrate and reduced invasion capability. Gene expression analysis of D492M and D492M$^{miR\text{-}203a}$ revealed peroxidasin (*PXDN*), a collagen IV cross-linking agent, as a novel target of miR-203a. We confirmed the binding of miR-203a to the 3'-UTR of *PXDN* using Luciferase assay.

In the final paper, I participated in work that demonstrated differential sensitivity of D492 and D492M cells to inhibition of the protein tyrosine phosphatase 1B (PTP1B). We showed that inhibition of PTP1B disrupted cell-cell adhesion and induced anoikis in D492 cells. Interestingly, D492M cells were more sensitive to PTP1B inhibition than D492 and in addition overexpression of miR-200c-141 in D492M made the cells more resistant to PTP1B inhibition. We hypothesized that PTP1B inhibition could potentially be used in cancer therapy involving the EMT phenotype.

Collectively, in my thesis I used isogenic breast epithelial cell lines with epithelial and mesenchymal phenotypes to explore the expression and functional roles of miRNAs in branching morphogenesis and EMT. I have elucidated the role of miR-200c-141 and miR-203a in these processes and identified *PXDN* as a novel target of miR-203a. In addition, it was shown that PTP1B inhibition disrupts cell–cell adhesion and induces anoikis in breast epithelial cells.

Keywords:

Branching morphogenesis, breast epithelial progenitor cells, miRNAs, EMT and MET.

Acknowledgements

The majority of the work presented in this thesis was carried out at the Stem Cell Research Unit (SCRU), Biomedical Center, Department of Anatomy, Faculty of Medicine, School of Health Sciences, University of Iceland.

First, I want to thank my supervisor Þórarinn Guðjónsson and co-supervisor Magnús Karl Magnússon for their guidance and mentorship during my PhD project. Their enthusiasm for science and moral support has been invaluable.

I also want to express my gratitude to both current and previous laboratory members at the Stem Cell Research Unit (SCRU) for a great teamwork. Amaranta, Anna Karen, Ari, Bryndís, Erika, Gunnhildur, Jennifer, Jón Pétur, Jón Þór, Kata, Sigríður Rut, Sophie, Sævar, Tobias and Zuzana.

Furthermore, I want to thank the doctoral committee, Erna Magnúsdótir, Hans Tómas Björnsson and Þórunn Rafnar, for their input and advice throughout the PhD project.

I want to thank the Center for Systems Biology at University of Iceland. I also want to thank my colleagues at the Biomedical Center at University of Iceland for their collaboration and assistance throughout this project. I also want to thank Páll Melsted for his guidance in using Kallisto and Sleuth for RNA-sequencing analysis.

I thank the University of Iceland and Landspitali – University Hospital for providing the infrastructure and support needed to carry out PhD studies in Iceland.

I also want to thank international collaborators: Maria Perander and Erik Knutsen at University of Tromsø, Norway; Winston Timp at Johns Hopkins University, USA; and Gunhild Mælandsmo at Oslo University Hospital, Norway.

I want to thank my family and friends, especially my parents for their support and encouragement.

Finally, I want to thank my wonderful Hanna Kristín for her endless love, support and patience throughout my PhD studies.

This work was supported by Grants from Landspitali University Hospital Science Fund, University of Iceland Research Fund, University of Iceland doctoral fund, and Icelandic Science and Technology Policy - Grant of Excellence: 152144051. ‘Göngum saman’, a supporting group for breast cancer research in Iceland also supported this work (www.gongumsaman.is).

Contents

List of abbreviations

2D culture	Two dimensional or monolayer culture
3D	Three dimensional
3D-rBM	Three-dimensional reconstituted basement membrane
3'-UTR	Three prime untranslated region
AGO	Argonaute
AREG	Amphiregulin
BM	Basement membrane
BRENCs	Breast endothelial cells
CDH1	E-cadherin or epithelial cadherin
CDH2	N-cadherin or neural cadherin
cDNA	Complementary DNA
DCIS	Ductal carcinoma in situ
DMEM	Dulbecco's Modified Eagle Medium
DNA	Deoxyribonucleic acid
ECM	Extracellular matrix
EDTA	Ethylenediaminetetraacetic acid
EGF	Epidermal growth factor
EGFR	Epidermal growth factor receptor
EGM	Endothelial cell growth medium
EMT	Epithelial to mesenchymal transition
EMT-TFs	Epithelial to mesenchymal transition transcription factors
EpCAM	Epithelial cell adhesion molecule
ER	Estrogen receptor
ERBB2	Receptor tyrosine-protein kinase erbB-2
ERα	Estrogen receptor α
EtOH	Ethanol
FBS	Fetal bovine serum
FDR	False discovery rate
FGF	Fibroblast growth factor
GFP	Green fluorescent protein
HEK-293T	Human embryonic kidney cells 293 containing SV40 T-antigen
HER2	Receptor tyrosine-protein kinase erbB-2
HMECs	Human mammary epithelial cells
HMLE	Immortalized human mammary epithelial cells
hTERT	Human telomerase reverse transcriptase
IDC	Invasive ductal carcinoma
IGF1	Insulin-like growth factor 1
iPSCs	Induced pluripotent stem cells
K	Keratin
KO	Gene knock out

LEP	Luminal epithelial cell
LGR5	Leucine rich repeat containing G protein coupled receptor 5
MACS	Magnetic cell sorting
MaSCs	Mammary stem cells
MeOH	Methanol
MEP	Myoepithelial cell
MET	Mesenchymal to epithelial transition
miRNA	MicroRNA
MUC	Sialomucin
ncRNAs	Non-coding RNAs
NGS	Next generation sequencing
PBS	Phosphate-buffered saline
PCR	Polymerase chain reaction
PFA	Paraformaldehyde
pre-miRNA	Precursor-miRNA
pri-miRNA	Primary transcript miRNA
PROCR	Protein C receptor
PTP1B	Protein tyrosine phosphatase 1B
PUMA	Pulmonary metastatic assay
PVDF membrane	Polyvinylidene difluoride membrane
PXDN	Peroxidasin
qPCR	Quantitative real-time polymerase chain reaction
rBM	Reconstituted basement membrane
RISC	RNA-induced silencing complex
RNA	Ribonucleic acid
RTK	Receptor tyrosine kinase
siRNA	Small interfering RNA
SNAI1	Snail family transcriptional repressor 1
SNAI2	Snail family transcriptional repressor 2
s-SHIP / Inpp5d	Inositol polyphosphate-5-phosphatase D
SV40ER	Simian Virus 40 early region
TDLUs	Terminal duct lobular units
TEBs	Terminal end buds
TF	Transcription factor
TGF-β	Transforming growth factor beta
TP63	Tumor protein p63
TWIST1	Twist family bHLH transcription factor 1
VEGF	Vascular endothelial growth factor
WB	Western blot
ZEB1	Zinc finger E-box binding homeobox 1
ZEB2	Zinc finger E-box binding homeobox 2

List of figures

List of tables

List of original papers

This thesis is based on the following original publications, which are referred to in the text by their numerals:

1. **MicroRNA-200c-141and ΔNp63 are required for breast epithelial differentiation and branching morphogenesis.**

   Bylgja Hilmarsdottir, Eirikur Briem, Valgardur Sigurdsson, Sigridur Rut Franzdottir, Markus Ringnér, Ari Jon Arason, Jon Thor Bergthorsson, Magnus Karl Magnusson and Thorarinn Gudjonsson. Developmental Biology, 403(2015)150–161.

2. **MiR-203a is differentially expressed during branching morphogenesis and EMT in breast progenitor cells and is a repressor of peroxidasin.**
   Eirikur Briem, Zuzana Budkova, Anna Karen Sigurdardottir, Bylgja Hilmarsdottir, Jennifer Kricker, Winston Timp, Magnus Karl Magnusson, Gunnhildur Traustadottir and Thorarinn Gudjonsson. (Submitted for publication in Developmental biology, April 2018).
3. **Inhibition of PTP1B disrupts cell-cell adhesion and induces anoikis in breast epithelial cells.**
   Bylgja Hilmarsdottir, Eirikur Briem, Skarphedinn Halldorsson, Jennifer Kricker, Sævar Ingthorsson, Sigrun Gustafsdottir, Gunhild M Mælandsmo, Magnus K Magnusson and Thorarinn Gudjonsson. Cell Death and Disease, (2017) 8(5): p. e2769.
4. **Application of breast epithelial stem cells and 3D culture to explore branching morphogenesis, EMT and cancer progression (Review).**
   Eirikur Briem, Saevar Ingthorsson, Gunnhildur Asta Traustadottir, Bylgja Hilmarsdottir and Thorarinn Gudjonsson. *Manuscript in preparation*.

In addition, some unpublished data is presented.

Declaration of contribution

Article 1. MicroRNA-200c-141 and ΔNp63 are required for breast epithelial differentiation and branching morphogenesis (published in Developmental Biology, 2015). In this paper the role of miR-200c-141 and ΔNp63 in epithelial integrity, differentiation and branching morphogenesis was described. In this paper, I am second author and performed some of the data analysis and the miR-200c-141 inhibition experiments. I worked on the final preparation of the manuscript in collaboration with Bylgja Hilmarsdottir and my supervisors.

Article 2. MiR-203a is differentially expressed during branching morphogenesis and EMT in breast progenitor cells and is a repressor of peroxidasin (submitted to Developmental biology, 2018). In this paper, where I am first author, I focused on miR-203a and its role in branching morphogenesis and EMT/MET. I designed the study in collaboration with my supervisors and performed majority of the experiments and analysis. I performed 2D and 3D cultures, small RNA sequencing and analysis, analyzed bisulfite sequencing data, RT-qPCR, designed and made lentiviral constructs, proliferation assay, DAB-staining, Western blots, anchorage independent growth, migration assay, flow sorting, RNA-isolation for polyA RNA-sequencing, alignment of polyA RNA sequencing reads, differential expression analysis of polyA RNA sequencing, bioinformatics analysis of miR-203a binding sites in the 3'-UTR of *PXDN* and assisted with the design of the luciferase experiments. Zuzana Budkova performed the apoptosis assay, invasion assay, transfection with miR-mimics, transfection with miR-inhibitors, RT-qPCR and luciferase assays. Anna Karen Sigurdardottir assisted in optimizing luciferase assay experiments and worked on Western blots for PXDN. Bylgja Hilmarsdottir performed bisulfite sequencing and provided material for RT-qPCR from primary cells. Winston Timp performed analysis of the HumanMethylation450 BedChip. Gunnhildur Traustadottir designed and optimized the luciferase assay. Jennifer Kricker proofread the manuscript. I wrote the manuscript in collaboration with my supervisors.

Article 3. Inhibition of PTP1B disrupts cell-cell adhesion and induces anoikis in breast epithelial cells (published in Cell death & disease, 2017). In this paper we described the role of PTP1B in cell adhesion and anoikis. In this paper I was the second author. I performed the knock down of

PTPN1 and proliferation assay, followed by RT-qPCR. I worked on the final preparation of the manuscript in collaboration with Bylgja Hilmarsdottir and my supervisors.

Article 4. Application of breast epithelial stem cells and 3D culture to explore branching morphogenesis, EMT and cancer progression (Review).

A review article describing the D492 model, which forms the foundation of the work done in this project. I wrote the manuscript in collaboration with my co-authors.

Unpublished data. Comprehensive transcriptomic and protein expression analysis of isogenic breast epithelial cell lines. Here, I describe the comprehensive transcriptomic and protein analysis I performed using the D492 / D492M cell culture model both in 2D and 3D. I designed the study and did all 2D and 3D culture experiments. PolyA RNA libraries were sequenced and I performed alignment, annotation and differential expression analysis. I extracted cells from 3D cultures and sent cell pellets to Bylgja Hilmarsdottir, who isolated proteins and shipped samples to USA for reverse protein array analysis. I am writing the manuscript in collaboration with my supervisors.

1 Introduction

In my project, I have used cellular models that capture developmental traits of the human breast gland, including branching epithelial morphogenesis. These models were used to analyze the functional role of microRNAs and protein tyrosine phosphatases in these processes. I therefore find it appropriate to start the introduction of my thesis by describing the cellular context of the human breast and how different cell types interact with each other and the surrounding stroma.

1.1 The human breast gland: An anatomic view

The human female breast gland is composed of branching epithelial ducts, embedded in vascular rich stroma, terminating in terminal duct lobular units (TDLUs), which are the functional milk producing units of the gland (Howard and Gusterson 2000). The stromal compartment gives structural support to the branching glandular architecture and consists of extracellular matrix containing vascular cells, immune cells, adipocytes and fibroblasts (Wiseman and Werb 2002) (Figure 1).

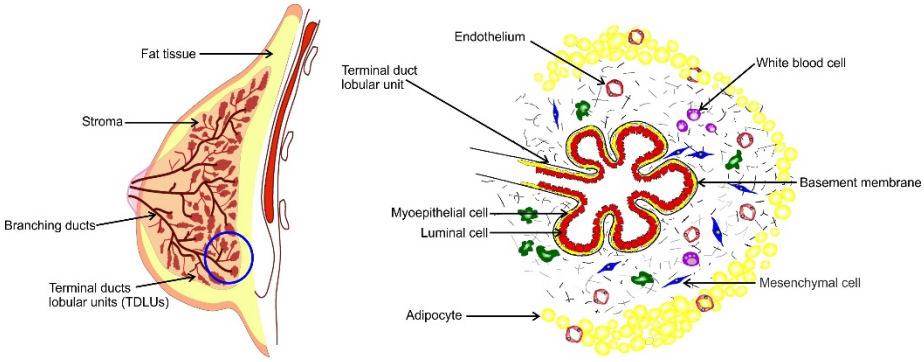

Figure 1. Schematic overview of the human female breast gland.

Left. Schematic figure of branching epithelial ducts that terminate in the TDLUs. Right. TDLU and the surrounding stroma. The TDLUs are composed of an inner layer of luminal epithelial cells and an outer layer of myoepithelial cells that are in contact with the basement membrane. The stroma is composed of the extracellular matrix (ECM), micro vessels, white blood cells and fibroblasts.

There is abundant evidence of cross-talk between the stroma and the epithelium, and studies have shown that stromal components can direct the

differentiation of the epithelial cells, including branching morphogenesis (Sakakura, Nishizuka et al. 1976, Propper 1978, Cunha, Young et al. 1995, Robinson, Karpf et al. 1999, Sigurdsson, Hilmarsdottir et al. 2011, Morsing, Klitgaard et al. 2016). From the onset of puberty, the mammary gland goes through repeated cycles of remodeling, which makes it a good model for studying the functional role of stem or progenitor cells in these processes. Traditionally, the epithelial cells of the mammary gland are divided into an inner layer of luminal epithelial cells (LEP) and an outer layer of contractile myoepithelial cells (MEP). LEPs and MEPs are believed to arise from a common stem cell within the epithelium (Pechoux, Gudjonsson et al. 1999, Gudjonsson, Villadsen et al. 2002, Villadsen, Fridriksdottir et al. 2007, Petersen and Polyak 2010, Fridriksdottir, Villadsen et al. 2017). LEPs in ducts and TDLUs, have apical-basal polarity, tight junctions and cell-cell anchoring junctions. LEPs and MEPs express specific linage related markers that aid in discriminating between these cell types, both *in situ* and *in vitro.* LEPs express e.g. EpCAM, MUC-1, E-cadherin, Keratins (K) 8,18 and 19 (Pechoux, Gudjonsson et al. 1999, Gudjonsson, Villadsen et al. 2002). During lactation LEPs secrete milk into the lumen of the TDLUs. MEPs are located on the basal side of the luminal cells and are in contact with the basement membrane. They express e.g. α-smooth muscle actin, P-cadherin, β4-integrin, P63, K5/6 and K14 (Gudjonsson, Adriance et al. 2005, Dewar, Fadare et al. 2011). During lactation, the infant activates nerves in the nipple that signal to the hypothalamus to produce oxytocin that is then released into the blood stream from the posterior pituitary. Oxytocin acts on myoepithelial cells by changing the mammary gland into a pump, by inducing contractility in MEPs that push the milk from the TDLUs into the ducts and towards the nipple (Ramsay, Kent et al. 2004). The fully differentiated myoepithelial cells have been considered to be terminally differentiated and their presence in cancer has been suggested to be tumor suppressive as their presence has been proposed to inhibit invasion of cancer cells into the surrounding stroma (Ingthorsson, Hilmarsdottir et al. 2015). Interestingly, Fridriksdottir et al. recently proposed that myoepithelial cells may be the actual stem cells in the epithelium and that these stem cells differ both in expression and function between ducts and TDLUs (Fridriksdottir, Villadsen et al. 2017).

Differentiation of the mammary gland can be divided into three major stages; embryonic, pubertal and reproductive. During embryogenesis and postnatal development epithelial-mesenchymal interactions direct development of the mammary gland, but after puberty, regulation by hormones (mainly estrogen and progesterone) and growth factors influence

these interactions as well (Macias and Hinck 2012). Pubertal growth is based on a balance between positive and negative regulators of branching morphogenesis (Macias and Hinck 2012). During puberty, the pituitary gland secrets growth hormone, which stimulates insulin-like growth factor 1 (IGF1) production in the liver and mammary stroma. This is important for ductal morphogenesis and terminal end bud formation in mice (Ruan and Kleinberg 1999, Gallego, Binart et al. 2001). In mouse mammary development, estrogen secreted by the ovaries signals through its receptor estrogen receptor α (ERα) in a subset of epithelial cells. This causes release of the epidermal growth factor family member amphiregulin (AREG), which binds to epidermal growth factor receptor (EGFR) on stromal fibroblasts. This leads to release of fibroblast growth factors (FGFs), which in turn signal to luminal epithelial cells to increase cell proliferation and branching (Sternlicht, Sunnarborg et al. 2005, Macias and Hinck 2012). The epithelial ERα and stromal EGFR signaling described in mouse mammary development, may shed light on why quiescent ERα-positive cells become proliferative in hormone dependent human ERα-positive breast tumors. Studies on hyperplastic enlarged lobular units in the adult female human breast have shown that both ERα and amphiregulin are upregulated in early lesions with a premalignant potential (Lee, Medina et al. 2007, Macias and Hinck 2012).

There are also negative regulators of pubertal ductal growth such as transforming growth factor beta 1 (TGFB1), which inhibits proliferation and ductal branching (Silberstein and Daniel 1987, Ewan, Shyamala et al. 2002, Pavlovich, Boghaert et al. 2011). At puberty, the mammary gland starts its monthly remodeling phases, through cell proliferation, differentiation and apoptosis, which further expands during pregnancy (Macias and Hinck 2012). The remodeling phases are under hormonal control, where estrogen and progesterone secreted by the ovaries play important roles (Brisken and O'Malley 2010). Estrogen stimulates growth of the milk ducts during the first half of the menstrual cycle and during the second half progesterone takes over and stimulates the formation of the acini in the murine mammary gland (Brisken and O'Malley 2010). At menarche, the mammary gland primes itself for further differentiation, which takes place during pregnancy. After birth of the offspring, the mammary gland fully differentiates as lactation begins and after weaning the mammary gland involutes and goes back to a state similar to the pre-pregnant state (Hansen and Bissell 2000). The mammary gland goes through repeated cycles of expansion and reduction, characterized by increased proliferation, differentiation and apoptosis (Hansen and Bissell 2000, Macias and Hinck 2012). The ability of the mammary gland to go

through constant remodeling during the menstrual cycle, pregnancy and lactation requires stem cells to repopulate the gland after cycles of growth and involution (Inman, Robertson et al. 2015).

1.2 Stem cells and tissue remodeling

Cellular remodeling of the mammary epithelium is dependent on the presence of stem cells that maintain cell proliferation to keep up with cell loss that occurs during involution. Numbers of studies have demonstrated the presence of stem cells in the mammary gland (Faulkin and Deome 1960, Kordon and Smith 1998, Gudjonsson, Villadsen et al. 2002, Shackleton, Vaillant et al. 2006, Stingl, Eirew et al. 2006, Villadsen, Fridriksdottir et al. 2007, Visvader and Stingl 2014, Fridriksdottir, Villadsen et al. 2017). These studies date back to the 1950´s when work on mouse mammary glands showed that when small numbers of mammary epithelial cells were transplanted into cleared mammary fat pads they were able to reconstitute the glandular epithelium and form epithelial branching structures that filled the fat pad, reviewed in (Faulkin and Deome 1960, Inman, Robertson et al. 2015). Later work, where single mammary epithelial cells were shown to form functionally active mammary glands, demonstrated that there is a stem cell population within the mammary gland (Kordon and Smith 1998, Shackleton, Vaillant et al. 2006, Stingl, Eirew et al. 2006). Mammary stem cells (MaSCs) have been described as morphologically distinct cells in the murine mammary gland, but the characteristics for a clear definition of MaSCs have not yet been determined. Specific markers, such as inositol polyphosphate-5-phosphatase D (s-SHIP) (Bai and Rohrschneider 2010), leucine-rich-repeat-containing G-protein coupled-receptor 5 (Lgr5) (Barker, Tan et al. 2013) and protein C receptor (Procr) (Wang, Cai et al. 2015) have all been associated with stem cell properties in the mouse mammary gland.

Although similarities can be found between the mouse mammary gland and the human breast, there are many differences between the two species (Dontu and Ince 2015). These include histological differences, differences in life span and differences in sensitivity to carcinogenic insults (Dontu and Ince 2015). In humans, breast epithelial cells with progenitor properties have been described as being restricted to the basal cell compartment and have an $EpCAM^{low}CD49f^{hi}$ phenotype, have repopulating capacity *in vivo* and a bipotent differentiation capacity *in vitro* (Stingl, Eaves et al. 1998, Stingl, Eaves et al. 2001). In contrast, Keller et al. reported that both luminal and basal/myoepithelial populations have cells with progenitor properties (Keller, Arendt et al. 2012). Probably, the most likely putative stem and progenitor breast cells are the suprabasal cells, which express bilineage markers, are

sialomucin negative (MUC-) and EpCAM positive (ESA+) and can form both luminal and basal cells (Gudjonsson, Villadsen et al. 2002). Interestingly, recently the myoepithelial cells have shown to be potential stem cell candidates (Fridriksdottir, Villadsen et al. 2017). Collectively, there are number of studies that show the presence of cells with stem cell properties both in the mouse mammary gland and in the human female breast.

There are significant parallels between cellular plasticity during embryonic development and carcinoma progression (Yang and Weinberg 2008). Cancer cells can hijack tissue regenerative functions of stem cells to promote malignancy and there is growing evidence linking epithelial to mesenchymal transition (EMT) to this acquisition of stem cell properties, which could be a contributing factor in the formation of cancer (Brabletz, Jung et al. 2005, Mani, Guo et al. 2008, Morel, Lievre et al. 2008).

1.3 Epithelial to mesenchymal transition / mesenchymal to epithelial transition

Epithelial to mesenchymal transition (EMT) is a process where epithelial cells lose their polarity, cell-cell adhesion and gain migratory and invasive properties (Thiery, Acloque et al. 2009). EMT and mesenchymal to epithelial transition (MET) are developmental processes that confer cellular plasticity to cells, which are important for both organ formation and maintenance (Thiery, Acloque et al. 2009). EMT is an important event during vertebrate development and takes place during gastrulation and neural crest formation (Duband, Monier et al. 1995, Viebahn 1995). During gastrulation, cells lose their epithelial characteristics by undergoing EMT enabling them to migrate from the epithelium of the epiblast through the primitive streak to form the primary germ layers, mesoderm and endoderm. Cells of the epiblast, that do not ingress, differentiate to form the ectoderm (Figure 2 a) (Ferrer-Vaquer, Viotti et al. 2010). Neural crest formation spans the time period from gastrulation to late organogenesis. The neural crest cells are a multipotent, migratory cell population that gives rise to a vast array of derivatives, ranging from the peripheral nervous system to the craniofacial skeleton and pigment cells (Sauka-Spengler and Bronner-Fraser 2008). After neural tube closure, neural crest cells undergo EMT forming a migratory mesenchymal cell type that migrates to diverse locations in the embryo (Bronner 2012). EMT also plays a role during wound healing and fibrosis (Figure 2 b). EMT can also be a part of cancer progression (Figure 2 c), when primary tumor cells lose their epithelial characteristics, such as apical to basal polarity, E-cadherin and keratin expression and gain mesenchymal characteristics, for instance increased mobility and expression of N-cadherin and vimentin (Nieto, Huang et al. 2016).

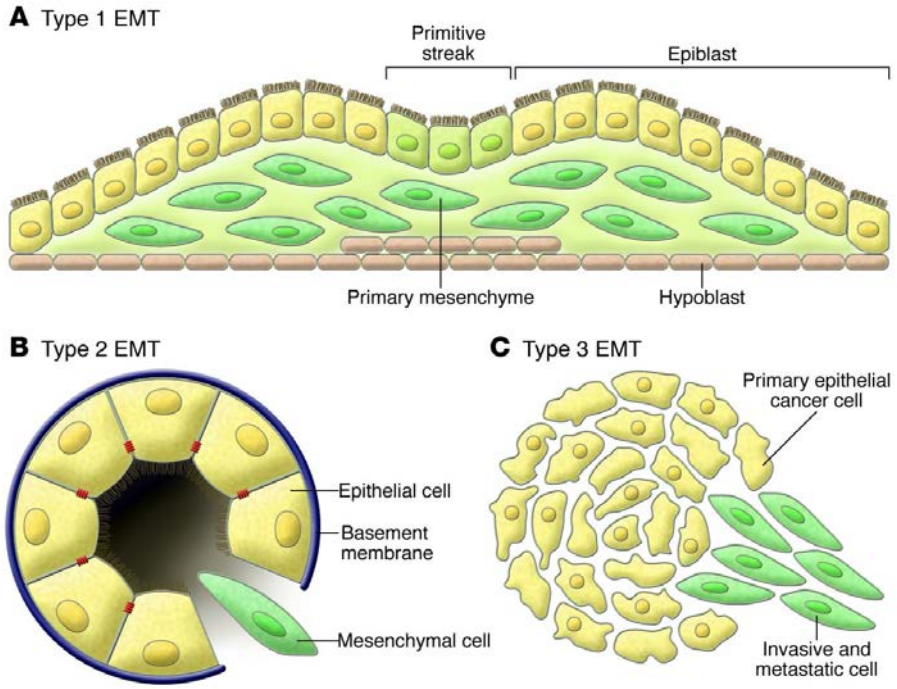

Figure 2. Different types of EMT.

Three different types of EMT a) during embryonic development, b) during inflammation and fibrosis and c) during cancer progression. *Adapted from (Kalluri and Weinberg 2009).*

It is important to note, that interpreting the contribution of EMT to metastatic colonization needs to be done with caution. There is debate about the importance of EMT to metastatic colonization, as collective migration of keratin 14 expressing tumor cells has been shown to form metastases without EMT (Fischer, Durrans et al. 2015, Cheung, Padmanaban et al. 2016). A change in phenotype due to EMT is often seen in the invasive front of primary tumors and is thought to make tumor cells more capable of breaching the basement membrane and gain access to the vasculature (Thiery 2002, Kalluri and Weinberg 2009, Smith and Bhowmick 2016, Sistigu, Di Modugno et al. 2017). This may enable cancer cells to disperse and form metastases in distant sites through the reverse process MET, where cancer cells regain an epithelial phenotype to colonize distant organs (Figure 3) (Nieto, Huang et al. 2016).

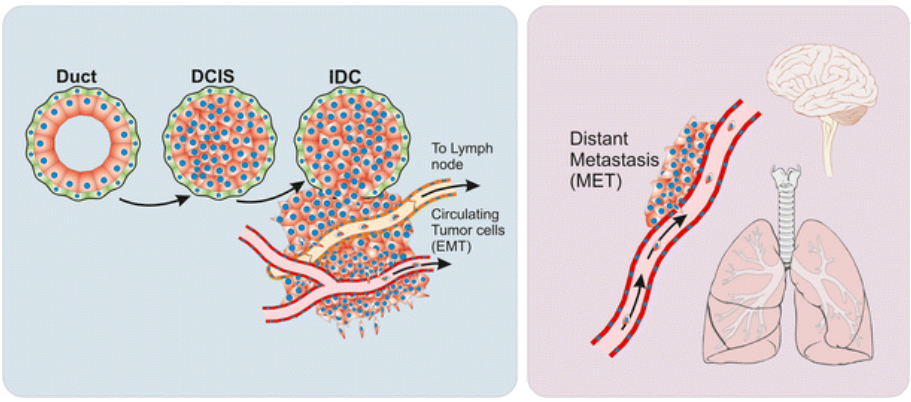

Figure 3. EMT and MET during cancer progression and metastasis.

When epithelial cells undergo EMT they lose their epithelial characteristics such as apical basal polarity and gain mesenchymal traits such as increased mobility and invasion. When tumor cells breach the basement membrane they gain access to the vasculature and disperse to distant organs were they can undergo MET thereby regaining epithelial characteristics to form distant metastases. DCIS: Ductal carcinoma in situ, IDC: Invasive ductal carcinoma. *Adapted from (Ingthorsson, Briem et al. 2016).*

In cancer, EMT is associated with unfavourable prognosis and cancer cells with an EMT phenotype are more migratory and in general more resistant to apoptosis than their epithelial counterparts (Thiery, Acloque et al. 2009). Therefore, it is challenging to identify novel targets in cancer cells with an EMT phenotype and since mesenchymal derivatives of cancer cells are less likely to be targeted by conventional chemotherapeutics it is important to identify these targets (Shang, Cai et al. 2013). This is partially the focus of article # 3, which will be discussed later in this thesis. Recently, EMT has been described as a dynamic process with intermediate EMT phenotypes, which transition between epithelial and mesenchymal states instead of being a binary decision (Tam and Weinberg 2013, Nieto, Huang et al. 2016). Cells with a hybrid phenotype have been described as being “metastable” meaning that they have flexibility to go through or reverse the EMT process (Tam and Weinberg 2013). Breast cancer cell plasticity has been suggested to arise from partial reactivation of the EMT program, since a complete EMT would render cells unable to fully metastasize to distant organs (Moyret-Lalle, Ruiz et al. 2014). The EMT program therefore needs to be under strict regulation, where cross-regulation of EMT transcription factors (EMT-TFs) and non-coding RNAs (ncRNAs) seem to be important mechanisms for breast cancer cells to acquire a stem cell like state. In recent years, ncRNAs, in particular micro RNAs (miRNAs) have been linked to cellular plasticity and regulation of

cellular fate. This is evidenced by a number of papers, showing how different miRNAs regulate EMT-TFs (Korpal, Lee et al. 2008, Wellner, Schubert et al. 2009, van Kempen, van den Hurk et al. 2012, Jang, Ahn et al. 2014, Moyret-Lalle, Ruiz et al. 2014).

1.4 MicroRNAs in EMT and branching morphogenesis

It is increasingly apparent that the non-coding portion of the genome is crucial in normal development and disease, its function however, is still largely unknown (Huang, Alvarez et al. 2013, Zhu, Fu et al. 2013). The most well-defined class of ncRNAs are miRNAs, which have been shown to have functions in normal development and disease. MiRNAs are small non-coding RNAs, which are ~22 nucleotides in length, and target the majority of protein coding transcripts in humans, where more than 60% of protein coding genes contain at least one conserved miRNA binding site (Friedman, Farh et al. 2009, Ha and Kim 2014). In canonical biogenesis of miRNAs, transcription is usually performed by RNA polymerase II, where the resulting primary (pri-miRNA) transcript is processed by the microprocessor, which is composed of the RNA-binding protein DGCR8 and the RNase III enzyme Drosha to a ~70 nucleotides precursor-miRNA (pre-miRNA) (Lee, Ahn et al. 2003, Han, Lee et al. 2004). The pre-miRNA is then exported from the nucleus, which is mediated by Exportin-5, and further processed by Dicer in the cytoplasm to form the mature miRNA/miRNA* duplex (Bernstein, Caudy et al. 2001, Carthew and Sontheimer 2009, Ha and Kim 2014).

Non-canonical pathways of miRNA biogenesis, which are independent of the RNase III proteins, Drosha and Dicer, have also been described (Miyoshi, Miyoshi et al. 2010). The small RNA duplex, generated by Dicer, is loaded onto an argonaute (AGO) protein to form the RNA-induced silencing complex (RISC) where the passenger miRNA strand is removed and the remaining strand works as a guide to base pair with a target mRNA, usually in the mRNA three prime untranslated region (3'-UTR), which induces translational repression by mRNA deadenylation and mRNA decay (Ha and Kim 2014).

In recent years, there has been increased focus on how various miRNAs act in different biological processes, such as embryogenesis, development, organ cellular maintenance, stem cell regulation and in cancer progression (Varner and Nelson 2014, Bhatia, Monkman et al. 2017, Gross, Kropp et al. 2017, Li, Long et al. 2017). As mentioned above, noncoding RNAs and in particular miRNAs are involved in regulation of epithelial-mesenchymal plasticity and they have been shown to target key EMT-TFs, such as snail

family transcriptional repressor 1 and 2 (SNAI1/2), zinc finger E-box binding homeobox 1 and 2 (ZEB1/2) and twist family bHLH transcription factor 1 (TWIST1) (Figure 4) (Guo, Parker Kerrigan et al. 2014, Bhatia, Monkman et al. 2017).

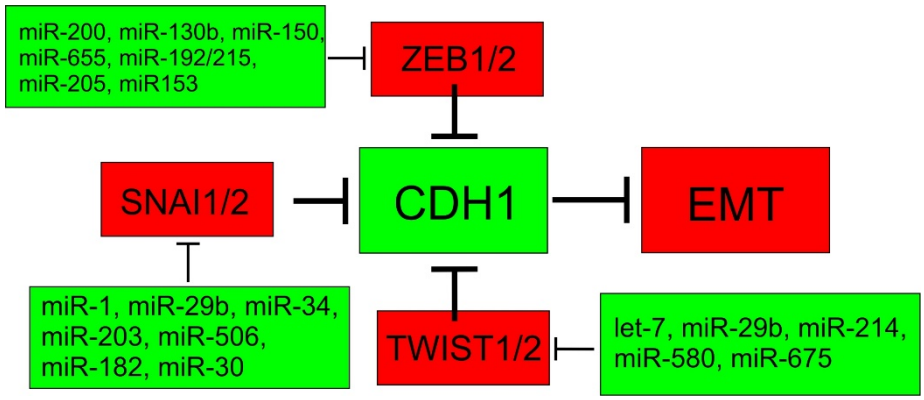

Figure 4. MicroRNAs regulating EMT transcription factors.

MiRNAs influence EMT by targeting EMT-TFs ZEB1/2, SNAI1/2 and TWIST1/2. Adapted from (Guo, Parker Kerrigan et al. 2014).

1.5 Receptor tyrosine kinases and phosphatases

Breast morphogenesis including formation of branching structures and cellular plasticity depends on multiple signaling pathways. Receptor tyrosine kinases (RTK) and phosphatases are important signaling molecules that participate in these processes. Our group has previously shown how RTKs such as EGFR and ERBB2 participate in branching morphogenesis, EMT and tumorigenesis (Ingthorsson, Andersen et al. 2016). Furthermore, our group has also shown how sprouty-1 (SPRY1) an important regulator of EGFR signaling regulates branching morphogenesis of D492 in 3D culture (Sigurdsson, Ingthorsson et al. 2013). In general, RTKs are considered oncogenes as amplification or overexpression of different RTKs are found in number of cancer types reviewed in (Gschwind, Fischer et al. 2004). In contrast phosphatases are in general believed to be tumor suppressors as their role is to dampen the signaling power of RTKs. Interestingly some phosphatases have been linked to cancer (Stuible, Doody et al. 2008, Lessard, Stuible et al. 2010, Aceto, Sausgruber et al. 2012). Protein tyrosine phosphatase 1B (PTP1B) has been linked to both cancer suppression and cancer progression (Yip, Saha et al. 2010, Liu, Wu et al. 2015). In breast cancer, overexpression of PTP1B is associated with the HER2 subtype (Bentires-Alj and Neel 2007, Julien, Dube et al. 2007) and this has been

linked to adverse prognosis (Tanner, Tirkkonen et al. 1996). PTP1B is a key enzyme in dephosphorylating the insulin receptor and its downstream signaling components and it takes part in the leptin signaling pathway by dephosphorylating upstream signaling molecules (Elchebly, Payette et al. 1999, Klaman, Boss et al. 2000, Zabolotny, Bence-Hanulec et al. 2002). Inhibitors for PTP1B have previously been developed as potential drugs for treatment of obesity (Shrestha, Bhattarai et al. 2007, Lantz, Hart et al. 2010).

1.6 *In vitro* modeling of human breast morphogenesis

To be able to study organ formation, tissue maintenance and diseases such as cancer it is necessary to have good access to both *in vivo* and *in vitro* models. *In vivo* models, in particular mice, have been very useful in studying mammary gland morphogenesis and breast cancer. Mice have been useful to study gene functions and many mutated mouse strains are available that can be used to study the continuous or conditional effects of gene knock out (KO) (Asselin-Labat, Vaillant et al. 2008, Borowsky 2011, Arendt and Kuperwasser 2015). Although many similarities exist between the mouse mammary gland and the human female breast, there are important differences worth discussing. In mice branching epithelial ducts end in simple terminal end buds (TEBs). In contrast, in the human female breast the branching ducts terminate in terminal duct lobular units (TDLUs), which are much more elaborate than the TEBs of the mouse mammary gland. TEBs in mice are embedded in adipose tissue, but in humans TDLUs are surrounded by vascularized loose connective tissue with a number of stromal cell types, such as fibroblasts and immune cells (Fridriksdottir, Petersen et al. 2011, Visvader and Stingl 2014, Inman, Robertson et al. 2015, Morsing, Klitgaard et al. 2016). At the nulliparous state the mouse mammary gland is less developed than the human mammary gland. The human gland contains glandular tissue within lobular structures, where the adult mouse contains a ductal network capped by a terminal end bud, lacking lobules (Dontu and Ince 2015). During pregnancy, the already existing human lobules expand and increase in numbers, while the mouse lobular development begins and undergoes full expansion only during pregnancy (Dontu and Ince 2015). During involution, the mouse mammary gland reverts to a state similar to the nulliparous state, but human female lobules can exist in various states of differentiation (Russo and Russo 2004, Fridriksdottir, Petersen et al. 2011). Therefore, the notable differences that exist between mouse and human mammary gland development may reflect hormonal action and functions with relevance to cancer susceptibility and progression (Carroll, Hickey et al. 2017).

It is also important to keep in mind that the mammary gland developmental stages in mice are much shorter than in humans. Furthermore, spatial localization and phenotypic properties of stem cells in the mouse mammary gland and the human breast gland are different. In mice, the MaSCs have been described to remain at the travelling TEBs, leaving behind daughter cells (Scheele, Hannezo et al. 2017) but in humans the stem cells have been described to be distributed in a stem cell niche in ducts and zones containing progenitor cells in lobules (Villadsen, Fridriksdottir et al. 2007). Although mice have been valuable for studies of breast morphogenesis and breast cancer research, there are as mentioned before, differences between the two species that need to be taken into account. This means that it is also important to use human cell models.

Tissues from reduction mammoplasties are a rich source of primary cells and these cells have been used extensively in breast morphogenesis and epithelial-stromal interactions studies (Gudjonsson, Ronnov-Jessen et al. 2002, Petersen, Nielsen et al. 2003, Sigurdsson, Fridriksdottir et al. 2006, Ingthorsson, Sigurdsson et al. 2010, Duss, Brinkhaus et al. 2014, Fridriksdottir, Kim et al. 2015). Primary cultures from reduction mammoplasties are important, but their main disadvantage is a finite lifespan of the cells, limiting long term studies. Therefore, well characterized immortalized cell lines have provided useful material for studies on breast morphogenesis and cancer progression. In particular, isogenic cell lines that capture the phenotypic diversity of breast morphogenesis are of great value. Various cell lines have been generated for normal breast and cancer research, such as the normal like MCF-10A, HMT-3522, HMLE and many more (Briand, Petersen et al. 1987, Tait, Soule et al. 1990, Elenbaas, Spirio et al. 2001). MCF-10A and HMT-3522 are the most widely used cell lines for normal breast gland research and are both derived from normal breast tissue (Debnath and Brugge 2005). The MCF-10A breast epithelial cell line is derived from benign proliferative breast tissue, spontaneously immortalized, is non-tumorigenic and estrogen receptor negative (Tait, Soule et al. 1990, Qu, Han et al. 2015). MCF-10A is widely used as a human normal breast cell model and has amplification of the MYC proto-oncogene, bHLH transcription factor (MYC) and a depletion of the chromosomal locus containing the cyclin dependent kinase inhibitor 2A (CDKN2A), which regulates senescence (Qu, Han et al. 2015). MCF-10A cells express basal/myoepithelial and luminal markers and also stem/progenitor markers (Qu, Han et al. 2015).

The HMT-3522 cell line, which was isolated from a reduction mammoplasty of a patient with fibrocystic breast disease, was spontaneously

immortalized and is a non-malignant human breast epithelial cell line (Briand, Petersen et al. 1987, Rizki, Weaver et al. 2008). The HMT-3522 subline S1 is a continuation of HMT-3522 from passage 34 (Nielsen and Briand 1989) and is non-tumorigenic and dependent on EGF for growth (Briand, Nielsen et al. 1996). When S1 was continuously cultured without EGF, a heterogeneous non-malignant population of cells called S2 was generated (Madsen, Lykkesfeldt et al. 1992). Continued culturing of S2 cells, without EGF, resulted in a drastic change in phenotype in passage 238, when the cells became tumorigenic in nude mice and in two mouse-culture passages resulted in a cell line called T4-2 (Briand, Nielsen et al. 1996). T4-2 cells have an invasive phenotype and form large and disorganized colonies in rBM (Weaver, Petersen et al. 1997). Another set of sublines, called S3 were generated from culturing S2 cells in rBM and then selecting colonies by size. The S3 cells are non-invasive but have increased potential of becoming invasive compared to the original S2 cells (Rizki, Weaver et al. 2008). There are similarities between the S3 and T4-2 models, where S3 shows a progression to a pre-invasive phenotype but the T4-2 shows a progression to an invasive phenotype. In conclusion, the HMT-3522 and its sublines represent a cell line model that is useful for identifying functional changes in transition from a pre-invasive to an invasive phenotype in metaplastic breast cancer (Rizki, Weaver et al. 2008). Finally, it is noteworthy, that the use of an *in vitro* rBM culture model was essential for capturing the phenotypic changes, which occur in the HMT-3522 breast cancer progression model.

Another useful cell line is the HMLE cell line, which originates from a reduction mammoplasty, where human mammary epithelial cells (HMECs) were immortalized using introduction of Simian Virus 40 early region (SV40ER) and the catalytic subunit of human telomerase (hTERT) (Elenbaas, Spirio et al. 2001). The HMLE cell line has been widely used to study EMT and sublines have been generated that have properties of stem cells and increased tumorigenicity (Mani, Guo et al. 2008, Taube, Herschkowitz et al. 2010).

The cell lines mentioned above MCF-10A, HMT-3522 and HMLE are all estrogen receptor (ER) negative and are therefore useful for modeling ER-negative breast cancers. ER negative breast cancers comprise approximately one-third of all breast cancers, are poorly differentiated, and have worse clinical outcome than those expressing the ER (Lapidus, Nass et al. 1998). Therefore, MCF-10A, HMT-3522 and HMLE are useful non-malignant equivalents to basal like breast cancers and are valuable for understanding basal breast cancer evolution. In contrast, seventy percent of breast cancers

are ER positive (Lumachi, Brunello et al. 2013) and the current understanding of ER expression, and the function of estrogen in the human breast, mostly relies on experiments with the MCF-7 cell line that was derived from a metastatic lesion (Soule, Vazguez et al. 1973). A non-malignant equivalent of luminal ER positive breast cells has been lacking. Until recently, it has been impossible to isolate and culture ER positive normal cells from reduction mammoplasty, but Fridriksdottir et al. have succeeded in isolating and propagating ER positive cells in culture (Fridriksdottir, Kim et al. 2015). This was done by refining cell culture conditions, which also involved inhibition of the transforming growth factor beta receptor (TGFbR) pathway that was necessary for expansion of ER positive cells (Fridriksdottir, Kim et al. 2015). To be able to do long term studies on these non-malignant ER positive cells the same group established an immortalized ER positive cell line (iHBEC^{ERpos}) with hTERT/shp16 that rendered the cells immortal while remaining true to the luminal lineage including expression of functional ER (Hopkinson, Klitgaard et al. 2017). The making of an ER positive non-malignant cell line may be useful for understanding differences in ER regulation and function between normal breast and breast cancer. To capture the full characteristics of various cell lines, it is important to culture them in conditions that resemble *in vivo* environments. To that end three-dimensional (3D) culturing models have been developed.

1.6.1 The importance of three-dimensional reconstituted basement membrane cultures

As is evident from the discussion above, 3D culturing models enable cells to proliferate and differentiate, in a way, more similar to *in vivo* conditions, therefore providing insights into developmental processes such as lumen formation and polarization, and cancer progression. When studying breast morphogenesis *in vitro* it is necessary to create microenvironments that capture the phenotypic traits of *in vivo* morphogenesis. In that regard, 3D cell culture assays are valuable as they allow for recreation of the microenvironment that supports cellular differentiation and morphogenesis. Originally 3D cultures were based on floating collagen gels and using this method morphological characteristics of differentiation were maintained and acinus-like structures formed below the surface of the gel (Emerman and Pitelka 1977, Vidi, Bissell et al. 2013).

The recapitulation of phenotypically normal acinar structures usually requires the presence of basement membrane (BM) components (Petersen, Ronnov-Jessen et al. 1992, Plachot, Chaboub et al. 2009). Reconstituted basement membrane (rBM), is widely used for 3D culture and is rich in laminins and collagen IV. In epithelial tissues, the BM forms the platform for

the epithelium and has been shown to be important for polarization of epithelial cells and tissue morphogenesis. The BM is composed of a polymeric network of collagen IV and laminins, which are interconnected by nidogen and perlecan (Vidi, Bissell et al. 2013). Peroxidasin plays a role in crosslinking collagen IV in the basement membrane (Ero-Tolliver, Hudson et al. 2015, Colon and Bhave 2016) and is discussed in more detail in article #2. The BM is a specialized form of extracellular matrix (ECM) linking epithelial and connective tissues and the adjacent stroma. The cell-cell and cell-ECM interactions form mechanistic constraints and a biochemical signaling network, which is necessary for differentiation and homeostasis of the glandular epithelium (Vidi, Bissell et al. 2013). In the mammary gland luminal cells are in contact with myoepithelial cells and in certain areas they are in contact with the BM (Vidi, Bissell et al. 2013).

Basal polarity is determined by laminin and α6β4 integrin dimers, which form the hemidesmosomes (Taddei, Faraldo et al. 2003). The basal-apical polarity axis is a key feature of luminal epithelial cells and is determined by cell-ECM anchoring junctions at the basal side of cells, cell-cell anchoring junctions on the lateral side and the location of tight junctions at the uppermost apical cell-cell adhesion complex, which separates the apical and basolateral membranes (Lelievre 2010). The separation of the apical and lateral surface of the cell membrane is important for intracellular signaling. The cytoskeleton and the basoapical polarity axis permit directional secretion of milk components into the lumen and integrations of mechanical and hormonal signals from the microenvironment (Vidi, Bissell et al. 2013). The loss of apical polarity is believed to be a critical event in tumor development (Chandramouly, Abad et al. 2007) and in invasive stages breakage of the BM allows cells to invade the ECM (Sternlicht, Lochter et al. 1999).

It is clear that the microenvironment of cells is a critical factor when studying breast development and breast cancer progression. Therefore, 3D cultures are ideal for recapitulating events that occur in real tissues. Monolayer cultures (2D cultures) are not as physiologically relevant as the flattened cell morphology and the spatial plane of cell-cell contacts are very different from what is seen in tissues and 3D cultures. Even though 2D cultures have their drawbacks they have been valuable for gene discovery and for early work on viral transformation (Vidi, Bissell et al. 2013). From the discussion above, it is clear that differences between 2D and 3D cultures are important to bear in mind, when studying developmental processes that occur in breast cells, as cell shape influences cell behavior and gene expression (Bissell, Weaver et al. 1999).

1.6.2 The D492 cell lines

In my PhD project, I mostly used the D492 breast epithelial cell line and its sublines. An important step in the search for breast epithelial stem cells was the initial separation of luminal epithelial- and myoepithelial cells and subsequent findings that subpopulation of luminal epithelial cells could give rise to myoepithelial cells (Pechoux, Gudjonsson et al. 1999). In a follow-up paper, it was demonstrated that MUC1 negative and EpCAM positive suprabasal cells had stem cell properties. Isolated MUC1 negative and EpCAM positive suprabasal cells were immortalized by transduction of the E6/E7 genes from human papilloma virus type 16. This cell line was initially referred to as suprabasal cell line (Gudjonsson, Villadsen et al. 2002, Villadsen, Fridriksdottir et al. 2007) and later renamed as D492 (Sigurdsson, Hilmarsdottir et al. 2011). D492 has stem cell properties as measured by its ability to form luminal- and myoepithelial cells in monolayer culture and to generate branching colonies akin to TDLUs when cultured in 3D-rBM. Interestingly, co-expression of both luminal and myoepithelial keratins (K14 and K19) is found in subpopulations of D492 cells. Co-expression of these two keratins is also found in suprabasal cells of the breast gland *in situ* (Villadsen 2005, Villadsen, Fridriksdottir et al. 2007) and has been associated with stem cell properties. Although, D492 cells show stem cell properties by giving rise to both luminal- and myoepithelial cells they are not able to give rise to estrogen receptor (ER) positive luminal epithelial cells.

One of the greatest advantages of 3D culture is the recapitulation of morphogenesis *in vitro* through the ability of cells to interact with each other. One important platform is to create co-culture conditions between epithelial and stromal cells. It has been shown in a number of studies that stroma confers instructive signals to epithelial cells (Ronnov-Jessen, Petersen et al. 1996, Hansen and Bissell 2000, Bissell, Radisky et al. 2002). Using the D492 cell line we have established a co-culture system where D492 cells were cultured with organotypic breast endothelial cells (BRENCs) derived from reduction mammoplasty (Sigurdsson, Fridriksdottir et al. 2006, Sigurdsson, Hilmarsdottir et al. 2011). Interestingly, when embedded into 3D-rBM, BRENCs stay as single cells inside the gel and do not proliferate. They are, however, metabolically active as evidenced by their ability to take up acetylated low-density lipoprotein (Sigurdsson, Fridriksdottir et al. 2006, Ingthorsson, Sigurdsson et al. 2010). In co-culture, BRENCs stimulate proliferation and branching morphogenesis of D492 cells. This is evident when D492 are seeded at clonal density. In 3D-rBM monoculture of D492 seeded at clonal density, no growth occurs. In contrast, in co-culture with

BRENCs, large branching structures are seen that are remarkably reminiscent of the terminal duct lobular units (TDLUs) of the breast. In addition to enhanced branching, BRENCS induced growth of spindle-like mesenchymal colonies in D492 cells. Cells isolated from a mesenchymal structure gave rise to a subline referred to as D492M. D492M has a mesenchymal phenotype, measured by a spindle like phenotype in culture and by marker expression. D492M has lost epithelial markers such as keratins, E-cadherin and transcription factors such as P63. In contrast, D492M gained mesenchymal markers including N-cadherin, Vimentin and alpha smooth muscle actin. D492M has acquired a cancer stem cell phenotype measured by increased CD44/CD24 ratio, anchorage independent growth, resistance to apoptosis and increased migration/invasion. However, when D492M cells are transplanted into nude mice, they are non-tumorigenic. A manuscript of a comprehensive review of D492 and its sublines is included with the thesis (article #4).

Due to the nature of stem cells they are linked to cellular plasticity, which is a term that explains the ability of a particular cell or cell type to change its phenotype. EMT and MET are cellular processes that inherently involve cellular plasticity. In this thesis, I apply the D492/D492M model to investigate cellular plasticity and processes involved in EMT/MET.

2 Aims

Developmental processes underlying mammary gland morphogenesis are under complex transcriptional control. Non-coding RNAs (ncRNAs) and in particular miRNAs have emerged as important regulators of gene transcription and have been shown to be important for stem cell regulation and epithelial plasticity, differentiation and disease. Epithelial plasticity refers to the ability of cells to change phenotypes as a response to intrinsic or extrinsic factors. Epithelial to mesenchymal transition (EMT) and its reverse process mesenchymal to epithelial transition (MET) are examples of cellular plasticity that occur both in normal development and in disease, such as cancer. EMT and MET are regulated by transcription factors, which in turn can be regulated by miRNAs. Cancer cells with an EMT phenotype are often more resistant to cancer therapy than cells with an epithelial phenotype, making it an ambitious goal to search for drug candidates that can eliminate cancer cells with such a phenotype. Three-dimensional cultures capture the phenotypic traits of branching morphogenesis and EMT in the human breast gland. This provides a platform for identification of agents that can facilitate, inhibit or reverse these events.

The general aim of this thesis was to apply the breast epithelial progenitor cell line, D492 and its mesenchymal derivative, D492M and 3D culture to study the role of miRNAs in branching morphogenesis and EMT with primary focus on the miR-200 family and miR-203a. In addition, the protein tyrosine phosphatase 1B (PTP1B) was studied, to see if its inhibition plays a role in viability of breast cells with epithelial or mesenchymal phenotype and further if miRNAs could to some extent counteract viability of cells after PTP1B inhibition.

2.1 Specific aims:

1) Analyze the role of miR-200c-141 in breast morphogenesis and EMT/MET.
2) Explore the temporal expression, novel targets and the functional role of miR-203a in branching morphogenesis and EMT.
3) Analyze the effects of PTP1B inhibition in breast cells with epithelial and mesenchymal phenotypes.

3 Materials and methods

In this chapter I will list up the methods that have I applied in my thesis and briefly describe the rationale for choosing these particular methods. More detailed descriptions of materials and methods are found in the papers included in this thesis and in the chapter on technical considerations.

3.1 Cell culture

3.1.1 Monolayer (2D) culture

D492 and D492M were maintained in H14 medium as described previously (Sigurdsson, Hilmarsdottir et al. 2011) and cultured on collagen I coated flasks. Primary luminal epithelial cells ($EpCAM^+$) and myoepithelial cells ($EpCAM^-$) were isolated from primary cultures of breast epithelial cells derived from reduction mammoplasties by magnetic cell sorting (MACS) and maintained in CDM3 and CDM4, respectively, as previously described (Pechoux, Gudjonsson et al. 1999). Primary human breast endothelial cells (BRENCs) were isolated from breast reduction mammoplasties and cultured in endothelial growth medium (EGM) + 5% FBS, referred to as EGM5 (Sigurdsson, Fridriksdottir et al. 2006). All cell lines were regularly authenticated with genotype profiling.

3.1.2 Three dimensional (3D) monoculture

In general, 3D monocultures were carried out in 24-well culture plates. Growth factor reduced reconstituted basement membrane (rBM, purchased as Matrigel, Corning #354230) was used for 3D cultures. Cells were suspended in 300 µl of rBM in a 24-well plate and incubated at 37°C in 5% CO_2 for 30 minutes. The cells were then supplemented with media and maintained in culture for up to three weeks. Cell culture media was changed three times per week.

3.1.3 3D co-culture

3D co-culture experiments were carried out with either 500 or 1000 epithelial cells mixed with 100,000 – 200,000 BRENCs in 300 µl of rBM in each well of a 24-well plate and cultured in EGM5 for 14 - 21 days. Under these conditions BRENCS are quiescent but viable in the rBM. Branching, solid and spindle-like structures were then isolated from the rBM with gentle shaking on ice in PBS - EDTA solution as previously described (Lee, Kenny et al. 2007).

3.2 Anchorage independence, migration and invasion assays

Anchorage independent growth was determined using 24-well ultra-low attachment plates, where triplicates of 500 cells of D492M$^{miR\text{-}203a}$ and D492M^{Empty} were single-cell filtered and cultured in EGM5 medium for 9 days.

For migration analysis, triplicates of 10,000 starved D492M$^{miR\text{-}203a}$ and D492M^{Empty} cells were seeded in DMEM/F12, HEPES medium on collagen I coated transwell filters with 8 µm pore size, with EGM5 medium in the lower chamber and then incubated for 24 hours. Non-migrated cells were removed with a cotton swab and washed away with PBS. Migrated cells were fixed in 3.7% formaldehyde in PBS for 10 minutes and then washed with 1 x PBS. Cells were then stained with 0.1% crystal violet solution in ethanol for 15 minutes and then washed with water. Images were acquired and migrated cells counted, 3 images per filter.

Invasion assay was performed using transwell filters with 8 µm pore size that were coated with 100 µl diluted rBM in H14 media. D492M$^{miR\text{-}203a}$ and D492M^{Empty} (25,000 cells) were seeded in H14 media on top of rBM coated filters and H14 + 5% FBS added to the lower chamber and incubated for 44 hours. rBM was then removed with a cotton swab and washed with PBS. Cells were fixed in 3.7% formaldehyde in PBS for 15 minutes and washed four times with water. Cells were then stained with 0.1% crystal violet solution in ethanol for 15 minutes and then washed with water. Images were acquired and migrated cells counted, 3 images per filter.

3.3 Western blot

Equal amounts (5 µg) of proteins in RIPA buffer were separated on NuPAGE™ 10% Bis-Tris Protein Gels and transferred to a PVDF membrane. Antibodies used are listed in the papers and manuscript. The Odyssey Infrared Imaging System (Li-Cor) was used for detection. Fluorescent images were converted to gray scale.

3.4 Immunochemistry

Cells from monolayer cultures were fixed using 4% paraformaldehyde (PFA) or methanol (MeOH). Nuclear fixation was performed using 1:1 Methanol:Acetone. For multiple labeling experiments, fluorescent isotype specific secondary antibodies were used. Specimens were visualized on a Leica DMI3000 B inverted microscope, Zeiss LSM 5 Pascal laser-scanning microscope (Carl Zeiss) or Olympus Fluoview 1200.

3.5 Proliferation assay

Cells were seeded in triplicates in 24-well plates and cultures stopped every 24 hours. Cells were fixed in 3.7% formaldehyde in PBS for 10 minutes, washed once with 1 x PBS, stained with 0.1% crystal violet in 10% ethanol for 15 minutes, washed four times with water and dried. Density of cells was evaluated by extracting the crystal violet stain in 10% acetic acid and measuring optical density at 595 nm using a spectrometer.

Proliferation was also measured using IncuCyte Zoom (Essen Bioscience) per manufacturer's instructions.

3.6 Apoptosis assay

Resistance to chemically induced apoptosis was measured using 10 µM camptothecin as an apoptosis-inducing agent and caspase-3/7 reagents (Essen Bioscience, #4440). The experiment was performed using IncuCyte Zoom per manufacturer's instructions (Essen Bioscience).

3.7 DNA isolation and methylation bead chip array

D492 (1 x 10^4 cells) and D492M (2.5 x 10^4 cells) were grown in 3D-rBM in triplicate in a 24-well plate for 14 days and colonies extracted from 3D-rBM with gentle shaking on ice in PBS - EDTA solution as previously described (Lee, Kenny et al. 2007). DNA was extracted using the PureLink Genomic DNA Mini Kit and DNA was bisulfite converted using the EZ-96 DNA Methylation-Gold Kit, per manufacturer´s protocols. The samples were hybridized to the Infinium HumanMethylation450 BeadChip array. Data was analyzed using the minfi Bioconductor package (Aryee, Jaffe et al. 2014).

3.8 Bisulfite sequencing

DNA (0.5 - 1 µg) was bisulfite converted using the EpiTect Bisulfite Kit. Target DNA sequences were amplified using nested PCR. Methylation levels were analyzed by sequencing the bisulfite modified promoter regions on a 3130 Genetic Analyzer (Applied Biosystems). Methylation data from bisulfite sequencing was analyzed and visualized using the BiQ Analyzer v2.0 (Bock, Reither et al. 2005).

3.9 Quantitative reverse transcription PCR analysis

Total RNA was extracted with Tri-Reagent and reverse transcription performed using random hexamers and SuperScript IV Reverse Transcriptase. One µg of RNA was used for each cDNA reaction. A list of

primers that were used for mRNA qRT-PCR analysis can be found in the materials and methods sections of each paper and manuscript. Maxima Probe/ROX qPCR Master Mix (2X) was used for TaqMan qRT-PCR analysis.

Quantitative RT-PCR analysis of miRNAs was performed using the universal cDNA synthesis kit II from Exiqon and ExiLENT SYBR Green master mix. The primer sets from Exiqon that were used for miRNA qRT-PCR analysis can be found in the materials and methods sections of each paper and manuscript. All qRT-PCRs were performed on the Applied Biosystems 7500 Real-Time PCR system and relative expression differences were calculated using the $2^{\Delta Ct}$ method.

3.10 Small RNA sequencing

Total RNA was isolated from branching and spindle-like colonies from D492 and D492M, respectively using Tri-Reagent. For the D492 branching time point experiment, RNA was isolated from 3D-rBM culture on days 7, 14 and 21. Samples were pooled in triplicates from each time point, before small RNA library preparation. Small RNA libraries were prepared using the TruSeq Small RNA Library Kit from Illumina, per manufacturer´s protocol. The small RNA libraries were then sequenced using the Illumina MiSeq platform and V2 sequencing chemistry. FASTQ files were generated with MiSeq Reporter (Illumina). Small RNA sequence analysis was performed using the CLC Genomics Workbench and miRBase – release 21 was used for annotation. Samples were normalized by totals and counts reported as reads per million. Reads above 29 nt and below 15 nt in length were discarded. Proportion-based statistical analysis was done using the test of Kal (Kal, van Zonneveld et al. 1999). Hierarchal clustering of features was performed using Log2 transformed expression values, Euclidean distance and single linkage.

3.11 PolyA mRNA sequencing

RNA was isolated from 3D and 2D cultures using the Exiqon miRCURY RNA Isolation Kit - Cell and Plant and quality control of RNA samples was performed using BioAnalyzer. Libraries were prepared using polyA mRNA library kit from Illumina and sequenced on a HiSeq sequencer from Illumina. Alignment of reads and annotation was performed using Kallisto and differential expression analysis was done using Sleuth.

3.12 Cloning of miR-203a into pCDH lentivector

The miR-203a miRNA construct was amplified from D492 genomic DNA using nested PCR (see manuscript). From miR-203a-outer amplicon, EcoRI and NotI restriction sites were incorporated with PCR. Phusion High-Fidelity

DNA Polymerase was used for PCR and amplicons were purified using the GeneJET PCR purification kit. Double digestions of miR-203a-inner amplicon and pCDH vector were performed using EcoRI and NotI. The miR-203a-inner amplicon was cloned into pCDH lentivector using T4 DNA ligase. Empty pCDH lentivector and miR-203a-pCDH lentivector were transformed into *E. coli* DH5alpha competent cells and inserts confirmed with colony PCR. Lentivectors were produced in cultures of DH5alpha and isolated using GeneJET Plasmid Miniprep kit. The cloned miR-203a insert sequence was then confirmed by Sanger sequencing. The pCDH lentivector has a RFP+Puro fusion containing the T2A element to enable co-expression of balanced levels of RFP and Puro genes. Viral particles were produced in HEK-293T cells using TurboFect transfection reagent and virus containing supernatant collected after 48 and 72 hours. Target cells were transfected with virus titer and stable cell lines and control (empty-lentivector) cells were isolated with puromycin followed by flow-sorting selecting for RFP expressing cells.

3.13 Transient transfection with miR-203a mimic

Briefly, D492M cells were separately transfected with 50 pmole of mirVANA miR-203a-3p mimic or miRNA mimic negative control #1 using RNAiMAX per manufacturer's instructions for mirVana miRNA mimics.

3.14 Transient transfection with miR-203a inhibitor

Briefly, D492M$^{miR\text{-}203a}$ cells were separately transfected with 50 pmole of mirVANA miR-203a-3p inhibitor or mirVana miRNA Inhibitor, Negative Control #1 using RNAiMAX per manufacturer's instructions for mirVana miRNA inhibitors.

3.15 Plasmid vector constructs and luciferase activity assay

Synthetic oligonucleotides containing the hsa-miR203-3p target sequence of human *PXDN* 3'-UTR, a mismatched version of the target site or a deletion thereof were cloned into pmirGLO Dual-Luciferase miRNA Target Expression Vector. The miRNA target expression vectors and miR-203a-3p mimics were then transfected into HEK-293T cells. Luciferase activity was measured using the Dual-Glo Luciferase Assay System from Promega. Normalized firefly luciferase activity (background subtracted firefly luciferase activity / background subtracted Renilla luciferase activity) for each construct was compared to that of the pmirGLO vector no-insert control.

3.16 Statistical analysis

Data are presented as means of triplicate samples and standard deviations are represented as error bars, unless stated otherwise. Student two – tailed T-test was used to carry out statistical analysis between samples. P-values below 0.05 were considered significant.

4 Results and discussion

In this chapter, I will discuss my data both published and unpublished and put my work into perspective with the past and current literature. Published papers and manuscript are enclosed at the end of my thesis.

4.1 Article #1. MicroRNA-200c-141 and ΔNp63 are required for breast epithelial differentiation and branching morphogenesis (published in Developmental Biology 2015)

As discussed in the introduction, miRNAs are now being recognized as important players in regulating cell fate and differentiation. In this paper, we were interested in analyzing differences in miRNA expression between the human mammary progenitor cell line D492 and its mesenchymal derivative D492M. MiRNAs were isolated from monolayer cultures of D492 and D492M and analyzed using miRNA expression arrays. We analyzed 599 miRNAs and identified 186 miRNAs that were differentially expressed between the two cell lines. The miRNA expression data are accessible through GEO Series accession number GSE60524. Among the most downregulated miRNAs in D492M were miRNAs belonging to the miRNA-200 family (Figure 5), a family of miRNAs that has been shown to be important for preserving epithelial integrity (Gregory, Bert et al. 2008, Wellner, Schubert et al. 2009, Mongroo and Rustgi 2010, Davalos, Moutinho et al. 2012). The miRNA-200 family is composed of five miRNAs located in two gene clusters in humans; miR-200a, miR-200b, and miR-429 are located on chromosome 1 and miR-200c and miR-141 are located on chromosome 12. In this study, we focused on miR-200c and miR-141, which are located on chromosome 12 and share the same promoter. We demonstrated that the transcriptional silencing of miR-200c-141 in D492M was through DNA methylation of the CpG islands in the promoter area. No methylation of miR-200c-141 promoter area was found in D492 (Figure 6). This indicated that the expressional control of miR-200c-141 was a regulated event, which we decided to investigate further.

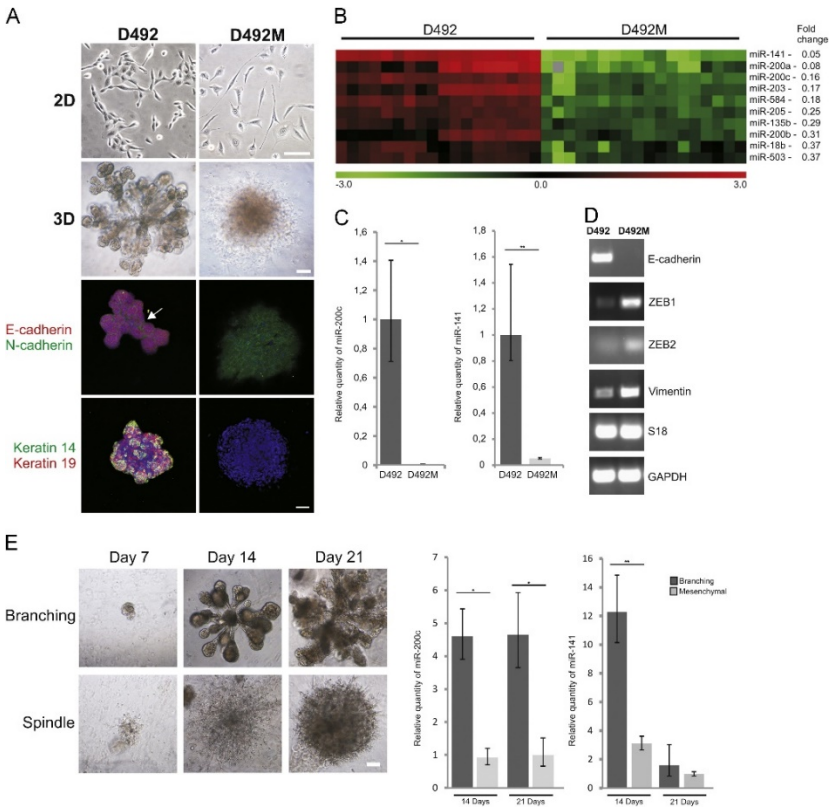

Figure 5. The miR-200 family is downregulated in breast epithelial stem cells undergoing EMT.

(A) D492 and D492M generate branching and mesenchymal-like structures in 3D culture, respectively. D492 a breast epithelial cell line with stem cell properties forms cuboidal epithelial phenotype in 2D culture and elaborate branching structures in 3D culture in reconstituted basement membrane (rBM) matrix. In contrast, D492M forms a spindle-like phenotype in 2D and 3D cultures. Immunostaining shows reduced expression of E-cadherin (red) and increased expression of N-cadherin (green) in D492M. K14 (green) and K19 (red) that are present in the branching structures of D492 in 3D culture are lost in the spindle-like colonies of cultured D492M cells. Note, the N-cadherin expression in the branching structures of D492 is restricted to the interface between lobular units (arrow) compared to the overall staining in D492M. Cells were counterstained with TO-PRO-3 nuclearstain. Bar=100 μM. (B) miRNA expression analysis shows drastic difference between D492 and D492M. Heatmap of differentially expressed miRNAs shows a drastic difference between D492 and D492M. Of the top 10 downregulated miRNAs in D492M, four where from the miR-200 family (miR-200a, miR-200b, miR-200c and miR-141). There was not significant difference in the expression of the fifth miR-200 family member, miR-429. (C) Validation of miR-200c and miR-141 expression in D492 and D492M. miR-200c and miR-141 downregulation in D492M was verified with qPCR. The expression of miR-200c was shown to be more than 500 fold in D492 relative to D492M. miR-141 expression was almost 20 fold higher in D492 than D492M. miRNA levels were

normalized to U6. (D) Expression of ZEB1 and ZEB2 is increased in D492M. PCR expression analysis of selected targets regulated by miR-200c-141 shows different expressions between D492 and D492M. E-cadherin was lost in D492M accompanied by increased expression of ZEB1, ZEB2 and vimentin. S18 and GAPDH as loading control. (E) miR-200c and -141 are downregulated in newly formed mesenchymal structures. D492 cells were embedded into matrigel in coculture with endothelial cells in order to form branching and spindle like structures. After 14 and 21 days in culture, RNA was isolated from newly formed mesenchymal colonies. qPCR for miR-200c and -141 demonstrated significantly higher expression of these miRNAs in newly formed branching colonies than in mesenchymal colonies. miRNA levels were normalized to SNORD48. Bar=100 µM. (Figure 1 in article #1)

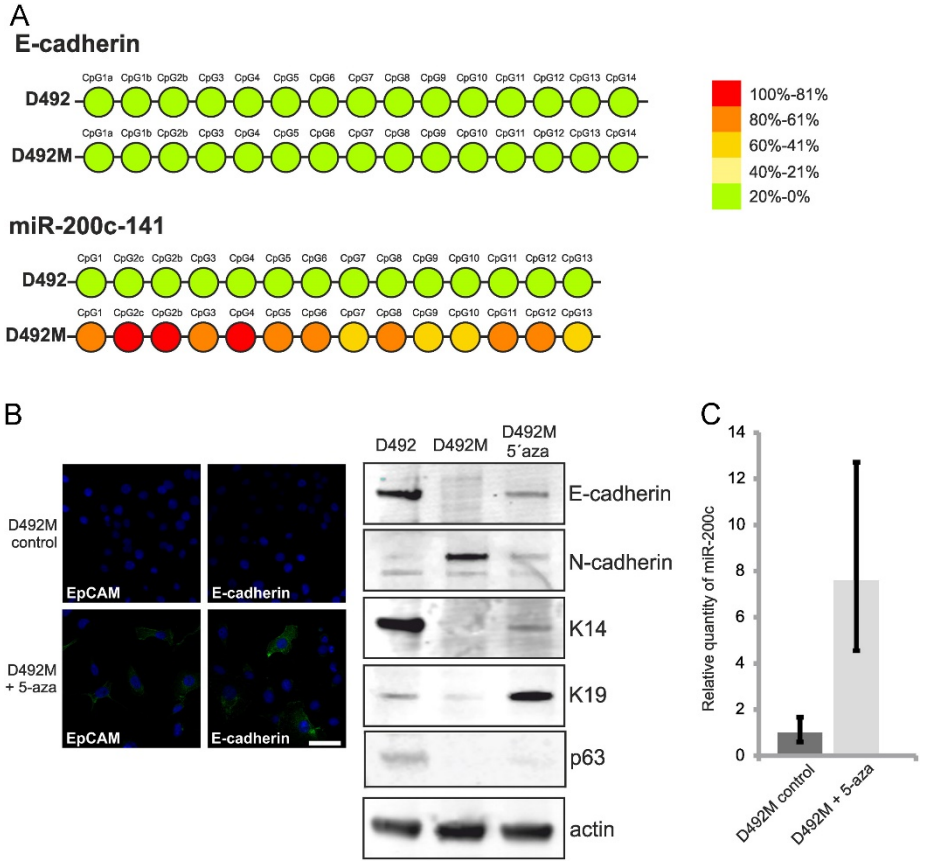

Figure 6. The promoter region of miR-200c-141 is methylated in D492M.

(A) The promoter area of miR-200c-141 is methylated in D492M. Bisulfite sequencing shows no methylation at the promoter region of E-cadherin in D492 and D492M. In contrast the promoter region of miR-200c-141 is methylated D492M only, where miR-200c and -141 expression is reduced. The color column on the right indicates percentage levels of methylation at CpG island promoter areas in E-cadherin and miR-200c-141. (B) 5-Azacytidine (5-Aza) treatment of D492M partially reverses the

EMT phenotype. Immunostaining for E-cadherin and EpCAM (green) (left) demonstrates that expression is partially reestablished in D492M after treatment with a demethylation agent (5-aza). Cells were counterstained with TO-PRO-3 nuclearstain. Western blot demonstrated gain of epithelial phenotype in 5-aza treated cells as seen by increased expression of E-cadherin, K14 and K19 and decreased expression of N-cadherin but no change in p63 expression (right). Actin was used as a loading control. (C) 5-Aza treatment of D492M induces expression of miR-200c. U6 as loading control. (Figure 2 in article #1)

To study the ability of miR-200c-141 to preserve epithelial integrity of D492, we overexpressed miR-200c-141 in D492 and cultured the cells in co-culture with breast endothelial cells (BRENCS), which had previously been shown to induce EMT in D492 (Sigurdsson, Hilmarsdottir et al. 2011). The $D492^{miR\text{-}200c\text{-}141}$ cells only formed branching and solid round epithelial colonies and no mesenchymal colonies, in co-culture with BRENCs, showing that the overexpression of miR-200c-141 was sufficient to inhibit endothelial-induced EMT and to maintain epithelial integrity of D492 without affecting branching (Figure 7). Endothelial induced EMT has been reported in other cell types such as in human pancreatic (PANC-1) cancer cell line, lung cancer (A549) cell line, mouse mammary epithelial cell line (NMuMg) and in primary human squamous cell carcinoma cells (SCC) (Kimura, Hayashi et al. 2013, Zhang, Dong et al. 2014, Shenoy and Lu 2016). Having found it interesting that miR-200c-141 can inhibit endothelial induced EMT in D492 cells it would also be interesting to investigate if overexpression of miR200c-141 could also inhibit EMT in other cell types known to undergo endothelial-induced EMT.

Next, we wanted to see if miR-200c-141 expression would suffice to re-induce an epithelial phenotype in D492M. When miR-200c-141 was overexpressed in D492M we indeed saw a mesenchymal to epithelial transition (MET), albeit only to the luminal epithelial phenotype. This indicated that some important myoepithelial regulators were not induced by overexpression of miR-200c-141 in D492M (see below). $D492M^{miR\text{-}200c\text{-}141}$ had cuboidal epithelial morphology in 2D and irregular branching like structures in 3D. When $D492M^{miR\text{-}200c\text{-}141}$ were grown in co-culture with breast endothelial cells (BRENCS) they only formed epithelial solid round colonies and no mesenchymal colonies, and they failed to form elaborate branching structures like D492 does. When we tested for marker expression of $D492M^{miR\text{-}200c\text{-}141}$ we saw that these cells had lost N-cadherin expression but gained expression of luminal markers, such as EpCAM, E-cadherin and K19, but did not gain expression of myoepithelial markers (Figure 8). We concluded that miR-200c-141 overexpression reverted the mesenchymal cells towards a luminal epithelial phenotype, but, in contrast to the parental

D492 cell line, failed to generate branching structures in 3D culture. We hypothesized that the absence of myoepithelial cell differentiation made it impossible for the cells to form branching structures.

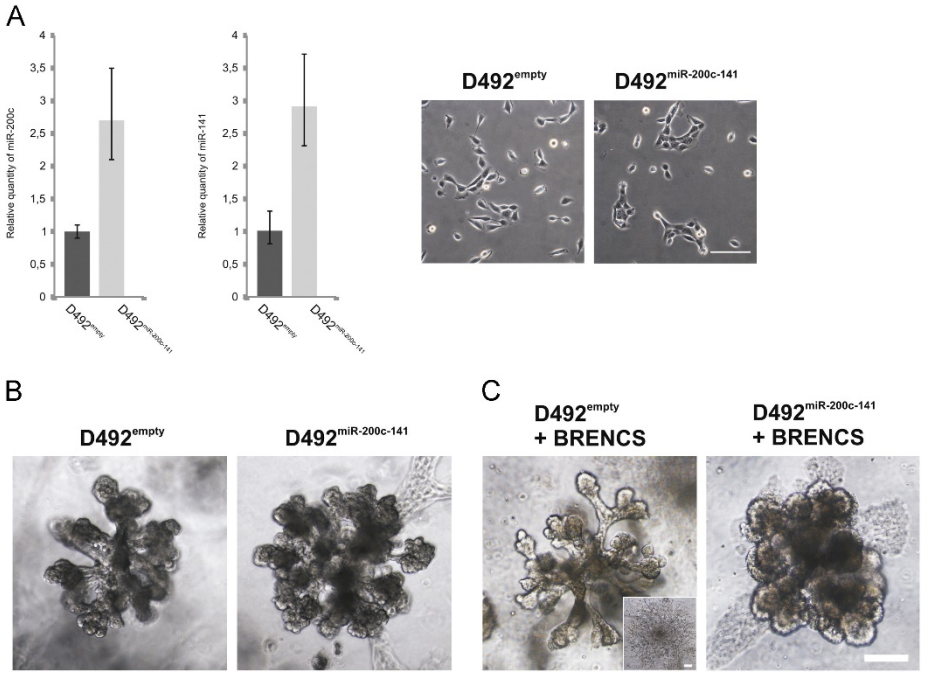

Figure 7. Overexpression of miR-200c-141 in D492 inhibits EMT, but does not affect branching.

(A) qPCR analysis verifies the overexpression of miR-200c and -141 in D492. D492M cells were transduced with a lentiviral construct containing miR-200c-141 ($D492^{miR\text{-}200c\text{-}141}$). Expression levels of miR-200c and -141 were 2–3 fold higher in $D492^{miR\text{-}200c\text{-}141}$ than in $D492^{empty}$ cells. miRNA levels were normalized to U6. (B) $D492^{miR\text{-}200c\text{-}141}$ cells cultured in rBM monoculture form branching colonies similar to $D492^{empty}$. (C) $D492^{miR\text{-}200c\text{-}141}$ are resistent to EMT in coculture with endothelial cells. $D492^{miR\text{-}200c\text{-}141}$ only form branching structures in coculture with BRENCS while $D492^{empty}$ form branching and mesenchymal colonies in coculture. (Figure 3 in article #1)

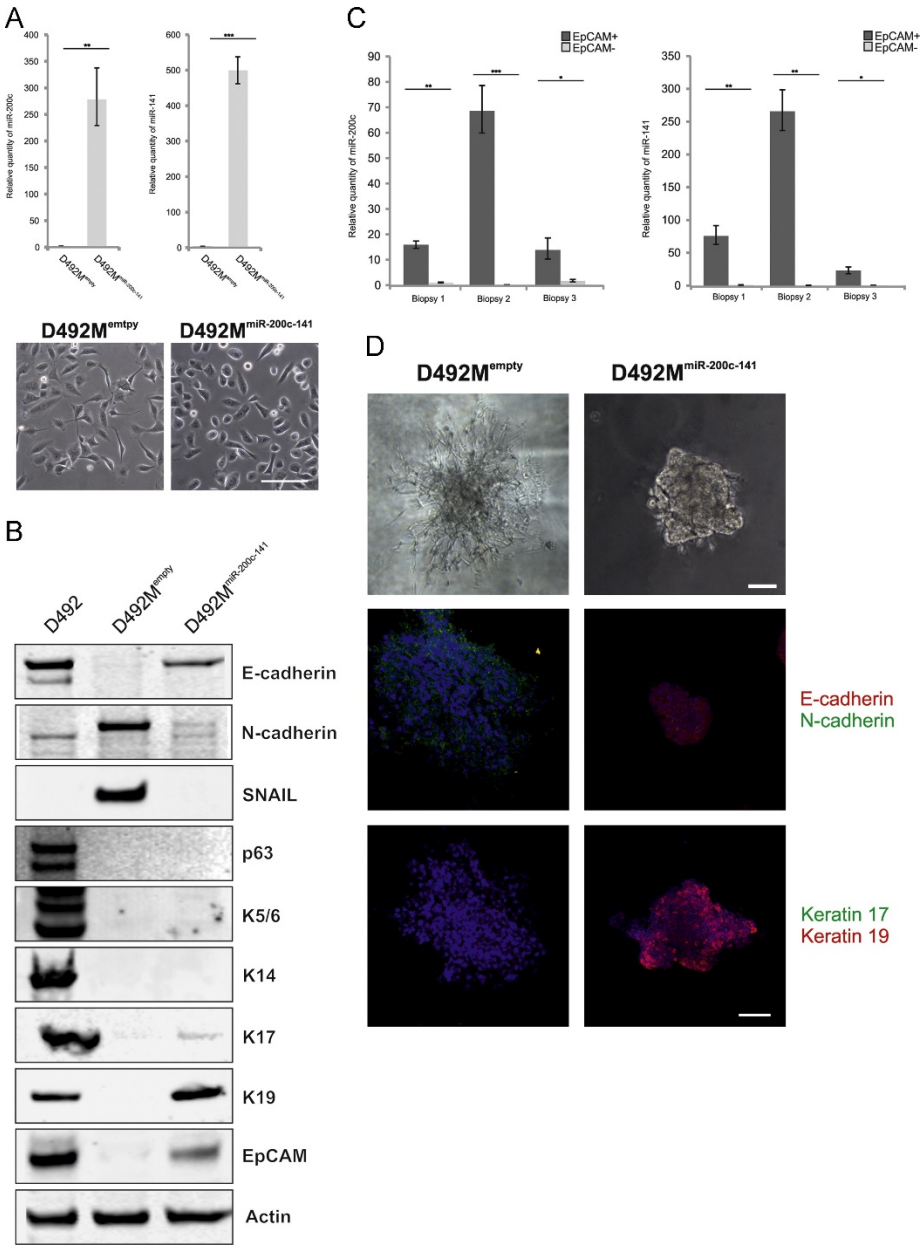

Figure 8. Forced expression of miR-200c-141 induces luminal epithelial differentiation.

(A) Overexpression of miR-200c-141 in D492M induces epithelial morphology in 2D culture. D492M cells were transduced with a lentiviral construct containing miR-200c-141 (D492M$^{miR\text{-}200c\text{-}141}$). The expression was 300–500 fold higher in D492M$^{miR\text{-}200c\text{-}141}$ than in D492M^{empty} cells. Phase contrast image of D492M$^{miR\text{-}200c\text{-}141}$ shows cuboidal epithelial phenotype in culture. miRNA levels were normalized to U6. Bar=100 µM. (B)

D492M$^{miR\text{-}200c\text{-}141}$ acquires luminal epithelial phenotype. Western blot demonstrates expression of E-cad, EpCAM and K19 in D492M$^{miR\text{-}200c\text{-}141}$ cells. In contrast little or no expression of p63, K14, K5/6, or K17 is seen. Also, the expression of the EMT markers N-cad and SNAIL is reduced compared to D492M^{empty}. Actin was used as a loading control. (C) miR-200c and miR-141 are luminal epithelial markers in the breast. qPCR analysis shows that EpCAM positive cells (luminal), express 5–7 fold more miR-200c and 40–120 fold more miR-141 than EpCAM negative cells (myoephithelial). Measurement was done in paired luminal and myoepithelial cells from three different biopsies. miRNA levels were normalized to SNORD48. (D) D492M^{empty} and D492M$^{miR\text{-}200c\text{-}141}$ form spindle and irregular branching like structures in 3D rBM culture, respectively. Immunostaining shows vague expression of N-cad (green) and strong E-cad (red) expression in D492M$^{miR\text{-}200c\text{-}141}$. Note the lack of polarity in N-cad expression (compared with Fig. 1A). D492M$^{miR\text{-}200c\text{-}141}$ retain K19 (red) expression in 3D culture but lack expression of K17 (green). Cells were counterstained with TO-PRO-3 nuclearstain. Bar=100 µM. (Figure 4 in article #1)

Myoepithelial cells have been shown to be important for polarization and differentiation of luminal epithelial cells (Gudjonsson, Ronnov-Jessen et al. 2002). Therefore, we tested if introduction of myoepithelial regulators into D492M and D492M$^{miR\text{-}200c\text{-}141}$ would induce myoepithelial differentiation and branching morphogenesis, respectively. We decided to focus on tumor protein p63 (TP63), which is an important basal cell transcription factor in many epithelial tissues, such as skin, lung, salivary glands and breast (Blanpain and Fuchs 2007, Senoo, Pinto et al. 2007, Candi, Cipollone et al. 2008). TP63 is also widely expressed in myoepithelial cells in the breast. TP63 has two major isoforms, ΔNp63 and TA-p63 (Yang, Kaghad et al. 1998). The ΔNp63 isoform is the dominant form in most tissues and has been shown to be a regulator of the basal cell markers P-cadherin, K5 and K14 (Romano, Birkaya et al. 2007, Shimomura, Wajid et al. 2008, Romano, Ortt et al. 2009). Because ΔNp63 has lower expression in D492M than D492, we decided to overexpress ΔNp63 in D492M. Interestingly, overexpression of ΔNp63 in D492M caused a switch in cadherin expression, from N-cadherin to E- and P-cadherin, increased expression of the myoepithelial marker K17, but not the luminal epithelial marker EpCAM. K14 was not induced after ΔNp63 overexpression in D492M and D492M$^{\Delta Np63}$ cells maintained mesenchymal morphology in 2D culture, but formed dense mesenchymal/epithelial hybrid colonies in 3D culture but were not able to branch (Figure 9).

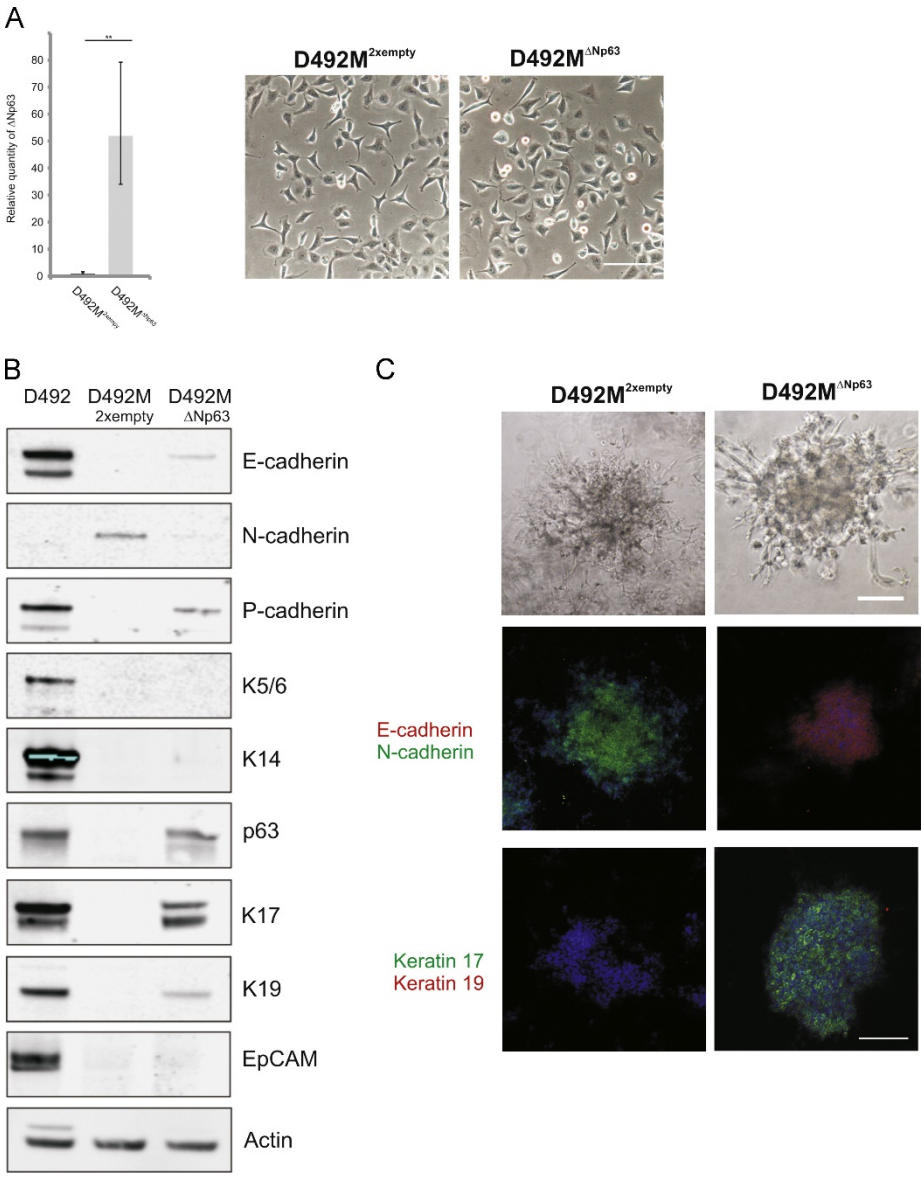

Figure 9. Forced expression of ΔNp63 induces myoepithelial differentiation.

(A) ΔNp63 overexpression has little effect on morphology of D492M in 2D culture. D492M cells were transduced with a lentiviral construct containing ΔNp63 ($D492M^{\Delta Np63}$). The expression levels of ΔNp63 were 50 fold higher in $D492M^{\Delta Np63}$ than in $D492^{2\times empty}$ cells. Phase contrast image of $D492M^{\Delta Np63}$ shows minor effect of ΔNp63 overexpression on cell morphology. miRNA levels were normalized to U6. Bar=100 µM. (B) $D492M^{\Delta Np63}$ acquires myoepithelial phenotype. Western blot shows strong expression of the myoepithelial markers p63, K17 and P-cadherin and a vague K14 expression. Also, the expression of the EMT marker N-cad is reduced compared

to D492M^{empty}. Actin was used as a loading control. (C) D492M$^{\Delta Np63}$ cell in rBM monoculture form irregular colonies. D492M$^{\Delta Np63}$ form structures with slightly more dense morphology than D492M, but retain the mesenchymal morphology of the parental cell line. IF staining shows strong expression of E-cad (red) and K17 (green) but lack of N-cad (green) and K19 (red) expression. Cells were counterstained with TO-PRO-3 nuclearstain. Bar=100 µM. (Figure 5 in article #1)

We concluded that overexpression of ΔNp63 in D492M induced myoepithelial marker expression in D492M, although not completely, as K14 expression was lacking. It is important to note that even though we concluded that the myoepithelial differentiation was incomplete, as some important markers such as alpha-smooth muscle actin were not expressed, there is a question if we should rather have called this basal cell differentiation instead of myoepithelial differentiation.

Next, we were interested in studying the effects of overexpressing ΔNp63 in D492M$^{miR\text{-}200c\text{-}141}$ to see if we would also get an induction of basal/myoepithelial markers. In fact, this is what happened where co-expression of miR-200c-141 and ΔNp63 in D492M induced both luminal and myoepithelial markers and a switch from N- to E-cadherin expression. Interestingly, D492M$^{miR\text{-}200c\text{-}141\text{-}\Delta Np63}$ expressed K5/6 and K14 that were not expressed in D492M$^{miR\text{-}200c\text{-}141}$ or D492M$^{\Delta Np63}$. In 2D culture D492M$^{miR\text{-}200c\text{-}141\text{-}\Delta Np63}$ showed cuboidal epithelial phenotype and in 3D culture they formed irregular branching colonies (Figure 10). It is noteworthy that when D492M$^{miR\text{-}200c\text{-}141\text{-}\Delta Np63}$ were pre-clustered in ultra-low adhesion plates, thereby allowing the cells to pre-arrange in multi-cell clusters before 3D culture, the cells were able to form elaborate branching structures resembling D492 (Figure 11). From this data, we concluded that ectopic expression of miR-200c-141 and ΔNp63 was sufficient to induce branching in D492M, which resembled branching of D492, and with the same key epithelial marker expression profile as D492.

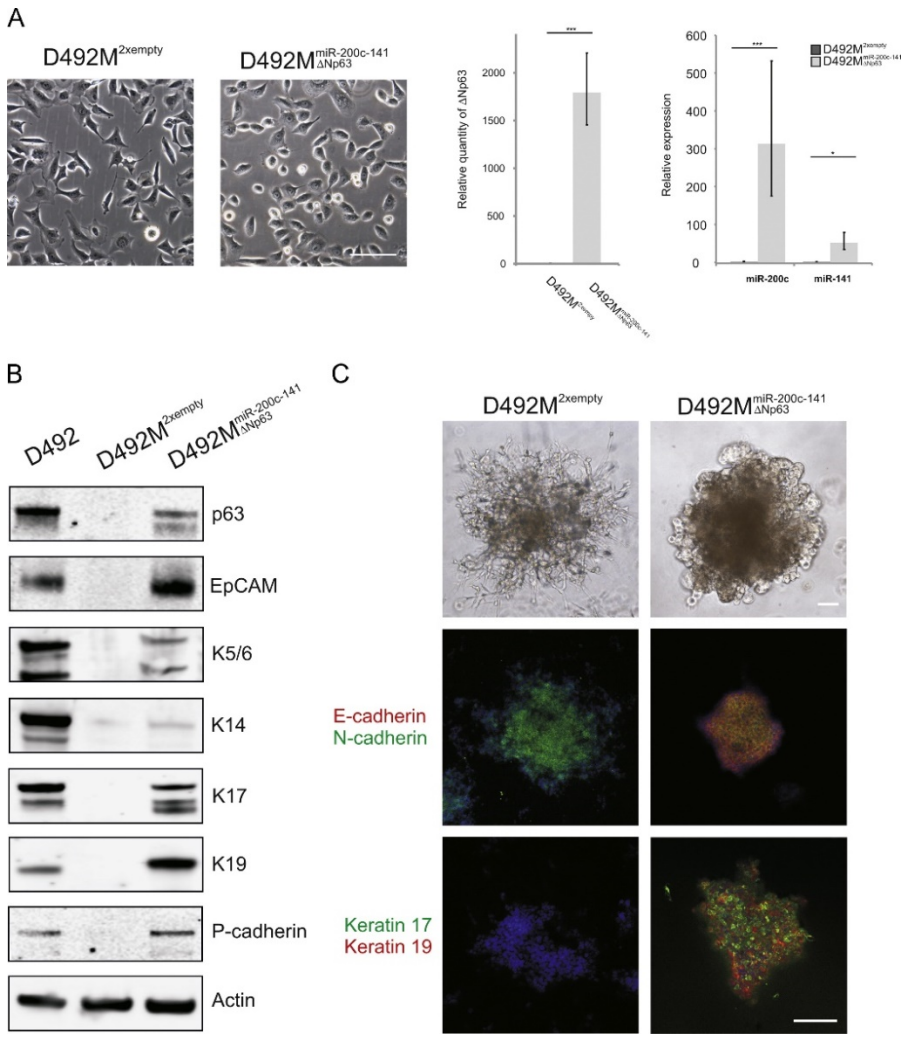

Figure 10. Co-expression of mir-200c-141 and ΔNp63 induces LEP and MEP differentiation.

(A) Co-expression of miR-200c-141 and ΔNp63 in D492M. D492M$^{\text{miR-200c-141}}$ were transduced with a lentiviral construct containing ΔNp63 (D492M$^{\text{miR-200c-141-ΔNp63}}$). Phase contrast image of D492M$^{\text{miR-200c-141-ΔNp63}}$ shows cuboidal epithelial phenotype in culture. miR-200c, miR-141 and ΔNp63 expression levels were 50–1700 fold higher in D492M$^{\text{miR-200c-141-ΔNp63}}$ than in D492$^{\text{2×empty}}$ cells, respectively. miRNA levels were normalized to U6. Bar=100 µM. (B) miR-200c-141 and ΔNp63 coexpression induces expression of luminal and myoepithelial markers. Western blot shows strong expression of the myoepithelial markers p63, K5/6, K17 and P-cadherin and a vague K14 expression in D492M$^{\text{miR-200c-141-ΔNp63}}$. The luminal markers EpCAM and K19 are also expressed. Actin as loading control. (C) D492M$^{\text{miR-200c-141-ΔNp63}}$ cells in rBM monoculture form irregular branching colonies. Immunostaining shows co-expression of N-cad (green) and E-cad (red) D492M$^{\text{miR-200c-141-Δp63}}$. Note the lack of polarity in N-cad expression (compared with Fig. 1A). D492M$^{\text{miR-200c-141-ΔNp63}}$ expresses both luminal marker K19 (red) and myoepithelial marker K17 (green). Cells were counterstained with TO-PRO-3 nuclearstain. Bar=100 µM. (Figure 6 in article #1)

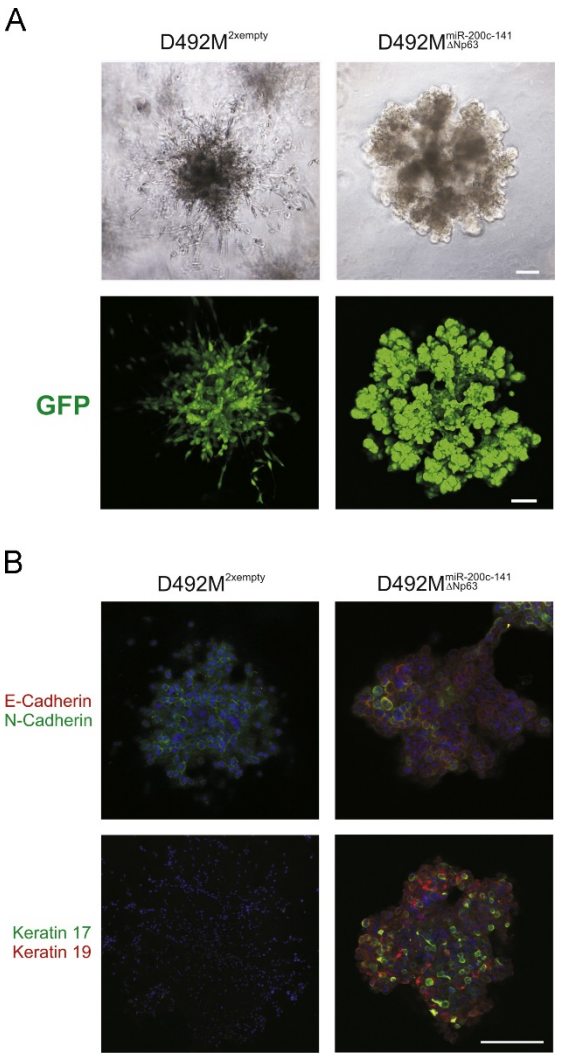

Figure 11. Co-expression of mir-200c-141 and ΔNp63 in D492M rescues the luminal–myoepithelial phenotype and induces branching.

(A) D492M$^{miR\text{-}200c\text{-}141\text{-}\Delta Np63}$ form epithelial branching structures in cluster assay. Cells were preclustered in an ultra low adhesion plate for 24 h, embedded into matrigel and cultured for 8 days. D492M$^{miR\text{-}200c\text{-}141\text{-}\Delta Np63}$ form elaborate branching structures similar to D492 (see Fig. 1A) while D492M form mesenchymal structures in cluster assay (upper bright field, lower GFP). Bar=100 µM. (B) Expression of luminal and myoeithelial markers in D492M$^{miR\text{-}200c\text{-}141\text{-}\Delta Np63}$. Immunostaining shows low N-cad (green) and strong E-cad (red) expression in D492M$^{miR\text{-}200c\text{-}141\text{-}\Delta p63}$ as well as K17 (green) and K19 (red) expression. Cells were counterstained with TO-PRO-3 nuclearstain. Bar=100 µM. (Figure 7 in article #1)

Collectively, we showed in this study that the miR-200c-141 cluster is an important regulator of cellular plasticity, including EMT/MET and luminal differentiation in D492 and its mesenchymal derivative D492M. We also showed that ΔNp63 is important for myoepithelial differentiation and can restore epithelial characteristics in D492M. To restore full progenitor properties and branching potential in D492M it was necessary to co-express ΔNp63 and miR-200c-141, which resulted in a bipotential luminal and myoepithelial phenotype and branching morphogenesis in 3D culture.

A recent paper Knezevic et al. demonstrated that miR-200c induces differentiation, increases chemosensitivity and reduces metastatic potential in *in vivo* models of claudin-low subtype of breast cancer (Knezevic, Pfefferle et al. 2015). This subtype is classified within the group of triple negative breast cancer and is characterized by being enriched in the EMT phenotype (Prat, Parker et al. 2010, Jordan, Johnson et al. 2011, Nieto, Huang et al. 2016). Furthermore, Koo et al. demonstrated that overexpression of miR-200c in several cancer cell lines including the breast cancer cell line MDA-MB-468 increased radiosensitivity and this was due to downregulation of p-EGFR and p-AKT (Koo, Cho et al. 2017). This data indicates that miR-200c could act as a tumor suppressor in cancer types with an EMT phenotype by reverting the EMT phenotype through MET, which is associated with increased chemo- and radiosensitivity. This could however be a double-edged sword, because miR-200c-141 has also been linked to increased metastatic potential of cancer cells (Dykxhoorn, Wu et al. 2009, Korpal, Ell et al. 2011, Jin, Suk Kim et al. 2017, Zhang, Zhang et al. 2017). It is possible that miR-200c could act as a tumor suppressor in the early phase of tumor development, inhibiting formation of a migrating/invasive EMT phenotype. In advanced cancer, miR-200c could act as metastatic driver by helping the cancer cells to colonize in distant organs. To analyze if this could be the case we conducted a pulmonary metastatic assay (PUMA) on D492M and D492M$^{miR\text{-}200c\text{-}141}$. There was a dramatic increases in colonization of D492M$^{miR\text{-}200c\text{-}141}$ compared to D492M^{Ctrl} (Hilmarsdottir 2016). This shows that the expression of miR-200c-141 increases colonization potential of D492M in the lung. High expression levels of miR-200c and miR-141 have been reported in breast cancer patients and animal models with metastatic disease and poor clinical prognosis (Korpal, Ell et al. 2011, Pecot, Rupaimoole et al. 2013, Le, Hamar et al. 2014, Tuomarila, Luostari et al. 2014, Jin, Suk Kim et al. 2017). This is in concordance with our results from the PUMA assay.

Collectively, this study shows that miR-200c-141 are important for differentiation and cellular fate decision. MiR-200c-141 expression is

important for maintaining epithelial differentiation and for branching morphogenesis, especially luminal differentiation. In breast cancer, the loss of miR-200c-141 expression can result in cells undergoing EMT, where cells gain increased mobility and invasive capabilities and therefore ability to intravasate. Expression of miR-200c-141 may be important for forming metastasis as the cancer cells need to colonize foreign tissues and regain epithelial characteristics. Higher levels of miR-200c and miR-141 have been reported in serum from breast cancer patients with metastatic disease compared to healthy controls (Madhavan, Zucknick et al. 2012, Madhavan, Peng et al. 2016). The higher levels of miR-200c and miR-141 could be derived from the primary tumor or metastatic sites. ΔNp63 expression induced MET in D492M, restored myoepithelial differentiation, and was necessary for complete MET in D492M$^{miR\text{-}200c\text{-}141}$. ΔNp63 has been reported to drive metastasis in breast cancer cells (Di Franco, Turdo et al. 2016) and it would be interesting to see if D492M$^{miR\text{-}200c\text{-}141\text{-}\Delta Np63}$ are more malignant than D492M$^{miR\text{-}200c\text{-}141}$. These studies will be performed in the laboratory in the near future.

4.2 Article #2. MiR-203a is differentially expressed during branching morphogenesis and EMT in breast progenitor cells and is a repressor of peroxidasin (submitted to Developmental biology, April 2018).

In this paper, of which I am the first author, I focused on miR-203a and its role in branching morphogenesis and EMT/MET. In the miRNA expression array data described above, miR-203a, was similar to the miR-200 family, one of the most downregulated miRNAs in D492M. Here, I conducted miRNA expression analysis of D492 and D492M cells in 3D-rBM culture using small RNA sequencing. This showed that miR-203a expression increases during branching morphogenesis of D492 cells and that it is highly downregulated in D492M.

4.2.1 Comparison of miRNA expression in D492 and D492M from 3D-rBM cultures

To get a more comprehensive view of the miRNA profiles, I conducted small RNA sequencing on D492 and D492M in 3D-rBM culture. As was discussed in the introduction, ncRNAs play an important role in development, differentiation, EMT/MET and cancer progression. We had previously shown that when D492 breast epithelial progenitor cells undergo EMT there are drastic changes in gene expression (article #1). Previous expression analysis of D492 and D492M were performed on cells from monolayer cultures and next I wanted to expand the analysis to 3D-rBM cultures. It is well documented that mRNA expression is different between 2D and 3D-rBM cultures and therefore I thought it was interesting to study if this would also apply to miRNA expression (Dangles, Lazar et al. 2002, Ghosh, Spagnoli et al. 2005, Kenny, Lee et al. 2007, Yu, Lin et al. 2012, Zschenker, Streichert et al. 2012). I changed platforms and moved from gene expression microarrays to next generation sequencing (NGS). First, I did small RNA sequencing on D492 and its mesenchymal derivative D492M, from 3D-rBM cultures, and performed differential miRNA expression analysis. Forty-seven miRNAs were differentially expressed (> 2-fold), 24 were down-regulated and 23 were up-regulated in D492M. Interestingly, there was strong concordance between these results and the miRNA microarray analysis from monolayer (Figure 12 a-b). The most downregulated miRNAs in D492M, in both assays, have been strongly associated with epithelial integrity, such as the miRNA-200 family, miR-205 and miR-203a (Gregory, Bert et al. 2008, Wellner, Schubert et al. 2009, Feng, Wang et al. 2014). This showed that there was little difference in expression of key miRNAs preserving epithelial integrity between D492 and D492M grown in 2D and 3D-rBM cultures.

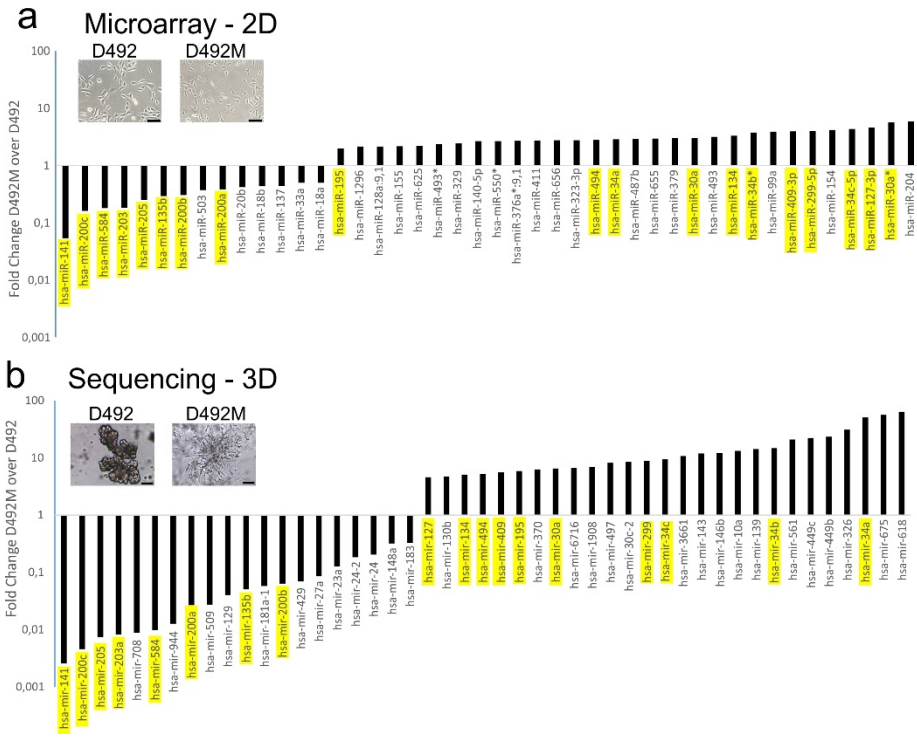

Figure 12. The most significantly differentially expressed miRNAs are consistently dysregulated in both 2D and 3D-rBM cultures of D492 and D492M.

Differentially expressed miRNAs between D492M and D492 in 2D culture based on a) microarray data and in b) 3D-rBM culture based on small RNA-sequencing data. There is concordance between a) and b) (highlighted in yellow) especially in the most downregulated miRNAs, i.e. the miRNA 200 family, miR-203, miR-205 and miR-584. Scale bar = 100 µm

4.2.2 Downregulation of miR-203a is not due to promoter DNA methylation

We had previously shown that expression of miR-200c-141 was suppressed in D492M through DNA promoter methylation (article #1). Therefore, I decided to investigate if transcriptional control of miR-205 and miR-203a was also due to methylation of CpG islands in the promoter area of these miRNAs. Bisulfite sequencing analysis of miR-200c-141 and miR-205 revealed hyper-methylation in the promoter area, while the promoter area in miR-203a remained un-methylated in D492M (Figure 13). This is in contrast to previously published results in human mammary epithelial cells (HMLE) undergoing EMT (Taube, Malouf et al. 2013) and some metastatic breast cancer cell lines (Zhang, Zhang et al. 2011) where the promoter of miR-203a becomes methylated.

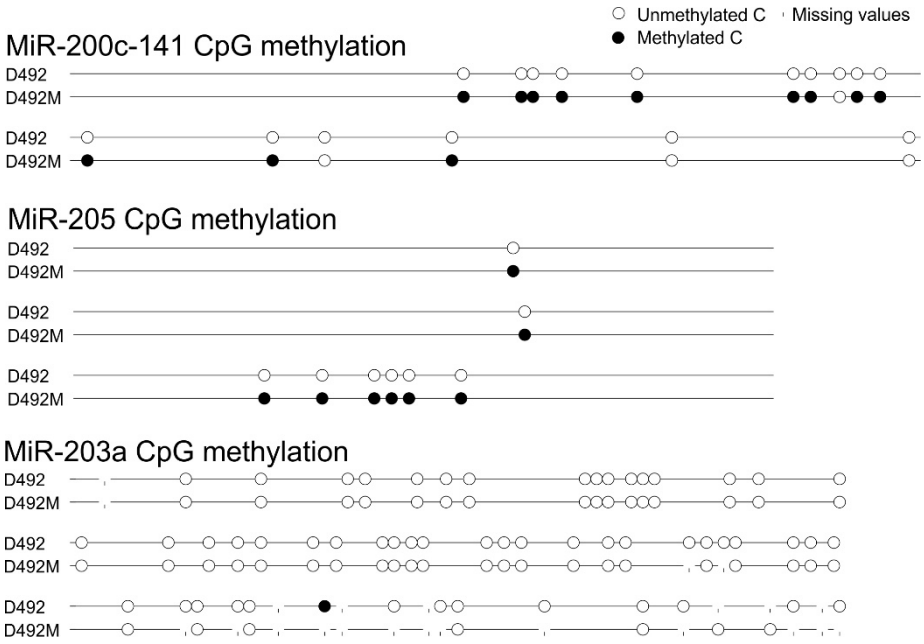

Figure 13. Promoter DNA methylation of miR-200c-141, miR-205 and miR-203a.

Bisulfite sequencing of miRNA promoters in D492 and D492M. The promoters of miR-200c-141, miR-205 and miR-203a are un-methylated in D492. In D492M, the promoter of miR-203a remains un-methylated, while the promoters of miR-200c-141 and miR-205 are methylated.

4.2.3 MiR-203a expression is restricted to epithelial cells and is mainly associated with luminal epithelial cells and shows temporal changes in expression during D492 branching morphogenesis

The promoter DNA methylation data indicated that transcriptional control of miR-203a is different in D492M compared to other breast EMT cell lines. According to a study from Park et al. expression of miR-203 was higher in more differentiated luminal epithelial cancer cell lines such as MCF-7 and T47D, but was lower in less differentiated mesenchymal-like cancer cell lines, such as MDA-MB-231, SUM159 and Hs578T (Park, Gaur et al. 2008). When I investigated miR-203a expression in various breast cell lines I found that miR-203a expression was restricted to cell lines with an epithelial phenotype, i.e. D492, HMLE and MCF10A, but was absent in mesenchymal derivatives of D492 and HMLE (D492M and HMLEmes) and the triple negative MDA-MB-231 (Figure 14 a). Furthermore, when I analyzed miR-203a expression in primary breast cells, it was expressed in the epithelial cells, predominantly in luminal epithelial cells, but not fibroblasts and breast endothelial cells (Figure

14 b).

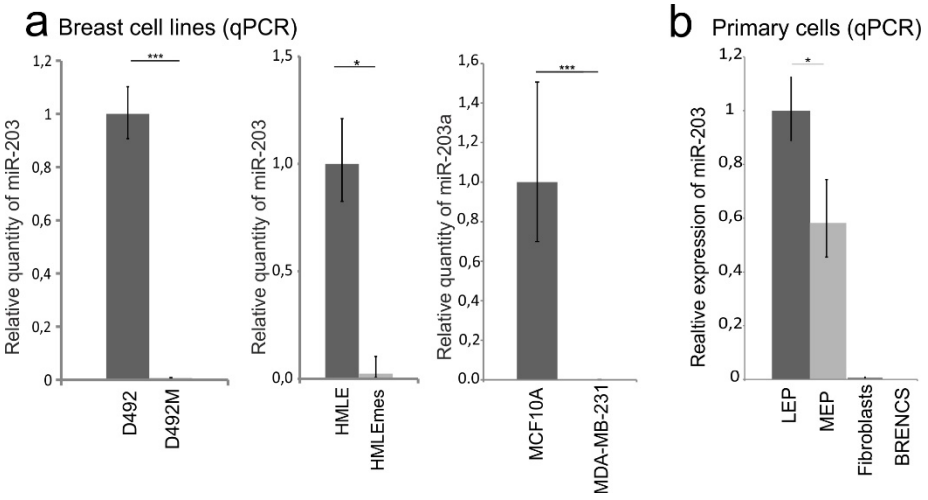

Figure 14. MiR-203a expression in breast cell lines.

a) Expression of miR-203a is restricted to cell lines with an epithelial phenotype. Expression of miR-203a in mesenchymal derivatives of D492 and HMLE, i.e. D492M and HMLEmes, is downregulated with little or no expression in the mesenchymal state. MCF10A, a normal like breast cell line, has high expression of miR-203a, while the triple negative mesenchymal breast cancer cell line MDA-MB-231 has no expression of miR-203a. b) Expression of miR-203a from primary breast cells. MiR-203a is expressed in the epithelial cells, mostly luminal epithelial cells, but not fibroblasts and BRENCS.

With this data in mind, I decided to investigate miR-203a expression in D492 at various stages of differentiation. I analyzed miR-203a expression at different time points during branching morphogenesis in 3D-rBM culture, i.e. during pre-branching (day 7), branching (day 14) and late-branching (day 21) and in different sub-populations of D492, i.e. EpCAM^{high} and EpCAM^{low} cells. I found that expression of miR-203a was higher in more differentiated D492 cells, i.e. miR-203a expression increased with increasing differentiation of the D492 branching colonies (Figure 15 a-b).

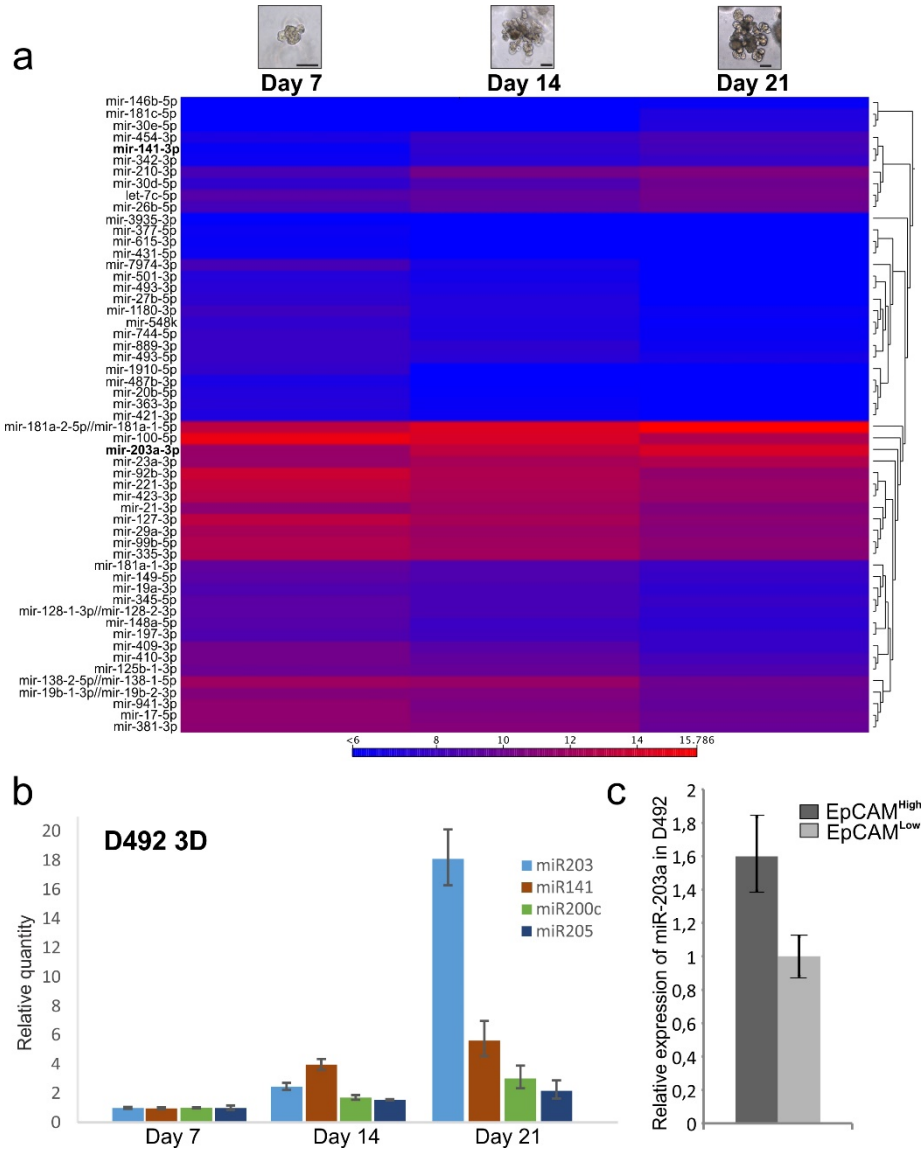

Figure 15. Differentially expressed miRNAs in D492 during branching.

a) Heatmap showing differentially expressed miRNAs in D492 at different time points during branching morphogenesis (day 7, 14 and 21). MiR-203a expression increases during branching of D492. Heatmap shows miRNAs with > 2-fold change in expression (FDR corrected p-values < 0.1). Scale bar = 100 µm. b) RT-qPCR showing that the expression of miR-203a and miR-141 significantly increases between time points during branching morphogenesis. Interestingly, expression of miR-203a increases markedly in late branching at day 21. c) RT-qPCR showing higher expression of miR-203a in EpCAM high D492 cells.

There was also increased expression of miR-141 during branching although not to the same extent as miR-203a at day 21 (Figure 15 a-b). In contrast, expression of miR-205 and miR-200c was constant throughout the branching process (Figure 15 b). This indicates that miR-203a and miR-141 may play a role in differentiation of the epithelial cells during branching morphogenesis.

I also found that, miR-203a expression was higher in the $EpCAM^{high}$ sub-population of D492, which represents more luminally differentiated cells compared to $EpCAM^{low}$ cells (Figure 15 c). This data is similar to results published by DeCastro et al. where they demonstrated that expression of miR-203a is induced during lactogenic- and luminal differentiation (DeCastro, Dunphy et al. 2013).

In summary, miR-203a expression was highest in the epithelial compartment of the breast and was most prominent in the more differentiated luminal cells. Expression of miR-203a was lost when the breast epithelial cell lines D492 and HMLE underwent EMT and was absent in mesenchymal derivatives of epithelial cells and breast cancer cell lines with a mesenchymal appearance. Transcriptional control of miR-203a expression in D492/D492M was not through hyper-methylation of the promoter as in HMLE/HMLE-mesenchymal derivatives and MDA-MB-231. Expression of miR-203a increased during D492 branching morphogenesis as the cells differentiated. Interestingly, in a study characterizing miRNA expression in post-natal mouse mammary gland development, miR-203a expression increased during early development and gestation followed by lower expression during the lactation and involution stages (Avril-Sassen, Goldstein et al. 2009). The D492 3D-rBM model therefore shows similar results, in terms of miR-203a expression, as *in vivo* experiments done in mice during early development of the post-natal gland. A limitation to our D492 3D-rBM model is that it does not capture the pregnancy and lactation stages and therefore is not suitable for studying miR-203a expression during these stages.

4.2.4 MiR-203a expression reduces mesenchymal characteristics of D492M cells

Next, I decided to do functional experiments with miR-203a in D492 and D492M cells. Previously we had shown that overexpression of miR-200c-141 in D492M reverted the mesenchymal phenotype to an epithelial phenotype through MET (article #1). Therefore, I wanted to know if miR-203a would also induce MET in D492M. Overexpression of miR-203a in D492M ($D492M^{miR\text{-}203a}$) induced subtle changes in cell morphology but did not revert the cells to an epithelial morphology. Phase contrast images of $D492M^{miR\text{-}203a}$ cultured in monolayer show that there is increased adherence between cells.

Furthermore, when D492M$^{miR-203a}$ cells were cultured in 3D-rBM they formed more compact colonies, although the colonies still had cellular protrusions, typical of mesenchymal cells (Figure 16).

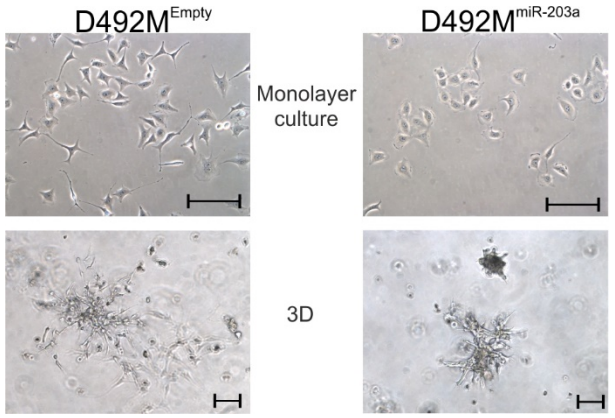

Figure 16. D492M$^{miR-203a}$ cells cultured in 2D and 3D.

Phase contrast images of D492M$^{miR-203a}$ show that in monolayer culture the cells adhere more to each other and in 3D-rBM the colonies are more compact but still have protrusions showing mesenchymal characteristics.

There was visible reduction in immunostaining of the mesenchymal marker N-cadherin and increased staining of the epithelial markers E-cadherin, K14 and K19 in D492M$^{miR-203a}$ cultured in monolayer (Figure 17 a). D492M$^{miR-203a}$ showed reduced N-cadherin and increased E-cadherin protein expression in Western blot (WB) (Figure 17 b), but showed no changes in K14 and K19 protein expression.

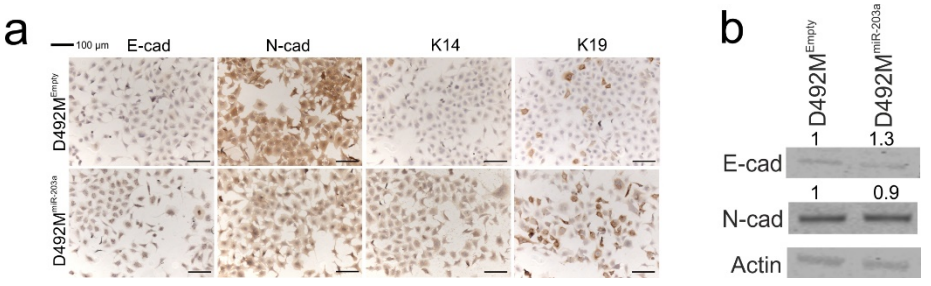

Figure 17. D492M$^{miR-203a}$ cells show reduced expression of the mesenchymal marker N-cadherin and increased expression of the epithelial marker E-cadherin.

a) DAB staining of D492M$^{miR-203a}$ cells show decrease in staining of the mesenchymal marker N-cadherin and increase in staining of the epithelial marker E-cadherin. There is also increased DAB staining of K14 and K19 in D492M$^{miR-203a}$.b) Decreased expression of N-cadherin and increased expression of E-cadherin was also seen in WB.

Overexpression of miR-203a in D492M reduced the proliferation rate of the cells in monolayer and when the cells were cultured in low-attachment plates, anchorage independent growth was negatively affected (Figure 18 a). The ability of cells to grow in suspension has been described as a progenitor/stem cell property (Dontu, Abdallah et al. 2003) and the reduced ability of D492M$^{miR-203a}$ cell to form mammospheres in suspension indicates that miR-203a induces cellular differentiation.

As mesenchymal cells have increased mobility compared to epithelial cells, I analyzed the ability of D492M$^{miR-203a}$ cells to migrate and invade. Indeed, D492M$^{miR-203a}$ cells showed reduced ability to migrate through transwell filters and to invade through matrigel coated transwell filters, indicating suppression of mesenchymal characteristics (Figure 18 b).

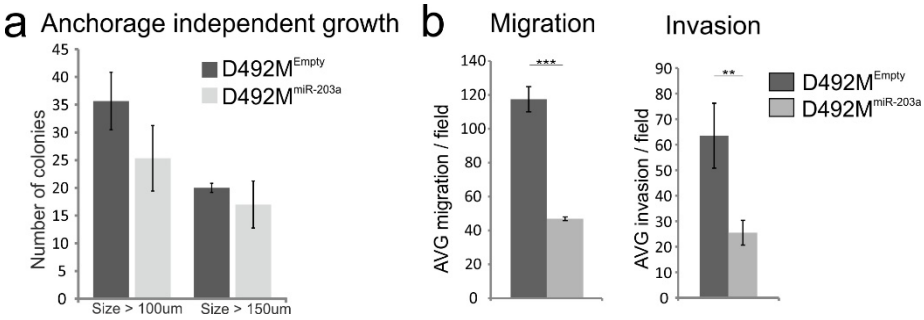

Figure 18. D492M$^{miR-203a}$ cells show reduced progenitor/stem cell properties and reduced mesenchymal characteristics.

a) D492M$^{miR-203a}$ cells have reduced capability to form mammospheres indicating loss of a progenitor/stem characteristic in low-attachment assay. b) D492M$^{miR-203a}$ cells migrate less in transwell migration- and invasion assays, showing reduced mesenchymal traits.

Since the EMT phenotype has been associated with apoptosis resistance, I decided to investigate sensitivity of D492M$^{miR-203a}$ cells to camptothecin, a chemical inducer of apoptosis. Interestingly, D492M$^{miR-203a}$ cells were less resistant to chemically induced apoptosis (Figure 19).

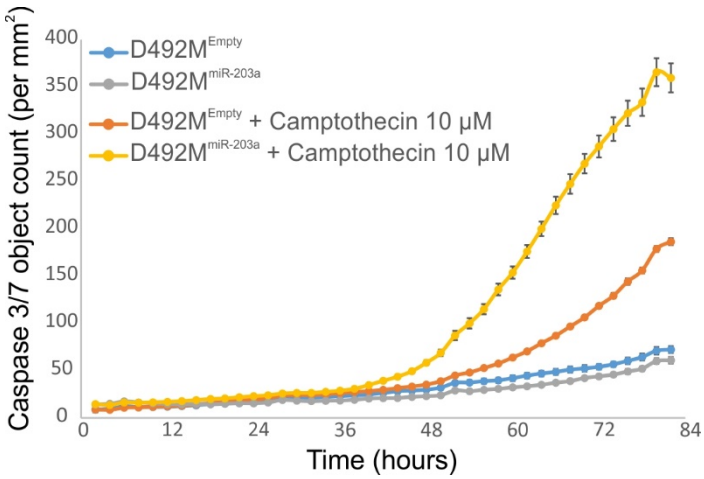

Figure 19. D492M$^{miR-203a}$ cells are more sensitive to camptothecin induced apoptosis.

D492M$^{miR-203a}$ cells are more sensitive to chemically induced apoptosis. D492M^{Empty} (blue) and D492M$^{miR-203a}$ (grey) were treated with DMSO and D492M^{Empty} (orange) and D492M$^{miR-203a}$ (yellow) were treated with 10 µM camptothecin. D492M$^{miR-203a}$ (yellow) are more sensitive to camptothecin than D492M^{Empty} (orange) as is evident by the caspase 3/7 object count.

In summary, although phenotypic changes were not drastic, we saw clear differences in functional testing such as reduced anchorage independent growth, reduced migration/invasion and increased sensitivity towards chemical induced apoptosis. In summary, there was reduction in mesenchymal traits in D492M$^{miR-203a}$ cells.

4.2.5 Peroxidasin is a potential target of miR-203a

I also performed RNA-sequencing on D492M$^{miR-203a}$ to search for potential target genes of miR-203a. The most significantly downregulated gene was peroxidasin (*PXDN*) (Figure 20 a), which codes for a protein that has been described in other organs to be involved in crosslinking collagen IV in the basement membrane and is believed to be important for normal development (Colon, Page-McCaw et al. 2017). Its function has not been previously described in breast morphogenesis but, importantly, overexpression of *PXDN* in HER2 positive breast cancer is associated with poor prognosis (MTCI database). My analysis identified a novel link between miR-203a and *PXDN*, where *PXDN* is a potential target of miR-203a, and is more highly expressed in D492M than D492. Using bioinformatics analysis, I discovered that miR-203a has a highly conserved binding motif (8 nucleotides) along with two

other poorly conserved motifs in the 3´-UTR of *PXDN* (Figure 20 b). When D492M cells were treated with miR-203a-mimic, expression of *PXDN* was reduced and when D492M$^{miR\text{-}203a}$ cells were treated with a miR-203a-inhibitor, *PXDN* expression was increased (Figure 20 c), showing negative correlation between miR-203a expression and *PXDN* expression. *PXDN* is upregulated in mesenchymal derivatives of both D492 and HMLE, i.e. D492M and HMLEmes respectively (Figure 20 d). Finally, binding of miR-203a to the *PXDN* 3'-UTR was confirmed with a luciferase assay (Figure 20 e). HEK293T cells were transfected with a plasmid containing the conserved binding site for miR-203a and the surrounding sequence from the PXDN 3'-UTR or a plasmid with only the miR-203a conserved binding site deleted. Cells transfected with the plasmid containing the miR-203a binding site had reduced luciferase activity compared to the empty plasmid control and the plasmid with the deleted miR-203a binding site, indicating binding of the miR-203a-3p mimic to the target sequence.

In conclusion, I used branching morphogenesis of D492 progenitor cells in 3D-rBM to model breast development and differentiation. MiR-203a expression coincided with increased differentiation status of the breast epithelial cells *in vitro* and correlates with differentiation stages in the mammary epithelium *in vivo*. MiR-203a expression is highest in luminal epithelial cells and is more expressed in differentiated epithelial cells compared to stem/basal cells. When I analyzed miR-203a expression in normal and cancerous human breast epithelial cell lines the expression was highest in cell lines with a luminal epithelial phenotype. When miR-203a was overexpressed in D492M, I only observed subtle changes towards MET and the effect was primarily evident in functional assays. Furthermore, I have demonstrated a novel link between miR-203a and *PXDN*, which is highly expressed in D492M.

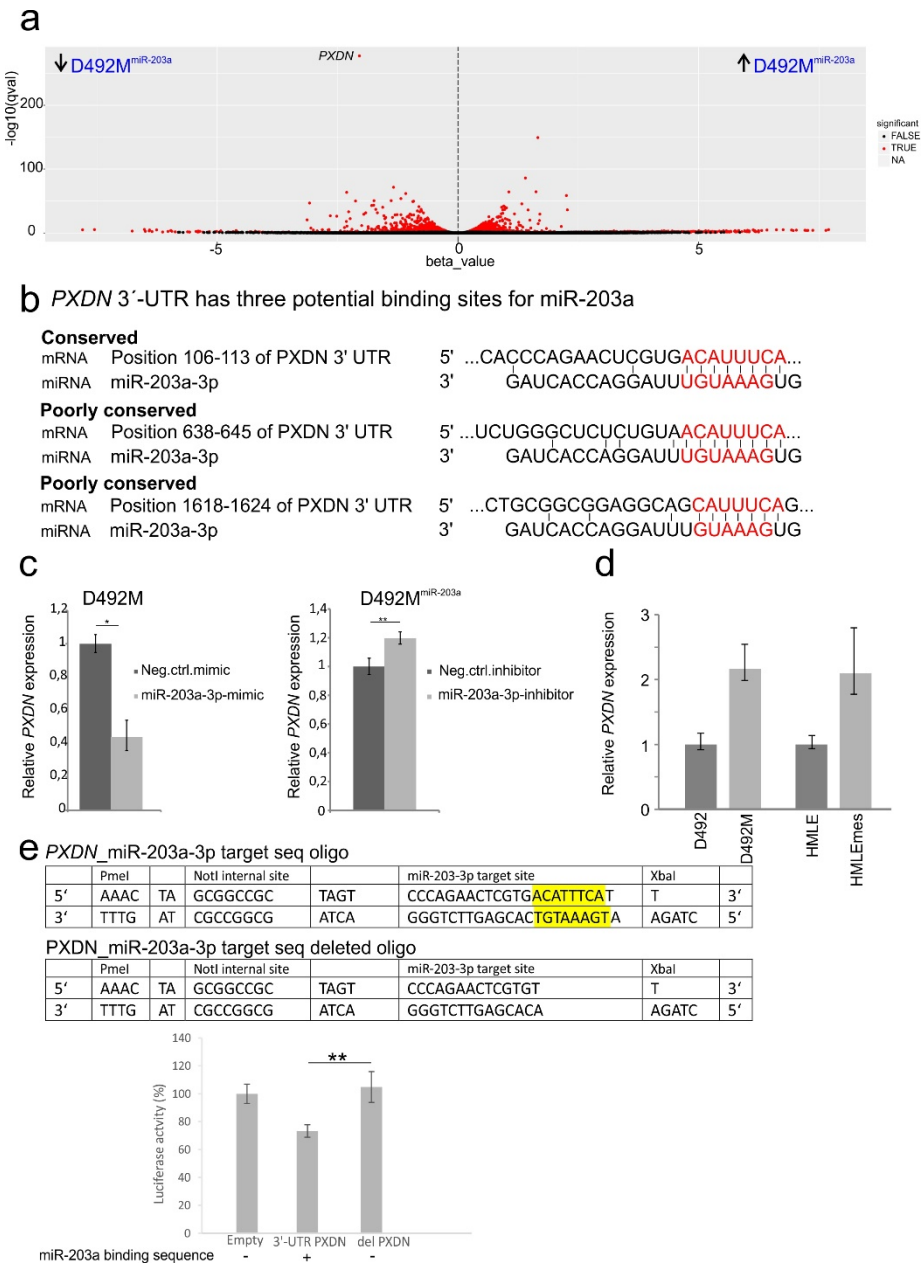

	PmeI		NotI internal site		miR-203-3p target site	XbaI	
5'	AAAC	TA	GCGGCCGC	TAGT	CCCAGAACTCGTGACATTTCAT	T	3'
3'	TTTG	AT	CGCCGGCG	ATCA	GGGTCTTGAGCACTGTAAAGTA	AGATC	5'

	PmeI		NotI internal site		miR-203-3p target site	XbaI	
5'	AAAC	TA	GCGGCCGC	TAGT	CCCAGAACTCGTGT	T	3'
3'	TTTG	AT	CGCCGGCG	ATCA	GGGTCTTGAGCACA	AGATC	5'

Figure 20. *PXDN*, a potential target of miR-203a, is more highly expressed in mesenchymal derivatives of D492 and HMLE.

a) *PXDN* was the most significantly downregulated gene in D492M$^{miR-203}$ b) and it has three potential binding sites for miR-203a in its 3'-UTR (based on TargetScan). c) When D492M cells were treated with miR-203a-mimic, there was significant downregulation of *PXDN* and when D492M$^{miR-203a}$ cells were treated with a miR-203a-

3p-inhibitor there was significant upregulation of *PXDN* expression, indicating a potential interaction between miR-203a and *PXDN*. *PXDN* expression was determined by RT-qPCR. d) *PXDN* expression is higher in mesenchymal derivatives of both D492 and HMLE, i.e. D492M and HMLEmes respectively (RT-qPCR). e) Luciferase assay showing HEK293T cells transfected with a empty plasmid control, plasmid containing the miR-203a binding site from *PXDN* 3‘-UTR or plasmid with the deleted miR-203a binding site. There was significantly reduced luciferase activity in cells transfected with the plasmid containing the miR-203a binding site compared to the plasmid with the deleted miR-203a binding site.

4.3 Article 3. Inhibition of PTP1B disrupts cell-cell adhesion and induces anoikis in breast epithelial cells

Due to PTP1B involvement in breast cancer and the fact that very little is known about its expression and function in the normal breast gland we decided to analyze PTP1B in normal breast and in D492 breast epithelial progenitor cells.

In article #3, we studied PTP1B in normal breast tissue, breast primary cells and breast cell lines, with primary focus on D492 and D492M. In normal breast tissue PTP1B was expressed in both luminal and myoepithelial cells and in fibroblasts. PTP1B was predominantly expressed in myoepithelial cells and fibroblasts but showed little expression in breast endothelial cells (Figure 21).

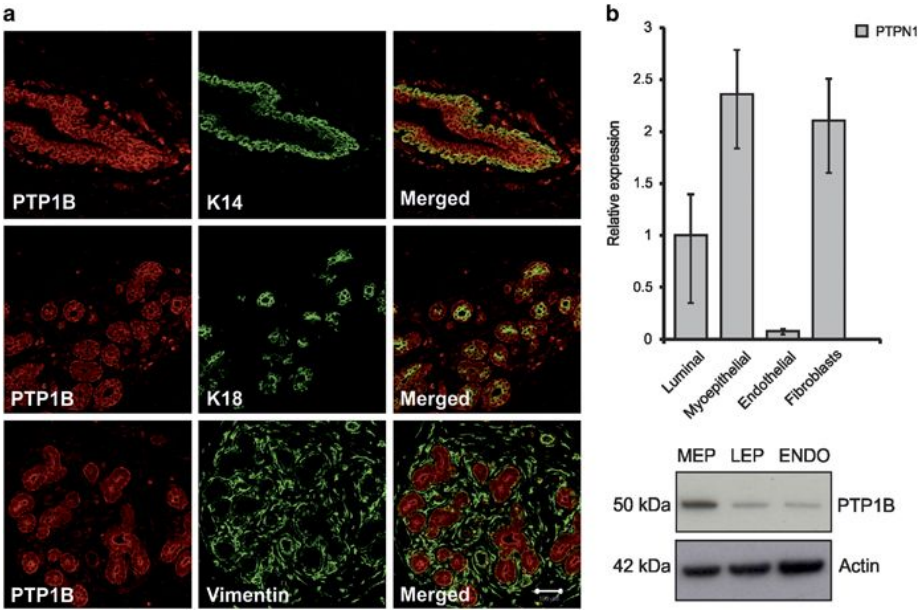

Figure 21. PTP1B is highly expressed in normal human breast tissue.

(a) PTP1B is expressed both in the epithelial and stromal compartments of the breast. Immunohistochemical stainings show prominent co-expression of PTP1B (red) and K14 (green) in myoepithelial cells (top row), PTP1B (red) and K18 (green) in luminal epithelial cells (middle row), PTP1B (red) and vimentin (green) stains myoepithelial and fibroblasts (bottom row). Bar 100 µm. (b) PTP1B is predominantly expressed in myoepithelial cells and fibroblasts in the breast gland. qPCR mRNA analysis shows that PTP1B expression is higher in myoepithelial cells (MEP) and fibroblasts than in luminal epithelial cells (LEP) and endothelial cells (ENDO). Expression levels were normalized to GAPDH (upper). Western blot confirmed high expression of PTP1B in myoepithelial cells (lower). Actin was used as a loading control. (Figure 1 in article #3)

To study the role of PTP1B in breast epithelial cells we used D492 and treated it with a PTP1B inhibitor. PTP1B inhibition caused reduced proliferation rate of D492 and affected survival of the cells. PTP1B inhibition leads to apoptosis in D492, more specifically anoikis which is a form of programmed cell death that occurs in the absence of cell-matrix interactions (Frisch and Francis 1994). Reduced proliferation was also seen when PTP1B was knocked down with siRNAs (Figure 22).

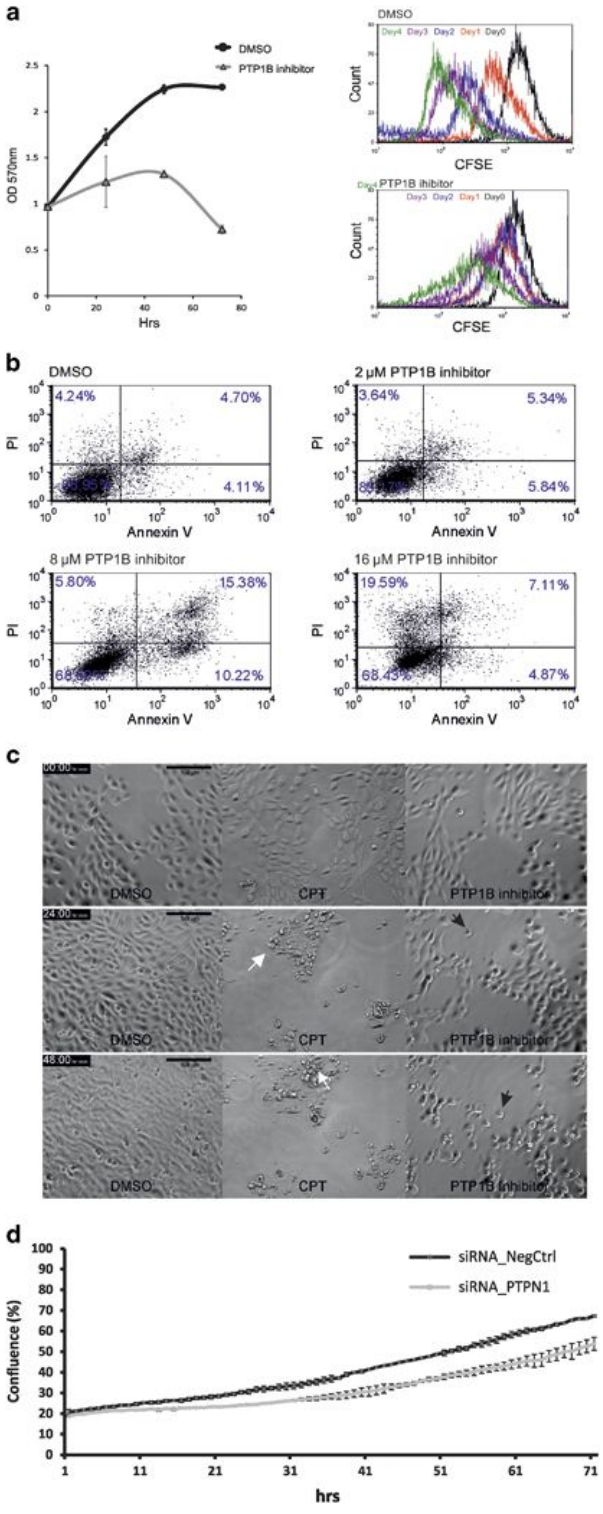
a
DMSO
PTP1B inhibitor
OD 570nm
Hrs
Count
CFSE
b
DMSO
2 μM PTP1B inhibitor
8 μM PTP1B inhibitor
16 μM PTP1B inhibitor
PI
Annexin V
4.24%
4.70%
4.11%
3.64%
5.34%
5.84%
5.80%
15.38%
10.22%
19.59%
7.11%
4.87%
c
DMSO
CPT
PTP1B inhibitor
d
siRNA_NegCtrl
siRNA_PTPN1
Confluence (%)
hrs

Figure 22. PTP1B is important for proliferation and survival of breast epithelial cells.

(a) Inhibition of PTP1B reduces cell division and affects survival of D492 cells. Left cell survival assay reveals that PTP1B inhibitor causes reduction in proliferation and cell death in D492. D492 were treated with DMSO (control) or 16 μM of a specific PTP1B inhibitor for 3 days, stained with crystal violet and the optical density at 570 nm determined. All experiments were conducted in triplicate. Right, D492 cells were stained with CFSE fluorescent dye, treated with DMSO or 8 μM of PTP1B inhibitor and analyzed using flow cytometry over a period of 4 days. Note, reduced cell division in D492 after PTP1B inhibition. (b) Inhibition of PTP1B results in apoptosis of D492 cells. Annexin V and PI staining shows that PTP1B inhibitor induces apoptotic cell death in D492. D492 cells were treated with DMSO (control) and various concentrations of PTP1B inhibitor. (c) Cell death induced by the PTP1B inhibitor shows the characteristics of anoikis. CPT induces classical apoptosis of D492 cells over time in culture (middle column). D492 cells were treated with DMSO as a control (left column). Treatment with PTP1B inhibitor results in failure of cells to establish a confluent monolayer with a number of cells forming a rounded detached appearance as in cells undergoing anoikis. (d) Knockdown of PTPN1 reduces proliferation of D492 cells. D492 cells were transfected with siRNA PTPN1 s11507 or negative control no. 1 siRNA at 50 nM and cell confluence was monitored for 72 h using IncuCyte Zoom Live Cell Analysis System. Knockdown of PTPN1 resulted in an inhibition of confluency, whereby D492 cells treated with siRNA against PTPN1 demonstrated significantly less cell proliferation than cells treated with negative control siRNA. All experiments were done in triplicate. (Figure 2 in article #3)

D492 cultured in 3D-rBM formed elaborate branching structures where PTP1B expression was widespread throughout the branching structures, like in the normal breast gland and furthermore the expression of PTP1B was highest in the lobular ends. When D492 branching structures were treated with PTP1B inhibitor, cells lost cell-cell contact and formed grapelike structures with no caspase 3 staining. In contrast, when the branching structures were treated with camptothecin it caused shrinkage, blebbing of cells and accumulation of cell debris positive for caspase 3 staining indicating apoptosis (Figure 23).

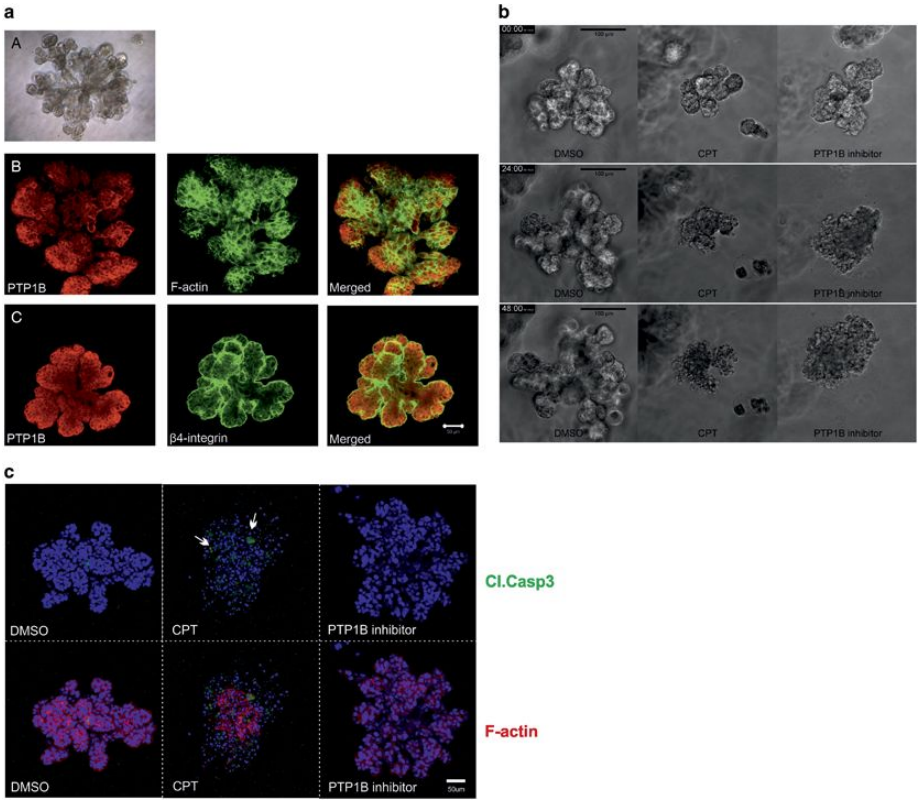

Figure 23. Inhibition of PTP1B affects branching morphogenesis and induces anoikis-like effects in D492 cells cultured in 3D.

(a) Expression of PTP1B in TDLU-like structures generated by D492 cells in 3D culture. (A) D492 cells form branching structures when cultured in 3D rBM matrix. (B) Expression of F-actin (green), PTP1B (red) and (C) expression of β4-integrin (green) and PTP1B in D492 cells cultured in 3D rBM. Note, the strong expression of PTP1B at the lobular ends. Bar 50 µm. (b) Inhibition of PTP1B induces loss of cell adhesion in 3D structures. D492 cells cultured in 3D rBM were treated with 10 µM of CPT, 32 µM of the PTP1B inhibitor or DMSO as control for 48 h. (c) D492 cells treated with PTP1B inhibitor die by anoikis. D492 cells treated with the PTP1B inhibitor do not show staining for cleaved caspase 3 in 3D culture (green). CPT was used as a positive control for apoptosis, arrows point to cells positive for cleaved caspase 3. Phalloidin stains F-actin (red). DAPI was used for nuclear staining (blue). (Figure 3 in article #3)

We concluded that PTP1B inhibition caused disturbed morphogenesis in D492 and controlled cell death through anoikis in 3D culture. In retrospect, we could also have stained for caspase 8. Caspase 8 is activated in anoikis by the ligation of death receptors on the cell surface resulting in assembly of a death-inducing signaling complex (DISC) that has the role of recruiting and activating caspase 8 (Gilmore 2005).

PTP1B has previously been reported to be an activator of Src kinase by dephosphorylating the inhibitory tyrosine phosphorylation site (Y529) (Bjorge, Pang et al. 2000). We decided to investigate if PTP1B inhibition would decrease Src activity in D492. D492 cells treated with the PTP1B inhibitor had increased phosphorylation of the inhibitory phosphorylation site (Y529) and decreased PTP1B-Src protein interaction (Figure 24). This showed that Src activity in D492 was dependent on PTP1B.

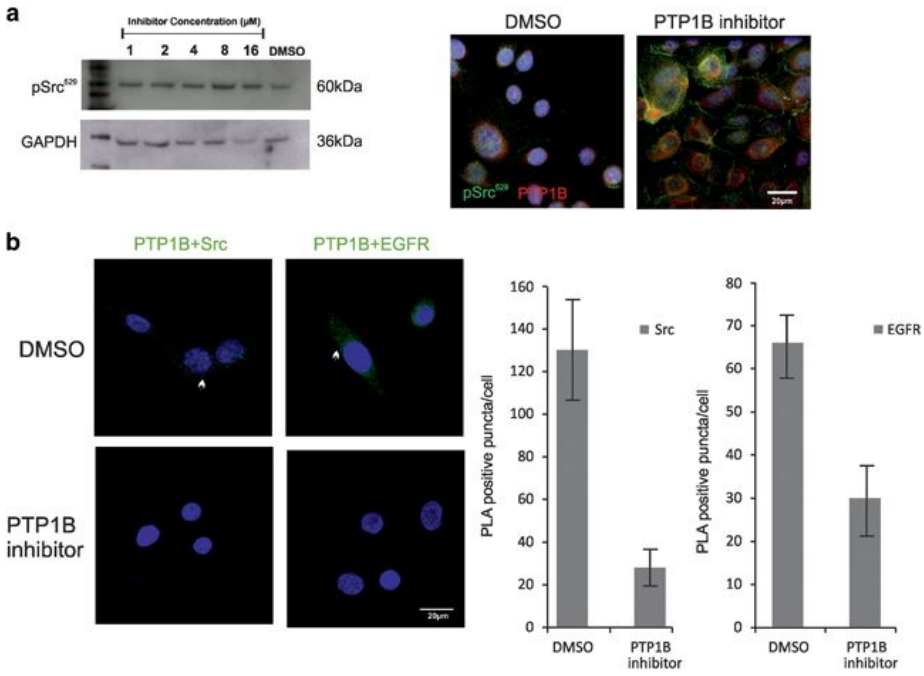

Figure 24. PTP1B inhibitor decreases Src activation in D492 cells.

(a) Treatment with PTP1B inhibitor results in increased phosphorylation of the inhibitory SrcY529. Left, western blot analysis of pSrcY529 shows that PTP1B inhibitor increases phosphorylation of pSrcY529. Protein extracts from D492 cells after treatment with DMSO and various concentrations of PTP1B inhibitor for 48 h. GAPDH as loading control. Right, Immunofluorescence staining of pSrc in D492 cells treated with the PTP1B inhibitor confirms increased phosphorylation of pSrcY529 after PTP1B inhibition. pSrc (green), PTP1B (red), TOPRO-3 nuclear staining (blue). Bar 20 μm. (b) Inhibition of PTP1B disrupts PTP1B protein interactions. PLA shows that PTP1B complexes with Src (left) and EGFR (right) (green arrows) are disassembled (left). DAPI nuclear stain (blue). Cell profiler was used to quantify frequency of positive puncta per cell (right). (Figure 4 in article #3)

Next, we decided to study how PTP1B affects cell adhesion. D492 cells were treated with PTP1B inhibitor for 48 hours and then cell detachment was measured after 1 minute of trypsinization compared to total number of cells,

where D492 cells detached more easily with increasing concentration of the PTP1B inhibitor. Expression of cell adhesion molecules was also measured, which showed decreased expression of Claudin 1, FAK and E-cadherin with increasing concentration of PTP1B inhibitor. In addition, actin polymerization was completely lost in D492 cells when they were treated with the PTP1B inhibitor, but total actin levels were unchanged (Figure 25). To summarize, PTP1B inhibition induced loss of adhesion in D492.

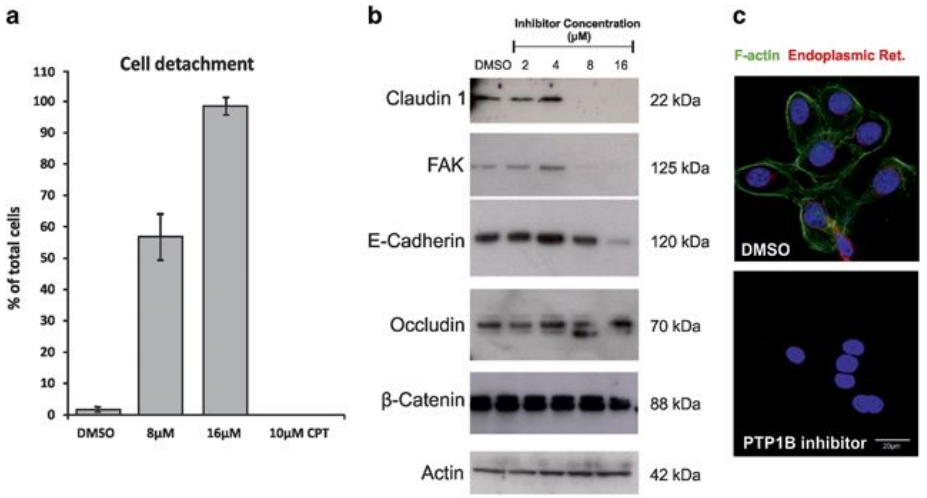

Figure 25. PTP1B inhibition affects expression of cell adhesion molecules and actin polymerization.

(a) D492 cells treated with PTP1B inhibitor show loose surface attachment. D492 cells were treated with 8 or 16 μM of the PTP1B inhibitor, 10 μM of CPT or DMSO as control for 24 h, and assayed for sensitivity to trypsinization. (b) Expression of various cell adhesion molecules is reduced in D492 cells after PTP1B inhibition for 48 h. D492 cells were treated with various concentrations of the PTP1B inhibitor for 48 h followed by protein isolation. Claudin-1, FAK and E-cadherin expression is lost when treated with 16 μM of the inhibitor. PTP1B inhibition does not affect occludin, β-catenin and actin expression. (c) F-actin polymerization is lost in D492 cells treated with inhibitor for 5 h. Phalloidin stains F-actin (green), Concavalin A stains endoplasmic reticulum (red). (Figure 5 in article #3)

Epithelial cells that undergo EMT lose cell-cell adhesion and gain increased migratory and invasion capability. We decided to investigate the effects of PTP1B inhibition on D492M, an EMT derivative of D492. Interestingly, D492M cells were more sensitive to PTP1B inhibition, than their epithelial counterpart, and were not as viable. The same applied to the breast epithelial progenitor cell line HMLE and its mesenchymal derivative HMLEMmes. Interestingly, mesenchymal derivatives of mammary epithelial cells are more sensitive to PTP1B inhibition than their epithelial counterparts.

Possibly, PTP1B inhibition makes the mesenchymal cells more sensitive to induction of cell death making PTP1B a potential therapeutic target in a subset of breast cancer tumors enriched in cells showing an EMT phenotype.

Then we decided to see if PTP1B inhibition would have less effect on D492M overexpressing miR-200c-141, which has an epithelial phenotype. When cells were trypsinized, $D492M^{Ctrl}$ were more loosely attached than $D492M^{miR\text{-}200c\text{-}141}$ showing reduced effects of the PTP1B inhibitor on a cell line with epithelial characteristics (Figure 26).

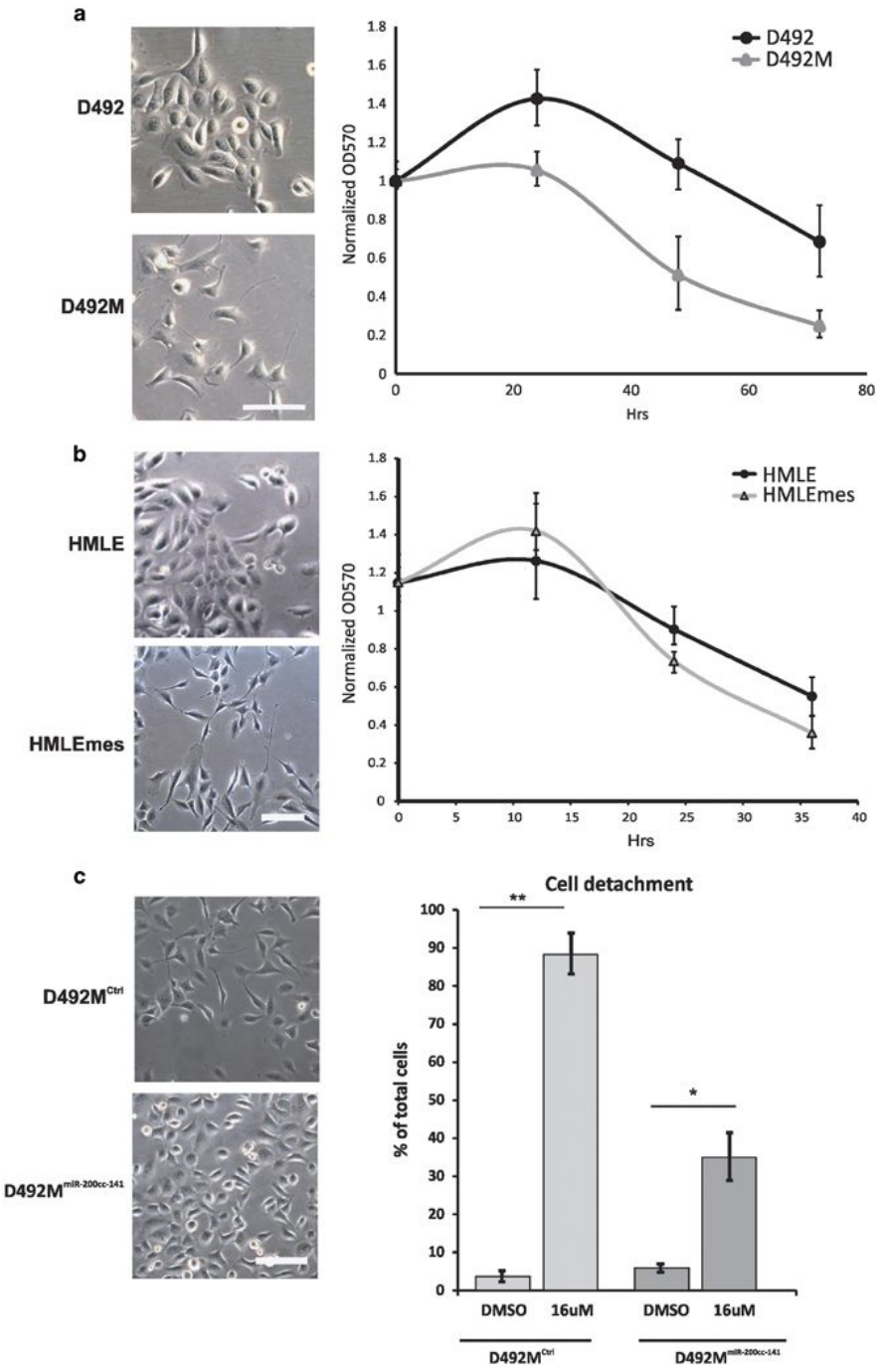

Figure 26. Cells with mesenchymal phenotype are more sensitive to PTP1B inhibition than their isogenic epithelial counterparts.

(a) D492M is more sensitive toward PTP1B inhibition than D492. The isogenic cell lines D492M and D492 that show mesenchymal and epithelial phenotype, respectively, were treated with DMSO (control) or 16 μM of a specific PTP1B inhibitor for 3 days. Cells were stained with crystal violet at different time points and optical density measured at 570 nm to evaluate the survival of cells. Note how D492M cells show lesser survival than D492. All experiments were conducted in triplicate. (b) HMLEmes is more sensitive to PTP1B inhibition than HMLE. HMLE and HMLEmes were treated with DMSO (control) or 16 μM of a specific PTP1B inhibitor for 3 days, stained with crystal violet and the optical density at 570 nm determined. (c) MET reverses sensitivity to PTP1B inhibition in D492M. $D492M^{Ctrl}$ (mesenchymal) and $D492M^{miR\text{-}200c\text{-}141}$ (epithelial) were treated with 16 μM of the PTP1B inhibitor or DMSO as control for 24 h and assayed for sensitivity to trypsinization. (Figure 6 in article #3)

We also treated $D492M^{miR\text{-}203a}$ cells with the PTP1B inhibitor and interestingly the cells were more sensitive to PTP1B inhibition than $D492M^{Empty}$ cells. This could be because $D492M^{miR\text{-}203a}$ cells only show a partial reversion towards the epithelial phenotype, which is not enough to increase resistance to PTP1B inhibition and possibly miR-203a overexpression makes the D492M cells more sensitive to induction of cell death by PTP1B inhibition.

Collectively, we showed that PTP1B has a role in cell adhesion and anoikis. We also hypothesized that PTP1B inhibition could have a therapeutic role in a subset of breast cancers, enriched in cells with an EMT phenotype.

4.4 Unpublished data.

In addition to the published data and manuscript in submission I have substantial unpublished data I would like discuss in this chapter. As mentioned earlier miRNA expression analysis was conducted on D492 and D492M cultured in both monolayer and 3Dr-BM. D492 form branching TDLU-like structures over 21 days in culture, whereas D492M form colonies of spindle-shaped cells, which do not change in morphology during the culture period. Therefore, RNA was only collected on day 14 from D492M but from three time points in D492, from day 7 (pre-branching), day 14 (branching) and day 21 (late branching) (Figure 27).

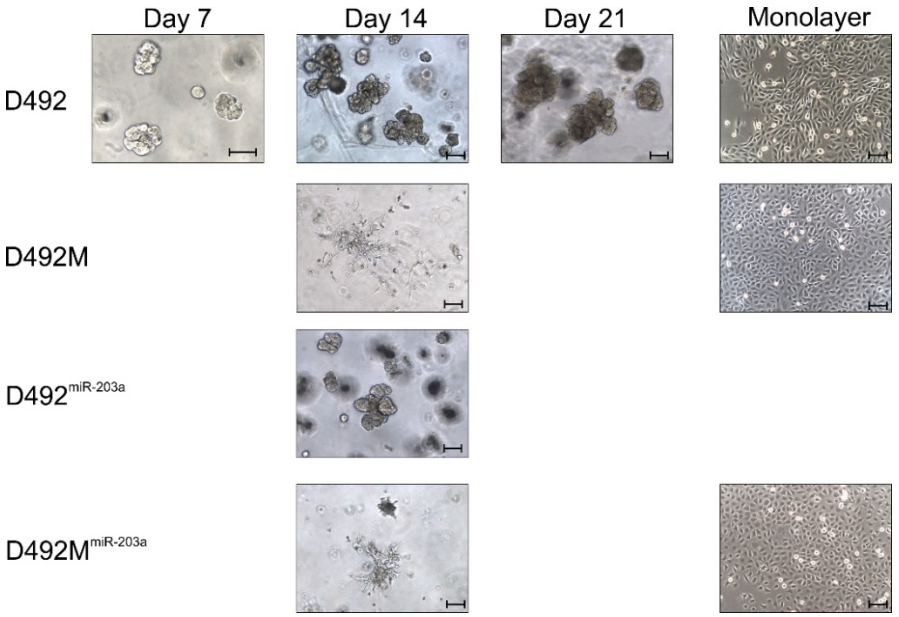

Figure 27. Experimental setup of mRNA-sequencing.

RNA-sequencing was performed on D492 from 3D-rBM culture at three time points (day 7, 14 and 21) and 2D culture. RNA-sequencing was performed on D492M, $D492^{miR\text{-}203a}$ and $D492M^{miR\text{-}203a}$ from day 14 in 3D-rBM culture and 2D culture. All samples were mRNA-sequenced in triplicates.

I performed mRNA sequencing and small-RNA sequencing of D492 and D492M in addition to $D492^{miR\text{-}203a}$ and $D492M^{miR\text{-}203a}$ cultivated in both monolayer and 3D-rBM cultures (Figure 27). As was mentioned above it has been well documented that gene expression differs between 2D and 3DrBM culture (Yu, Lin et al. 2012, Zschenker, Streichert et al. 2012) and see below. I was therefore expecting to see great differences in miRNA expression between 2D and 3D in D492 and D492M. It was, however, surprising to see how similar the miRNA expression pattern was between monolayer and 3D cultures (Figure 12). The small-RNA sequencing on cells from monolayer correlated very well with the microarray analysis conducted in article #1. In addition to miR200c-141, other miRNAs did show dramatic down regulation in D492M including miR-203a and miR-205, which are well known miRNAs that have been under the spotlight as being important regulators of cellular fate decision and epithelial differentiation (Greene, Herschkowitz et al. 2010, Moes, Le Bechec et al. 2012, DeCastro, Dunphy et al. 2013, Ding, Park et al. 2013, Taube, Malouf et al. 2013). Table 1 summarizes miRNAs that were overexpressed in D492 or D492M and are discussed in this thesis. Overexpression of many of these miRNAs in D492M did not result in any phenotypic changes.

Table 1. Summary of cell lines, which I generated during my project and are discussed in this thesis.

miRNA	Cell line	Changes in cellular Phenotype
miR-200c-141	D492	Inhibition of endothelial induced EMT
miR-200c-141	D492M	Reversion to luminal epithelial phenotype
miR-203a	D492M+miR-203a	Partial changes towards an epithelial phenotype
miR-203a	D492+miR-203a	No observed changes
miRZip-203a	D492+miRZip-203	No observed changes
miR-205	D492M+miR-205	Mild changes in phenotype
miR-584	D492M+miR-584	No observed changes
miR-1908	D492+miR-1908	No observed changes

4.4.1 Overexpression and knockdown studies.

MiR-200c, miR-141, miR-203a, miR-205 and miR-584A were among the most downregulated miRNAs in D492 in both datasets (microarray and NGS). MiR-200c and miR-141 formed the basis for article #1 and miR-203a formed the basis of article #2. Overexpression of miR-584 and miR-205, in D492M, did not induce changes to the same extent as miR-200c-141 and miR-203a.

4.4.2 Analysis of miR-584 expression

MiR-584 was one of the most downregulated miRNAs in D492M, compared to D492, and little was known about its function in the breast gland, so I decided to investigate it further. First, I did breast cancer survival analysis using the Molecular Therapeutics for Cancer, Ireland (MTCI) database, which is based on an algorithm developed to identify subsets of genes/miRNAs associated with disease progression in breast cancer and its subtypes. MiR-584 expression was associated with better prognosis in lymph node negative patients and patients with luminal B subtype of breast cancer. In contrast, miR-584 expression was associated with poorer prognosis in lymph node positive patients. Next, I performed functional analysis of miR-584 in D492M. First, the downregulation of miR-584 in D492M was confirmed by RT-qPCR. Interestingly, miR-584 expression was also down-regulated in D492 3D cultures boosted with EGM5 and in D492 cells grown in 2D EGM5 or H14+5%FBS compared to D492 grown in H14. As is mentioned in the technical considerations chapter of this thesis, D492 cells boosted with EGM5 in 3D or grown in EGM5 or H14+5%FBS in 2D, have a mesenchymal phenotype. In D492/D492M miR-584 expression therefore seemed to be associated with the epithelial phenotype. Next, I checked for miR-584

expression within the epithelial cell compartment of breast tissue and checked for expression in primary luminal- and myoepithelial cells (LEP and MEP). MiR-584 was expressed in LEPs and MEPs but to a higher extent in LEPs. A logical next step in my analysis was to overexpress miR-584 in D492M. The D492M$^{miR-584}$ cell line was characterized with respect to epithelial and mesenchymal properties along with performing functional assays. D492M$^{miR-584}$ cells did not show any changes in morphology and maintained a mesenchymal phenotype, both in 2D and 3D culture. In Western blot analysis D492M$^{miR-584}$ maintained mesenchymal marker expression and did not show increase in tested epithelial markers, except for a slight increase in K19. No changes in proliferation rate, migration in a wound healing assay or changes in resistance to camptothecin induced apoptosis were detected. This was in contrast to a study describing miR-584 function in breast cancer cells lines, where miR-584 inhibited breast cancer cell migration through regulation of its target, protein phosphatase and actin regulator 1 PHACTR1 (Fils-Aime, Dai et al. 2013). This may be explained by the fact that PHACTR1 is not highly expressed in D492 and D492M and therefore not relevant for my study. In conclusion, miR-584 overexpression in D492M had little or no impact on the mesenchymal properties of D492M.

4.4.3 Analysis of miR-205 expression

Another downregulated miRNA in D492M, miR-205, which was the highest expressed miRNA in D492, was chosen for further analysis. MTCI breast cancer survival analysis of miR-205 revealed that miR-205 expression was associated with better prognosis in breast cancer as a whole. Overexpression of miR-205 in D492M resulted in 340-fold overexpression compared to D492M^{Empty}. Even though the overexpression of miR-205 in D492M was high, it did not reach the miR-205 levels in D492, in fact the miR-205 expression in D492M$^{miR-205}$ was only 1/3 of the expression in D492. D492M$^{miR-205}$ cells maintained a mesenchymal morphology, both in 2D and 3D culture. Western blot analysis of D492M$^{miR-205}$ compared to D492M^{Empty} revealed a slight induction of the epithelial markers E-cadherin, K14 and K19 and a slight decrease in N-cadherin. The expression of the EMT transcription factors ZEB1 and ZEB2, which are both validated targets of miR-205, was reduced in D492M$^{miR-205}$ determined by RT-qPCR. D492M$^{miR-205}$ cells showed increased migration in a wound healing assay and increased sensitivity to camptothecin induced apoptosis. The D492M$^{miR-205}$ cell line showed more phenotypic changes than D492M$^{miR-584}$, but did not show as drastic changes as we saw in D492M$^{miR-200c-141}$. At this point in my PhD project, I had concerns that the changes I saw in D492M$^{miR-205}$ were not convincing enough

and since there were already publications on the role of miR-205 in EMT, I decided to pursue another miRNA, which in contrast to miR-584 and miR-205 was upregulated in D492M.

4.4.4 Analysis of miR-1908 expression

In contrast to what I had done previously, I decided to overexpress a D492M upregulated miRNA, i.e. miR-1908, in D492. MTCI breast cancer survival analysis of miR-1908 associated high expression of miR-1908 with worse prognosis in breast cancer as a whole, in lymph node positive breast cancer and the basal subtype. $D492^{miR\text{-}1908}$ had ~20-fold overexpression of miR-1908 compared to $D492^{Empty}$. $D492^{miR\text{-}1908}$ maintained epithelial morphology in 2D culture and formed branching colonies in 3D-rBM culture. There was no change in proliferation rate of $D492^{miR\text{-}1908}$ compared to $D492^{Empty}$. RT-qPCR analysis revealed a slight downregulation of N-cadherin and approximately 40% downregulation of apolipoprotein E (APOE), a validated target of miR-1908, but no change in E-cadherin expression or the validated miR-1908 target genes TGFβ1, DnaJ heat shock protein family (Hsp40) member A4 (DNAJA4) and MAM domain containing glycosylphosphatidylinositol anchor 1 (MDGA1). There was no change in expression of E-cadherin and K14 in Western blot analysis.

4.4.5 Knock down of miR-203a in D492

Overexpression of miR-203a in D492M showed promising results and formed the basis for article #2, but some parts of the miR-203a project were problematic, such as silencing of miR-203a in D492. To assess the functional effects of knocking down miR-203a in D492, I used a permanent miRNA interference approach (miRZip). This method is based on asymmetric hairpins optimized for anti-sense miRNA production, where miRZip anti-sense miRNAs suppress specific endogenous miRNAs. Characterization of the cell line $D492^{miRZip\text{-}203}$ by Western blot analysis for E-cadherin, N-cadherin, K14, K19, ΔNp63 and EGFR revealed no changes in expression of these markers. This could be because D492 has very high endogenous expression of miR-203a, which may explain the ineffective knock-down of using this method, which was only 25% reduction of miR-203a measured by qPCR).

In conclusion, there were little effects from overexpressing miR-584, miR-205 and miR-1908 in D492 and D492M and no effects of silencing miR-203a in D492 with a miRZip method.

4.4.6 Transcriptome profiling of D492 cells grown in 2D and 3D culture.

Three-dimensional cultures have advantages over 2D cultures in providing more physiologically relevant data and bear a better resemblance to *in vivo* like conditions. In 3D cultures, cells are surrounded by extracellular matrix that put physical constrains on cells and affects spatial organization of cell surface receptors. This can influence signal transduction and impacts gene expression of cells grown in 3D leading to differences in cellular responses and behavior (Edmondson, Broglie et al. 2014).

I set out to investigate gene expression differences in D492 grown in 2D and 3DrBM cultures. There were 146 differentially expressed genes (qval < 0.05), 111 genes were upregulated and 35 genes were downregulated in 3D-rBM. KEGG pathway analysis of the up-regulated genes in 3D, revealed extracellular matrix receptor interaction as the top hit. Gene ontology enrichment analysis revealed enrichment in biological processes relating to development, cell differentiation, adhesion, keratinization and cell junction organization. This is in concordance with previous reports comparing epithelial cells grown in 3D-rBM and 2D, where extracellular matrix and cell-to-cell interactions are enriched in 3DrBM culture (Bissell, Weaver et al. 1999, Vidi, Bissell et al. 2013).

Gene expression analysis was also performed on D492M grown in 2D and 3D-rBM cultures. There were many more differentially expressed genes between 2D and 3D-rBM for the mesenchymal cell line, 6791 transcripts were up-regulated in 3DrBM and 3368 transcripts were down-regulated (qval < 0.05). When performing KEGG pathway analysis for the top 150 up-regulated genes in 3D-rBM of D492M the top hit was cell cycle, containing the following 5 genes, CCND1, ATR, ANAPC1, PLK1 and BUB1. Interestingly, four of these genes have GO molecular function classification “protein serine/threonine kinase activity”. An interesting candidate for further investigation is MET proto-oncogene (hepatocyte growth factor receptor), which belongs to the focal adhesion, pathways in cancer and melanoma KEGG gene sets, which is up-regulated in D492M 3D-rBM compared to D492M 2D. Previously, our group reported that endothelial induced EMT in D492 was partially blocked by inhibition of HGF signaling (Sigurdsson, Hilmarsdottir et al. 2011) and it is worth studying if MET plays an important role in endothelial induced EMT of D492.

Collectively, I have substantial unpublished data and resources that have already been fed into other PhD projects at the laboratory. In addition, I have

started working on a manuscript that takes all this together (experiments from Figure 27). Using the EMT model (D492/D492M) as presented in this thesis and exploring the differentiation pattern in 3D and linking transcriptomic data and microRNA profiles together is interesting and published.

5 Technical considerations and retrospective view on experimental design

A PhD study in experimental life sciences requires acquisition of theoretical and technical skills. In my project, some methods and protocols were fairly well established when I started. Others needed to be improved and in some cases changed drastically. In this chapter, I will discuss my experimental approach and obstacles that I met during my study. I also want to use this chapter, to be self-critical regarding my theoretical and technical background and discuss things I could have done differently. In addition to my experimental studies, I have enhanced my skills in the field of bioinformatics, which I will elaborate on later in this chapter.

5.1 Cell culture approaches

In vitro culture of cells is in a way an artifact because cells are removed from their natural context in the body and exposed to hostile environments, such as plastic surfaces in cell culture flasks, serum rich culture media etc. that can have drastic effects on their gene expression and phenotype. In the introduction chapter, I touched on the pros and cons of *in vivo* and *in vitro* models. In this chapter, I will elaborate on my *in vitro* cell culture approaches and discuss some of the obstacles I had to overcome. I used both two-dimensional (2D, cells cultured in monolayer on plastic) and three-dimensional (3D, cells embedded into extracellular matrix) cultures. Culturing cells in 2D and 3D environments requires different experimental setups and in particular 3D cultures need advanced expertise before designing a study. This is because in 3D cultures, one tries to recapitulate the phenotypic traits of an *in vivo* condition.

In my PhD project, I focused on the D492 breast epithelial progenitor cell line and its mesenchymal derivative D492M. D492M was generated from 3D co-culture of D492 and breast endothelial cells (BRENCs) in growth factor reduced reconstituted basement membrane matrix (rBM) (Figure 28) (Sigurdsson, Hilmarsdottir et al. 2011, Ingthorsson, Briem et al. 2016).

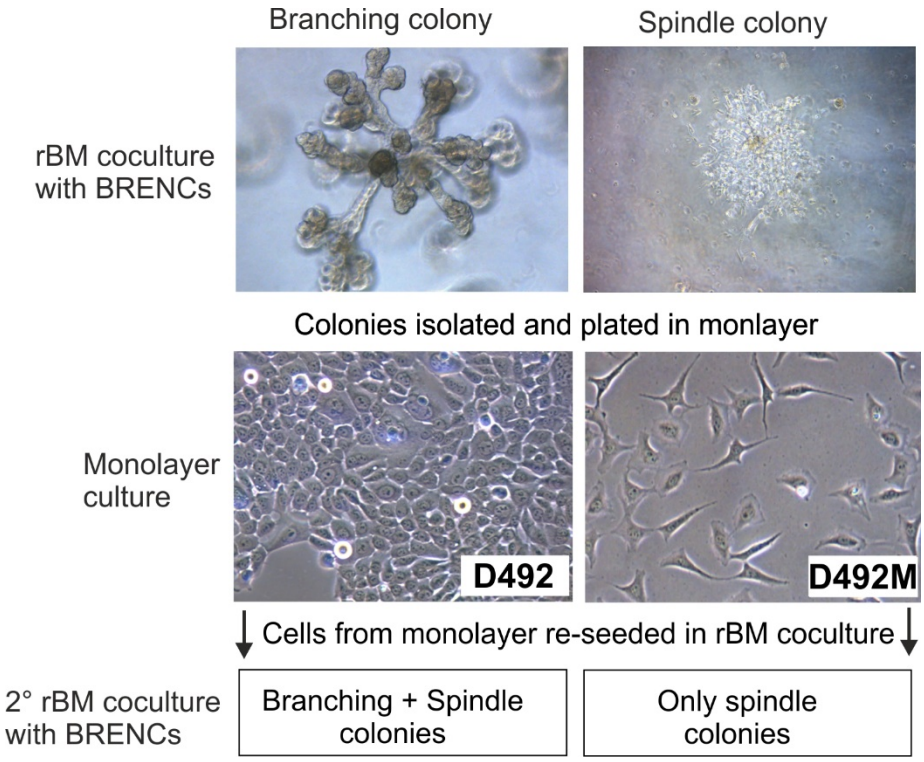

Figure 28. Establishment of the D492M cell line.

Upper panel, 1° coculture of D492 and BRENCs in 3D-rBM. D492 form both branching and spindle colonies in coculture with BRENCs. Branching and spindle colonies were isolated from rBM and plated separately in monolayer cultures (lower panel). Cells from a mesenchymal colony were renamed D492M (mesenchymal). D492, left and D492M, right. D492 and D492M were then re-seeded into 3D-rBM 2° coculture with BRENCs. Coculture derived from branching colonies (D492) formed both branching and spindle colonies, but cells derived from spindle colonies (D492M) (right) formed only spindle colonies. *Adapted from* (Sigurdsson, Hilmarsdottir et al. 2011).

When culturing cells in 3D-rBM, cell numbers (for each cell line) need to be optimized (Lee, Kenny et al. 2007). Number of cells per milliliter of rBM depends on experimental aims and growth properties of each cell line. When D492 is cultured alone in 3D-rBM a minimum of 10.000 cells per 300 µL of rBM (24-well plate) are needed for a viable culture. To achieve maximal branching morphogenesis for D492 cells, seeded cells must be within the range of 10.000 - 20.000 cells per 300 µL of rBM. Seeding too many cells can result in fusion of colonies or steric hindrance from adjacent colonies that reduces the ability of D492 to form single cell derived branching structures (Figure 29) (Bergthorsson, Magnusson et al. 2013).

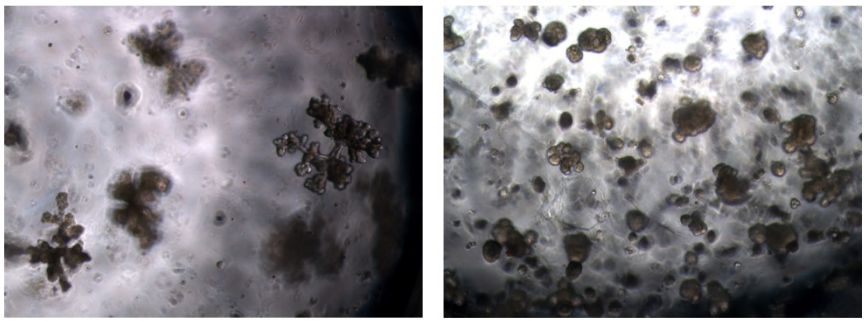

Figure 29. Seeding density of D492 affects colony formation and branching morphogenesis in 3D-rBM culture.

Left, optimal D492 cell density. Note, how branching colonies are formed from single cells. Right, increased D492 cell density. Note, lack of branching colony formation due to steric hindrance from adjacent colonies and in some cases fusion of colonies.

During the initial phase of my PhD project, one of the obstacles I had to overcome was to optimize 3D-rBM cell culture conditions. Unfortunately, I got mixed results on how many cells were needed per milliliter of rBM. After thorough investigation into what was causing these variations, I learned that it was necessary to titrate cell density for each rBM lot number and to use lot numbers with similar protein concentrations. This is because of variability inherent to biological materials such as rBM, which is extracted from Engelbreth-Holm-Swarm mouse sarcoma, a tumor rich in extracellular matrix proteins. Interestingly, in co-culture of breast epithelial cells and BRENCs, it was possible to seed much fewer epithelial cells (down to single cells), than if the epithelial cells were cultured alone. This is because when BRENCs are embedded into rBM they are non-proliferative, but viable, and act as feeder cells that induce growth and proliferation of epithelial cells (Ingthorsson, Sigurdsson et al. 2010, Sigurdsson, Hilmarsdottir et al. 2011). Co-cultures of BRENCs and D492 were setup in EGM5 medium that is rich in growth factors; such as FGF, EGF and VEGF and contains 5% serum; and is the recommended medium for endothelial cells (Sigurdsson, Fridriksdottir et al. 2006). D492 cells are commonly cultured in H14, a serum free medium, containing DMEM/F12, estrogen, insulin, hydrocortisone, transferrin, EGF, selenium and prolactin (Blaschke, Howlett et al. 1994). However, it is important to note that endothelial cells do not survive in H14 medium due to their needs for serum or serum supplements in the media and therefore EGM5 was used for all co-culture studies. Previous experiments had shown that if D492 cells were cultured alone in 3D-rBM and boosted with EGM5 overnight, fewer D492 cells were needed per milliliter of rBM to get branching

structures. To my surprise, when culturing D492 and boosting them for 24 hours with EGM5, most colonies adopted a mesenchymal phenotype (not seen before), and only a small number of colonies had an epithelial or branching phenotype (Figure 30 a).

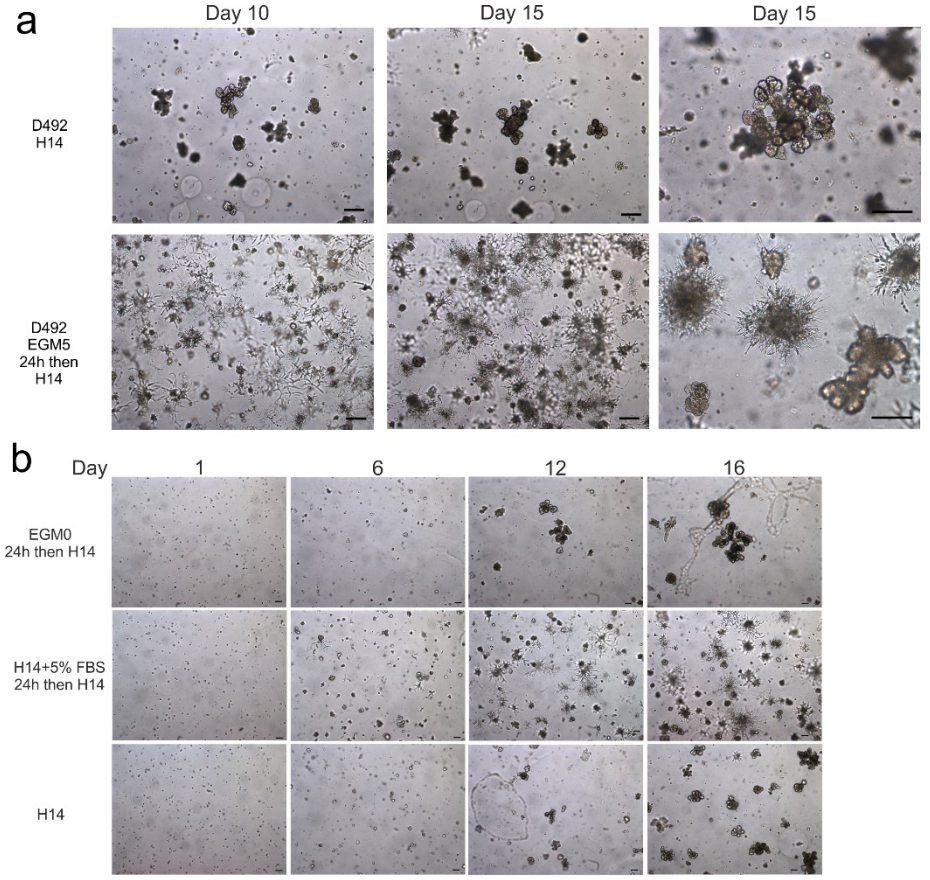

Figure 30. Effects of different culture media on D492 cells in 3D-rBM culture.

a) D492 cells cultured in 3D-rBM in H14 (top row) and boosted with EGM5 for 24 hours and then H14 for the rest of the culture period (bottom row). Colonies in the top row have a branching epithelial phenotype, while colonies from EGM5 boosted cultures in the bottom row acquire branching and mesenchymal phenotypes. b) D492 cells boosted with EGM0 for 24 hours then H14 (top row), D492 cells boosted with H14+5% FBS for 24 hours then H14 (middle row) and D492 cells only cultured in H14 (bottom row). The spindle like phenotype was only seen in cultures boosted with media containing serum (middle row). Scale bar = 100 µm

This was unexpected, as the conclusion from earlier studies was that endothelial cells were the dominant factor in inducing EMT in D492, not the EGM5. A possible explanation for this was that EGM5 medium is rich in growth factors (EGF, FGF and VEGF) and serum, which are known inducers of EMT (Moustakas and Heldin 2007, Lamouille, Xu et al. 2014). To follow up on this observation, I cultivated D492 in either EGM5 or H14, in both 3D-rBM and 2D, and tested for expression of epithelial and mesenchymal markers. D492 cultured in EGM5 media in 2D showed downregulation of epithelial markers, but little change in mesenchymal markers. I speculated that the growth factors and/or serum in EGM5 might be causing partial EMT in D492, and therefore I decided to culture D492 in H14+5% FBS to see if the serum was inducing EMT. D492 cells grown in H14+5% FBS showed reduced staining for E-cadherin, but not to the same extent as D492 cells cultured in EGM5. D492 cells cultured in EGM5 or H14+5% FBS had spindle-like morphology in 2D. In trying to tease out which factors in EGM5 and/or serum might be responsible for inducing EMT in D492, I treated D492 cells with TGF-β or VEGF to see if these factors were inducing EMT. The results showed no apparent changes in morphology or marker expression in D492 treated cells by either factor, except that D492 cells treated with TGF-β on day 0 in 3D-rBM culture did not branch or branched little in comparison with un-boosted D492 cells. This is in concordance with reports on the role of TGF-β as an inhibitor of ductal growth and branching (Silberstein and Daniel 1987, Ewan, Shyamala et al. 2002, Pavlovich, Boghaert et al. 2011). Finally, I cultured D492 in 3D-rBM and boosted them for 24 hours with EGM without serum (EGM0), H14+5% FBS or H14. D492 cells boosted with EGM0 and H14 formed branching colonies, while the H14+5% FBS boosted D492 cells formed mesenchymal colonies (Figure 30 b). Interestingly, cells boosted with EGM0 formed fewer but larger branching colonies. This led to the conclusion that the serum was inducing EMT in D492. To summarize, I got some unexpected results when learning 3D-rBM culture techniques. D492 cells grown in 3D-rBM treated with EGM5 underwent EMT, something not seen before. After comparing D492 cells grown in EGM5 and H14+5% FBS, I concluded that components in the serum were inducing EMT. Furthermore, D492 cells grown in 2D/EGM5 showed a stronger phenotypic switch than D492 cultured in 2D/H14+5% FBS, indicating additional effects of growth factors in the EGM medium.

Collectively, I spent 6-8 months on optimizing 3D-rBM cell culture conditions in my initial phase of the PhD project. At that time, this caused frustration and I thought this was wasted time and effort. However, in

retrospect, this time and difficulties taught me a valuable lesson in cell culture and the importance of designing cell culture experiments carefully. I definitely benefitted from this experience when I set out to investigate gene expression differences in D492 grown in 2D and 3D-rBM cultures.

5.2 Overexpression and knockdown studies.

In recent years micro RNAS (miRNAs) have been linked to many developmental processes and diseases such as cancer. One of the aims of my project was to analyze miRNAs that were differentially expressed between D492 and D492M in 3D-rBM cultures. Since the 3D-rBM culture experiments proved to be more cumbersome than expected, I decided to start performing functional analyses of candidate miRNAs from the microarray study, which formed the basis for article #1. Among the most downregulated miRNAs in D492 compared to D492M in the microarray dataset were miR-200c and miR-141, which Bylgja Hilmarsdottir a previous PhD student at the laboratory had been working on. Other downregulated miRNAs in D492 included miR-203a, miR-205 and miR-584. I decided to investigate miR-203a, miR-205 and miR-584 further in my project. Although data from miR-584 overexpression experiments in D492M were negative, I find it important to discuss this data, as it paved the way for subsequent studies. During this time of my project, I optimized and became skilled in methods used to investigate miRNAs.

In retrospect, it might have been a better approach to do a fast screening process by transiently transfecting interesting miRNAs and test for epithelial/mesenchymal markers in D492 and D492M. Larger numbers of miRNAs could have been tested and less effort spent on making stable cell lines. MiRNAs showing promising results could then have been chosen to make stable cell lines for further characterization. RNA-sequencing of these cell lines could then have been performed and interesting genes or pathways, not necessarily related to EMT/MET, could have been investigated further. On a positive note, the stable cell lines I generated during my project are now available to other researchers in the lab.

For knockdown studies, it might have been better to do transient knockdown with miRNA inhibitors to screen for effects or/and do a CRISPR/Cas9 knockout or repression with dCas9 of specific miRNAs. The CRISPR/Cas9 technology was being implemented in the laboratory in 2014 with many problems in the beginning. It is now well established in the laboratory and I assume that I would have used this technology if I were doing these experiments today.

5.3 Expression studies and data mining.

In my project, I have mainly been working with isogenic cell lines and analyzing phenotypic changes after extrinsic or intrinsic insults. When I started the project, I received miRNA array data from Bylgja Hilmarsdottir, a previous PhD student at the laboratory. This data formed the basis for article #1. The miRNAs in article #1 were isolated from monolayer culture. In article #2, I repeated the miRNA expression study but now in 3D-rBM culture and used NGS instead of microarrays. The reason I did this, is because 3D-rBM cultures are closer to *in vivo* conditions than monolayer (Gudjonsson, Ronnov-Jessen et al. 2003, Kenny, Lee et al. 2007, Antoni, Burckel et al. 2015). When I started my PhD studies, I already had extensive experience in making NGS libraries through my previous work at Roche NimbleGen and the Feinberg laboratory at Johns Hopkins. I was experienced in running samples on sequencers and had mastered the workflow all the way to data analysis. However, I was lacking experience and expertise in conducting bioinformatics analysis of NGS data. I went to Heidelberg in Germany and completed the EMBL introductory course: “Statistical Bioinformatics using R and Bioconductor”. This course was focused on NGS data analysis and was a good first step towards analyzing transcriptional datasets. Following the course, I learned how to use Kallisto for quantifying abundances of transcripts from RNA-seq data (Bray, Pimentel et al. 2016) and Sleuth for differential expression analysis (Pimentel, Bray et al. 2016). Here, I got supervision from one of the developers of the programs Pall Melsted, Assistant Professor in the Faculty of Industrial Engineering, Mechanical Engineering and Computer Science, University of Iceland. For miRNA sequencing analysis, I used the CLC Genomics Workbench (Qiagen, Aarhus Denmark) with assistance from our collaborators Maria Perander and Erik Knutsen (University of Tromso, Norway). The knowledge I have acquired during my PhD studies, has allowed me to capture the full NGS-workflow, from cell culture to analyzed transcriptomic datasets.

5.4 2D vs 3D-rBM cultures, primary cultures vs. cell lines.

Cell cultures are important and necessary tools in biomedical sciences. Cultures of human cells bridge the gap between *in vivo* studies in animals and studies in humans. However, it is important to think about the context of cells in the body and that they are the building blocks of structures that form the basis of functions of tissues and organs. When cells are removed from a tissue and cultured under favorable artificial conditions, they are called primary cells and usually have limited lifespans. Therefore, researchers have

developed various methods to immortalize primary cells (see below). The majority of cell cultures are conducted in monolayer on a plastic surface. This has been highly useful in a number of studies, but has certain drawbacks in studies focusing on tissue morphogenesis. It is important to think about cells, in particular epithelial cells in 3D context and how these cells interact with the surrounding microenvironment, often referred to as stroma. It is well documented that stroma can have instructive and dominant effects on epithelial plasticity (Ronnov-Jessen, Petersen et al. 1996, Shekhar, Pauley et al. 2003, Parmar and Cunha 2004, Ronnov-Jessen and Bissell 2009, Ingthorsson, Sigurdsson et al. 2010). Therefore, it is important to realize that when culturing cells, we are taking cells out of context, which may have drastic effects on gene expression and phenotype resulting in artifacts that have no or little correlation with *in vivo* conditions (Vidi, Bissell et al. 2013). Although not perfect, 3D cultures allow for structural morphogenesis so cells can capture to some extent *in-vivo*-like phenotypes. In general, this was clear from the start of my study. However, it has taken time and effort to realize how much structural context matters.

In my study, I have almost exclusively been working with the D492 progenitor cell line and its derivative D492M along with isogenic sublines overexpressing genes of interest. This model has been used in the laboratory for a number of years and is very useful when studying breast morphogenesis, EMT and cancer progression. It is, however, important to mention that D492 was initially generated by transfecting primary breast epithelial cells with E6 and E7 oncogenes from human papilloma virus 16. The E6 and E7 proteins target the p53 and retinoblastoma pRB tumor suppressor proteins, respectively (Wazer, Liu et al. 1995). Although, they are not cancer cells these cell lines cannot be considered completely normal. Another useful cell line for breast research is the HMLE cell line, which originates from a reduction mammoplasty, where human mammary epithelial cells (HMECs) were immortalized using introduction of Simian Virus 40 early region (SV40ER) and the catalytic subunit of human telomerase (hTERT) (Elenbaas, Spirio et al. 2001). The HMLE cell line has been used to study EMT and for generation of sublines with properties of stem cells and increased tumorigenicity (Mani, Guo et al. 2008, Taube, Herschkowitz et al. 2010). As with D492, it is important to mention that the HMLE cells are not considered completely normal as they have also been immortalized.

An alternative to working with immortalized cells is to use primary cells. Until now, one of the biggest problems in working with primary cells is the short lifespan of the cells that limits possibility of long-term studies. Recently,

methods have been established that allow for long-term expansion of breast primary cells using 3D-rBM cultures and breast cancer organoid medium, which helps in overcoming many of the issues that arise from working with immortalized cell lines (Sachs, de Ligt et al. 2018). Another alternative is to use human induced pluripotent stem cells (iPSCs) and differentiating them into mammary-like organoids (Qu, Han et al. 2017).

As mentioned above, immortalized cell lines have been very useful for studying developmental pathways and cancer progression but have limitations, as they cannot be considered normal due to their immortalization. Therefore, it is important to move our experiments more into primary cultures and possibly iPSCs models for future studies. These methods are currently being established at the laboratory and will pave the way for upcoming projects.

6 Concluding remarks

Branching morphogenesis is a developmental process seen across species wherever it is necessary to increase surface area due to some specific function. In the mammary gland (independent of mammalian species) branching epithelial morphogenesis is necessary to increase the size of the glandular tree to prepare for lactation. The branching morphogenesis occurs during each menstruation cycle and if fertilization fails, drop in estrogen and progesterone production results in menstruation in the uterus and involution of the mammary epithelium. However, if pregnancy occurs sustained production of these hormones extends the branching morphogenesis of the mammary gland to reach the maximal size and differentiation during lactation. Understanding these developmental events is necessary to increase our knowledge about the origin and progression of breast cancer. In the human female breast gland, breast cancer often originates in the TDLUs resulting in abnormal histoarchitecture and changed phenotype of the epithelial cells. The core focus of my PhD project has been to understand the cellular and molecular mechanism behind branching morphogenesis in the human breast. The branching process requires cellular plasticity that allows cells to invade the surrounding stroma. In my project, I have applied the D492 breast epithelial stem cell line and its isogenic mesenchymal cell line D492M to explore the molecular mechanisms of branching morphogenesis and cellular plasticity including EMT and MET. I have applied 3D-rBM cultures that allow for generation of *in-vivo*-like structures. At the molecular level, I have focused on miRNAs in these processes.

My data demonstrate an important role of miRNAs in breast development, which may be valuable for further understanding of the complex molecular interactions that occur during these processes. Deregulation of miRNAs can change cell fate and increased knowledge of the mechanisms underlying transcriptional control of these ncRNAs is important to better understand normal development and cancer progression. I have analyzed changes in miRNA expression of D492 and D492M in monolayer and 3D-rBM cultures. Furthermore, I have designed and conducted systematic analysis of D492 during branching morphogenesis in 3D-rBM culture. In that regard, I have selected a culture period of 21 days, which is the period needed for maximal branching morphogenesis of D492 cells. By isolating small RNAs, mRNAs

and proteins from day 7, 14 and 21 in 3D-rBM culture, I was able to predict interactions between miRNAs, mRNAs and proteins during the branching period allowing me to identify novel miRNA targets. This was demonstrated in the case of miR-203a targeting *PXDN*. Because D492M forms uniformly one phenotype in 3D-rBM culture (spindle shaped, mesenchymal like colonies), I decided to select only one time-point for D492M, day 14. In comparison between D492 and D492M, I have discovered that the most downregulated miRNAs in D492M are associated with the epithelial phenotype. Furthermore, I have shown that many miRNAs are differentially expressed in a temporal manner during branching morphogenesis in 3D-rBM culture. I have analyzed the effects of overexpressing selected miRNAs from my expression data set in D492 and D492M and put these results in perspective with other cell lines, *in vivo* experiments, primary cell culture and breast cancer databases. I have studied miRNA expression in respect to different variables, such as different culturing conditions, time course analysis and phenotypes. I have focused on miRNAs that have been reported to be associated with epithelial integrity, suppressing stem cell properties and inducing luminal differentiation. Initially, we showed that miR-200c-141 preserved epithelial integrity in D492 by inhibiting endothelial-induced EMT. Furthermore, we demonstrated that overexpression of miR-200c-141 in D492M reverted the EMT phenotype through MET, albeit only to the luminal epithelial phenotype. To identify the missing myoepithelial factor, we decided to introduce P63 a well-known transcription factor for myoepithelial cells into D492M$^{miR\text{-}200c\text{-}141}$. This resulted in complete reversion to the original phenotype of D492. Collectively, we have shown that miR-200c-141 and P63 are necessary for fate decision of luminal- and myoepithelial cells, respectively. Furthermore, our unpublished data shows that D492M$^{miR\text{-}200c\text{-}141}$, colonize better than D492M in a metastatic assay, indicating that the MET process in D492M may facilitate metastasis. Based on these findings, one can speculate that miR-200c-141 can both work as a tumor suppressor and an oncogene, depending on the cellular context and tumor stage. In primary breast tumors, high expression of miR-200c-141 may inhibit cancer progression, but when EMT cells regain expression of miR-200c-141 it may promote metastasis by helping the cancer cells to colonize other tissues.

A large part of my work was devoted to studying another miRNA, namely miRNA-203a. Similar to miR-200c-141, expression of miR-203a is often downregulated in EMT. In addition, miR-203a like miR-200c-141, has been described as being a suppressor of stem cell properties and to promote luminal differentiation in breast tissue. In my studies, I analyzed if miR-203a

could induce MET in D492M. Unlike miR-200c-141, which was able to induce MET in these cells, miR-203a only partially reverted the phenotype, indicating that miR-203a is a weak inducer of MET at least in the D492/D492M model. In addition to analysis of EMT/MET profiling, I also focused on analyzing expression and the role of miR-203a in branching morphogenesis. Expression of miR-203a increased between time points in 3D-rBM culture, indicating that it may play a role in differentiation of the cells as they fully form the branching structures. MiR-203a has been described as a suppressor of stem cell properties. It is a known suppressor of the basal cell marker P63 and increased expression of miR-203a during differentiation may suppress P63 as the cells differentiate into luminal epithelial cells. Overexpressing miR-203a in D492M revealed new potential targets of miR-203a. Transcriptional analysis of D492M$^{miR\text{-}203a}$ revealed peroxidasin (*PXDN*) as a potential target of miR-203a. It was the most downregulated gene in D492M$^{miR\text{-}203a}$ both in monolayer and in 3D-rBM cultures and has three potential binding sites for miR-203a in its 3'-UTR, one conserved and two poorly conserved. Interestingly, *PXDN* expression is increased in mesenchymal derivatives of both D492 and HMLE, i.e. D492M and HMLEmes, respectively. The upregulation of *PXDN* is therefore not exclusive to D492M but also occurs after EMT in HMLE cells. PXDN is secreted to the extracellular matrix and plays a role in reinforcing collagen IV (COL4A1) in the basement membrane. Interestingly, COL4A1 is also downregulated in D492M$^{miR\text{-}203a}$ and has a potential binding site in its 3'-UTR for miR-203a. miR-203a could therefore be targeting two interacting components important for extracellular matrix modifications. Importantly, when studying breast cancer patient survival based on breast cancer subtypes, *PXDN* expression seems to be associated with worse prognosis in HER2 positive breast cancer. Therefore, PXDN may be a potential target for drug development in HER2 positive breast cancer and is an especially promising candidate since it is secreted to the extracellular matrix and is therefore more accessible for drug treatment.

Finally, we showed that inhibition of protein tyrosine phosphatase 1B (PTP1B) disrupts cell-cell adhesion and induces anoikis in breast epithelial cells. PTP1B has been described as either being a tumor suppressor or an oncogene in breast cancer. PTP1B is expressed in the normal breast gland, where the expression is highest in the myoepithelial cells and fibroblasts. PTP1B was highly expressed during branching morphogenesis of D492 in 3D-rBM culture. We showed that after D492 and HMLE cells had undergone EMT the cells were more sensitive to PTP1B inhibition, making PTP1B a

potential drug candidate in breast cancer involving the EMT phenotype. This is important because EMT is believed to play an important role in cancer progression and development of resistance to cancer treatment. We hypothesized that because of low expression of cell adhesion proteins in D492M cells they tolerate less interference of cell attachment complexes where PTP1B is involved.

6.1 Future perspective

Linking stem cells, branching morphogenesis and cellular plasticity together and applying cell culture models to understand these developmental processes are of importance not only regarding our understanding of normal development but also for better understanding of breast cancer origin and progression. The 3D-rBM culture models that I have established and applied in my studies are currently being used in other projects in the laboratory. I believe that 3D-rBM models of branching morphogenesis and EMT can be useful in future studies to identify novel molecular interactions between noncoding RNAs and proteins. All the expression data from my studies are available for further studies and this has already given rise to two other PhD projects that are currently ongoing in the laboratory. One project focuses on the functional role PXDN in breast morphogenesis and cancer. My initial analysis of RNA-sequencing and small RNA profiling identified a novel link between miR-203a and peroxidasin (*PXDN*), a gene that has been described in other organs to be involved in crosslinking collagen IV in the basement membrane. Its function has however not been well described in breast morphogenesis or breast cancer. We have found two other miRNAs that are downregulated in D492M, which have binding sites in the *PXDN* 3'-UTR, namely miR-23a and miR-29, which will be investigated further. The other project focuses on unraveling the functions of ncRNAs on chromosome 14q32. Our transcriptomic data shows that the maternally expressed ncRNAs including the lncRNA MEG3 and clusters of miRNAs on the imprinted locus at 14q32 chromosome region (DLK1-DIO3) are highly upregulated in D492M compared to the parental cell line, D492. Thus, the aim of that project is to elucidate the functional roles of the maternally expressed ncRNAs of the DLK1-DIO3 locus in branching morphogenesis and EMT.

Although the D492 model works well and is highly useful for studies of molecular and phenotypic changes, which occur during branching morphogenesis and EMT, it has several shortcomings. It is an *in vitro* model and in the long run the findings extracted from this model need to be verified using *in vivo* models or captured by primary cell cultures. An example of this

are the next steps in studying spatial and temporal expression of PXDN in the mammary gland, which include analyses of expression in virgin, early pregnant, late pregnant, lactating and involute mouse mammary glands. In addition, isolation of primary human breast epithelial cells from reduction mammoplasties using flow cytometry, and analysis of expression of PXDN in 3D culture organoid models, as well as in breast biopsies are important.

Collectively, during my PhD study I have gained valuable experience including technical and theoretical expertise to build up model systems and to apply them to answer developmental questions regarding branching morphogenesis and EMT. This model system can be applied to other epithelial cell lines and pathways important for branching morphogenesis and EMT can be elucidated. Proteins from the same time points for D492 and D492M both in 3D-rBM and 2D cultures, were extracted and analyzed on a reverse phase protein array, designed with focus on proteins relevant to cancer. Analysis of this dataset has recently begun and the aim is to correlate this dataset with the transcriptomic data. In addition to the transcriptomic data and the reverse protein array, we have access to mass spectrometry data from cell lysates and cell culture media of D492 and D492M from 2D cultures and the next step is to link this data with the transcriptomic and the reverse protein array data.

References

Aceto, N., N. Sausgruber, H. Brinkhaus, D. Gaidatzis, G. Martiny-Baron, G. Mazzarol, S. Confalonieri, M. Quarto, G. Hu, P. J. Balwierz, M. Pachkov, S. J. Elledge, E. van Nimwegen, M. B. Stadler and M. Bentires-Alj (2012). "Tyrosine phosphatase SHP2 promotes breast cancer progression and maintains tumor-initiating cells via activation of key transcription factors and a positive feedback signaling loop." Nat Med **18**(4): 529-537.

Antoni, D., H. Burckel, E. Josset and G. Noel (2015). "Three-dimensional cell culture: a breakthrough in vivo." Int J Mol Sci **16**(3): 5517-5527.

Arendt, L. M. and C. Kuperwasser (2015). "Form and function: how estrogen and progesterone regulate the mammary epithelial hierarchy." J Mammary Gland Biol Neoplasia **20**(1-2): 9-25.

Aryee, M. J., A. E. Jaffe, H. Corrada-Bravo, C. Ladd-Acosta, A. P. Feinberg, K. D. Hansen and R. A. Irizarry (2014). "Minfi: a flexible and comprehensive Bioconductor package for the analysis of Infinium DNA methylation microarrays." Bioinformatics **30**(10): 1363-1369.

Asselin-Labat, M. L., F. Vaillant, M. Shackleton, T. Bouras, G. J. Lindeman and J. E. Visvader (2008). "Delineating the epithelial hierarchy in the mouse mammary gland." Cold Spring Harb Symp Quant Biol **73**: 469-478.

Avril-Sassen, S., L. D. Goldstein, J. Stingl, C. Blenkiron, J. Le Quesne, I. Spiteri, K. Karagavriilidou, C. J. Watson, S. Tavare, E. A. Miska and C. Caldas (2009). "Characterisation of microRNA expression in post-natal mouse mammary gland development." BMC Genomics **10**: 548.

Bai, L. and L. R. Rohrschneider (2010). "s-SHIP promoter expression marks activated stem cells in developing mouse mammary tissue." Genes Dev **24**(17): 1882-1892.

Barker, N., S. Tan and H. Clevers (2013). "Lgr proteins in epithelial stem cell biology." Development **140**(12): 2484-2494.

Bentires-Alj, M. and B. G. Neel (2007). "Protein-tyrosine phosphatase 1B is required for HER2/Neu-induced breast cancer." Cancer Res **67**(6): 2420-2424.

Bergthorsson, J. T., M. K. Magnusson and T. Gudjonsson (2013). "Endothelial-rich microenvironment supports growth and branching morphogenesis of prostate epithelial cells." Prostate **73**(8): 884-896.

Bernstein, E., A. A. Caudy, S. M. Hammond and G. J. Hannon (2001). "Role for a bidentate ribonuclease in the initiation step of RNA interference." Nature **409**(6818): 363-366.

Bhatia, S., J. Monkman, A. K. L. Toh, S. H. Nagaraj and E. W. Thompson (2017). "Targeting epithelial-mesenchymal plasticity in cancer: clinical and preclinical advances in therapy and monitoring." Biochem J **474**(19): 3269-3306.

Bissell, M. J., D. C. Radisky, A. Rizki, V. M. Weaver and O. W. Petersen (2002). "The organizing principle: microenvironmental influences in the normal and malignant breast." Differentiation **70**(9-10): 537-546.

Bissell, M. J., V. M. Weaver, S. A. Lelievre, F. Wang, O. W. Petersen and K. L. Schmeichel (1999). "Tissue structure, nuclear organization, and gene expression in normal and malignant breast." Cancer Res **59**(7 Suppl): 1757-1763s; discussion 1763s-1764s.

Bjorge, J. D., A. Pang and D. J. Fujita (2000). "Identification of protein-tyrosine phosphatase 1B as the major tyrosine phosphatase activity capable of dephosphorylating and activating c-Src in several human breast cancer cell lines." J Biol Chem **275**(52): 41439-41446.

Blanpain, C. and E. Fuchs (2007). "p63: revving up epithelial stem-cell potential." Nat Cell Biol **9**(7): 731-733.

Blaschke, R. J., A. R. Howlett, P. Y. Desprez, O. W. Petersen and M. J. Bissell (1994). "Cell differentiation by extracellular matrix components." Methods Enzymol **245**: 535-556.

Bock, C., S. Reither, T. Mikeska, M. Paulsen, J. Walter and T. Lengauer (2005). "BiQ Analyzer: visualization and quality control for DNA methylation data from bisulfite sequencing." Bioinformatics **21**(21): 4067-4068.

Borowsky, A. D. (2011). "Choosing a mouse model: experimental biology in context--the utility and limitations of mouse models of breast cancer." Cold Spring Harb Perspect Biol **3**(9): a009670.

Brabletz, T., A. Jung, S. Spaderna, F. Hlubek and T. Kirchner (2005). "Opinion: migrating cancer stem cells - an integrated concept of malignant tumour progression." Nat Rev Cancer **5**(9): 744-749.

Bray, N. L., H. Pimentel, P. Melsted and L. Pachter (2016). "Near-optimal probabilistic RNA-seq quantification." Nature Biotechnology **34**(5): 525-527.

Briand, P., K. V. Nielsen, M. W. Madsen and O. W. Petersen (1996). "Trisomy 7p and malignant transformation of human breast epithelial cells following epidermal growth factor withdrawal." Cancer Res **56**(9): 2039-2044.

Briand, P., O. W. Petersen and B. Van Deurs (1987). "A new diploid nontumorigenic human breast epithelial cell line isolated and propagated in chemically defined medium." In Vitro Cell Dev Biol **23**(3): 181-188.

Brisken, C. and B. O'Malley (2010). "Hormone action in the mammary gland." Cold Spring Harb Perspect Biol **2**(12): a003178.

Bronner, M. E. (2012). "Formation and migration of neural crest cells in the vertebrate embryo." Histochem Cell Biol **138**(2): 179-186.

Candi, E., R. Cipollone, P. Rivetti di Val Cervo, S. Gonfloni, G. Melino and R. Knight (2008). "p63 in epithelial development." Cell Mol Life Sci **65**(20): 3126-3133.

Carroll, J. S., T. E. Hickey, G. A. Tarulli, M. Williams and W. D. Tilley (2017). "Deciphering the divergent roles of progestogens in breast cancer." Nat Rev Cancer **17**(1): 54-64.

Carthew, R. W. and E. J. Sontheimer (2009). "Origins and Mechanisms of miRNAs and siRNAs." Cell **136**(4): 642-655.

Chandramouly, G., P. C. Abad, D. W. Knowles and S. A. Lelievre (2007). "The control of tissue architecture over nuclear organization is crucial for epithelial cell fate." J Cell Sci **120**(Pt 9): 1596-1606.

Cheung, K. J., V. Padmanaban, V. Silvestri, K. Schipper, J. D. Cohen, A. N. Fairchild, M. A. Gorin, J. E. Verdone, K. J. Pienta, J. S. Bader and A. J. Ewald (2016). "Polyclonal breast cancer metastases arise from collective dissemination of keratin 14-expressing tumor cell clusters." Proc Natl Acad Sci U S A **113**(7): E854-863.

Colon, S. and G. Bhave (2016). "Proprotein Convertase Processing Enhances Peroxidasin Activity to Reinforce Collagen IV." J Biol Chem **291**(46): 24009-24016.

Colon, S., P. Page-McCaw and G. Bhave (2017). "Role of Hypohalous Acids in Basement Membrane Homeostasis." Antioxid Redox Signal **27**(12): 839-854.

Cunha, G. R., P. Young, K. Christov, R. Guzman, S. Nandi, F. Talamantes and G. Thordarson (1995). "Mammary phenotypic expression induced in epidermal cells by embryonic mammary mesenchyme." Acta Anat (Basel) **152**(3): 195-204.

Dangles, V., V. Lazar, P. Validire, S. Richon, M. Wertheimer, V. Laville, J. L. Janneau, M. Barrois, C. Bovin, T. Poynard, G. Vallancien and D. Bellet (2002). "Gene expression profiles of bladder cancers: evidence for a striking effect of in vitro cell models on gene patterns." Br J Cancer **86**(8): 1283-1289.

Davalos, V., C. Moutinho, A. Villanueva, R. Boque, P. Silva, F. Carneiro and M. Esteller (2012). "Dynamic epigenetic regulation of the microRNA-200 family mediates epithelial and mesenchymal transitions in human tumorigenesis." Oncogene **31**(16): 2062-2074.

Debnath, J. and J. S. Brugge (2005). "Modelling glandular epithelial cancers in three-dimensional cultures." Nat Rev Cancer **5**(9): 675-688.

DeCastro, A. J., K. A. Dunphy, J. Hutchinson, A. L. Balboni, P. Cherukuri, D. J. Jerry and J. DiRenzo (2013). "MiR203 mediates subversion of stem cell properties during mammary epithelial differentiation via repression of DeltaNP63alpha and promotes mesenchymal-to-epithelial transition." Cell Death Dis **4**: e514.

Dewar, R., O. Fadare, H. Gilmore and A. M. Gown (2011). "Best practices in diagnostic immunohistochemistry: myoepithelial markers in breast pathology." Arch Pathol Lab Med **135**(4): 422-429.

Di Franco, S., A. Turdo, A. Benfante, M. L. Colorito, M. Gaggianesi, T. Apuzzo, R. Kandimalla, A. Chinnici, D. Barcaroli, L. R. Mangiapane, G. Pistone, S. Vieni, E. Gulotta, F. Dieli, J. P. Medema, G. Stassi, V. De Laurenzi and M. Todaro (2016). "DeltaNp63 drives metastasis in breast cancer cells via PI3K/CD44v6 axis." Oncotarget **7**(34): 54157-54173.

Ding, X., S. I. Park, L. K. McCauley and C. Y. Wang (2013). "Signaling between transforming growth factor beta (TGF-beta) and transcription factor SNAI2 represses expression of microRNA miR-203 to promote epithelial-mesenchymal transition and tumor metastasis." J Biol Chem **288**(15): 10241-10253.

Dontu, G., W. M. Abdallah, J. M. Foley, K. W. Jackson, M. F. Clarke, M. J. Kawamura and M. S. Wicha (2003). "In vitro propagation and transcriptional profiling of human mammary stem/progenitor cells." Genes Dev **17**(10): 1253-1270.

Dontu, G. and T. A. Ince (2015). "Of mice and women: a comparative tissue biology perspective of breast stem cells and differentiation." J Mammary Gland Biol Neoplasia **20**(1-2): 51-62.

Duband, J. L., F. Monier, M. Delannet and D. Newgreen (1995). "Epithelium-mesenchyme transition during neural crest development." Acta Anat (Basel) **154**(1): 63-78.

Duss, S., H. Brinkhaus, A. Britschgi, E. Cabuy, D. M. Frey, D. J. Schaefer and M. Bentires-Alj (2014). "Mesenchymal precursor cells maintain the differentiation and proliferation potentials of breast epithelial cells." Breast Cancer Res **16**(3): R60.

Dykxhoorn, D. M., Y. Wu, H. Xie, F. Yu, A. Lal, F. Petrocca, D. Martinvalet, E. Song, B. Lim and J. Lieberman (2009). "miR-200 enhances mouse breast cancer cell colonization to form distant metastases." PLoS One **4**(9): e7181.

Edmondson, R., J. J. Broglie, A. F. Adcock and L. Yang (2014). "Three-dimensional cell culture systems and their applications in drug discovery and cell-based biosensors." Assay Drug Dev Technol **12**(4): 207-218.

Elchebly, M., P. Payette, E. Michaliszyn, W. Cromlish, S. Collins, A. L. Loy, D. Normandin, A. Cheng, J. Himms-Hagen, C. C. Chan, C. Ramachandran, M. J. Gresser, M. L. Tremblay and B. P. Kennedy (1999). "Increased insulin sensitivity and obesity resistance in mice lacking the protein tyrosine phosphatase-1B gene." Science **283**(5407): 1544-1548.

Elenbaas, B., L. Spirio, F. Koerner, M. D. Fleming, D. B. Zimonjic, J. L. Donaher, N. C. Popescu, W. C. Hahn and R. A. Weinberg (2001). "Human breast cancer cells generated by oncogenic transformation of primary mammary epithelial cells." Genes Dev **15**(1): 50-65.

Emerman, J. T. and D. R. Pitelka (1977). "Maintenance and induction of morphological differentiation in dissociated mammary epithelium on floating collagen membranes." In Vitro **13**(5): 316-328.

Ero-Tolliver, I. A., B. G. Hudson and G. Bhave (2015). "The Ancient Immunoglobulin Domains of Peroxidasin Are Required to Form Sulfilimine Cross-links in Collagen IV." J Biol Chem **290**(35): 21741-21748.

Ewan, K. B., G. Shyamala, S. A. Ravani, Y. Tang, R. Akhurst, L. Wakefield and M. H. Barcellos-Hoff (2002). "Latent transforming growth factor-beta activation in mammary gland: regulation by ovarian hormones affects ductal and alveolar proliferation." Am J Pathol **160**(6): 2081-2093.

Faulkin, L. J., Jr. and K. B. Deome (1960). "Regulation of growth and spacing of gland elements in the mammary fat pad of the C3H mouse." J Natl Cancer Inst **24**: 953-969.

Feng, X., Z. Wang, R. Fillmore and Y. Xi (2014). "MiR-200, a new star miRNA in human cancer." Cancer Lett **344**(2): 166-173.

Ferrer-Vaquer, A., M. Viotti and A. K. Hadjantonakis (2010). "Transitions between epithelial and mesenchymal states and the morphogenesis of the early mouse embryo." Cell Adh Migr **4**(3): 447-457.

Fils-Aime, N., M. Dai, J. Guo, M. El-Mousawi, B. Kahramangil, J. C. Neel and J. J. Lebrun (2013). "MicroRNA-584 and the protein phosphatase and actin regulator 1 (PHACTR1), a new signaling route through which transforming growth factor-beta Mediates the migration and actin dynamics of breast cancer cells." J Biol Chem **288**(17): 11807-11823.

Fischer, K. R., A. Durrans, S. Lee, J. Sheng, F. Li, S. T. Wong, H. Choi, T. El Rayes, S. Ryu, J. Troeger, R. F. Schwabe, L. T. Vahdat, N. K. Altorki, V. Mittal and D. Gao (2015). "Epithelial-to-mesenchymal transition is not required for lung metastasis but contributes to chemoresistance." Nature.

Fridriksdottir, A. J., J. Kim, R. Villadsen, M. C. Klitgaard, B. M. Hopkinson, O. W. Petersen and L. Ronnov-Jessen (2015). "Propagation of oestrogen receptor-positive and oestrogen-responsive normal human breast cells in culture." Nat Commun **6**: 8786.

Fridriksdottir, A. J., O. W. Petersen and L. Ronnov-Jessen (2011). "Mammary gland stem cells: current status and future challenges." Int J Dev Biol **55**(7-9): 719-729.

Fridriksdottir, A. J., R. Villadsen, M. Morsing, M. C. Klitgaard, J. Kim, O. W. Petersen and L. Ronnov-Jessen (2017). "Proof of region-specific multipotent progenitors in human breast epithelia." Proc Natl Acad Sci U S A **114**(47): E10102-e10111.

Friedman, R. C., K. K. Farh, C. B. Burge and D. P. Bartel (2009). "Most mammalian mRNAs are conserved targets of microRNAs." Genome Res **19**(1): 92-105.

Frisch, S. M. and H. Francis (1994). "Disruption of epithelial cell-matrix interactions induces apoptosis." J Cell Biol **124**(4): 619-626.

Gallego, M. I., N. Binart, G. W. Robinson, R. Okagaki, K. T. Coschigano, J. Perry, J. J. Kopchick, T. Oka, P. A. Kelly and L. Hennighausen (2001). "Prolactin, growth hormone, and epidermal growth factor activate Stat5 in different compartments of mammary tissue and exert different and overlapping developmental effects." Dev Biol **229**(1): 163-175.

Ghosh, S., G. C. Spagnoli, I. Martin, S. Ploegert, P. Demougin, M. Heberer and A. Reschner (2005). "Three-dimensional culture of melanoma cells profoundly affects gene expression profile: a high density oligonucleotide array study." J Cell Physiol **204**(2): 522-531.

Gilmore, A. P. (2005). "Anoikis." Cell Death Differ **12 Suppl 2**: 1473-1477.

Greene, S. B., J. I. Herschkowitz and J. M. Rosen (2010). "The ups and downs of miR-205: identifying the roles of miR-205 in mammary gland development and breast cancer." RNA Biol **7**(3): 300-304.

Gregory, P. A., A. G. Bert, E. L. Paterson, S. C. Barry, A. Tsykin, G. Farshid, M. A. Vadas, Y. Khew-Goodall and G. J. Goodall (2008). "The miR-200 family and miR-205 regulate epithelial to mesenchymal transition by targeting ZEB1 and SIP1." Nat Cell Biol **10**(5): 593-601.

Gross, N., J. Kropp and H. Khatib (2017). "MicroRNA Signaling in Embryo Development." Biology (Basel) **6**(3).

Gschwind, A., O. M. Fischer and A. Ullrich (2004). "The discovery of receptor tyrosine kinases: targets for cancer therapy." Nat Rev Cancer **4**(5): 361-370.

Gudjonsson, T., M. C. Adriance, M. D. Sternlicht, O. W. Petersen and M. J. Bissell (2005). "Myoepithelial cells: their origin and function in breast morphogenesis and neoplasia." J Mammary Gland Biol Neoplasia **10**(3): 261-272.

Gudjonsson, T., L. Ronnov-Jessen, R. Villadsen, M. J. Bissell and O. W. Petersen (2003). "To create the correct microenvironment: three-dimensional heterotypic collagen assays for human breast epithelial morphogenesis and neoplasia." Methods **30**(3): 247-255.

Gudjonsson, T., L. Ronnov-Jessen, R. Villadsen, F. Rank, M. J. Bissell and O. W. Petersen (2002). "Normal and tumor-derived myoepithelial cells differ in their ability to interact with luminal breast epithelial cells for polarity and basement membrane deposition." Journal of Cell Science **115**(1): 39-50.

Gudjonsson, T., R. Villadsen, H. L. Nielsen, L. Ronnov-Jessen, M. J. Bissell and O. W. Petersen (2002). "Isolation, immortalization, and characterization of a human breast epithelial cell line with stem cell properties." Genes Dev **16**(6): 693-706.

Guo, F., B. C. Parker Kerrigan, D. Yang, L. Hu, I. Shmulevich, A. K. Sood, F. Xue and W. Zhang (2014). "Post-transcriptional regulatory network of epithelial-to-mesenchymal and mesenchymal-to-epithelial transitions." J Hematol Oncol **7**: 19.

Ha, M. and V. N. Kim (2014). "Regulation of microRNA biogenesis." Nat Rev Mol Cell Biol **15**(8): 509-524.

Han, J., Y. Lee, K. H. Yeom, Y. K. Kim, H. Jin and V. N. Kim (2004). "The Drosha-DGCR8 complex in primary microRNA processing." Genes Dev **18**(24): 3016-3027.

Hansen, R. K. and M. J. Bissell (2000). "Tissue architecture and breast cancer: the role of extracellular matrix and steroid hormones." Endocr Relat Cancer **7**(2): 95-113.

Hilmarsdottir, B. (2016). Extrinsic and intrinsic regulation of breast epithelial plasticity and survival. Ph.D. Doctoral dissertation, University of Iceland.

Hopkinson, B. M., M. C. Klitgaard, O. W. Petersen, R. Villadsen, L. Ronnov-Jessen and J. Kim (2017). "Establishment of a normal-derived estrogen receptor-positive cell line comparable to the prevailing human breast cancer subtype." Oncotarget **8**(6): 10580-10593.

Howard, B. A. and B. A. Gusterson (2000). "Human breast development." J Mammary Gland Biol Neoplasia **5**(2): 119-137.

Huang, T., A. Alvarez, B. Hu and S. Y. Cheng (2013). "Noncoding RNAs in cancer and cancer stem cells." Chin J Cancer **32**(11): 582-593.

Ingthorsson, S., K. Andersen, B. Hilmarsdottir, G. M. Maelandsmo, M. K. Magnusson and T. Gudjonsson (2016). "HER2 induced EMT and tumorigenicity in breast epithelial progenitor cells is inhibited by coexpression of EGFR." Oncogene **35**(32): 4244-4255.

Ingthorsson, S., E. Briem, J. T. Bergthorsson and T. Gudjonsson (2016). "Epithelial Plasticity During Human Breast Morphogenesis and Cancer Progression." J Mammary Gland Biol Neoplasia **21**(3-4): 139-148.

Ingthorsson, S., B. Hilmarsdottir, J. Kricker, M. K. Magnusson and T. Gudjonsson (2015). "Context-Dependent Function of Myoepithelial Cells in Breast Morphogenesis and Neoplasia." Curr Mol Biol Rep **1**(4): 168-174.

Ingthorsson, S., V. Sigurdsson, A. Fridriksdottir, Jr., J. G. Jonasson, J. Kjartansson, M. K. Magnusson and T. Gudjonsson (2010). "Endothelial cells stimulate growth of normal and cancerous breast epithelial cells in 3D culture." BMC Res Notes **3**: 184.

Ingthorsson, S., V. Sigurdsson, A. J. Fridriksdottir, J. G. Jonasson, J. Kjartansson, M. K. Magnusson and T. Gudjonsson (2010). "Endothelial cells stimulate growth of normal and cancerous breast epithelial cells in 3D culture." BMC Res Notes **3**(1): 184.

Inman, J. L., C. Robertson, J. D. Mott and M. J. Bissell (2015). "Mammary gland development: cell fate specification, stem cells and the microenvironment." Development **142**(6): 1028-1042.

Jang, K., H. Ahn, J. Sim, H. Han, R. Abdul, S. S. Paik, M. S. Chung and S. J. Jang (2014). "Loss of microRNA-200a expression correlates with tumor progression in breast cancer." Transl Res **163**(3): 242-251.

Jin, T., H. Suk Kim, S. Ki Choi, E. Hye Hwang, J. Woo, H. Suk Ryu, K. Kim, A. Moon and W. Kyung Moon (2017). "microRNA-200c/141 upregulates SerpinB2 to promote breast cancer cell metastasis and reduce patient survival." Oncotarget **8**(20): 32769-32782.

Jordan, N. V., G. L. Johnson and A. N. Abell (2011). "Tracking the intermediate stages of epithelial-mesenchymal transition in epithelial stem cells and cancer." Cell Cycle **10**(17): 2865-2873.

Julien, S. G., N. Dube, M. Read, J. Penney, M. Paquet, Y. Han, B. P. Kennedy, W. J. Muller and M. L. Tremblay (2007). "Protein tyrosine phosphatase 1B deficiency or inhibition delays ErbB2-induced mammary tumorigenesis and protects from lung metastasis." Nat Genet **39**(3): 338-346.

Kal, A. J., A. J. van Zonneveld, V. Benes, M. van den Berg, M. G. Koerkamp, K. Albermann, N. Strack, J. M. Ruijter, A. Richter, B. Dujon, W. Ansorge and H. F. Tabak (1999). "Dynamics of gene expression revealed by comparison of serial analysis of gene expression transcript profiles from yeast grown on two different carbon sources." Mol Biol Cell **10**(6): 1859-1872.

Kalluri, R. and R. A. Weinberg (2009). "The basics of epithelial-mesenchymal transition." J Clin Invest **119**(6): 1420-1428.

Keller, P. J., L. M. Arendt, A. Skibinski, T. Logvinenko, I. Klebba, S. Dong, A. E. Smith, A. Prat, C. M. Perou, H. Gilmore, S. Schnitt, S. P. Naber, J. A. Garlick and C. Kuperwasser (2012). "Defining the cellular precursors to human breast cancer." Proc Natl Acad Sci U S A **109**(8): 2772-2777.

Kenny, P. A., G. Y. Lee, C. A. Myers, R. M. Neve, J. R. Semeiks, P. T. Spellman, K. Lorenz, E. H. Lee, M. H. Barcellos-Hoff, O. W. Petersen, J. W. Gray and M. J. Bissell (2007). "The morphologies of breast cancer cell lines in three-dimensional assays correlate with their profiles of gene expression." Mol Oncol **1**(1): 84-96.

Kimura, C., M. Hayashi, Y. Mizuno and M. Oike (2013). "Endothelium-dependent epithelial-mesenchymal transition of tumor cells: exclusive roles of transforming growth factor beta1 and beta2." Biochim Biophys Acta **1830**(10): 4470-4481.

Klaman, L. D., O. Boss, O. D. Peroni, J. K. Kim, J. L. Martino, J. M. Zabolotny, N. Moghal, M. Lubkin, Y. B. Kim, A. H. Sharpe, A. Stricker-Krongrad, G. I. Shulman, B. G. Neel and B. B. Kahn (2000). "Increased energy expenditure, decreased adiposity, and tissue-specific insulin sensitivity in protein-tyrosine phosphatase 1B-deficient mice." Mol Cell Biol **20**(15): 5479-5489.

Knezevic, J., A. D. Pfefferle, I. Petrovic, S. B. Greene, C. M. Perou and J. M. Rosen (2015). "Expression of miR-200c in claudin-low breast cancer alters stem cell functionality, enhances chemosensitivity and reduces metastatic potential." Oncogene **34**(49): 5997-6006.

Koo, T., B. J. Cho, D. H. Kim, J. M. Park, E. J. Choi, H. H. Kim, D. J. Lee and I. A. Kim (2017). "MicroRNA-200c increases radiosensitivity of human cancer cells with activated EGFR-associated signaling." Oncotarget **8**(39): 65457-65468.

Kordon, E. C. and G. H. Smith (1998). "An entire functional mammary gland may comprise the progeny from a single cell." Development **125**(10): 1921-1930.

Korpal, M., B. J. Ell, F. M. Buffa, T. Ibrahim, M. A. Blanco, T. Celia-Terrassa, L. Mercatali, Z. Khan, H. Goodarzi, Y. Hua, Y. Wei, G. Hu, B. A. Garcia, J. Ragoussis, D. Amadori, A. L. Harris and Y. Kang (2011). "Direct targeting of Sec23a by miR-200s influences cancer cell secretome and promotes metastatic colonization." Nat Med **17**(9): 1101-1108.

Korpal, M., E. S. Lee, G. Hu and Y. Kang (2008). "The miR-200 family inhibits epithelial-mesenchymal transition and cancer cell migration by direct targeting of E-cadherin transcriptional repressors ZEB1 and ZEB2." J Biol Chem **283**(22): 14910-14914.

Lamouille, S., J. Xu and R. Derynck (2014). "Molecular mechanisms of epithelial-mesenchymal transition." Nat Rev Mol Cell Biol **15**(3): 178-196.

Lantz, K. A., S. G. Hart, S. L. Planey, M. F. Roitman, I. A. Ruiz-White, H. R. Wolfe and M. P. McLane (2010). "Inhibition of PTP1B by trodusquemine (MSI-1436) causes fat-specific weight loss in diet-induced obese mice." Obesity (Silver Spring) **18**(8): 1516-1523.

Lapidus, R. G., S. J. Nass and N. E. Davidson (1998). "The loss of estrogen and progesterone receptor gene expression in human breast cancer." J Mammary Gland Biol Neoplasia **3**(1): 85-94.

Le, M. T., P. Hamar, C. Guo, E. Basar, R. Perdigao-Henriques, L. Balaj and J. Lieberman (2014). "miR-200-containing extracellular vesicles promote breast cancer cell metastasis." J Clin Invest **124**(12): 5109-5128.

Lee, G. Y., P. A. Kenny, E. H. Lee and M. J. Bissell (2007). "Three-dimensional culture models of normal and malignant breast epithelial cells." Nat Methods **4**(4): 359-365.

Lee, S., D. Medina, A. Tsimelzon, S. K. Mohsin, S. Mao, Y. Wu and D. C. Allred (2007). "Alterations of gene expression in the development of early hyperplastic precursors of breast cancer." Am J Pathol **171**(1): 252-262.

Lee, Y., C. Ahn, J. Han, H. Choi, J. Kim, J. Yim, J. Lee, P. Provost, O. Radmark, S. Kim and V. N. Kim (2003). "The nuclear RNase III Drosha initiates microRNA processing." Nature **425**(6956): 415-419.

Lelievre, S. A. (2010). "Tissue polarity-dependent control of mammary epithelial homeostasis and cancer development: an epigenetic perspective." J Mammary Gland Biol Neoplasia **15**(1): 49-63.

Lessard, L., M. Stuible and M. L. Tremblay (2010). "The two faces of PTP1B in cancer." Biochim Biophys Acta **1804**(3): 613-619.

Li, N., B. Long, W. Han, S. Yuan and K. Wang (2017). "microRNAs: important regulators of stem cells." Stem Cell Res Ther **8**(1): 110.

Liu, H., Y. Wu, S. Zhu, W. Liang, Z. Wang, Y. Wang, T. Lv, Y. Yao, D. Yuan and Y. Song (2015). "PTP1B promotes cell proliferation and metastasis through activating src and ERK1/2 in non-small cell lung cancer." Cancer Lett **359**(2): 218-225.

Lumachi, F., A. Brunello, M. Maruzzo, U. Basso and S. M. Basso (2013). "Treatment of estrogen receptor-positive breast cancer." Curr Med Chem **20**(5): 596-604.

Macias, H. and L. Hinck (2012). "Mammary gland development." Wiley Interdiscip Rev Dev Biol **1**(4): 533-557.

Madhavan, D., C. Peng, M. Wallwiener, M. Zucknick, J. Nees, S. Schott, A. Rudolph, S. Riethdorf, A. Trumpp, K. Pantel, C. Sohn, J. Chang-Claude, A. Schneeweiss and B. Burwinkel (2016). "Circulating miRNAs with prognostic value in metastatic breast cancer and for early detection of metastasis." Carcinogenesis **37**(5): 461-470.

Madhavan, D., M. Zucknick, M. Wallwiener, K. Cuk, C. Modugno, M. Scharpff, S. Schott, J. Heil, A. Turchinovich, R. Yang, A. Benner, S. Riethdorf, A. Trumpp, C. Sohn, K. Pantel, A. Schneeweiss and B. Burwinkel (2012). "Circulating miRNAs as surrogate markers for circulating tumor cells and prognostic markers in metastatic breast cancer." Clin Cancer Res **18**(21): 5972-5982.

Madsen, M. W., A. E. Lykkesfeldt, I. Laursen, K. V. Nielsen and P. Briand (1992). "Altered gene expression of c-myc, epidermal growth factor receptor, transforming growth factor-alpha, and c-erb-B2 in an immortalized human breast epithelial cell line, HMT-3522, is associated with decreased growth factor requirements." Cancer Res **52**(5): 1210-1217.

Mani, S. A., W. Guo, M. J. Liao, E. N. Eaton, A. Ayyanan, A. Y. Zhou, M. Brooks, F. Reinhard, C. C. Zhang, M. Shipitsin, L. L. Campbell, K. Polyak, C. Brisken, J. Yang and R. A. Weinberg (2008). "The epithelial-mesenchymal transition generates cells with properties of stem cells." Cell **133**(4): 704-715.

Miyoshi, K., T. Miyoshi and H. Siomi (2010). "Many ways to generate microRNA-like small RNAs: non-canonical pathways for microRNA production." Mol Genet Genomics **284**(2): 95-103.

Moes, M., A. Le Bechec, I. Crespo, C. Laurini, A. Halavatyi, G. Vetter, A. Del Sol and E. Friederich (2012). "A novel network integrating a miRNA-203/SNAI1 feedback loop which regulates epithelial to mesenchymal transition." PLoS One **7**(4): e35440.

Mongroo, P. S. and A. K. Rustgi (2010). "The role of the miR-200 family in epithelial-mesenchymal transition." Cancer Biol Ther **10**(3): 219-222.

Morel, A. P., M. Lievre, C. Thomas, G. Hinkal, S. Ansieau and A. Puisieux (2008). "Generation of breast cancer stem cells through epithelial-mesenchymal transition." PLoS One **3**(8): e2888.

Morsing, M., M. C. Klitgaard, A. Jafari, R. Villadsen, M. Kassem, O. W. Petersen and L. Ronnov-Jessen (2016). "Evidence of two distinct functionally specialized fibroblast lineages in breast stroma." Breast Cancer Res **18**(1): 108.

Moustakas, A. and C. H. Heldin (2007). "Signaling networks guiding epithelial-mesenchymal transitions during embryogenesis and cancer progression." Cancer Sci **98**(10): 1512-1520.

Moyret-Lalle, C., E. Ruiz and A. Puisieux (2014). "Epithelial-mesenchymal transition transcription factors and miRNAs: "Plastic surgeons" of breast cancer." World J Clin Oncol **5**(3): 311-322.

Nielsen, K. V. and P. Briand (1989). "Cytogenetic analysis of in vitro karyotype evolution in a cell line established from nonmalignant human mammary epithelium." Cancer Genet Cytogenet **39**(1): 103-118.

Nieto, M. A., R. Y. Huang, R. A. Jackson and J. P. Thiery (2016). "Emt: 2016." Cell **166**(1): 21-45.

Park, S. M., A. B. Gaur, E. Lengyel and M. E. Peter (2008). "The miR-200 family determines the epithelial phenotype of cancer cells by targeting the E-cadherin repressors ZEB1 and ZEB2." Genes Dev **22**(7): 894-907.

Parmar, H. and G. R. Cunha (2004). "Epithelial-stromal interactions in the mouse and human mammary gland in vivo." Endocr Relat Cancer **11**(3): 437-458.

Pavlovich, A. L., E. Boghaert and C. M. Nelson (2011). "Mammary branch initiation and extension are inhibited by separate pathways downstream of TGFbeta in culture." Exp Cell Res **317**(13): 1872-1884.

Pechoux, C., T. Gudjonsson, L. Ronnov-Jessen, M. J. Bissell and O. W. Petersen (1999). "Human mammary luminal epithelial cells contain progenitors to myoepithelial cells." Dev Biol **206**(1): 88-99.

Pecot, C. V., R. Rupaimoole, D. Yang, R. Akbani, C. Ivan, C. Lu, S. Wu, H. D. Han, M. Y. Shah, C. Rodriguez-Aguayo, J. Bottsford-Miller, Y. Liu, S. B. Kim, A. Unruh, V. Gonzalez-Villasana, L. Huang, B. Zand, M. Moreno-Smith, L. S. Mangala, M. Taylor, H. J. Dalton, V. Sehgal, Y. Wen, Y. Kang, K. A. Baggerly, J. S. Lee, P. T. Ram, M. K. Ravoori, V. Kundra, X. Zhang, R. Ali-Fehmi, A. M. Gonzalez-Angulo, P. P. Massion, G. A. Calin, G. Lopez-Berestein, W. Zhang and A. K. Sood (2013). "Tumour angiogenesis regulation by the miR-200 family." Nat Commun **4**: 2427.

Petersen, O. W., H. L. Nielsen, T. Gudjonsson, R. Villadsen, F. Rank, E. Niebuhr, M. J. Bissell and L. Ronnov-Jessen (2003). "Epithelial to mesenchymal transition in human breast cancer can provide a nonmalignant stroma." Am J Pathol **162**(2): 391-402.

Petersen, O. W. and K. Polyak (2010). "Stem cells in the human breast." Cold Spring Harb Perspect Biol **2**(5): a003160.

Petersen, O. W., L. Ronnov-Jessen, A. R. Howlett and M. J. Bissell (1992). "Interaction with basement membrane serves to rapidly distinguish growth and differentiation pattern of normal and malignant human breast epithelial cells." Proc Natl Acad Sci U S A **89**(19): 9064-9068.

Pimentel, H. J., N. Bray, S. Puente, P. Melsted and L. Pachter (2016). "Differential analysis of RNA-Seq incorporating quantification uncertainty." bioRxiv.

Plachot, C., L. S. Chaboub, H. A. Adissu, L. Wang, A. Urazaev, J. Sturgis, E. K. Asem and S. A. Lelievre (2009). "Factors necessary to produce basoapical polarity in human glandular epithelium formed in conventional and high-throughput three-dimensional culture: example of the breast epithelium." BMC Biol **7**: 77.

Prat, A., J. S. Parker, O. Karginova, C. Fan, C. Livasy, J. I. Herschkowitz, X. He and C. M. Perou (2010). "Phenotypic and molecular characterization of the claudin-low intrinsic subtype of breast cancer." Breast Cancer Res **12**(5): R68.

Propper, A. Y. (1978). "Wandering epithelial cells in the rabbit embryo milk line. A preliminary scanning electron microscope study." Dev Biol **67**(1): 225-231.

Qu, Y., B. Han, B. Gao, S. Bose, Y. Gong, K. Wawrowsky, A. E. Giuliano, D. Sareen and X. Cui (2017). "Differentiation of Human Induced Pluripotent Stem Cells to Mammary-like Organoids." Stem Cell Reports **8**(2): 205-215.

Qu, Y., B. Han, Y. Yu, W. Yao, S. Bose, B. Y. Karlan, A. E. Giuliano and X. Cui (2015). "Evaluation of MCF10A as a Reliable Model for Normal Human Mammary Epithelial Cells." PLoS One **10**(7): e0131285.

Ramsay, D. T., J. C. Kent, R. A. Owens and P. E. Hartmann (2004). "Ultrasound imaging of milk ejection in the breast of lactating women." Pediatrics **113**(2): 361-367.

Rizki, A., V. M. Weaver, S. Y. Lee, G. I. Rozenberg, K. Chin, C. A. Myers, J. L. Bascom, J. D. Mott, J. R. Semeiks, L. R. Grate, I. S. Mian, A. D. Borowsky, R. A. Jensen, M. O. Idowu, F. Chen, D. J. Chen, O. W. Petersen, J. W. Gray and M. J. Bissell (2008). "A human breast cell model of preinvasive to invasive transition." Cancer Res **68**(5): 1378-1387.

Robinson, G. W., A. B. Karpf and K. Kratochwil (1999). "Regulation of mammary gland development by tissue interaction." J Mammary Gland Biol Neoplasia **4**(1): 9-19.

Romano, R. A., B. Birkaya and S. Sinha (2007). "A functional enhancer of keratin14 is a direct transcriptional target of deltaNp63." J Invest Dermatol **127**(5): 1175-1186.

Romano, R. A., K. Ortt, B. Birkaya, K. Smalley and S. Sinha (2009). "An active role of the DeltaN isoform of p63 in regulating basal keratin genes K5 and K14 and directing epidermal cell fate." PLoS One **4**(5): e5623.

Ronnov-Jessen, L. and M. J. Bissell (2009). "Breast cancer by proxy: can the microenvironment be both the cause and consequence?" Trends Mol Med **15**(1): 5-13.

Ronnov-Jessen, L., O. W. Petersen and M. J. Bissell (1996). "Cellular changes involved in conversion of normal to malignant breast: importance of the stromal reaction." Physiol Rev **76**(1): 69-125.

Ruan, W. and D. L. Kleinberg (1999). "Insulin-like growth factor I is essential for terminal end bud formation and ductal morphogenesis during mammary development." Endocrinology **140**(11): 5075-5081.

Russo, J. and I. H. Russo (2004). "Development of the human breast." Maturitas **49**(1): 2-15.

Sachs, N., J. de Ligt, O. Kopper, E. Gogola, G. Bounova, F. Weeber, A. V. Balgobind, K. Wind, A. Gracanin, H. Begthel, J. Korving, R. van Boxtel, A. A. Duarte, D. Lelieveld, A. van Hoeck, R. F. Ernst, F. Blokzijl, I. J. Nijman, M. Hoogstraat, M. van de Ven, D. A. Egan, V. Zinzalla, J. Moll, S. F. Boj, E. E. Voest, L. Wessels, P. J. van Diest, S. Rottenberg, R. G. J. Vries, E. Cuppen and H. Clevers (2018). "A Living Biobank of Breast Cancer Organoids Captures Disease Heterogeneity." Cell **172**(1-2): 373-386 e310.

Sakakura, T., Y. Nishizuka and C. J. Dawe (1976). "Mesenchyme-dependent morphogenesis and epithelium-specific cytodifferentiation in mouse mammary gland." Science **194**(4272): 1439-1441.

Sauka-Spengler, T. and M. Bronner-Fraser (2008). "A gene regulatory network orchestrates neural crest formation." Nat Rev Mol Cell Biol **9**(7): 557-568.

Scheele, C. L., E. Hannezo, M. J. Muraro, A. Zomer, N. S. Langedijk, A. van Oudenaarden, B. D. Simons and J. van Rheenen (2017). "Identity and dynamics of mammary stem cells during branching morphogenesis." Nature **542**(7641): 313-317.

Senoo, M., F. Pinto, C. P. Crum and F. McKeon (2007). "p63 Is essential for the proliferative potential of stem cells in stratified epithelia." Cell **129**(3): 523-536.

Shackleton, M., F. Vaillant, K. J. Simpson, J. Stingl, G. K. Smyth, M. L. Asselin-Labat, L. Wu, G. J. Lindeman and J. E. Visvader (2006). "Generation of a functional mammary gland from a single stem cell." Nature **439**(7072): 84-88.

Shang, Y., X. Cai and D. Fan (2013). "Roles of epithelial-mesenchymal transition in cancer drug resistance." Curr Cancer Drug Targets **13**(9): 915-929.

Shekhar, M. P., R. Pauley and G. Heppner (2003). "Host microenvironment in breast cancer development: extracellular matrix-stromal cell contribution to neoplastic phenotype of epithelial cells in the breast." Breast Cancer Res **5**(3): 130-135.

Shenoy, A. K. and J. Lu (2016). "Cancer cells remodel themselves and vasculature to overcome the endothelial barrier." Cancer Lett **380**(2): 534-544.

Shimomura, Y., M. Wajid, L. Shapiro and A. M. Christiano (2008). "P-cadherin is a p63 target gene with a crucial role in the developing human limb bud and hair follicle." Development **135**(4): 743-753.

Shrestha, S., B. R. Bhattarai, K. H. Lee and H. Cho (2007). "Mono- and disalicylic acid derivatives: PTP1B inhibitors as potential anti-obesity drugs." Bioorg Med Chem **15**(20): 6535-6548.

Sigurdsson, V., A. J. Fridriksdottir, J. Kjartansson, J. G. Jonasson, M. Steinarsdottir, O. W. Petersen, H. M. Ogmundsdottir and T. Gudjonsson (2006). "Human breast microvascular endothelial cells retain phenotypic traits in long-term finite life span culture." In Vitro Cell Dev Biol Anim **42**(10): 332-340.

Sigurdsson, V., B. Hilmarsdottir, H. Sigmundsdottir, A. J. Fridriksdottir, M. Ringner, R. Villadsen, A. Borg, B. A. Agnarsson, O. W. Petersen, M. K. Magnusson and T. Gudjonsson (2011). "Endothelial induced EMT in breast epithelial cells with stem cell properties." PLoS One **6**(9): e23833.

Sigurdsson, V., S. Ingthorsson, B. Hilmarsdottir, S. M. Gustafsdottir, S. R. Franzdottir, A. J. Arason, E. Steingrimsson, M. K. Magnusson and T. Gudjonsson (2013). "Expression and functional role of sprouty-2 in breast morphogenesis." PLoS One **8**(4): e60798.

Silberstein, G. B. and C. W. Daniel (1987). "Reversible inhibition of mammary gland growth by transforming growth factor-beta." Science **237**(4812): 291-293.

Sistigu, A., F. Di Modugno, G. Manic and P. Nistico (2017). "Deciphering the loop of epithelial-mesenchymal transition, inflammatory cytokines and cancer immunoediting." Cytokine Growth Factor Rev **36**: 67-77.

Smith, B. N. and N. A. Bhowmick (2016). "Role of EMT in Metastasis and Therapy Resistance." J Clin Med **5**(2).

Soule, H. D., J. Vazguez, A. Long, S. Albert and M. Brennan (1973). "A human cell line from a pleural effusion derived from a breast carcinoma." J Natl Cancer Inst **51**(5): 1409-1416.

Sternlicht, M. D., A. Lochter, C. J. Sympson, B. Huey, J. P. Rougier, J. W. Gray, D. Pinkel, M. J. Bissell and Z. Werb (1999). "The stromal proteinase MMP3/stromelysin-1 promotes mammary carcinogenesis." Cell **98**(2): 137-146.

Sternlicht, M. D., S. W. Sunnarborg, H. Kouros-Mehr, Y. Yu, D. C. Lee and Z. Werb (2005). "Mammary ductal morphogenesis requires paracrine activation of stromal EGFR via ADAM17-dependent shedding of epithelial amphiregulin." Development **132**(17): 3923-3933.

Stingl, J., C. J. Eaves, U. Kuusk and J. T. Emerman (1998). "Phenotypic and functional characterization in vitro of a multipotent epithelial cell present in the normal adult human breast." Differentiation **63**(4): 201-213.

Stingl, J., C. J. Eaves, I. Zandieh and J. T. Emerman (2001). "Characterization of bipotent mammary epithelial progenitor cells in normal adult human breast tissue." Breast Cancer Res Treat **67**(2): 93-109.

Stingl, J., P. Eirew, I. Ricketson, M. Shackleton, F. Vaillant, D. Choi, H. I. Li and C. J. Eaves (2006). "Purification and unique properties of mammary epithelial stem cells." Nature **439**(7079): 993-997.

Stuible, M., K. M. Doody and M. L. Tremblay (2008). "PTP1B and TC-PTP: regulators of transformation and tumorigenesis." Cancer Metastasis Rev **27**(2): 215-230.

Taddei, I., M. M. Faraldo, J. Teuliere, M. A. Deugnier, J. P. Thiery and M. A. Glukhova (2003). "Integrins in mammary gland development and differentiation of mammary epithelium." J Mammary Gland Biol Neoplasia **8**(4): 383-394.

Tait, L., H. D. Soule and J. Russo (1990). "Ultrastructural and immunocytochemical characterization of an immortalized human breast epithelial cell line, MCF-10." Cancer Res **50**(18): 6087-6094.

Tam, W. L. and R. A. Weinberg (2013). "The epigenetics of epithelial-mesenchymal plasticity in cancer." Nat Med **19**(11): 1438-1449.

Tanner, M. M., M. Tirkkonen, A. Kallioniemi, J. Isola, T. Kuukasjarvi, C. Collins, D. Kowbel, X. Y. Guan, J. Trent, J. W. Gray, P. Meltzer and O. P. Kallioniemi (1996). "Independent amplification and frequent co-amplification of three nonsyntenic regions on the long arm of chromosome 20 in human breast cancer." Cancer Res **56**(15): 3441-3445.

Taube, J. H., J. I. Herschkowitz, K. Komurov, A. Y. Zhou, S. Gupta, J. Yang, K. Hartwell, T. T. Onder, P. B. Gupta, K. W. Evans, B. G. Hollier, P. T. Ram, E. S. Lander, J. M. Rosen, R. A. Weinberg and S. A. Mani (2010). "Core epithelial-to-mesenchymal transition interactome gene-expression signature is associated with claudin-low and metaplastic breast cancer subtypes." Proc Natl Acad Sci U S A **107**(35): 15449-15454.

Taube, J. H., G. G. Malouf, E. Lu, N. Sphyris, V. Vijay, P. P. Ramachandran, K. R. Ueno, S. Gaur, M. S. Nicoloso, S. Rossi, J. I. Herschkowitz, J. M. Rosen, J. P. Issa, G. A. Calin, J. T. Chang and S. A. Mani (2013). "Epigenetic silencing of microRNA-203 is required for EMT and cancer stem cell properties." Sci Rep **3**: 2687.

Thiery, J. P. (2002). "Epithelial-mesenchymal transitions in tumour progression." Nat Rev Cancer **2**(6): 442-454.

Thiery, J. P., H. Acloque, R. Y. Huang and M. A. Nieto (2009). "Epithelial-mesenchymal transitions in development and disease." Cell **139**(5): 871-890.

Tuomarila, M., K. Luostari, Y. Soini, V. Kataja, V. M. Kosma and A. Mannermaa (2014). "Overexpression of microRNA-200c predicts poor outcome in patients with PR-negative breast cancer." PLoS One **9**(10): e109508.

van Kempen, L. C., K. van den Hurk, V. Lazar, S. Michiels, V. Winnepenninckx, M. Stas, A. Spatz and J. J. van den Oord (2012). "Loss of microRNA-200a and c, and microRNA-203 expression at the invasive front of primary cutaneous melanoma is associated with increased thickness and disease progression." Virchows Arch **461**(4): 441-448.

Varner, V. D. and C. M. Nelson (2014). "Cellular and physical mechanisms of branching morphogenesis." Development **141**(14): 2750-2759.

Vidi, P. A., M. J. Bissell and S. A. Lelievre (2013). "Three-dimensional culture of human breast epithelial cells: the how and the why." Methods Mol Biol **945**: 193-219.

Viebahn, C. (1995). "Epithelio-mesenchymal transformation during formation of the mesoderm in the mammalian embryo." Acta Anat (Basel) **154**(1): 79-97.

Villadsen, R. (2005). "In search of a stem cell hierarchy in the human breast and its relevance to breast cancer evolution." Apmis **113**(11-12): 903-921.

Villadsen, R., A. J. Fridriksdottir, L. Ronnov-Jessen, T. Gudjonsson, F. Rank, M. A. LaBarge, M. J. Bissell and O. W. Petersen (2007). "Evidence for a stem cell hierarchy in the adult human breast." J Cell Biol **177**(1): 87-101.

Visvader, J. E. and J. Stingl (2014). "Mammary stem cells and the differentiation hierarchy: current status and perspectives." Genes Dev **28**(11): 1143-1158.

Wang, D., C. Cai, X. Dong, Q. C. Yu, X. O. Zhang, L. Yang and Y. A. Zeng (2015). "Identification of multipotent mammary stem cells by protein C receptor expression." Nature **517**(7532): 81-84.

Wazer, D. E., X. L. Liu, Q. Chu, Q. Gao and V. Band (1995). "Immortalization of distinct human mammary epithelial cell types by human papilloma virus 16 E6 or E7." Proc Natl Acad Sci U S A **92**(9): 3687-3691.

Weaver, V. M., O. W. Petersen, F. Wang, C. A. Larabell, P. Briand, C. Damsky and M. J. Bissell (1997). "Reversion of the malignant phenotype of human breast cells in three-dimensional culture and in vivo by integrin blocking antibodies." J Cell Biol **137**(1): 231-245.

Wellner, U., J. Schubert, U. C. Burk, O. Schmalhofer, F. Zhu, A. Sonntag, B. Waldvogel, C. Vannier, D. Darling, A. zur Hausen, V. G. Brunton, J. Morton, O. Sansom, J. Schuler, M. P. Stemmler, C. Herzberger, U. Hopt, T. Keck, S. Brabletz and T. Brabletz (2009). "The EMT-activator ZEB1 promotes tumorigenicity by repressing stemness-inhibiting microRNAs." Nat Cell Biol **11**(12): 1487-1495.

Wiseman, B. S. and Z. Werb (2002). "Stromal effects on mammary gland development and breast cancer." Science **296**(5570): 1046-1049.

Yang, A., M. Kaghad, Y. Wang, E. Gillett, M. D. Fleming, V. Dotsch, N. C. Andrews, D. Caput and F. McKeon (1998). "p63, a p53 homolog at 3q27-29, encodes multiple products with transactivating, death-inducing, and dominant-negative activities." Mol Cell **2**(3): 305-316.

Yang, J. and R. A. Weinberg (2008). "Epithelial-mesenchymal transition: at the crossroads of development and tumor metastasis." Dev Cell **14**(6): 818-829.

Yip, S. C., S. Saha and J. Chernoff (2010). "PTP1B: a double agent in metabolism and oncogenesis." Trends Biochem Sci **35**(8): 442-449.

Yu, M., G. Lin, N. Arshadi, I. Kalatskaya, B. Xue, S. Haider, F. Nguyen, P. C. Boutros, A. Elson, L. B. Muthuswamy, N. K. Tonks and S. K. Muthuswamy (2012). "Expression profiling during mammary epithelial cell three-dimensional morphogenesis identifies PTPRO as a novel regulator of morphogenesis and ErbB2-mediated transformation." Mol Cell Biol **32**(19): 3913-3924.

Zabolotny, J. M., K. K. Bence-Hanulec, A. Stricker-Krongrad, F. Haj, Y. Wang, Y. Minokoshi, Y. B. Kim, J. K. Elmquist, L. A. Tartaglia, B. B. Kahn and B. G. Neel (2002). "PTP1B regulates leptin signal transduction in vivo." Dev Cell **2**(4): 489-495.

Zhang, G., W. Zhang, B. Li, E. Stringer-Reasor, C. Chu, L. Sun, S. Bae, D. Chen, S. Wei, K. Jiao, W. H. Yang, R. Cui, R. Liu and L. Wang (2017). "MicroRNA-200c and microRNA- 141 are regulated by a FOXP3-KAT2B axis and associated with tumor metastasis in breast cancer." Breast Cancer Res **19**(1): 73.

Zhang, Z., Z. Dong, I. S. Lauxen, M. S. Filho and J. E. Nor (2014). "Endothelial cell-secreted EGF induces epithelial to mesenchymal transition and endows head and neck cancer cells with stem-like phenotype." Cancer Res **74**(10): 2869-2881.

Zhang, Z., B. Zhang, W. Li, L. Fu, L. Fu, Z. Zhu and J. T. Dong (2011). "Epigenetic Silencing of miR-203 Upregulates SNAI2 and Contributes to the Invasiveness of Malignant Breast Cancer Cells." Genes Cancer **2**(8): 782-791.

Zhu, J., H. Fu, Y. Wu and X. Zheng (2013). "Function of lncRNAs and approaches to lncRNA-protein interactions." Sci China Life Sci **56**(10): 876-885.

Zschenker, O., T. Streichert, S. Hehlgans and N. Cordes (2012). "Genome-wide gene expression analysis in cancer cells reveals 3D growth to affect ECM and processes associated with cell adhesion but not DNA repair." PLoS One **7**(4): e34279.

Original publications

Paper I

Developmental Biology 403 (2015) 150–161

Contents lists available at ScienceDirect

Developmental Biology

journal homepage: www.elsevier.com/locate/developmentalbiology

MicroRNA-200c-141 and ΔNp63 are required for breast epithelial differentiation and branching morphogenesis

Bylgja Hilmarsdóttir [a,b], Eirikur Briem [a,b], Valgardur Sigurdsson [a], Sigrídur Rut Franzdóttir [a], Markus Ringnér [d], Ari Jon Arason [a,b], Jon Thor Bergthorsson [a,b], Magnus Karl Magnusson [a,b,c], Thorarinn Gudjonsson [a,b,*]

[a] Stem Cell Research Unit, Biomedical Center, Department of Anatomy, Faculty of Medicine, School of Health Sciences, University of Iceland, Iceland
[b] Department of Laboratory Hematology, Landspitali-University Hospital, Iceland
[c] Department of Medical Pharmacology and Toxicology, Faculty of Medicine, School of Health Sciences, University of Iceland, Iceland
[d] Division of Oncology and Pathology, Department of Clinical Sciences Lund, Lund University, Sweden

ARTICLE INFO

Article history:
Received 6 October 2014
Received in revised form
18 April 2015
Accepted 5 May 2015
Available online 9 May 2015

Keywords:
MiR-200c-141
ΔNp63
Breast cancer
Breast morphogenesis
Stem cells
EMT

ABSTRACT

The epithelial compartment of the breast contains two lineages, the luminal- and the myoepithelial cells. D492 is a breast epithelial cell line with stem cell properties that forms branching epithelial structures in 3D culture with both luminal- and myoepithelial differentiation. We have recently shown that D492 undergo epithelial to mesenchymal transition (EMT) when co-cultured with endothelial cells. This 3D co-culture model allows critical analysis of breast epithelial lineage development and EMT. In this study, we compared the microRNA (miR) expression profiles for D492 and its mesenchymal-derivative D492M. Suppression of the miR-200 family in D492M was among the most profound changes observed. Exogenous expression of miR-200c-141 in D492M reversed the EMT phenotype resulting in gain of luminal but not myoepithelial differentiation. In contrast, forced expression of ΔNp63 in D492M restored the myoepithelial phenotype only. Co-expression of miR-200c-141 and ΔNp63 in D492M restored the branching morphogenesis in 3D culture underlining the requirement for both luminal and myoepithelial elements for obtaining full branching morphogenesis in breast epithelium. Introduction of a miR-200c-141 construct in both D492 and D492M resulted in resistance to endothelial induced EMT. In conclusion, our data suggests that expression of miR-200c-141 and ΔNp63 in D492M can reverse EMT resulting in luminal- and myoepithelial differentiation, respectively, demonstrating the importance of these molecules in epithelial integrity in the human breast.

Introduction

Maintaining tissue integrity while allowing remodeling capacity in organs depends on the presence of tissue stem cells. This is particularly applicable in tissue with fast cellular remodeling such as blood, skin, gastrointestinal epithelium and the breast gland that is subjected to periodic tissue remodeling and branching morphogenesis from the onset of menarche to menopause (Raouf et al., 2012; Reya et al., 2001; Villadsen et al., 2007; Woodward et al., 2005). The breast epithelium consists of an inner layer of polarized luminal epithelial cells and an outer layer of myoepithelial cells that can be discriminated by marker expression (Gudjonsson et al., 2002a; Pechoux et al., 1999). Luminal cells express simple keratins (K) such as K18 and K19, the adhesion molecules E-cadherin and EpCAM and tight junction proteins such as claudin, occludin and ZO-1. In contrast myoepithelial cells express basal keratins such as K5/6, 14 and 17, P-cadherin, vimentin, alpha-smooth muscle actin and the basal cell marker p63 (Gudjonsson et al., 2002a; Pechoux et al., 1999). Although phenotypically and functionally different, luminal- and myoepithelial cells are generally thought to arise from common stem cells (Gudjonsson et al., 2002b; Pechoux et al., 1999; Raouf et al., 2012; Villadsen et al., 2007; Woodward et al., 2005). Furthermore, these stem cells or their downstream progenitors are believed to be the preferred targets of cancer initiation (Raouf et al., 2012; Smalley and Ashworth, 2003).

Epithelial to mesenchymal transition (EMT) is a conserved developmental process where epithelial cells loose epithelial properties and adapt a mesenchymal phenotype. This is observed during gastrulation, neural crest formation and wound healing. EMT is also a driving force in tumor cell invasion and metastasis manifested by loss of cell-to-cell adhesion and increased migration potential

* Correspondence to: Stem Cell Research Unit, Department of Medical Faculty, Biomedical Center, University of Iceland, Vatnsmyrarvegi 16, 101 Reykjavík, Iceland. Fax: +354 4884.
E-mail address: tgudjons@hi.is (T. Gudjonsson).

http://dx.doi.org/10.1016/j.ydbio.2015.05.007

(Hanahan and Weinberg, 2011). In addition, accumulating evidence suggests that EMT may provide differentiated epithelial cells with stem cell properties and contribute to cancer stem cell formation (reviewed in Ansieau (2013)).

MicroRNAs (miRNAs) have moved into the spotlight as master regulators in stem cell biology and fate decision (Hilmarsdottir et al., 2014; Yang and Rana, 2013; Zapata et al., 2012). Recent studies have shown that the miR-200 family plays a crucial role in regulating epithelial integrity and loss of its expression may drive cells through EMT (Hanahan and Weinberg, 2011; Howe et al., 2012). Members of the miR-200 family target the EMT associated transcription factors ZEB1 and ZEB2, which in turn suppress E-cadherin (Olson et al., 2009). The miR-200 gene family is located on two distinct clusters (miR-200ba-429 and miR-200c-141) on chromosomes 1 and 12, respectively (Mongroo and Rustgi, 2010).

The p63 transcription factor is expressed in the basal cells of various tissues, such as the skin, lung, prostate, salivary glands and breast (Blanpain and Fuchs, 2007). p63 is a member of the p53 family and has two major isoforms, ΔNp63 and TA-p63. The ΔN isoform is the dominant form in most tissues and has been identified as a regulator of basal cell associated markers such as K5, K14 and P-cadherin (Romano et al., 2007, 2009; Shimomura et al., 2008). The role of ΔNp63 has mostly been studied in the skin where it is crucial for adult stem cell maintenance. ΔNp63 has also been identified as an essential factor for epithelial stratification in the skin (Senoo et al., 2007) and lung (Daniely et al., 2004; Pellegrini et al., 2001). We have recently shown that knock-down of p63 in lung epithelial basal cells result in increased senescence and lack of pseudostratification (Arason et al., 2014).

The breast epithelial progenitor cell line D492 forms branching structures in 3D culture with differentiated luminal and myoepithelial cells (Gudjonsson et al., 2002b). Furthermore, in 3D coculture with endothelial cells the cell line displays two main morphotypes: branching colonies and spindle-like EMT colonies. The D492-mesenchymal (D492M) cell line was established from a single EMT colony (Sigurdsson et al., 2011, 2013). In this study, we show that D492 and D492M differ greatly in terms of miRNA expression. In particular the miR-200 family is downregulated in D492M. Methylation analysis shows that the promoter area of miR-200c-141 is methylated in D492M only. When introduced into the D492M, miR-200c-141 only reestablishes the luminal epithelial phenotype. Overexpression of miR-200c-141 in D492 and D492M prevents the endothelial-induced EMT demonstrating the importance of miR-200c-141 in preserving epithelial integrity. The missing myoepithelial phenotype was reestablished by introduction of ΔNp63 into D492M. Co-expression of both miR200c-141 and ΔNp63 in D492M reestablished the luminal- and myoepithelial expression seen in D492 and restored branching potential in 3D culture.

Materials and methods

Cell culture and 3D cultures

D492 and D492M were maintained in H14 medium as described previously (Sigurdsson et al., 2011). Primary luminal epithelial cells ($EpCAM^+$) and myoepithelial cells ($EpCAM^-$) were isolated by magnetic cell sorting (MACS) and maintained in CDM3 and CDM4 as described previously (Pechoux et al., 1999). Primary human breast endothelial cells (BRENCs) were isolated from breast reduction mammoplasties and cultured on endothelial growth medium (EGM-2) (Lonza)+5% FBS (Invitrogen) (Sigurdsson et al., 2006). Growth factor reduced reconstituted basement membrane (rBM, purchased as Matrigel, BD Biosciences) was used for 3D culture. 3D monocultures were carried out in 24 well culture plates (BD Falcon). 1×10^4 $D^4$92 cells were suspended in 300 μl of rBM. Co-culture experiments were carried out with 1×10^3 cells mixed with 1×10^5 BRENCs. 300 μl of mixed cells/rBM were seeded in each well of a 24 well plate and cultured on H14 (monoculture) or EGM5 (coculture) for 16 days. For detailed description of 3D cell culture see Sigurdsson et al. (2011).

Pre-cluster assay was adapted from Hirai et al. (1992). Briefly, 50,000 cells were mixed in 500 μl of EGM5 media and cultured on a 24 well low adhesion plate (plate coated with 12 μg/ml polyhema, for 24 h at 37 °C). After 24 h, cell clusters were collected with brief centrifugation and resuspended in 500 μl H14 media and 50 μl of preclustered organoids embedded in 100 μl of matrigel and seeded in 8 well chamber slite. The branching phenotype of cell clusters was determined after cultivation for 8 days.

Branching, solid and spindle-like structures were isolated from 3D cocultures with gentle shaking on ice in PBS-EDTA (5 mM) solution as described previously (Lee et al., 2007). Newly formed Mesenchymal and branching colonies were sorted under a stereomicroscope for RNA isolation.

MicroRNA expression array

RNA was isolated from D492 and D492M at 50% and 90% confluency in monolayer culture using RNeasy minikit (Qiagen). Experiments were conducted in triplicate, on three different time points (resulting in a total of 36 samples). RNA integrity was analyzed using the Agilent 2100 Bioanalyzer (Agilent). Microarray analysis was carried out at the SCIBLU Genomics Centre at Lund University (Lund, Sweden) using Illumina Human v2 MicroRNA Expression BeadChip (Illumina). To filter out unexpressed miRNAs, the 599 miRNA probes detected in at least 3 of the 36 samples (detection p-value ≤ 0.01) were selected for further analysis. For each probe, negative intensities after background correction were replaced by missing values, and then intensities were log-transfomed (base 2) followed by mean centering across samples to generate miRNA expression levels. To identify differentially expressed miRNA genes we used the MeV software (http://www.tm4.org) and the significance of microarrays (SAM) method (Tusher et al., 2001) using 10,000 permutations. The miRNA expression data discussed in this publication have been deposited in NCBI's Gene Expression Omnibus (Edgar et al., 2002) and are accessible through GEO Series accession number GSE60524 (http://www.ncbi.nlm.nih.gov/geo/query/acc.cgi?acc=GSE60524).

RT-PCR analysis

Total RNA was extracted with Tri-Reagent (Ambion). The RNA was DNAase treated and reverse transcribed with Hexanucleotide primers using RevertAid (#K1622, Fermentas). Resulting cDNA was used as template for RT-PCR performed using the primers listed in Supplementary Table 2.

qRT-PCR analysis

Quantitative RT-PCR of ΔNp63, ZEB1 and ZEB2 was performed on the same cDNA as the RT-PCR, described above. For quantification of p63, K14, K19, E-cadherin and N-cadherin SYBR green real-time PCR assay were used (Tp63 from IDT: HS.PT.58.38930512 other primers in Supplementary Table 2) and GAPDH as endogenous reference gene (primers in Supplementary Table 2). Primer pairs and probes from Applied Biosystems (TaqMan) were used for ZEB1 (Hs00232783_m1) and ZEB2 (Hs00207691_m1) quantification. GAPDH (4326317E) was used as endogenous reference gene.

Quantitative RT-PCR analysis of miRNAs was performed using miRCURY LNA™ microRNA PCR System (Exiqon). Gene expression levels were quantified using primers for hsa-miR-141 (#204504) and hsa-miR-200c (#2044852) (Exiqon). Normalization was done

with U6 RNA (#203907) or SNORD48 (#203903) (Exiqon). Relative expression differences was calculated with the $2^{\Delta Ct}$ method.

Immunochemistry

The following primary antibodies were used: Fibronectin (LabMab, (gift from D.E. Mosher (Chernousov et al., 1991))), K19 (ab7754, Abcam), K14 (NCL-LL002, NovoCastra), E-Cad (#610182, BD), N-Cad (#610920, BD), EpCAM (NCL-ESA, Novocastra), and p63 (NCL-p63, Novocastra). For double and triple labeling experiments we used fluorescence isotype specific secondary antibodies (Invitrogen) and fluorescent nuclear counterstain, TO-PRO-3 (Invitrogen). Specimens were visualized on a Zeiss LSM 5 Pa laser-scanning microscope (Carl Zeiss) and Olympus fluoview 1200.

Western blotting

Equal amounts (5 μg) of proteins in RIPA buffer were separated on 10% NuPage Bis-Tris gels (Invitrogen) and transferred to a PVDF membrane (Invitrogen). Antibodies: E-Cad (BD), Ncad (BD), K5/6 (Zymed), K8 (Abcam), K14 (Abcam), K17 (Dako), K19 (Abcam), Vimentin (Dako), Snail (Abcam), p63 (Abcam) actin, and EpCAM (Abcam) were used. Secondary antibodies were mouse or rabbit IRDey (Li-Cor) used at 1:10,000 and detected using the Odyssey Infrared Imaging System (Li-Cor). Fluorescent images were converted to gray scale.

5-Aza treatment

D492 and D492M were grown to 70% confluency. Cells were treated with 5 mM of 5-azacitidine (Sigma, A2385) in H14 medium and cultured for 4 days before IF staining or DNA, or protein isolation.

Bisulfite sequencing

Bisulfite conversion of DNA was performed with the Quiagen Epitech bisulfate kit (59,104) using 0.5–1 μg of DNA. The target DNA sequence was amplified using Nested PCR. Primer sequences are in Supplementary Table 2. DNA methylation analyses of bisulfite PCR amplicons were performed using Sequence scanner V1.0. DNA methylation level was scored as percentage methylation of individual CpG units in each sample.

miR-200c-141 and ΔNp63 overexpression

A miR-200c-141 construct was created by cloning the genomic region into a pLVTHM lentiviral vector purchased from Addgene (plasmid #12247 (Wiznerowicz and Trono, 2003)). The miR-200c-141 insert was amplified from genomic DNA using nested PCR (primers in Supplementary Table 2) and the sequence confirmed with sequencing. An empty vector was used as a control. The pLVTHM vector contains a green fluorescent protein (GFP) selection marker. Viral particles were produced in HEK-293T cells using Arrest-In transfection reagent (ATR1740; Open Biosystems) according to instructions. Virus-containing supernatants were collected 48 h after transfection and target cells were infected in the presence of 8 μg/μl polybrene. Stable, D492 and D492M with miR-200c-141 and control (empty) cells were isolated by flow-sorting, selecting GFP expressing cells using FACSaria. deltaNp63alpha-FLAG (Addgene, plasmid #26979 (Chatterjee et al., 2008)) was used to clone ΔNp63 into a pCDH lentiviral vector (System Biosciences), containing both RFP and a puromycin selection marker and viral particles were produced as described above. $D492M^{miR\text{-}200c\text{-}141}$ cells and $D492M^{empty}$ where transduced with the ΔNp63 overexpressing vector and $D492M^{empty}$ with empty pCDH vector as a control ($D492M^{2\times empty}$). Stable $D492M^{2\times empty}$, $D492M^{\Delta Np63}$ and $D492M^{miR\text{-}200c\text{-}141\Delta Np63}$ cells were selected using 2 μg/ml puromycin.

miR-200c-141 inhibition and ΔNp63 downregulation

miRCURY LNA™ microRNA Inhibitors from Exiqon were used to inhibit miR-200c-141 function, hsa-miR-200b, hsa-miR-200c (#450012-2) and hsa-miR-141, hsa-miR-200a (#450012-3). Exiqon negative control A inhibitor (#199004-04) was used as a control. Briefly, 75.000 D492 cells were seeded in each well of a 24 well plate and cultured on H14 for 24 h. Following the 24 h incubation media was removed and replaced with H14 without antibiotics, containing 25 nM inhibitor (#450012-2) and 25 nM inhibitor (#450012-3) or 50 nM negative inhibitor (#199004-04). Transfection was carried out by using 1.5 μl of Lipofectamine® RNAiMAX (Life Technologies #13778-075) per well. Cells were incubated for additional 24 h followed by RNA isolation, RT-PCR and qRT-PCR analysis. Samples were run in biological triplicates. ΔNp63 expression was downregulated using shp63alpha pLKO.1 puro lentiviral vector (Addgene plasmid 19,120 (Godar et al., 2008)) and pLKO.1 shSCR lentiviral vector (Addgene plasmid 17,920 (Saharia et al., 2008)) was used as control. Viral particles were produced in HEK-293 T cells using TurboFect transfection reagent (R0531; Life Technologies) according to manufacturer's instructions. Virus-containing supernatant was collected 48 h after transfection and target cells were infected in the presence of 8 μg/μl polybrene. Stable $D492^{Scr}$ and $D492^{p63KD}$ cells were selected using 2 μg/ml puromycin.

Statistical analysis

Data are presented as means with standard deviations of measurements. Statistical differences between samples were assessed with Student two-tailed *T*-test. *p*-Values below 0.05 were considered significant ($^{***}p \leq 0.001$, $^{**}p \leq 0.01$, $^{*}p \leq 0.05$).

Results

Endothelial-induced EMT in D492 breast epithelial stem cell line is associated with reduced expression of the miR-200 family

We have recently shown that endothelial cells can induce EMT in D492, a breast epithelial cell line with stem cell properties (Sigurdsson et al., 2011, 2013). A mesenchymal subline of D492, referred to as D492M shows irreversible EMT as evidenced by spindle-like phenotype in 2D and 3D culture, downregulation of E-cadherin, increased expression of N-cadherin and loss of K14 and K19 expression (Fig. 1A). In order to evaluate differences in miRNA expression profiles we carried out analysis of microRNA expression in D492 and D492M cells cultured in monolayer. We identified 186 miRNAs (false discovery rate = 0.002) differentially expressed between D492 and D492M, out of 599 analyzed miRNAs demonstrating large differences between D492 and D492M (Supplementary Table 1). Of the ten most downregulated miRNAs in D492M, four belonged to the miR-200 family (miR-141, -200a,-200c,-200b) (Fig. 1B). These microRNAs are emerging as major regulators of epithelial integrity in human and murine cells (Davalos et al., 2012; Gregory et al., 2008; Mongroo and Rustgi, 2010; Wellner et al., 2009). In particular, miR-200c and miR-141 have both been strongly linked to epithelial integrity (Davalos et al., 2012; Mongroo and Rustgi, 2010). miR-200c and miR-141 are colocalized on chromosome 12 (Fig. S1) and their expression is regulated from the same promoter (Mongroo and Rustgi, 2010).

Decreased expression of miR-200c and miR-141 in D492M compared to D492 was confirmed by qPCR (Fig. 1C). In addition,

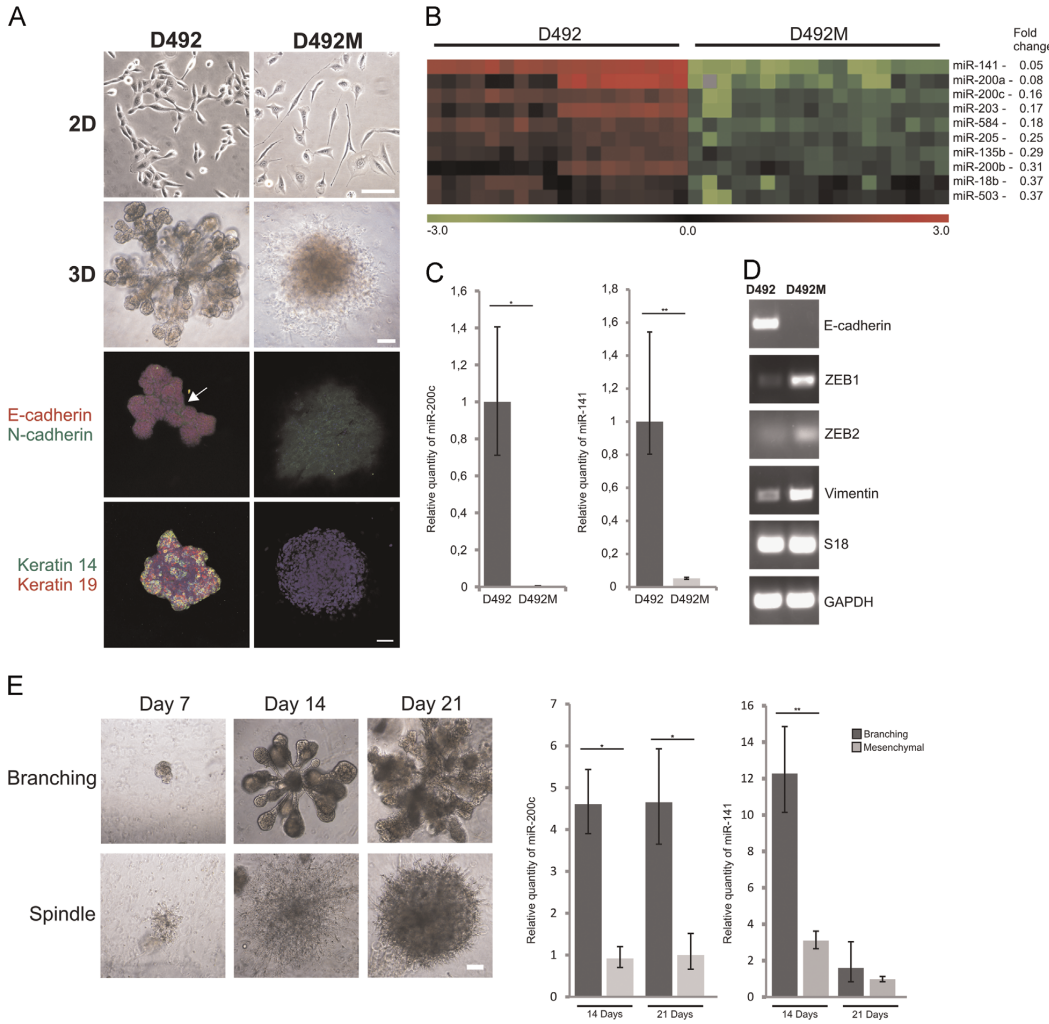

Fig. 1. The miR-200 family is downregulated in breast epithelial stem cells undergoing EMT. (A) D492 and D492M generate branching and mesenchymal-like structures in 3D culture, respectively. D492 a breast epithelial cell line with stem cell properties forms cuboidal epithelial phenotype in 2D culture and elaborate branching structures in 3D culture in reconstituted basement membrane (rBM) matrix. In contrast, D492M forms a spindle-like phenotype in 2D and 3D cultures. Immunostaining shows reduced expression of E-cadherin (red) and increased expression of N-cadherin (green) in D492M. K14 (green) and K19 (red) that are present in the branching structures of D492 in 3D culture are lost in the spindle-like colonies of cultured D492M cells. Note, the N-cadherin expression in the branching structures of D492 is restricted to the interface between lobular units (arrow) compared to the overall staining in D492M. Cells were counterstained with TO-PRO-3 nuclearstain. Bar = 100 μM. (B) miRNA expression analysis shows drastic difference between D492 and D492M. Heatmap of differentially expressed miRNAs shows a drastic difference between D492 and D492M. Of the top 10 downregulated miRNAs in D492M, four where from the miR-200 family (miR-200a, miR-200b, miR-200c and miR-141). There was not significant difference in the expression of the fifth miR-200 family member, miR-429. (C) Validation of miR-200c and miR-141 expression in D492 and D492M. miR-200c and miR-141 downregulation in D492M was verified with qPCR. The expression of miR-200c was shown to be more than 500 fold in D492 relative to D492M. miR-141 expression was almost 20 fold higher in D492 than D492M. miRNA levels were normalized to U6. (D) Expression of ZEB1 and ZEB2 is increased in D492M. PCR expression analysis of selected targets regulated by miR-200c-141 shows different expressions between D492 and D492M. E-cadherin was lost in D492M accompanied by increased expression of ZEB1, ZEB2 and vimentin. S18 and GAPDH as loading control. (E) miR-200c and -141 are downregulated in newly formed mesenchymal structures. D492 cells were embedded into matrigel in coculture with endothelial cells in order to form branching and spindle like structures. After 14 and 21 days in culture, RNA was isolated from newly formed mesenchymal colonies. qPCR for miR-200c and -141 demonstrated significantly higher expression of these miRNAs in newly formed branching colonies than in mesenchymal colonies. miRNA levels were normalized to SNORD48. Bar = 100 μM.

RT-PCR shows down-regulation of E-cadherin in D492M accompanied by up-regulation of downstream targets for miR-200c such as ZEB1, ZEB2 and vimentin (Fig. 1D). These data show that loss of miR-200c-141 is accompanied by increased expression of EMT regulators, reduced expression of epithelial markers and gain of mesenchymal phenotype.

We next validated the differences in miR-200c-141 expression in newly formed branching and mesenchymal structures from 3D cultures. D492 and BRENCS were co-cultured in 3D rBM and RNA was isolated from branching and spindle-like colonies at two different time points, after 14 and 21 days in culture (Fig. 1E). These two time points represent different phases of the branching process where extensive branching is occurring on day 14, but on day 21 colony growth and branching has stopped. qPCR confirmed that miR-200c and miR-141 are downregulated in mesenchymal structures relative to branching structures at day 14 but on day 21 miR-141

expression is downregulated in both branching and mesenchymal structures while miR-200c remains unchanged. The reason for downregulation of miR-141 during branching at this time point is unclear. It has however been shown that miRNAs biogenesis is under strict control and subject to many post-transcriptional regulation mechanisms (Ha and Kim, 2014).

The promoter region of miR-200c-141 is methylated in D492M but not in D492

Gene silencing by CpG methylation is widely used by cells to suppress gene expression. Recent papers have shown that the expression of the miR-200 family can be regulated through methylation of its CpG rich promoter region (Vrba et al., 2010; Wiklund et al., 2010). To see if this was the case in D492M we bisulfite sequenced the CpG islands in the promoter area of the miR-200c-141 and as shown in Fig. 2A methylation occurs only in D492M, suggesting that methylation might play a role in the differential expression. The promoter of E-cadherin is commonly methylated during EMT but bisulfate sequencing showed that neither D492 nor D492M were methylated at the E-cadherin promoter (Fig. 2A). CpG islands in the other miR-200 family promoters, miR-200ba-429 were methylated in both D492 and D492M (Fig. S2A). These data are consistent with previous reports, showing that the miR-200c-141 cluster is regulated by promoter methylation while histone methylation is more important for repression of the miR-200ba-429 cluster (Davalos et al., 2012).

To assess the methylation effects on the EMT phenotype in D492M, we treated D492M cells with the demethylation agent 5-azacytidine (5-aza). Phenotypic characterization after treatment showed that the epithelial phenotype could be partially restored in D492M as demonstrated by expression of EpCAM, E-cadherin, K14 and K19 and reduced expression of N-cadherin (Fig. 2B). Similarly miR-200c expression was significantly upregulated in D492M after 5-aza treatment (Fig. 2C) but there was no change in the expression of miR-141 which remained very low before and after treatment. The expression of p63 was unchanged after 5-aza treatment. Bisulfate sequencing showed reduction of methylation at the miR-200c-141 promoter after 5-aza treatment (Fig. S2B).

Having shown that both miR-200c and miR-141 are markedly down-regulated in D492M and that the miR-200c-141 promoter locus is methylated, suggesting a regulated event, we decided to ectopically express the miR-200c-141 locus in both D492 and D492M and monitor the effect on morphogenesis, epithelial integrity and stemness in our breast stem cell model.

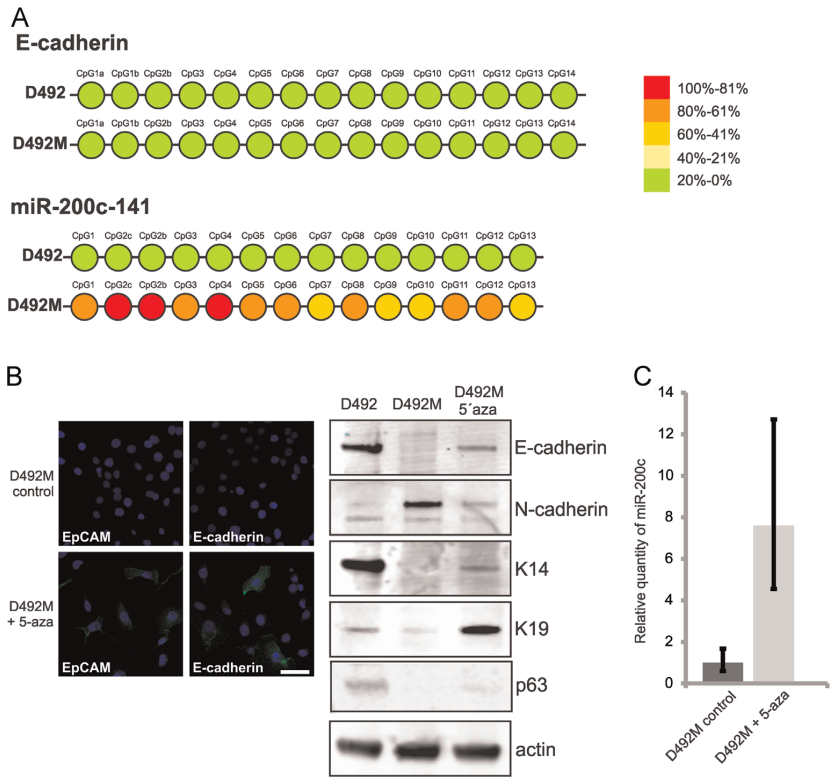

Fig. 2. The promoter region of miR-200c-141 is methylated in D492M. (A) The promoter area of miR-200c-141 is methylated in D492M. Bisulfite sequencing shows no methylation at the promoter region of E-cadherin in D492 and D492M. In contrast the promoter region of miR-200c-141 is methylated D492M only, where miR-200c and -141 expression is reduced. The color column on the right indicates percentage levels of methylation at CpG island promoter areas in E-cadherin and miR-200c-141. (B) 5-Azacytidine (5-Aza) treatment of D492M partially reverses the EMT phenotype. Immunostaining for E-cadherin and EpCAM (green) (left) demonstrates that expression is partially reestablished in D492M after treatment with a demethylation agent (5-aza). Cells were counterstained with TO-PRO-3 nuclearstain. Western blot demonstrated gain of epithelial phenotype in 5-aza treated cells as seen by increased expression of E-cadherin, K14 and K19 and decreased expression of N-cadherin but no change in p63 expression (right). Actin was used as a loading control. (C) 5-Aza treatment of D492M induces expression of miR-200c. U6 as loading control.

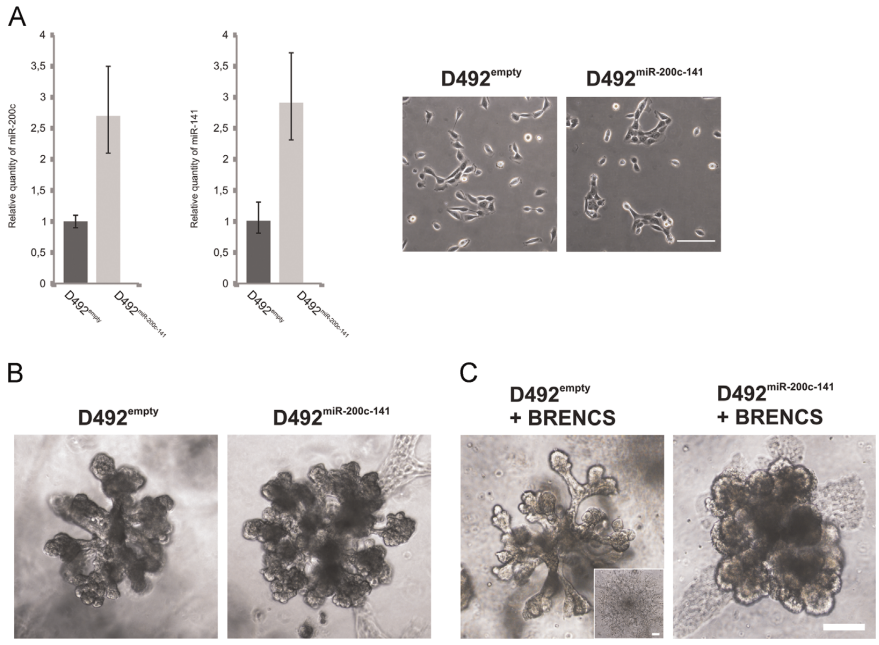

Fig. 3. Overexpression of miR-200c-141 in D492 inhibits EMT, but does not affect branching. (A) qPCR analysis verifies the overexpression of miR-200c and -141 in D492. D492M cells were transduced with a lentiviral construct containing miR-200c-141 ($D492^{miR\text{-}200c\text{-}141}$). Expression levels of miR-200c and -141 were 2–3 fold higher in $D492^{miR\text{-}200c\text{-}141}$ than in $D492^{empty}$ cells. miRNA levels were normalized to U6. (B) $D492^{miR\text{-}200c\text{-}141}$ cells cultured in rBM monoculture form branching colonies similar to $D492^{empty}$. (C) $D492^{miR\text{-}200c\text{-}141}$ are resistent to EMT in coculture with endothelial cells. $D492^{miR\text{-}200c\text{-}141}$ only form branching structures in coculture with BRENCS while $D492^{empty}$ form branching and mesenchymal colonies in coculture.

Overexpression of miR-200c-141 in D492 prevents endothelial induced EMT

Partial EMT (p-EMT) is a process previously described in wound healing and mammary tubulogenesis during branching morphogenesis (Leroy and Mostov, 2007). Our data shows that miR-200c and miR-141 are highly expressed in D492 to a level of approximately two fold that of primary breast epithelial cells (Fig. S3A). However miR-200c-141 could be locally downregulated at branching tips during branching morphogenesis as consequence of p-EMT. Local downregulation is not expected to influence levels of total miRNA and hence would not be detected in qPCR (Fig. 1E). To test if local downregulation of miR-200c and miR-141 is necessary for branching we constitutively overexpressed miR-200c-141 in D492 (Fig. 3A) thereby inhibiting possible partial downregulation by subpopulation of cells. $D492^{miR\text{-}200c\text{-}141}$ cells showed no differences in morphology in 2D culture (Fig. 3A) or in expression of critical epithelial markers (Fig. S3B). When embedded into rBM $D492^{miR\text{-}200c\text{-}141}$ showed a similar phenotype as $D492^{empty}$ (Fig. 3B). However, in contrast to $D492^{empty}$, $D492^{miR\text{-}200c\text{-}141}$ was unable to undergo EMT when cocultured with BRENCS and only formed branching structures, showing the efficiency of miR-200c-141 to maintain epithelial integrity and prevent EMT (Fig. 3C). We conclude that down-regulation of miR-200c-141 is necessary to undergo EMT, but not for branching morphogenesis in the breast.

Ectopic expression of miR-200c-141 in D492M induces luminal epithelial differentiation

To understand the importance of miR-200c-141 silencing in maintaining the mesenchymal phenotype seen in D492M, we constitutively overexpressed miR-200c-141 in D492M (Fig. 4A). Re-expression of miR-200c-141 in D492M reversed the mesenchymal phenotype allowing reemergence of cuboidal epithelial phenotype in monolayer culture and increased expression of luminal epithelial markers (EpCAM, E-cadherin, K19) and decreased expression of N-cadherin (Fig. 4A and B). Interestingly, $D492M^{miR\text{-}200c\text{-}141}$ does not express the myoepithelial keratins K5/6 and K14. Faint expression of K17 can be seen on western blot (Fig. 4B). Furthermore, $D492M^{miR\text{-}200c\text{-}141}$ fails to reestablish expression of the myoepithelial transcription factor p63 that is known to regulate expression of basal markers such as K14 and P-cadherin (Romano et al., 2007; Shimomura et al., 2008). Further characterization showed that the level of the EMT transcription factors, and targets of miR-200c and -141, ZEB1 and ZEB2 were decreased (Fig. S4A). These data indicate that miR-200c-141 is particularly important for maintaining the luminal epithelial phenotype. In order to support this further we analyzed the expression of miR-200c and -141 in purified primary luminal- and myoepithelial cells. The expression was 15–260 fold higher in the EpCAM positive luminal epithelial cells compared to the EpCAM negative fraction containing the myoepithelial cells (Fig. 4C). Having shown that forced expression of mir-200c-141 in D492M reestablished the luminal epithelial phenotype we evaluated its effect on the branching potential of D492M and the ability of the cell line to undergo endothelial-induced EMT.

D492MmiR-200c-141 cells form epithelial-like colonies in 3D culture and are resistant to endothelial-induced EMT

To evaluate the morphology of $D492M^{miR\text{-}200c\text{-}141}$ in 3D culture we seeded cells into rBM. In contrast to $D492M^{empty}$ that only generates mesenchymal/spindle-like structures, $D492M^{miR\text{-}200c\text{-}141}$ forms epithelial structures that, however, are not as complex as those generated from the original D492 cell line (compare Fig. 4D upper panel and Fig. 1A). Immunocytochemistry demonstrated a typical mesenchymal phenotype in the $D492M^{empty}$ cells as shown

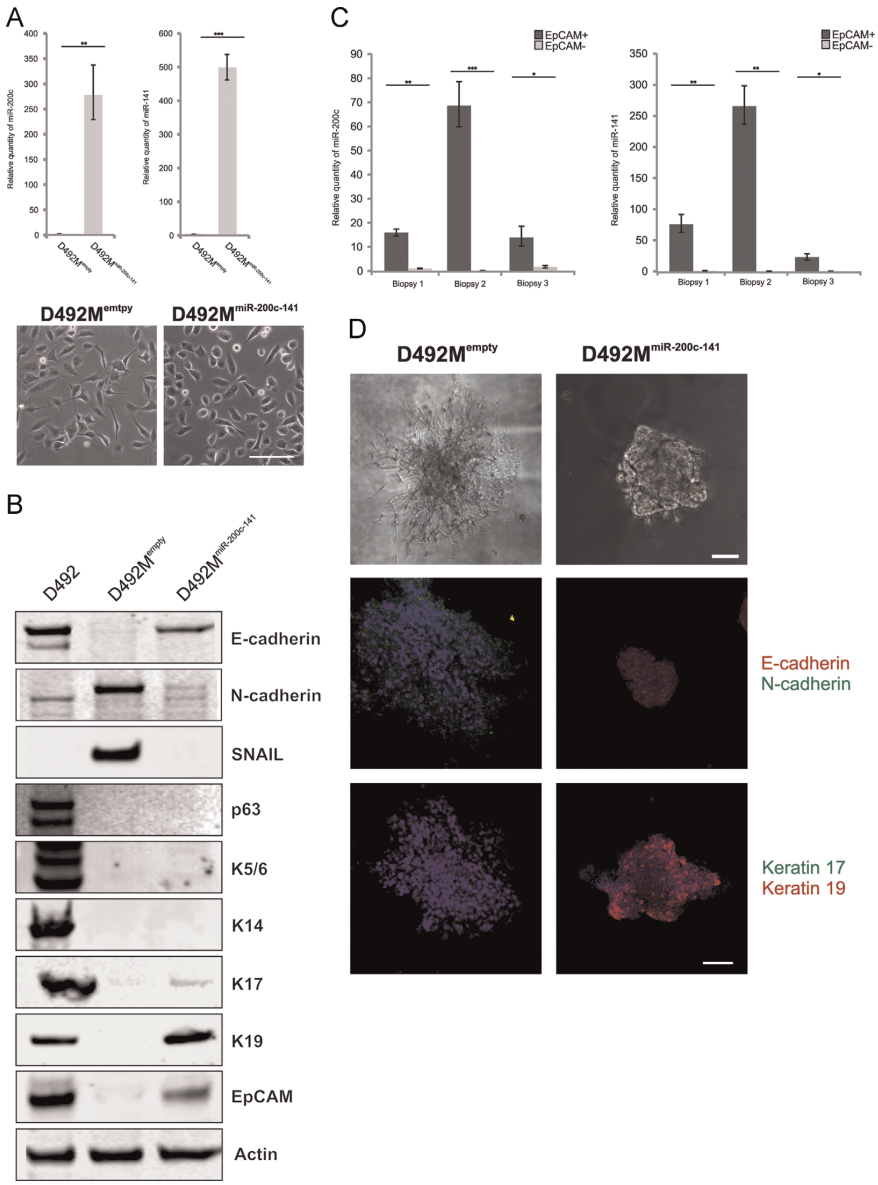

Fig. 4. Forced expression of miR-200c-141 induces luminal epithelial differentiation. (A) Overexpression of miR-200c-141 in D492M induces epithelial morphology in 2D culture. D492M cells were transduced with a lentiviral construct containing miR-200c-141 (D492M$^{miR\text{-}200c\text{-}141}$). The expression was 300–500 fold higher in D492M$^{miR\text{-}200c\text{-}141}$ than in D492M^{empty} cells. Phase contrast image of D492M$^{miR\text{-}200c\text{-}141}$ shows cuboidal epithelial phenotype in culture. miRNA levels were normalized to U6. Bar = 100 μM. (B) D492M$^{miR\text{-}200c\text{-}141}$ acquires luminal epithelial phenotype. Western blot demonstrates expression of E-cad, EpCAM and K19 in D492M$^{miR\text{-}200c\text{-}141}$ cells. In contrast little or no expression of p63, K14, K5/6, or K17 is seen. Also, the expression of the EMT markers N-cad and SNAIL is reduced compared to D492M^{empty}. Actin was used as a loading control. (C) miR-200c and miR-141 are luminal epithelial markers in the breast. qPCR analysis shows that EpCAM positive cells (luminal), express 5–7 fold more miR-200c and 40–120 fold more miR-141 than EpCAM negative cells (myoepithelial). Measurement was done in paired luminal and myoepithelial cells from three different biopsies. miRNA levels were normalized to SNORD48. (D) D492M^{empty} and D492M$^{miR\text{-}200c\text{-}141}$ form spindle and irregular branching like structures in 3D rBM culture, respectively. Immunostaining shows vague expression of N-cad (green) and strong E-cad (red) expression in D492M$^{miR\text{-}200c\text{-}141}$. Note the lack of polarity in N-cad expression (compared with Fig. 1A). D492M$^{miR\text{-}200c\text{-}141}$ retain K19 (red) expression in 3D culture but lack expression of K17 (green). Cells were counterstained with TO-PRO-3 nuclearstain. Bar = 100 μM.

by N-cadherin expression and lack of K14, K19 and E-cadherin expression. The D492M$^{miR\text{-}200c\text{-}141}$ cells showed a weak overall N-cadherin in 3D culture staining unlike D492 cells that expresses N-Cadherin particularly at the interface between lobular units. D492M$^{miR\text{-}200c\text{-}141}$ cells are E-cadherin positive and K19 positive, but negative for K17, confirming lack of myoepithelial differentiation in the cells. These results were confirmed by western blot analysis showing expression of luminal epithelial markers but not mesenchymal or myoepithelial markers in 3D (Fig. S4B). When cocultured with BRENCs previously shown to induce EMT in D492

(Sigurdsson et al., 2011), D492M$^{miR\text{-}200c\text{-}141}$ forms branching- and solid round colonies but not mesenchymal colonies (Fig. S5A–C). To further examine the role of miR-200c-141 in epithelial differentiation we treated D492 with miRNA inhibitors for miR-200c and miR-141 for 24 h and monitored the effect on known target genes (ZEB1 and ZEB2) and epithelial markers (Fig. S6). Significant changes were seen in ZEB2 expression, but there was no change in E-cadherin, N-cadherin, K14 and K19. ZEB1 expression was absent in both miR-200c-141 inhibitor treated D492 and the control D492 cell line. This data suggests that miR-200c-141 was only partly inhibited, potentially because of their high expression in D492, resulting in moderate effect in downstream targets, but not enough to induce phenotypic changes in D492.

p63 expression is necessary and sufficient for establishment of myoepithelial differentiation in D492M

The fact that miR-200c-141 was only able to rescue the luminal epithelial differentiation in D492M left us with the open question what regulates the myoepithelial differentiation in D492. p63 is a

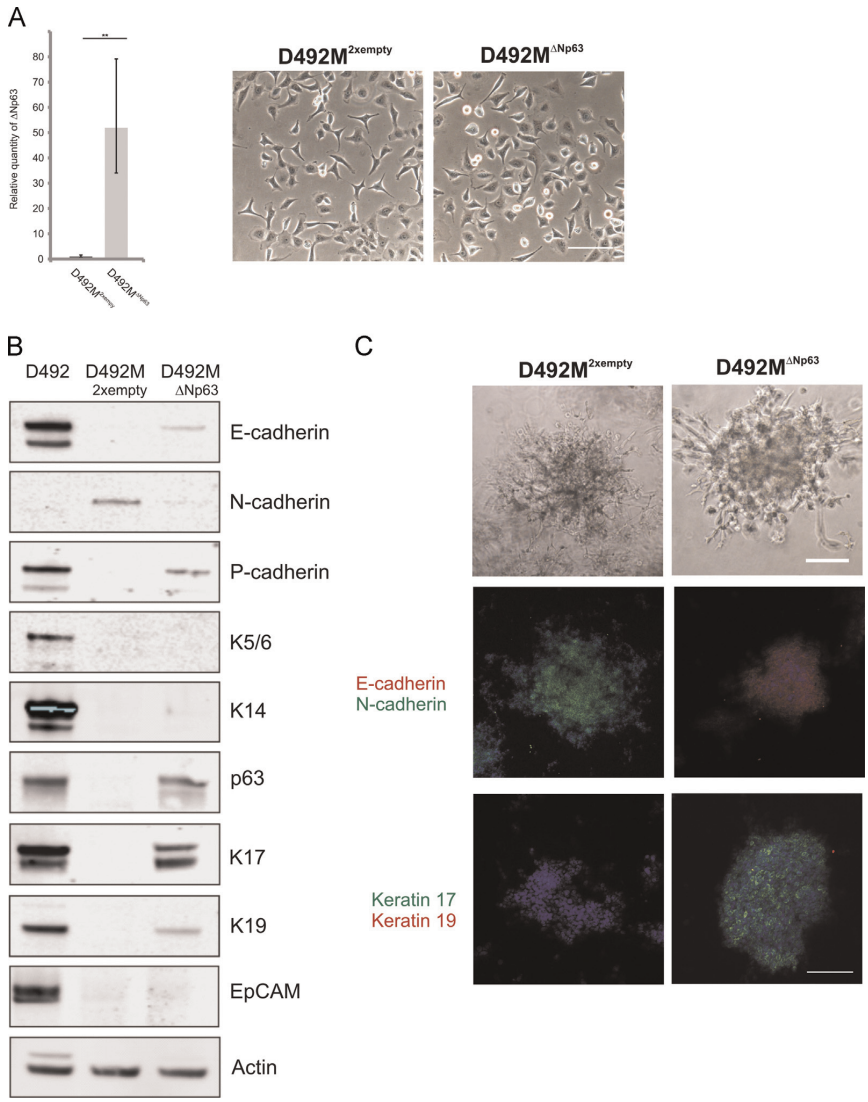

Fig. 5. Forced expression of ΔNp63 induces myoepithelial differentiation. (A) ΔNp63 overexpression has little effect on morphology of D492M in 2D culture. D492M cells were transduced with a lentiviral construct containing ΔNp63 (D492M$^{\Delta Np63}$). The expression levels of ΔNp63 were 50 fold higher in D492M$^{\Delta Np63}$ than in D492$^{2\times empty}$ cells. Phase contrast image of D492M$^{\Delta Np63}$ shows minor effect of ΔNp63 overexpression on cell morphology. miRNA levels were normalized to U6. Bar = 100 μM. (B) D492M$^{\Delta Np63}$ acquires myoepithelial phenotype. Western blot shows strong expression of the myoepithelial markers p63, K17 and P-cadherin and a vague K14 expression. Also, the expression of the EMT marker N-cad is reduced compared to D492M^{empty}. Actin was used as a loading control. (C) D492M$^{\Delta Np63}$ cell in rBM monoculture form irregular colonies. D492M$^{\Delta Np63}$ form structures with slightly more dense morphology than D492M, but retain the mesenchymal morphology of the parental cell line. IF staining shows strong expression of E-cad (red) and K17 (green) but lack of N-cad (green) and K19 (red) expression. Cells were counterstained with TO-PRO-3 nuclearstain. Bar = 100 μM.

known regulator of basal cells in number of epithelial organs such as the skin, lung, salivary glands and breast (Candi et al., 2008). Although the expression of p63 is associated with myoepithelial cells in the breast the functional role of this transcription factor in myoepithelial differentiation has not been thoroughly explored. ΔNp63 is downregulated in D492M compared to D492 (Fig. S7). We therefore overexpressed ΔNp63 in D492M (Fig. 5A). Expression of ΔNp63 in D492M resulted in a switch from N-cadherin to E-cadherin (Fig. 5B). Moreover D492M$^{\Delta Np63}$ cells expressed the myoepithelial markers K17 and P-cadherin but lack the luminal epithelial marker EpCAM. Upregulation of ΔNp63 in D492M induced expression of the luminal epithelial marker K19, but to a much lesser extent than miR-200c-141 (Fig. 4B). Surprisingly, ectopic expression of ΔNp63 did not result in K5/6 or K14 myoepithelial marker expression as reported in other organs (Romano et al., 2009). In 3D rBM culture the D492M$^{\Delta Np63}$ cells form structures with slightly more dense morphology than D492M, but retain the mesenchymal morphology of the parental cell line.

To confirm our results implicating ΔNp63 in linage decision of D492M we used lentiviral vector to knock down p63 in D492

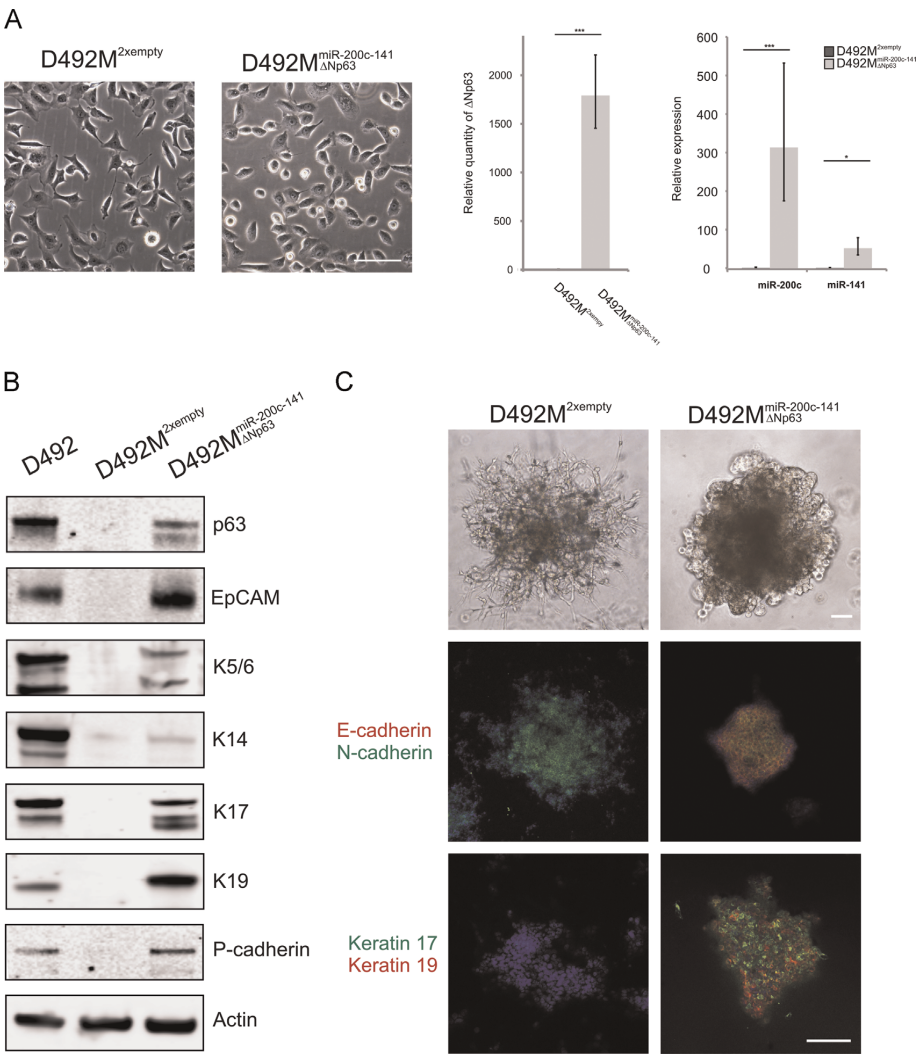

Fig. 6. Co-expression of mir-200c-141 and ΔNp63 induces LEP and MEP differentiation. (A) Co-expression of miR-200c-141 and ΔNp63 in D492M. D492M$^{\text{miR-200c-141}}$ were transduced with a lentiviral construct containing ΔNp63 (D492M$^{\text{miR-200c-141-}\Delta Np63}$). Phase contrast image of D492M$^{\text{miR-200c-141-}\Delta Np63}$ shows cuboidal epithelial phenotype in culture. miR-200c, miR-141 and ΔNp63 expression levels were 50–1700 fold higher in D492M$^{\text{miR-200c-141-}\Delta Np63}$ than in D492$^{2\times\text{empty}}$ cells, respectively. miRNA levels were normalized to U6. Bar = 100 μM. (B) miR-200c-141 and ΔNp63 coexpression induces expression of luminal and myoepithelial markers. Western blot shows strong expression of the myoepithelial markers p63, K5/6, K17 and P-cadherin and a vague K14 expression in D492M$^{\text{miR-200c-141-}\Delta Np63}$. The luminal markers EpCAM and K19 are also expressed. Actin as loading control. (C) D492M$^{\text{miR-200c-141-}\Delta Np63}$ cells in rBM monoculture form irregular branching colonies. Immunostaining shows co-expression of N-cad (green) and E-cad (red) D492M$^{\text{miR-200c-141-}\Delta p63}$. Note the lack of polarity in N-cad expression (compared with Fig. 1A). D492M$^{\text{miR-200c-141-}\Delta Np63}$ expresses both luminal marker K19 (red) and myoepithelial marker K17 (green). Cells were counterstained with TO-PRO-3 nuclearstain. Bar = 100 μM.

(Fig. S8A). Downregulation of p63 in D492 reduced expression of E-cadherin, P-cadherin and K14 but did not influence the levels of of N-cadherin and K19 (Fig. S8B and C).

Co-expression of mir-200c-141 and ΔNp63 in rescues the luminal–myoepithelial phenotype and induces branching

In an attempt to restore both luminal- and myoepthelial differentiation in D492M we transduced D492M with lentiviral vectors for the constitutive expression of miR-200c-141 and ΔNp63 (Fig. 6A). miR-200c-141 and ΔNp63 expression in D492M induced expression of various luminal and myoepithelial markers (Fig. 6B). Expression of key epithelial markers was similar to that found in D492. Interestingly, co-expression of these genes induces expression of K5/6 and K14, that were not expressed in D492M$^{miR\text{-}200c\text{-}141}$ or D492M$^{\Delta Np63}$. In 3D rBM culture the D492M$^{miR\text{-}200c\text{-}141\text{-}\Delta Np63}$ cells form epithelial structures with more mature branching than previously seen, but not as complex as D492 (Fig. 6C). Immunofluorescent staining of D492M expressing both miR-200c-141 and ΔNp63 shows induced expression of both K17 and K19 (Fig. 6C).

In regular 3D rBM culture, colonies result from the growth of a single cell. To further investigate the branching potential of D492M$^{miR\text{-}200c\text{-}141\text{-}\Delta Np63}$ we applied a cluster assay in which case the cells were preclustered in ultra-low adhesion plates for 24 h prior to seeding into matrigel. This assay allows the cells pre-arrange in multi-cell clusters before 3D culture. After 8 days culture period under this condition D492, D492M^{empty}, D492M$^{miR\text{-}200c\text{-}141}$ and D492M$^{\Delta Np63}$ form similar structures as described before, however, D492M$^{miR\text{-}200c\text{-}141\text{-}\Delta Np63}$ forms elaborate branching structures similar to D492 (Fig. 7A) which show overall expression of E-cad, K17 and K19 (Fig. 7B). Thus ectopic expression of both miR-200c-141 and ΔNp63 is necessary and sufficient to induce branching phenotype in D492M similar to D492.

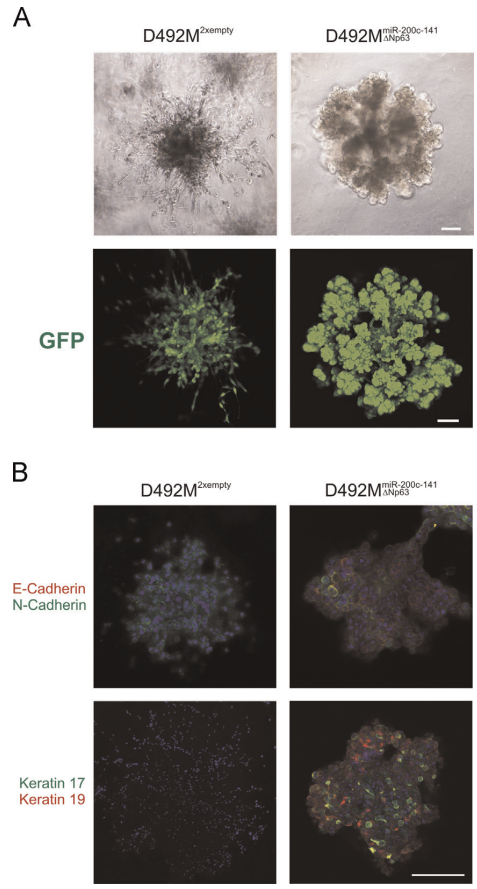

Fig. 7. Co-expression of mir-200c-141 and ΔNp63 in rescues the luminal–myoepithelial phenotype and induces branching. (A) D492M$^{miR\text{-}200c\text{-}141\text{-}\Delta Np63}$ form epithelial branching structures in cluster assay. Cells were preclustered in an ultra low adhesion plate for 24 h, embedded into matrigel and cultured for 8 days. D492M$^{miR\text{-}200c\text{-}141\text{-}\Delta Np63}$ form elaborate branching structures similar to D492 (see Fig. 1A) while D492M form mesenchymal structures in cluster assay (upper bright field, lower GFP). Bar = 100 μM. (B) Expression of luminal and myoeithelial markers in D492M$^{miR\text{-}200c\text{-}141\text{-}\Delta Np63}$. Immunostaining shows low N-cad (green) and strong E-cad (red) expression in D492M$^{miR\text{-}200c\text{-}141\text{-}\Delta p63}$ as well as K17 (green) and K19 (red) expression. Cells were counterstained with TO-PRO-3 nuclearstain. Bar = 100 μM.

Discussion

In this study we have identified critical elements controlling entry to the EMT program in breast epithelium using a model based on the human epithelial stem cell line D492. We found that forced expression of miR-200c-141 suppressed EMT in D492 and converted its mesenchymal derivative D492M towards epithelial phenotype of the luminal type. While expression of the miR-200c-141 construct did not rescue the branching potential of the original cell line, additional up-regulation of the myoepithelial marker ΔNp63 had a complimentary effect by restoring branching capacity. The results demonstrate the importance of miR-200c-141 for breast epithelial integrity in general and luminal epithelial differentiation in particular. They also underline the requirement for both luminal and myoepithelial elements for obtaining full branching morphogenesis in breast epithelium.

Our study was inspired by our initial observation showing that the permanent conversion of D492 to D492M was accompanied by dramatic down-regulation of the miR-200c-141 locus previously linked to epithelial integrity. After confirming our initial findings we demonstrated that the down-regulation is caused by methylation-based repression of the miR-200c-141 promoter. Previous studies are also in line with our data showing that GpC-rich promoter areas for miR-200c-141 are frequently methylated during EMT (Castilla et al., 2012; Vrba et al., 2010). Castilla et al. have shown that the miR-200c-141 locus is frequently hypermethylated in triple negative breast cancer and metablastic breast cancer both cancer subtypes showing prominent EMT phenotype. They also demonstrated hypermethylation of the miR-200-141 locus in cellular model of spontaneous EMT (Castilla et al., 2012). Vrba demonstrated that CpG island is unmethylated in promoter area of human miR-200/miR-141 expressing epithelial cells and in miR-200c/miR-141 positive tumor cells. They also also demonstrated that the CpG island is heavily methylated in human miR-200c/miR-141 negative fibroblasts and miR-200c/miR-141 negative tumor cells (Vrba et al., 2010).

In primary tissue, we found that expression levels of miR-200c and miR-141, was strong in luminal breast epithelium but levels were much lower in the myoepithelial compartment. This is in line with the results of Bockmeyer et al. who showed that miR-200c-141 expression in tissue from reduction mammoplasty was predominantly in the luminal epithelial compartment and to a much lesser extent in myoepithelial cells (Bockmeyer et al., 2011).

Our attempt to demonstrate the regulatory role of miR-200c-141 in EMT by forcing its expression in D492 resulted in complete inhibition of endothelial induced EMT, while allowing the cells to undergo branching morphogenesis. When the miR-200c-141 construct was expressed in D492M, it reestablished luminal epithelial

properties, accompanied with resistance towards endothelial induced EMT. However the inability of D492M$^{miR\text{-}200c\text{-}141}$ to restore full branching potential of the original cell line encouraged further search for complementary regulatory elements.

The strict commitment of D492M$^{miR\text{-}200c\text{-}141}$ to luminal differentiation suggested that either stem cell or myoepithelial/basal elements were missing for restoring the original branching potential. The p63 protein is being increasingly recognized as a master regulator of basal epithelial cells in stratified epithelium including skin, lung, prostate and the mammary gland (Blanpain and Fuchs, 2007; Senoo et al., 2007). Indeed, basal cells are considered stem cell or progenitor population in these organs (Blanpain and Fuchs, 2014). In the mammary gland, p63 is highly expressed in the basal layer that comprises both differentiated myoepithelial cells and candidate stem or progenitor cells (Yallowitz et al., 2014). Studies have revealed an important role for p63 during mammary gland development in both infant and adult mice. p63 knockout mice lack the mammary gland completely as consequence of absence of squamous epithelia and they are consequently not viable (McKeon, 2004; Yang et al., 1999). In the adult gland, Forster et al. showed that basal/myoepithelial cell specific p63 knock-out in virgin mice caused defects in luminal cell proliferation and differentiation resulting in failed lactation (Forster et al., 2014). Although expression of p63 is associated with myoepithelial and progenitor cells in the breast, its expression in the basal compartment is essential for luminal cell formation highlighting the importance of both cell types for TDLU formation in the breast. Since p63 expression is also down-regulated in D492M relative to D492 we hypothesized that restoration of the p63 protein levels would contribute to the branching potential. Forced expression of ΔNp63 in D492M resulted in increased expression of myoepithelial markers without influencing branching capacity. Simultaneous overexpression of miR-200c-141 and ΔNp63 in D492M resulted in complete reversion of the mesenchymal phenotype and D492M$^{miR\text{-}200c\text{-}141\Delta Np63}$ had the same profile of critical epithelial markers as D492. Furthermore, D492M$^{miR\text{-}200c\text{-}141\Delta Np63}$ was able to carry out complex branching morphogenesis in pre-clustered 3D assay.

In our study we demonstrate miR-200c-141 and p63 are strong regulators of luminal epithelial- and myoepithelial differentiation, respectively and coexpression of these molecules in D492M capture the branching morphogenesis seen in wild type D492. When D492 cells undergo EMT they lose stem cell properties measured by the ability to generate both luminal- and myoepithelial cells.

We have shown that in D492, EMT is associated with marked repression of the miR-200c-141 locus. Although the mesenchymal phenotype could be reversed with re-expression of miR-200c-141, the cells regain only the luminal epithelial phenotype suggesting that the bi-potential stem cell phenotype is dependent on additional factors. The reintroduction of transcription factor p63 into D492M induced mesenchymal to epithelial transition (MET) with a myoepithelial phenotype.

Recently, Shimono et al. showed that microRNAs including miR-200 family were downregulated in breast cancer stem cells and normal breast epithelial stem cells. In line with our results, they showed that miR-200c inhibited the ability of stem cells to generate mammary ducts and form tumors (Shimono et al., 2009). Although D492M$^{miR\text{-}200c\text{-}141}$ re-adapts the epithelial phenotype it is unable to generate branching structures at the same level as the parental cell line D492, possibly because of the requirement for basal/myoeptihelial factors in full branching. Interestingly, along with the fact that miR-200 family preserves epithelial integrity in normal tissue such as the breast gland and may as such act as tumor suppressors there are accumulating data showing that these miRNAs facilitate colonization and metastases of distant organs including the lung (Dykxhoorn et al., 2009; Korpal et al., 2011). This indicates that regulation of the miR-200 family may be context dependent both spatially and temporally.

In summary, our data suggest a key role for the miR-200c-141 locus in maintaining epithelial integrity, luminal differentiation and suppression of epithelial to mesenchymal transition in the human breast gland. ΔNp63, a myoepithelial marker in the breast gland, induced MET in D492M and restored myoepithelial differentiation. Co-expression of these genes resulted in complete MET and mature branching morphogenesis, underlining the importance of both luminal and myoepithelial compartments in breast morphogenesis.

Acknowledgment

This work was supported by Grants from Landspitali University Hospital Science Fund, University of Iceland Research Fund, Science and Technology Policy Council-Research Fund (Grant No. 120416022), “Göngum saman”, a supporting group for breast cancer research in Iceland (www.gongumsaman.is). The funders had no role in study design, data collection and analysis, decision to publish, or preparation of the manuscript.

Appendix A. Supplementary material

Supplementary data associated with this article can be found in the online version at doi:10.1016/j.ydbio.2015.05.007.

References

Ansieau, S., 2013. EMT in breast cancer stem cell generation. Cancer Lett. 338, 63–68.
Arason, A.J., Jonsdottir, H.R., Halldorsson, S., Benediktsdottir, B.E., Bergthorsson, J.T., Ingthorsson, S., Baldursson, O., Sinha, S., Gudjonsson, T., Magnusson, M.K., 2014. DeltaNp63 has a role in maintaining epithelial integrity in airway epithelium. PLoS One 9, e88683.
Blanpain, C., Fuchs, E., 2007. p63: revving up epithelial stem-cell potential. Nat. Cell Biol. 9, 731–733.
Blanpain, C., Fuchs, E., 2014. Stem cell plasticity. Plasticity of epithelial stem cells in tissue regeneration. Science 344, 1242281.
Bockmeyer, C.L., Christgen, M., Muller, M., Fischer, S., Ahrens, P., Langer, F., Kreipe, H., Lehmann, U., 2011. MicroRNA profiles of healthy basal and luminal mammary epithelial cells are distinct and reflected in different breast cancer subtypes. Breast Cancer Res. Treat. 130, 735–745.
Candi, E., Cipollone, R., Cervo, Rivetti di Val, Gonfloni, P., Melino, S., Knight, R., G., 2008. p63 in epithelial development. Cell. Mol. Life Sci. 65, 3126–3133.
Castilla, M.A., Diaz-Martin, J., Sarrio, D., Romero-Perez, L., Lopez-Garcia, M.A., Vieites, B., Biscuola, M., Ramiro-Fuentes, S., Isacke, C.M., Palacios, J., 2012. MicroRNA-200 family modulation in distinct breast cancer phenotypes. PLoS One 7, e47709.
Chatterjee, A., Upadhyay, S., Chang, X., Nagpal, J.K., Trink, B., Sidransky, D., 2008. U-box-type ubiquitin E4 ligase, UFD2a attenuates cisplatin mediated degradation of DeltaNp63alpha. Cell Cycle 7, 1231–1237.
Chernousov, M.A., Fogerty, F.J., Koteliansky, V.E., Mosher, D.F., 1991. Role of the I-9 and III-1 modules of fibronectin in formation of an extracellular fibronectin matrix. J. Biol. Chem. 266, 10851–10858.
Daniely, Y., Liao, G., Dixon, D., Linnoila, R.I., Lori, A., Randell, S.H., Oren, M., Jetten, A.M., 2004. Critical role of p63 in the development of a normal esophageal and tracheobronchial epithelium. Am. J. Physiol.—Cell Physiol. 287, C171–C181.
Davalos, V., Moutinho, C., Villanueva, A., Boque, R., Silva, P., Carneiro, F., Esteller, M., 2012. Dynamic epigenetic regulation of the microRNA-200 family mediates epithelial and mesenchymal transitions in human tumorigenesis. Oncogene 31, 2062–2074.
Dykxhoorn, D.M., Wu, Y., Xie, H., Yu, F., Lal, A., Petrocca, F., Martinvalet, D., Song, E., Lim, B., Lieberman, J., 2009. miR-200 enhances mouse breast cancer cell colonization to form distant metastases. PLoS One 4, e7181.
Edgar, R., Domrachev, M., Lash, A.E., 2002. Gene Expression Omnibus: NCBI gene expression and hybridization array data repository. Nucleic Acids Res. 30, 207–210.
Forster, N., Saladi, S.V., van Bragt, M., Sfondouris, M.E., Jones, F.E., Li, Z., Ellisen, L.W., 2014. Basal cell signaling by p63 controls luminal progenitor function and lactation via NRG1. Dev. Cell 28, 147–160.
Godar, S., Ince, T.A., Bell, G.W., Feldser, D., Donaher, J.L., Bergh, J., Liu, A., Miu, K., Watnick, R.S., Reinhardt, F., McAllister, S.S., Jacks, T., Weinberg, R.A., 2008. Growth-inhibitory and tumor- suppressive functions of p53 depend on its repression of CD44 expression. Cell 134, 62–73.

Gregory, P.A., Bert, A.G., Paterson, E.L., Barry, S.C., Tsykin, A., Farshid, G., Vadas, M.A., Khew-Goodall, Y., Goodall, G.J., 2008. The miR-200 family and miR-205 regulate epithelial to mesenchymal transition by targeting ZEB1 and SIP1. Nat. Cell Biol. 10, 593–601.

Gudjonsson, T., Ronnov-Jessen, L., Villadsen, R., Rank, F., Bissell, M.J., Petersen, O.W., 2002a. Normal and tumor-derived myoepithelial cells differ in their ability to interact with luminal breast epithelial cells for polarity and basement membrane deposition. J. Cell Sci. 115, 39–50.

Gudjonsson, T., Villadsen, R., Nielsen, H.L., Ronnov-Jessen, L., Bissell, M.J., Petersen, O.W., 2002b. Isolation, immortalization, and characterization of a human breast epithelial cell line with stem cell properties. Genes Dev. 16, 693–706.

Ha, M., Kim, V.N., 2014. Regulation of microRNA biogenesis. Nat. Rev. Mol. Cell Biol. 15, 509–524.

Hanahan, D., Weinberg, R.A., 2011. Hallmarks of cancer: the next generation. Cell 144, 646–674.

Hilmarsdottir, B., Briem, E., Bergthorsson, J.T., Magnusson, M.K., Gudjonsson, T., 2014. Functional role of the microrna-200 family in breast morphogenesis and neoplasia. Genes 5, 804–820.

Hirai, Y., Takebe, K., Takashina, M., Kobayashi, S., Takeichi, M., 1992. Epimorphin: a mesenchymal protein essential for epithelial morphogenesis. Cell 69, 471–481.

Howe, E.N., Cochrane, D.R., Richer, J.K., 2012. The miR-200 and miR-221/222 microRNA families: opposing effects on epithelial identity. J. Mammary Gland Biol. Neoplasia 17, 65–77.

Korpal, M., Ell, B.J., Buffa, F.M., Ibrahim, T., Blanco, M.A., Celia-Terrassa, T., Mercatali, L., Khan, Z., Goodarzi, H., Hua, Y., Wei, Y., Hu, G., Garcia, B.A., Ragoussis, J., Amadori, D., Harris, A.L., Kang, Y., 2011. Direct targeting of Sec23a by miR-200s influences cancer cell secretome and promotes metastatic colonization. Nat. Med. 17, 1101–1108.

Lee, G.Y., Kenny, P.A., Lee, E.H., Bissell, M.J., 2007. Three-dimensional culture models of normal and malignant breast epithelial cells. Nat. Methods 4, 359–365.

Leroy, P., Mostov, K.E., 2007. Slug is required for cell survival during partial epithelial-mesenchymal transition of HGF-induced tubulogenesis. Mol. Biol. Cell 18, 1943–1952.

McKeon, F., 2004. p63 and the epithelial stem cell: more than status quo? Genes Dev. 18, 465–469.

Mongroo, P.S., Rustgi, A.K., 2010. The role of the miR-200 family in epithelial-mesenchymal transition. Cancer Biol. Ther. 10, 219–222.

Olson, P., Lu, J., Zhang, H., Shai, A., Chun, M.G., Wang, Y., Libutti, S.K., Nakakura, E.K., Golub, T.R., Hanahan, D., 2009. MicroRNA dynamics in the stages of tumorigenesis correlate with hallmark capabilities of cancer. Genes Dev. 23, 2152–2165.

Pechoux, C., Gudjonsson, T., Ronnov-Jessen, L., Bissell, M.J., Petersen, O.W., 1999. Human mammary luminal epithelial cells contain progenitors to myoepithelial cells. Dev. Biol. 206, 88–99.

Pellegrini, G., Dellambra, E., Golisano, O., Martinelli, E., Fantozzi, I., Bondanza, S., Ponzin, D., McKeon, F., De Luca, M., 2001. p63 identifies keratinocyte stem cells. Proc. Natl. Acad. Sci. USA 98, 3156–3161.

Raouf, A., Sun, Y., Chatterjee, S., Basak, P., 2012. The biology of human breast epithelial progenitors. Semin. Cell Dev. Biol. 23, 606–612.

Reya, T., Morrison, S.J., Clarke, M.F., Weissman, I.L., 2001. Stem cells, cancer, and cancer stem cells. Nature 414, 105–111.

Romano, R.A., Birkaya, B., Sinha, S., 2007. A functional enhancer of keratin14 is a direct transcriptional target of deltaNp63. J. Investig. Dermatol. 127, 1175–1186.

Romano, R.A., Ortt, K., Birkaya, B., Smalley, K., Sinha, S., 2009. An active role of the DeltaN isoform of p63 in regulating basal keratin genes K5 and K14 and directing epidermal cell fate. PLoS One 4, e5623.

Saharia, A., Guittat, L., Crocker, S., Lim, A., Steffen, M., Kulkarni, S., Stewart, S.A., 2008. Flap endonuclease 1 contributes to telomere stability. Curr. Biol. 18, 496–500.

Senoo, M., Pinto, F., Crum, C.P., McKeon, F., 2007. p63 is essential for the proliferative potential of stem cells in stratified epithelia. Cell 129, 523–536.

Shimomura, Y., Wajid, M., Shapiro, L., Christiano, A.M., 2008. P-cadherin is a p63 target gene with a crucial role in the developing human limb bud and hair follicle. Development 135, 743–753.

Shimono, Y., Zabala, M., Cho, R.W., Lobo, N., Dalerba, P., Qian, D., Diehn, M., Liu, H., Panula, S.P., Chiao, E., Dirbas, F.M., Somlo, G., Pera, R.A., Lao, K., Clarke, M.F., 2009. Downregulation of miRNA-200c links breast cancer stem cells with normal stem cells. Cell 138, 592–603.

Sigurdsson, V., Fridriksdottir, A.J., Kjartansson, J., Jonasson, J.G., Steinarsdottir, M., Petersen, O.W., Ogmundsdottir, H.M., Gudjonsson, T., 2006. Human breast microvascular endothelial cells retain phenotypic traits in long-term finite life span culture. In Vitro Cell Dev. Biol. Anim. 42, 332–340.

Sigurdsson, V., Hilmarsdottir, B., Sigmundsdottir, H., Fridriksdottir, A.J., Ringner, M., Villadsen, R., Borg, A., Agnarsson, B.A., Petersen, O.W., Magnusson, M.K., Gudjonsson, T., 2011. Endothelial induced EMT in breast epithelial cells with stem cell properties. PLoS One 6, e23833.

Sigurdsson, V., Ingthorsson, S., Hilmarsdottir, B., Gustafsdottir, S.M., Franzdottir, S.R., Arason, A.J., Steingrimsson, E., Magnusson, M.K., Gudjonsson, T., 2013. Expression and functional role of sprouty-2 in breast morphogenesis. PLoS One 8, e60798.

Smalley, M., Ashworth, A., 2003. Stem cells and breast cancer: a field in transit. Nat. Rev. Cancer 3, 832–844.

Tusher, V.G., Tibshirani, R., Chu, G., 2001. Significance analysis of microarrays applied to the ionizing radiation response. Proc. Natl. Acad. Sci. USA 98, 5116–5121.

Villadsen, R., Fridriksdottir, A.J., Ronnov-Jessen, L., Gudjonsson, T., Rank, F., LaBarge, M.A., Bissell, M.J., Petersen, O.W., 2007. Evidence for a stem cell hierarchy in the adult human breast. J. Cell Biol. 177, 87–101.

Vrba, L., Jensen, T.J., Garbe, J.C., Heimark, R.L., Cress, A.E., Dickinson, S., Stampfer, M.R., Futscher, B.W., 2010. Role for DNA methylation in the regulation of miR-200c and miR-141 expression in normal and cancer cells. PLoS One 5, e8697.

Wellner, U., Schubert, J., Burk, U.C., Schmalhofer, O., Zhu, F., Sonntag, A., Waldvogel, B., Vannier, C., Darling, D., zur Hausen, A., Brunton, V.G., Morton, J., Sansom, O., Schuler, J., Stemmler, M.P., Herzberger, C., Hopt, U., Keck, T., Brabletz, S., Brabletz, T., 2009. The EMT-activator ZEB1 promotes tumorigenicity by repressing stemness-inhibiting microRNAs. Nat. Cell Biol. 11, 1487–1495.

Wiklund, E.D., Bramsen, J.B., Hulf, T., Dyrskjot, L., Ramanathan, R., Hansen, T.B., Villadsen, S.B., Gao, S., Ostenfeld, M.S., Borre, M., Peter, M.E., Orntoft, T.F., Kjems, J., Clark, S.J., 2010. Coordinated epigenetic repression of the miR-200 family and miR-205 in invasive bladder cancer. Int. J. Cancer 128, 1327–1334.

Wiznerowicz, M., Trono, D., 2003. Conditional suppression of cellular genes: lentivirus vector-mediated drug-inducible RNA interference. J. Virol. 77, 8957–8961.

Woodward, W.A., Chen, M.S., Behbod, F., Rosen, J.M., 2005. On mammary stem cells. J. Cell Sci. 118, 3585–3594.

Yallowitz, A.R., Alexandrova, E.M., Talos, F., Xu, S., Marchenko, N.D., Moll, U.M., 2014. p63 is a prosurvival factor in the adult mammary gland during post-lactational involution, affecting PI-MECs and ErbB2 tumorigenesis. Cell Death Differ. 21, 645–654.

Yang, A., Schweitzer, R., Sun, D., Kaghad, M., Walker, N., Bronson, R.T., Tabin, C., Sharpe, A., Caput, D., Crum, C., McKeon, F., 1999. p63 is essential for regenerative proliferation in limb, craniofacial and epithelial development. Nature 398, 714–718.

Yang, C.S., Rana, T.M., 2013. Learning the molecular mechanisms of the reprogramming factors: let's start from microRNAs. Mol. Biosyst. 9, 10–17.

Zapata, A.G., Alfaro, D., Garcia-Ceca, J., 2012. Biology of stem cells: the role of microenvironments. Adv. Exp. Med. Biol. 741, 135–151.

Paper II

Manuscript Details

Manuscript number	DEVELOPMENTALBIOLOGY_2018_143
Title	MiR-203a is differentially expressed during branching morphogenesis and EMT in breast progenitor cells and is a repressor of peroxidasin
Article type	Research Paper

Abstract

MicroRNAs regulate developmental events such as branching morphogenesis, epithelial to mesenchymal transition (EMT) and its reverse process mesenchymal to epithelial transition (MET). In this study, we performed small RNA sequencing of a breast epithelial progenitor cell line (D492), and its mesenchymal derivative (D492M) cultured in three-dimensional microenvironment. Among the most downregulated miRNAs in D492M was miR-203a, a miRNA that plays an important role in epithelial differentiation. Increased expression of miR-203a was seen in D492, concomitant with increased complexity of branching. When miR-203a was overexpressed in D492M, a partial reversion towards epithelial phenotype was seen. Gene expression analysis of D492M and D492MmiR-203a revealed peroxidasin, a collagen IV cross-linker, as the most significantly downregulated gene in D492MmiR-203a. Collectively, we demonstrate that miR-203a expression temporally correlates with branching morphogenesis and is suppressed in D492M. Overexpression of miR-203a in D492M induces a partial MET and reduces the expression of peroxidasin. Furthermore, we demonstrate that miR-203a is a novel repressor of peroxidasin. MiR-203-peroxidasin axis may be an important regulator in branching morphogenesis, EMT/MET and basement membrane remodeling.

Keywords	microRNA; niR-203a; breast morphogenesis; EMT; Stem cells; 3D culture; Peroxidasin
Manuscript category	Developmental Biology - Main

Corresponding Author	Thorarinn Gudjonsson
Corresponding Author's Institution	Univeristy of Iceland
Order of Authors	Thorarinn Gudjonsson, Eirikur Briem, Zuzana Budkova, Anna Karen Sigurdardottir, Jennifer Kricker, Gunnhildur Asta Traustadottir, Bylgja Hilmarsdottir, Magnus Karl Magnusson, Winston Timp

Submission Files Included in this PDF

File Name [File Type]

Briem et al Cover letter.doc [Cover Letter]

Briem et al Manuscript.docx [Manuscript File]

Figure 1 A-B.pdf [Figure]

Figure 2 A-B.pdf [Figure]

Figure 3 A.pdf [Figure]

Figure 3 B-C.pdf [Figure]

Figure 4 A-I.pdf [Figure]

Figure 5 A-C.pdf [Figure]

Figure 5 D.pdf [Figure]

Figure S1.pdf [Figure]

Table S1.docx [Table]

Submission Files Not Included in this PDF

File Name [File Type]

Table S2.xlsx [Table]

To view all the submission files, including those not included in the PDF, click on the manuscript title on your EVISE Homepage, then click 'Download zip file'.

Thursday, March 29, 2018

Dear editor.

Please find our manuscript entitled*"* **MiR-203a is differentially expressed during branching morphogenesis and EMT in breast progenitor cells and is a repressor of peroxidasin**" submitted by Eirikur Briem, Zuzana Budkova, Anna Karen Sigurdardottir, Bylgja Hilmarsdottir, Jennifer Kricker, Winston Timp, Magnus Karl Magnusson, Gunnhildur Traustadottir and Thorarinn Gudjonsson to Developmen. This is original data that has not been published elsewhere.

Corresponding author:
Thorarinn Gudjonsson. E-mail: tgudjons@hi.is
Stem Cell Research Unit, Biomedical Center, Department of Anatomy, Faculty of Medicine, School of Health Sciences, University of Iceland.

Co-authors:
Eirikur Briem (eib13@hi.is), Zuzana Budkova (zub1@hi.is) , Anna Karen Sigurdardottir (aks6@hi.is), Bylgja Hilmarsdottir (bylgjah@gmail.com), Jennifer Kricker (jennik11@gmail.com), Winston Timp (wtimp@jhu.edu), Magnus Karl Magnusson (magnuskm@hi.is), Gunnhildur Traustadottir (gutra@hi.is).

In this study, we applied D492 a breast epithelial stem cell line and its mesenchymal derivative D492M to analyze the role of microRNAs in branching morphogenesis and EMT. We performed small RNA sequencing on D492 and D492M cultured in three-dimensional reconstituted basement membrane matrix (3D-rBM). When analyzed over time (21 days) in 3D culture, increased expression of miR-203a was seen in D492, concomitant with increased complexity of the branching structures. This is consistent with changes previously shown to occur in the mouse mammary gland *in vivo*. When miR-203a was overexpressed in D492M (D492M$^{miR\text{-}203a}$), a partial reversion towards epithelial phenotype was seen. Gene expression analysis of D492M and D492M$^{miR\text{-}203a}$ revealed that peroxidasin (PXDN), a collagen IV cross-linker was the most significantly downregulated gene in D492M$^{miR\text{-}203a}$. Bioinformatics analysis revealed that PXDN has three putative binding sites for miR-203a in its 3'-UTR. To verify the binding of miR-203a to the 3'-UTR of PXDN we set up a luciferase reporter assay that confirmed the binding.
Collectively, we have shown that miR-203a expression temporally correlates with branching morphogenesis in 3D-rBM and is suppressed in the mesenchymal state. Overexpression of miR-203a in D492M induces a partial mesenchymal to epithelial transition. Finally, we demonstrate that miR-203a is a novel repressor of PXDN.

All authors have read the manuscript, agree with its contents, and have declared that no competing interests exist. This manuscript is submitted solely to Developmental, and has not been published elsewhere.

On behalf of my co-authors,
Yours Sincerely,

Thorarinn Gudjonsson, Professor

MiR-203a is differentially expressed during branching morphogenesis and EMT in breast progenitor cells and is a repressor of peroxidasin

Eirikur Briem[1], Zuzana Budkova[1], Anna Karen Sigurdardottir[1], Bylgja Hilmarsdottir[1,4], Jennifer Kricker[1], Winston Timp[5], Magnus Karl Magnusson[2,3], Gunnhildur Traustadottir[1] and Thorarinn Gudjonsson[1,2]

[1]Stem Cell Research Unit, Biomedical Center, Department of Anatomy, Faculty of Medicine, School of Health Sciences, University of Iceland, Iceland

[2]Department of Laboratory Hematology, Landspitali - University Hospital, Iceland

[3]Department of Pharmacology and Toxicology, Faculty of Medicine, School of Health Sciences, University of Iceland, Iceland

[4]Department of Tumor Biology, The Norwegian Radium Hospital, Oslo, Norway

[5]Department of Biomedical Engineering, Johns Hopkins University, USA

Correspondence: T Gudjonsson, Stem Cell Research Unit, Department of Medical Faculty, Biomedical Center, University of Iceland, Vatnsmyrarvegi 16, 101 Reykjavík, Iceland.
Tel: +354-525 4827; Fax: +354 525 4884. E-mail: tgudjons@hi.is

Summary statement

MiR-203a is highly upregulated during branching morphogenesis of D492 breast epithelial progenitor cells and is downregulated in its isogenic mesenchymal cell line D492M. Furthermore, miR-203a is a novel suppressor of peroxidasin, a collagen IV crosslinking agent. MiR-203a-Peroxdasin axis may be important regulator of branching morphogenesis and basement remodeling in the human breast gland.

Abstract

MicroRNAs regulate developmental events such as branching morphogenesis, epithelial to mesenchymal transition (EMT) and its reverse process mesenchymal to epithelial transition (MET). In this study, we performed small RNA sequencing of a breast epithelial progenitor cell line (D492), and its mesenchymal derivative (D492M) cultured in three-dimensional microenvironment. Among the most downregulated miRNAs in D492M was miR-203a, a miRNA that plays an important role in epithelial differentiation. Increased expression of miR-203a was seen in D492, concomitant with increased complexity of branching. When miR-203a was overexpressed in D492M, a partial reversion towards epithelial phenotype was seen. Gene expression analysis of D492M and D492M$^{miR\text{-}203a}$ revealed peroxidasin, a collagen IV cross-linker, as the most significantly downregulated gene in D492M$^{miR\text{-}203a}$. Collectively, we demonstrate that miR-203a expression temporally correlates with branching morphogenesis and is suppressed in D492M. Overexpression of miR-203a in D492M induces a partial MET and reduces the expression of peroxidasin. Furthermore, we demonstrate that miR-203a is a novel repressor of peroxidasin. MiR-203-peroxidasin axis may be an important regulator in branching morphogenesis, EMT/MET and basement membrane remodeling.

Introduction

Developmental events underlying breast epithelial morphogenesis are closely related to pathways important to cancer progression, i.e. epithelial to mesenchymal transition (EMT) and mesenchymal to epithelial transition (MET). Evidence shows that the two distinct epithelial cell lineages that make up branching morphogenesis in the breast, luminal- and myoepithelial cells, originate from common breast epithelial stem cells (Pechoux, Gudjonsson et al. 1999, Gudjonsson, Villadsen et al. 2002, Villadsen, Fridriksdottir et al. 2007, Petersen and Polyak 2010). These stem cells are responsible for continuous tissue remodeling throughout the reproductive period, as well as the extensive epithelial expansion and branching morphogenesis seen during pregnancy and lactation. D492 is a breast epithelial stem cell line that generates branching *in vivo*-like structures in 3D-rBM (Gudjonsson, Villadsen et al. 2002, Villadsen, Fridriksdottir et al. 2007, Sigurdsson, Hilmarsdottir et al. 2011). We have previously shown when D492 is co-cultured under 3D conditions, breast endothelial cells markedly stimulate their branching ability, but can also induce an irreversible EMT in the epithelial cells (Sigurdsson, Hilmarsdottir et al. 2011). This condition gave rise to the D492M cell line (Sigurdsson, Hilmarsdottir et al. 2011). In EMT, different pathways ultimately control transcriptional regulatory factors such as SNAI1, SNAI2, TWIST, ZEB1 and ZEB2 leading to increased expression of mesenchymal and decreased expression of epithelial markers (Moustakas and Heldin 2007). Downregulation of the epithelial cell-cell adhesion proteins, such as E-cadherin, is one of the hallmarks of EMT (Peinado, Olmeda et al. 2007). In addition, expression of epithelial specific keratins is often greatly reduced, while expression of mesenchymal markers, such as N-cadherin, vimentin, alpha smooth muscle actin and fibronectin are increased in EMT (Moustakas and Heldin 2007). Enhanced migration, invasion and resistance to apoptosis are also characteristic for cells that have undergone EMT (Hanahan and Weinberg 2011). The tightly regulated process of cell conversion seen in EMT is also a critical event seen in many cancer types, including breast cancer (Petersen, Lind Nielsen et al. 2001, Mani, Guo et al. 2008, Sarrio, Rodriguez-Pinilla et al. 2008) and EMT is typically associated with increased aggressiveness and metastatic behavior

(Hanahan and Weinberg 2011).

Interestingly, the mesenchymal transition from D492 to D492M is accompanied by drastic changes in microRNA (miRNA) expression (Hilmarsdottir, Briem et al. 2015). MiRNAs have been described as regulators of protein expression through their ability to bind and silence mRNAs, where silencing of certain transcription factors, which are important for gene regulation may cause marked changes in cell phenotype and fate (Hilmarsdottir, Briem et al. 2014). In recent years, miRNAs have been shown to be either tumor promoting or tumor suppressing depending on context and cancer type. For example, the miR-200 family has been linked to both stem cell regulation and cancer progression (Shimono, Zabala et al. 2009). This family of miRNAs is strongly downregulated in tumors with high metastatic potential (Olson, Lu et al. 2009) and miR-200c, a member of this family, is downregulated in human breast cancer stem cells and normal mammary stem cells (Shimono, Zabala et al. 2009). We have recently shown that the miRNA-200c-141 cluster is predominantly expressed in luminal breast epithelial cells, and that miRNA-200c-141 is highly expressed in D492, but not in D492M. Interestingly, overexpression of miR-200c-141 in D492M restored the luminal epithelial phenotype (Hilmarsdottir, Briem et al. 2015).

In this study, we compared the miRNA expression profile of D492 and D492M, when cultured in 3D reconstituted basement membrane matrix (3D-rBM). Small RNA sequencing revealed a striking difference in expression patterns between the two cell lines, with a number of known epithelial miRNAs, including miR-203a, downregulated in D492M. We demonstrated that miR-203a expression increases during branching morphogenesis *in vitro* similar to its expression pattern in mouse mammary gland *in vivo* (Avril-Sassen, Goldstein et al. 2009). Furthermore, overexpression of miR-203a in D492M induced partial phenotypic changes towards MET, reduced cell proliferation, migration, invasion, and increased sensitivity to chemically induced apoptosis. Finally, we identified miR-203a as a novel repressor of peroxidasin (PXDN), an extracellular matrix protein with peroxidase activity and a collagen IV crosslinking agent.

Results

Comparison of miRNA expression in the breast epithelial progenitor cell line D492 and its mesenchymal derivative D492M.

D492 and D492M are isogenic cell lines with epithelial and mesenchymal phenotypes, respectively. We have previously shown a profound difference in miRNA expression between these cell lines when cultured in monolayer (Hilmarsdottir, Briem et al. 2015). Here, we conducted an expression analysis in 3D culture. Due to its stem cell properties, D492 can generate branching structures in 3D-rBM culture reminiscent of terminal duct lobular units (TDLUs) in the breast. In contrast, D492M form disorganized mesenchymal-like structures with spindle shape protrusions of cells (Fig. 1A, top). To investigate the miRNA expression patterns between D492 and D492M in 3D-rBM we performed small RNA sequencing (Fig. 1A). This revealed 47 differentially expressed miRNAs (>1.5-fold change, $p<0.05$ and FDR<0.1) between D492 from (days 7, 14 and 21) and D492M at day 14 in 3D culture, where 20 of these miRNAs were downregulated in D492M. Among the most profound changes was downregulation of miR-200c, miR-141, miR-205 and miR-203a in D492M (Fig. 1A), all of which have been previously associated with epithelial integrity and repression of EMT (Gregory, Bert et al. 2008, Wellner, Schubert et al. 2009, Feng, Wang et al. 2014). These miRNAs were all downregulated with high statistical significance in D492M as shown in the volcano plot (Fig. 1B). The upregulated miRNAs in D492M do not show as clear involvement in EMT as the downregulated ones.

Downregulation of miR-203a in D492M is not due to methylation of its CpG islands in the promoter area.

Methylation of CpG islands in promoter areas is a common event during gene silencing. To further explore what causes downregulation of miRNAs in D492M, we explored the promoter DNA methylation status of differentially expressed miRNAs. We used the HumanMethylation450K BeadChip and looked at CpGs within 5 kb region of the promoter area of differentially expressed miRNAs. Two miRNAs did not have

probes within the 5 kb region of the gene but of the 45 which did, 8 miRNAs showed differential DNA methylation between D492 and D492M (Table S2). Our data shows that promoter areas upstream of miR-200c-141 and miR-205 were methylated in D492M, but not in D492 (Fig. 2A). In contrast, the promoter area of miR-203a was not differentially methylated between D492 and D492M (Fig. 2A). Bisulfite sequencing of the promoter area of miR-200c-141, miR-205 and miR-203a confirmed that the promoter of miR-203a was unmethylated in D492M, unlike the promoters of miR-200c-141 and miR-205 (Fig. 2B). This is in contrast to previously published results in human mammary epithelial cells (HMLE) undergoing EMT (Taube, Malouf et al. 2013) and some metastatic breast cancer cell lines (Zhang, Zhang et al. 2011), where the promoter of miR-203a becomes methylated. Our data shows that a profound downregulation of miR-203a could be mediated through other mechanisms than DNA methylation, such as histone modifications. Indeed, miR-203a expression has been shown to be suppressed by EZH2 in prostate cancer (Cao, Mani et al. 2011). In summary, the repression of miR-203a, in endothelial induced EMT of D492 is not due to promoter methylation.

MiR-203a shows temporal changes in expression during branching morphogenesis in 3D culture and is associated with luminal breast epithelial cells.

The breast gland is a dynamic organ during the reproduction period. In each menstruation cycle the breast epithelium undergoes changes associated with branching morphogenesis and if pregnancy occurs, the branching epithelium expands resulting in maximal differentiation during lactation. The glandular epithelium then is subject to apoptosis after breastfeeding during the involution phase (Javed and Lteif 2013). Using D492 breast progenitor cells that are capable of generating branching epithelial morphogenesis in 3D-rBM, it is possible to analyze temporal changes during the branching process. To investigate if changes in miRNA expression occur during formation of TDLU–like structures in 3D-rBM, we isolated RNA from 3D-rBM cultures at days 7, 14 and 21, and performed small RNA sequencing.

Fifty-five miRNAs were differentially expressed between individual time points (>2-fold change, FDR corrected p-value < 0.05), thereof 40 miRNAs were downregulated and 15 miRNAs were upregulated during branching (Fig. 3A). In particular, among the upregulated miRNAs were miR-141 and miR-203, which were also some of the most downregulated miRNAs in D492M (Fig. 1A). Thus, small RNA sequencing, and subsequent verification with RT-qPCR, demonstrates that expression of miR-203a and miR-141 increased between time points and peaked at the late branching stage (day 21) (Fig. 3A-B). In contrast, expression of miR-205 and miR-200c was constant throughout the branching process (Fig. 3B). This indicates that miR-203a and miR-141 may play a role in differentiation of the epithelial cells during branching morphogenesis. The human breast epithelium is composed of two epithelial lineages, the luminal epithelial and the myoepithelial cells. In order to investigate whether miR-203a expression was lineage specific with either luminal- or myoepithelial cells, we sorted primary breast epithelial cells with EpCAM positive magnetic beads, as EpCAM is a luminal associated adhesion molecule that is also highly useful for antibody-based enrichment of luminal epithelial cells. We measured miR-203a expression in EpCAM high and EpCAM low cells, and demonstrated that, miR-203a expression was predominately associated with the EpCAM high luminal epithelial cells (Fig. 3C, left). There was some expression in the EpCAM low/negative myoepithelial cells, but no or little expression in endothelial cells and fibroblast (Fig. 3C, left). Due to the bipotential properties of D492 cells, they are able to generate luminal- and myoepithelial cells and differentiation of D492 branching colonies, into the two epithelial lineages, is clearly demonstrated with immunostaining against luminal- and myoepithelial markers (Gudjonsson, Villadsen et al. 2002). Based on EpCAM sorting of D492 cells into EpCAM high and EpCAM low fractions, we further confirmed that miR-203a was more associated with the luminal epithelial population in D492 (Fig. 3C, right). Differential expression of miR-203a between D492 and D492M was confirmed by RT-qPCR (Fig. 3C, right). To determine if this was in concurrence with other breast cell lines with epithelial and mesenchymal phenotypes, we examined the expression levels of miR-203a in HMLE, its mesenchymal derivative HMLEmes (Fig. 3C, right), the normal cell-derived MCF10A, and the mesenchymal cancer cell line, MDA-MB-231 (Fig. 3C, right).

Expression of miR-203a was restricted to all three cell lines with an epithelial phenotype.

MiR-203a expression reduces the mesenchymal traits of D492M cells.

To analyze if the presence of miR-203a affects the phenotype of D492M, we overexpressed miR-203a in D492M (D492M$^{miR\text{-}203a}$), using a lentiviral based transfection system. D492M$^{miR\text{-}203a}$ expressed miR-203a 17,500-fold higher than control (D492M^{Empty}) (Fig. 4A). Interestingly, phase contrast images of monolayer cultures show that miR-203a overexpression in D492M causes increased adherence between cells (Fig. 4B). Furthermore, when D492M is cultivated in 3D-rBM, it forms spindle shaped mesenchymal-like colonies in contrast to D492M$^{miR\text{-}203a}$ that forms more compact colonies although the colonies still show cellular protrusions, typical of mesenchymal cells (Fig. 4B). When the cells were cultured in monolayer, overexpression of miR-203a in D492M reduces the proliferation rate of the cells (Fig. 4C). Furthermore, there was visible reduction in expression of the mesenchymal marker N-cadherin and increased expression of E-cadherin, K14 and K19 in D492M$^{miR\text{-}203a}$, indicating a moderate reduction in mesenchymal characteristics (Fig. 4D-E). The EMT transcription factor SNAI2 is a confirmed target of miR-203a, and miR-203a is in return suppressed by SNAI2 forming a negative feedback loop (Ding, Park et al. 2013). In concordance with SNAI2 being a target of miR-203a, there was reduced expression of SNAI2 when miR-203a was overexpressed in D492M (Fig. 4F). Since the EMT phenotype has been associated with apoptosis resistance and SNAI2 is a known inhibitor of apoptosis (Inoue, Seidel et al. 2002), we asked if D492M$^{miR\text{-}203a}$ cells were less resistant to chemically induced apoptosis compared to D492M^{Empty}. Indeed, D492M$^{miR\text{-}203a}$ cells were more sensitive than D492M^{Empty} to camptothecin, a chemical inducer of apoptosis (Fig. 4G).

The ability of cells to proliferate as non-adherent mammospheres in suspension has been described as a property of early progenitor/stem cells (Dontu, Abdallah et al. 2003). When D492 and D492M were cultured in low attachment plates both generated

mammospheres but D492M generated significantly larger and a higher number of colonies (Sigurdsson, Hilmarsdottir et al. 2011). Interestingly, overexpression of miR-203a in D492M negatively impacts anchorage independent growth, resulting in loss of progenitor/stem cell properties indicating that miR-203a overexpression in D492M induces cellular differentiation (Fig. 4H). As mesenchymal cells have increased motility compared to epithelial cells, we analyzed the effect of miR-203a overexpression on the ability of D492M to migrate and invade. D492M$^{miR\text{-}203a}$ cells showed reduced ability to migrate through transwell filters (Fig. 4I, left) and to invade through matrigel coated transwell filters (Fig. 4I, right) indicating a suppression of mesenchymal characteristics. Collectively, overexpressing miR-203a in D492M induced a reduction of mesenchymal characteristics, caused reduced proliferation, migration, invasion, and increased sensitivity towards chemically induced apoptosis.

Peroxidasin (PXDN) is a novel target of miR-203a

Due to the phenotypic differences between D492 and D492M in 3D culture and the fact that miR-203a is not expressed in D492M, we decided to compare the transcriptional profiling of D492, D492M and D492M$^{miR\text{-}203a}$, with emphasis on identifying novel targets of miR-203a. Herein, we identified peroxidasin (PXDN), a collagen IV crosslinking agent in the basement membrane, as the most significantly downregulated gene in D492M$^{miR\text{-}203a}$ compared to D492M (Fig. 5A). In addition, we identified three potential binding sites for miR-203a in the 3'-UTR of PXDN, one well conserved and two less conserved (Fig. 5B). To further investigate the potential interaction between miR-203a and PXDN we treated D492M and D492M$^{miR\text{-}203a}$ with miR-203a-mimic and miR-203a-inhibitor, respectively. PXDN expression was reduced (Fig. 5C, left) and increased (Fig. 5C, right) when D492M and D492M$^{miR\text{-}203a}$ were treated with miR-203 mimic and inhibitor, respectively, corroborating that miR-203a regulates PXDN expression. Furthermore, we demonstrated that PXDN expression was directly regulated by miR-203a by carrying out a dual luciferase reporter assay showing that the relative luciferase activity was significantly lower in the PXDN 3'-UTR containing the miR-203a target sequence compared with PXDN 3'-UTR with deleted

miR-203a binding sequence, when transfected with miR-203a mimic (**p < 0.008) (Fig. 5 D). This suggested that miR-203a could directly regulate the expression of PXDN through targeting its 3'-UTR.

Collectively, we have shown that miR-203 is a novel repressor of PXDN, a protein that plays an important role as a collagen IV cross-linker agent in the basement membrane and has been implicated in the EMT process, i.e. development, fibrosis and cancer.

Discussion

Modeling breast morphogenesis and EMT in 3D culture is an important tool to shed light on cellular and molecular mechanisms behind these developmental events and complements well *in vivo* models. Although animal models, in particular mice models, have contributed significantly to our understanding of mammary gland morphogenesis and breast cancer, they cannot replace the necessity for using human cells due to the molecular and cellular differences in mammary gland biology between species (Dontu and Ince 2015). In this study, we have applied two isogenic breast cell lines, D492 and D492M and 3D culture based on reconstituted basement membrane (rBM) to capture the phenotypic architecture of branching morphogenesis of breast epithelium and EMT, respectively. D492 is a breast epithelial progenitor cell line established from suprabasal epithelium of a normal breast gland (Gudjonsson, Villadsen et al. 2002, Villadsen, Fridriksdottir et al. 2007, Sigurdsson, Hilmarsdottir et al. 2011). D492M has a mesenchymal phenotype and is derived from D492 cells that have undergone EMT when co-cultured with breast endothelial cells (Sigurdsson, Hilmarsdottir et al. 2011). In this study, we analyzed differential expression of miRNAs in D492 and D492M on day 14 in 3D-rBM culture. Small RNA sequencing analysis revealed 47 differentially expressed miRNAs between D492 and D492M at day 14 in culture, of which 20 miRNAs were down-regulated in D492M. Among the most profound changes, was the downregulation of the miR-200 family, miR-205 and miR-203a in D492M. We have previously shown that these miRNAs are also downregulated in D492M when cultured in monolayer (Hilmarsdottir, Briem et al. 2015) indicating a comparable expression pattern between 2D and 3D conditions. In the same study we demonstrated that when miR-141 and miR-200c, which are under regulation of the same promoter on chromosome 12 (Hilmarsdottir, Briem et al. 2014, Hilmarsdottir, Briem et al. 2015), were overexpressed in D492M, a reversal towards epithelial phenotype was induced, albeit only towards the luminal epithelial phenotype (Hilmarsdottir, Briem et al. 2015). Unlike miR-200c-141 and miR-205, which are both heavily methylated in D492M, we did not observe any methylation of CpG islands in the promoter area of miR-203a. The unmethylated pattern of the miR-203a promoter in D492M is opposite to what has been described in other breast cell lines with a mesenchymal phenotype (Zhang,

Zhang et al. 2011, Taube, Malouf et al. 2013). This indicates that miR-203a down regulation in D492M may be through other processes, such as histone modification, or transcription factor repression.

Ectopic overexpression of miR-203a in D492M partially induced epithelial traits. The effect of increased miR-203a expression was primarily evident in functional assays, where it caused reduced cell proliferation, migration, and invasion. Morphologic and gene expression changes were subtle and indicated only partial MET, as evidenced by reduced expression of N-cadherin, and SNAI2, an EMT transcription factor known to silence expression of miR-203a. Moes et al. demonstrated that overexpression of SNAI1 in MCF-7 breast cancer cells resulted in repression of miR-203 (Moes, Le Bechec et al. 2012).

Branching morphogenesis of the D492 cells in 3D-rBM was used to mimic breast development and differentiation. We show that miR-203a expression coincides with increased differentiation status of the breast epithelial cells. In contrast, other epithelial associated miRNAs such as miR-205, miR-200c and miR-141 show constant or minimal fluctuation in expression throughout the branching period (21 days). In a miRNA expression study on mouse mammary gland development, Avril-Sassen et al. (Avril-Sassen, Goldstein et al. 2009) demonstrated that miR-203a showed temporal changes during different phases of mammary gland development. High expression was seen in early development and gestation followed by low expression in lactation and involution stages (Avril-Sassen, Goldstein et al. 2009). Reduced expression of miR-203a in lactation might be due to that fact that lactation requires functionally active p63 positive myoepithelial cells. MiR-203a is a repressor of p63 and therefore, downregulation of miR-203a is probably necessary for full activity of the myoepithelium.

Since D492 cells have stem cell properties, it is possible to separate cells into luminal epithelial and myoepithelial cells (Gudjonsson, Villadsen et al. 2002, Villadsen, Fridriksdottir et al. 2007). Based on EpCAM, a luminal associated epithelial adhesion molecule, we separated D492 cells into two cell populations: EpCAM-high and EpCAM-low. EpCAM-high cells showed significantly higher expression of miR-203a than EpCAM-low cells. This was also confirmed in primary luminal epithelial- and

myoepithelial cells. This result is in agreement with DeCastro et al. (DeCastro, Dunphy et al. 2013), where they demonstrated that miR-203a was significantly more expressed in mouse luminal epithelial progenitor cells and differentiated luminal epithelial cells compared to stem/basal cells. They also tested the expression levels of miR-203a in a number of normal and cancerous human breast epithelial cell lines: highest expression was predominantly in cell lines with a luminal epithelial phenotype.

To search for potential target genes for miR-203a we analyzed gene expression of D492M and D492M$^{miR\text{-}203a}$. The most significantly differential expressed gene between D492M and D492M$^{miR\text{-}203a}$ was PXDN. PXDN is a heme-containing peroxidase that produces hypobromous acid (HOBr) to form sulfilimine cross-links to stabilize the collagen IV network in the basement membrane and is believed to be important in normal development (Colon, Page-McCaw et al. 2017). PXDN has also been linked to EMT and disease conditions such as melanoma invasion and fibrosis (Tindall, Pownall et al. 2005, Cheng, Salerno et al. 2008, Peterfi, Donko et al. 2009, Liu, Carson-Walter et al. 2010, Tauber, Jais et al. 2010, Barnett, Arnold et al. 2011, Khan, Rudkin et al. 2011, Bhave, Cummings et al. 2012, Yan, Sabrautzki et al. 2014, Ero-Tolliver, Hudson et al. 2015, Colon and Bhave 2016, Jayachandran, Prithviraj et al. 2016, Sitole and Mavri-Damelin 2018).

Jayachandran et al. identified PXDN as consistently elevated in invasive mesenchymal-like melanoma cells and it was also found highly expressed in metastatic melanoma tumors. Gene silencing led to reduced melanoma invasion *in vitro* (Jayachandran, Prithviraj et al. 2016). Moreover, Peterti et al. have shown that PXDN is secreted from myofibrolasts and also from fibrotic kidney (Peterfi, Donko et al. 2009). Young et al. demonstrated that PXDN expression increases in PIK3CA mutant MCF10A cells and that the PXDN protein is mainly associated with secreted exosomes (Young, Zimmerman et al. 2015). When knocking down PXDN in four basal like breast cancer cell lines, all cell lines showed reduced proliferation and when PXDN was knocked down in the luminal cell line MDA-MB-361, which expresses little PXDN, there was also reduced proliferation (Young, Zimmerman et al. 2015). The reduced proliferation rate we saw in D492M$^{miR\text{-}203a}$, could be because of PXDN silencing by miR-203a. The fact that PXDN is overexpressed in the mesenchymal cell line D492M may link it to the EMT phenotype.

In summary, mammary gland development is mostly a post-natal process, where post-transcriptional regulation via miR-203a expression correlates with differentiation stages in the mammary epithelium. Using the D492 breast progenitor cells cultivated in 3D-rBM it is possible to capture the critical aspects of branching morphogenesis. Temporal changes in miR-203a expression during the *in vitro* branching process correlate well with *in vivo* conditions. Although miR-203a repression and overexpression are well documented in a number of studies, we observed only subtle changes towards MET when overexpressed in D492M. Furthermore, we have demonstrated a novel link between miR-203a and PXDN, which is highly expressed in D492M. Collectively, we conclude that the miR-203a repression of PXDN may be important to retain epithelial phenotype of breast epithelial cells.

Material and methods

Cell culture

D492 and D492M cells were maintained in H14 medium as described previously (Sigurdsson, Hilmarsdottir et al. 2011). Primary luminal epithelial cells ($EpCAM^+$) and myoepithelial cells ($EpCAM^-$) were isolated from primary culture of breast epithelial cells derived from reduction mammoplasties by magnetic cell sorting (MACS) and maintained in CDM3 and CDM4, respectively, as previously described (Pechoux, Gudjonsson et al. 1999). Primary human breast endothelial cells (BRENCs) were isolated from breast reduction mammoplasties and cultured in endothelial growth medium (EGM) (Lonza) + 5% FBS (Invitrogen), referred to as EGM5 (Sigurdsson, Fridriksdottir et al. 2006). Growth factor reduced reconstituted basement membrane (rBM, purchased as Matrigel, Corning #354230) was used for 3D cultures. 3D monocultures were carried out in 24-well culture plates (Corning). 1×10^4 D492 cells were suspended in 300 µl of rBM. Co-culture experiments were carried out with either 500, or 1×10^3 cells mixed with 1×10^5 - 2×10^5 BRENCs. 300 µl of mixed cells / rBM were seeded in each well of a 24-well plate and cultured on H14 (monoculture) or EGM5 (co-culture) for 14 - 21 days.

Branching, solid and spindle-like structures were isolated from 3D co-cultures with gentle shaking on ice in PBS - EDTA (5 mM) solution as previously described (Lee, Kenny et al. 2007).

Small RNA sequencing

Total RNA was isolated from branching and spindle-like colonies from D492 and D492M, respectively using Tri-Reagent (Thermo Fisher Scientific, #AM9738). For D492 branching time points, RNA was isolated from 3D-rBM culture on days 7, 14 and 21 but for D492M RNA was isolated only on day 14. Samples were pooled in triplicates from each time point before small RNA library preparation. Small RNA libraries were prepared using the TruSeq Small RNA Library Kit from Illumina (#RS-200-0012) per manufacturer´s protocol. The small RNA libraries were then sequenced using the Illumina MiSeq platform and V2 sequencing chemistry. FASTQ files were generated

with MiSeq Reporter (Illumina, San Diego, US-CA). Small RNA sequence analysis was performed using the CLC Genomics Workbench (CLC Bio-Qiagen, Aarhus, Denmark) and miRBase – release 21 was used for annotation. Samples were normalized by totals and counts reported as reads per million. Reads above 29 nt and below 15 nt in length were discarded. Proportion-based statistical analysis was done using the test of Kal (Kal, van Zonneveld et al. 1999). Hierarchal clustering of features was performed using Log2 transformed expression values, Euclidean distance and single linkage. For the D492 and D492M comparison samples from day 7, 14 and 21 from D492 were compared to D492M sample from day 14.

DNA isolation and methylation bead chip array

D492 (1 x 10^4 cells) and D492M (2.5 x 10^4 cells) were grown in 3D-rBM in triplicate in a 24-well plate for 14 days and colonies extracted from 3D-rBM with gentle shaking on ice in PBS - EDTA (5 mM) solution as previously described (Lee, Kenny et al. 2007). DNA was extracted using the PureLink Genomic DNA Mini Kit (Thermo Fisher Scientific, #K182002) and DNA was bisulfite converted using the EZ-96 DNA Methylation-Gold Kit (Zymo Research, #D5007) per manufacturer´s protocols. The samples were hybridized to the Infinium HumanMethylation450 BeadChip array (Illumina, # WG-314-1003). Data was analyzed using the minfi Bioconductor package (Aryee, Jaffe et al. 2014).

Bisulfite sequencing

DNA (0.5 - 1 µg) was bisulfite converted using the EpiTect Bisulfite Kit (Qiagen, #59104). Target DNA sequences were amplified using nested PCR (see primers in Table S1). Methylation levels were analyzed by sequencing the bisulfite modified promoter regions on a 3130 Genetic Analyzer (Applied Biosystems). Methylation data from bisulfite sequencing was analyzed and visualized using the BiQ Analyzer v2.0 (Bock, Reither et al. 2005).

Quantitative reverse transcription PCR analysis

Total RNA was extracted with Tri-Reagent (Thermo Fisher Scientific, #AM9738) and reverse transcription performed using random hexamers (Thermo Fisher Scientific, #N8080127) and SuperScript IV Reverse Transcriptase (Thermo Fisher Scientific, #18090050). The following primers were used for mRNA qRT-PCR analysis, SNAI2 (Hs00950344_m1) (Thermo Fisher Scientific, #4331182) and GAPDH as endogenous reference gene (Thermo Fisher Scientific, # 4326317E). Maxima Probe/ROX qPCR Master Mix (2X) (Thermo Fisher Scientific, # K0231) was used for TaqMan qRT-PCR analysis.

Quantitative RT-PCR analysis of miRNAs was performed using the universal cDNA synthesis kit II (Exiqon, #203301) and ExiLENT SYBR Green master mix (Exiqon, #203402). The following primer sets from Exiqon were used for miRNA qRT-PCR analysis, hsa-miR-203a (#205914), hsa-miR-141-3p (#204504), hsa-miR-200c-3p (#204482), hsa-miR-205-5p (#204487) and U6 snRNA (#203907) was used as endogenous reference. All qRT-PCRs were performed on the Applied Biosystems 7500 Real-Time PCR system and relative expression differences were calculated with the $2^{\Delta Ct}$ method.

Cloning of miR-203a into pCDH lentivector

The miR-203a miRNA construct was amplified from D492 genomic DNA using nested PCR with the following outer primers, miR-203a-outer-F 5'-ATCAGTCGCGGGACCTATG-3' and miR-203a-outer-R 5'-GAATTCCACGGAGTTTCGAG-3'. From miR-203a-outer amplicon, EcoRI and NotI restriction sites were incorporated with PCR using the following inner primers, miR-203a-EcoRI-F-5'-TAAGCAGAATTCaggcgagggcgtctaagg-3' and miR-203a-NotI-R-5'-TGCTTAGCGGCCGCacctcccagcagcacttg-3'. Phusion High-Fidelity DNA Polymerase (NEB, # M0530S) was used for PCR and amplicons were purified using the GeneJET PCR purification kit (Thermo Fisher Scientific, #K0701). Double digestions of miR-203a-inner amplicon and pCDH vector (System Biosciences, #CD516B-2) were performed using EcoRI (NEB, #R0101) and NotI (Thermo Fisher Scientific, #ER0591). The miR-203a-inner amplicon was cloned into pCDH lentivector at insert-to-vector molar ratio 10:1 using T4 DNA ligase (Thermo Fisher Scientific, #15224041). Empty

pCDH lentivector and miR-203a-pCDH lentivector were transformed into *E. coli* DH5alpha competent cells and inserts confirmed with colony PCR. Lentivectors were produced in cultures of DH5alpha and isolated using GeneJET Plasmid Miniprep kit (Thermo Fisher Scientific, #K0502). The cloned miR-203a insert sequence was then confirmed with sequencing. The pCDH lentivector has a RFP+Puro fusion containing the T2A element to enable co-expression of balanced levels of RFP and Puro genes. Viral particles were produced in HEK-293T cells using TurboFect transfection reagent (Thermo Fisher Scientific, #R0531) and virus containing supernatant collected after 48 and 72 hours, centrifuged and filtered through 0.45 µm filter. Target cells were transfected with virus titer in the presence of 8 µg/µl polybrene. Stable cell lines and control (empty-lentivector) cells were isolated with puromycin (2 µg/ml) (Thermo Fisher Scientific, # A1113803) followed by flow-sorting (Sony SH800), selecting for RFP expressing cells.

Immunochemistry

The following primary antibodies were used for DAB staining (Dako, # K3467), E-cadherin (BD, # 610182), N-cadherin (BD, # 610921), K14 (Abcam, #ab7800) and K19 (Abcam, #ab7754). Specimens were visualized on a Leica DMI3000 B inverted microscope.

Western blotting

Equal amounts (5 µg) of proteins in RIPA buffer were separated on NuPAGE™ 10% Bis-Tris Protein Gels (Thermo Fisher Scientific, #NP0302BOX) and transferred to a PVDF membrane (Millipore, #IPFL00010). Antibodies: SNAI2 (Cell Signaling, #9585) and Histone H3 (Cell Signaling, #4499). Secondary antibodies were mouse or rabbit IRDey (Li-Cor) used at 1:20,000 and detected using the Odyssey Infrared Imaging System (Li-Cor). Fluorescent images were converted to gray scale.

Proliferation assay

Cells were seeded in triplicates in 24-well plates and cultures stopped every 24 hours. Cells were fixed in 3.7% formaldehyde in PBS for 10 minutes, washed once with 1 x

PBS, stained with 0.1% crystal violet in 10% ethanol for 15 minutes, washed four times with water and dried. Density of cells was evaluated by extracting the crystal violet stain in 10% acetic acid and measuring optical density at 595 nm using a spectrometer.

Apoptosis assay

Resistance to chemically induced apoptosis with 10 µM camptothecin (Sigma-Aldrich, #C9911) was determined using IncuCyte Caspase-3/7 Reagents (Essen Bioscience, #4440) and imaging on IncuCyte Zoom (Essen Bioscience) per manufacturer's instructions.

Anchorage independence, migration and invasion assays

Anchorage independent growth was determined using 24-well ultra-low attachment plates (Corning, #3473), where triplicates of 500 cells of D492M$^{miR\text{-}203a}$ and D492M^{Empty} were single cell filtered and cultured using EGM5 medium for 9 days. For migration analysis, triplicates of 10,000 starved D492M$^{miR\text{-}203a}$ and D492M^{Empty} cells were seeded in DMEM/F12, HEPES medium (Thermo Scientific, #31330038) on collagen I (Advanced BioMatrix, #5005-B) coated transwell filters with 8 µm pore size (Corning, #353097) with EGM5 medium in the lower chamber and incubated for 24 hours. Filters were rinsed with 1 x PBS and cells on the apical layer wiped off with a cotton swab (Q-tip) and migrated cells fixed in 3.7% formaldehyde in PBS for 10 minutes, washed with 1 x PBS, stained with 0.1% crystal violet in 10% ethanol for 15 minutes and washed with water and then dried. Images were acquired and migrated cells counted, 3 images per filter.

Invasion assay was performed using transwell filters with 8 µm pore size (Corning, #353097) that were coated with 100 µl diluted matrigel (Corning, #354230) 1:10 in H14 media. D492M$^{miR\text{-}203a}$ and D492M^{Empty} (25,000 cells) were seeded in H14 media on top of matrigel coated filters and H14 + 5% FBS added to the lower chamber and incubated for 44 hours. Matrigel was then removed with a cotton swab and washed with PBS. Cells were fixed in 3.7% formaldehyde in PBS for 15 minutes and washed four times with water. Images were acquired and migrated cells counted, 3 images per filter.

Transient transfection with miR-203a mimic

Briefly, D492M cells were separately transfected with 50 pmol of mirVANA miR-203a-3p mimic (Thermo Fisher, #4464066, Assay ID MC10152) and miRNA mimic negative control #1 (Thermo Fisher, #4464058) using RNAiMAX (Thermo Fisher, #13778075) per manufacturer's instructions for mirVana miRNA mimics.

Transient transfection with miR-203a inhibitor

Briefly, D492M$^{miR\text{-}203a}$ cells were separately transfected with 50 pmol of mirVANA miR-203a-3p inhibitor (Thermo Fisher, # 4464084, Assay ID MH10152) and mirVana miRNA Inhibitor, Negative Control #1 (Thermo Fisher, # 4464076) using RNAiMAX (Thermo Fisher, #13778075) per manufacturer's instructions for mirVana miRNA inhibitors.

Plasmid vector constructs and Luciferase activity assay

Synthetic oligonucleotides containing the hsa-miR203-3p target sequence of human PXDN 3'-UTR or a deletion thereof (Table 1) were cloned into pmirGLO Dual-Luciferase miRNA Target Expression Vector (Promega Corporation, Madison, WI, USA). As a positive control we cloned the target sequence of p63 3'-UTR, a known hsa-miR203-3p target, into pmirGLO, as well as a mismatched version of the p63 target site or a deletion thereof (Fig. S1). The correct sequence and orientation was verified by sequencing.

Table 1. Synthetic oligonucleotides containing the has-mir-203-3p target sequence of human PXDN 3'-UTR or a deletion thereof.

PXDN 3'-UTR sense	/5Phos/AAACTAGCGGCCGCTAGTCCCAGAACTCGTGACATTTCATT
PXDN 3'-UTR antisense	/5Phos/CTAGAATGAAATGTCACGAGTTCTGGGACTAGCGGCCGCTAGTTT
PXDN del sense	/5Phos/AAACTAGCGGCCGCTAGTCCCAGAACTCGTGTT
PXDN del antisense	/5Phos/CTAGAACACGAGTTCTGGGACTAGCGGCCGCTAGTTT

P63 3'-UTR sense	/5Phos/AAACTAGCGGCCGCTAGTGAATGAGTCCTTGATTTCAAAT
P63 3'-UTR antisense	/5Phos/CTAGATTTGAAATCAAGGACTCATTCACTAGCGGCCGCTAGTTT
P63 del sense	/5Phos/AAACTAGCGGCCGCTAGTGAATGAGTCCTTGAT
P63 del antisense	/5Phos/CTAGATCAAGGACTCATTCACTAGCGGCCGCTAGTTT

549

550 HEK293T cells were plated in a 96-well plate 3.0 x 10^4per well and incubated
551 overnight. Cells were first transfected with hsa-miR203-3p mimics (mirVana™ miRNA
552 Mimics, Thermo Fisher Scientific, #4464070) with final concentration of 100 nM, using
553 Lipofectamine RNAiMAX (Thermo Fisher Scienttific, #13778150) transfection reagent
554 (according to manufacturer's instructions, with minor changes: using serum free and
555 antibiotic-free high glucose DMEM medium instead of Opti-MEM® Medium). 24 hours
556 after transfection with miRNA mimics, cells were transfected (according to
557 manufacturer's instructions) with 200 ng/well luciferase plasmids (pmirGLO
558 constructs), using Lipofectamine 3000 (Thermo Fisher Scientific, #L3000015).
559 Twentyfour hours after, plasmid-transfection cells were analyzed for luciferase activity
560 using the Dual-Glo® Luciferase Assay System (Promega Corporation, Madison, WI,
561 USA). Normalized firefly luciferase activity (background subtracted firefly luciferase
562 activity/ background subtracted renilla luciferase activity) for each construct was
563 compared to that of the pmirGLO vector no-insert control. For each transfection,
564 luciferase activity was averaged from four replicates.

565

566 **Acknowledgements**

567 We thank Erik Knutsen and Isac Lee for their contribution to this work.

568

569 **Competing interests**

570 No competing interests declared.

571

572 **Funding**

573 This work was supported by Grants from Landspitali University Hospital Science Fund,
574 University of Iceland Research Fund, and Icelandic Science and Technology Policy -
575 Grant of Excellence: 152144051. 'Göngum saman', a supporting group for breast

cancer research in Iceland (www.gongumsaman.is). The funders had no role in study design, data collection and analysis, decision to publish, or preparation of the manuscript. Primary cells were received from reduction mammoplasty after acquiring informed consent from the donor. Approved by the Icelandic National Bioethics Committee VSN-13-057.

Data availability

NCBI GEO: https://www.ncbi.nlm.nih.gov/geo/query/acc.cgi?acc=GSE112306

The data discussed in this publication have been deposited in NCBI's Gene Expression Omnibus (Edgar, Domrachev et al. 2002) and are accessible through GEO Series accession number GSE112306.

(https://www.ncbi.nlm.nih.gov/geo/query/acc.cgi?acc=GSE112306).

References

Aryee, M. J., A. E. Jaffe, H. Corrada-Bravo, C. Ladd-Acosta, A. P. Feinberg, K. D. Hansen and R. A. Irizarry (2014). "Minfi: a flexible and comprehensive Bioconductor package for the analysis of Infinium DNA methylation microarrays." Bioinformatics **30**(10): 1363-1369.

Avril-Sassen, S., L. D. Goldstein, J. Stingl, C. Blenkiron, J. Le Quesne, I. Spiteri, K. Karagavriilidou, C. J. Watson, S. Tavaré, E. A. Miska and C. Caldas (2009). "Characterisation of microRNA expression in post-natal mouse mammary gland development." BMC Genomics **10**: 548.

Barnett, P., R. S. Arnold, R. Mezencev, L. W. Chung, M. Zayzafoon and V. Odero-Marah (2011). "Snail-mediated regulation of reactive oxygen species in ARCaP human prostate cancer cells." Biochem Biophys Res Commun **404**(1): 34-39.

Bhave, G., C. F. Cummings, R. M. Vanacore, C. Kumagai-Cresse, I. A. Ero-Tolliver, M. Rafi, J. S. Kang, V. Pedchenko, L. I. Fessler, J. H. Fessler and B. G. Hudson (2012). "Peroxidasin forms sulfilimine chemical bonds using hypohalous acids in tissue genesis." Nat Chem Biol **8**(9): 784-790.

Bock, C., S. Reither, T. Mikeska, M. Paulsen, J. Walter and T. Lengauer (2005). "BiQ Analyzer: visualization and quality control for DNA methylation data from bisulfite sequencing." Bioinformatics **21**(21): 4067-4068.

Cao, Q., R. S. Mani, B. Ateeq, S. M. Dhanasekaran, I. A. Asangani, J. R. Prensner, J. H. Kim, J. C. Brenner, X. Jing, X. Cao, R. Wang, Y. Li, A. Dahiya, L. Wang, M. Pandhi, R. J. Lonigro, Y. M. Wu, S. A. Tomlins, N. Palanisamy, Z. Qin, J. Yu, C. A. Maher, S. Varambally and A. M. Chinnaiyan (2011). "Coordinated regulation of polycomb group complexes through microRNAs in cancer." Cancer Cell **20**(2): 187-199.

Cheng, G., J. C. Salerno, Z. Cao, P. J. Pagano and J. D. Lambeth (2008). "Identification and characterization of VPO1, a new animal heme-containing peroxidase." Free Radic Biol Med **45**(12): 1682-1694.

Colon, S. and G. Bhave (2016). "Proprotein Convertase Processing Enhances Peroxidasin Activity to Reinforce Collagen IV." J Biol Chem **291**(46): 24009-24016.

Colon, S., P. Page-McCaw and G. Bhave (2017). "Role of Hypohalous Acids in Basement Membrane Homeostasis." Antioxid Redox Signal **27**(12): 839-854.
DeCastro, A. J., K. A. Dunphy, J. Hutchinson, A. L. Balboni, P. Cherukuri, D. J. Jerry and J. DiRenzo (2013). "MiR203 mediates subversion of stem cell properties during mammary epithelial differentiation via repression of DeltaNP63alpha and promotes mesenchymal-to-epithelial transition." Cell Death Dis **4**: e514.
Ding, X., S. I. Park, L. K. McCauley and C. Y. Wang (2013). "Signaling between transforming growth factor beta (TGF-beta) and transcription factor SNAI2 represses expression of microRNA miR-203 to promote epithelial-mesenchymal transition and tumor metastasis." J Biol Chem **288**(15): 10241-10253.
Dontu, G., W. M. Abdallah, J. M. Foley, K. W. Jackson, M. F. Clarke, M. J. Kawamura and M. S. Wicha (2003). "In vitro propagation and transcriptional profiling of human mammary stem/progenitor cells." Genes Dev **17**(10): 1253-1270.
Dontu, G. and T. A. Ince (2015). "Of mice and women: a comparative tissue biology perspective of breast stem cells and differentiation." J Mammary Gland Biol Neoplasia **20**(1-2): 51-62.
Edgar, R., M. Domrachev and A. E. Lash (2002). "Gene Expression Omnibus: NCBI gene expression and hybridization array data repository." Nucleic Acids Res **30**(1): 207-210.
Ero-Tolliver, I. A., B. G. Hudson and G. Bhave (2015). "The Ancient Immunoglobulin Domains of Peroxidasin Are Required to Form Sulfilimine Cross-links in Collagen IV." J Biol Chem **290**(35): 21741-21748.
Feng, X., Z. Wang, R. Fillmore and Y. Xi (2014). "MiR-200, a new star miRNA in human cancer." Cancer Lett **344**(2): 166-173.
Gregory, P. A., A. G. Bert, E. L. Paterson, S. C. Barry, A. Tsykin, G. Farshid, M. A. Vadas, Y. Khew-Goodall and G. J. Goodall (2008). "The miR-200 family and miR-205 regulate epithelial to mesenchymal transition by targeting ZEB1 and SIP1." Nat Cell Biol **10**(5): 593-601.
Gudjonsson, T., R. Villadsen, H. L. Nielsen, L. Ronnov-Jessen, M. J. Bissell and O. W. Petersen (2002). "Isolation, immortalization, and characterization of a human breast epithelial cell line with stem cell properties." Genes Dev **16**(6): 693-706.
Hanahan, D. and R. A. Weinberg (2011). "Hallmarks of cancer: the next generation." Cell **144**(5): 646-674.
Hilmarsdottir, B., E. Briem, J. T. Bergthorsson, M. K. Magnusson and T. Gudjonsson (2014). "Functional Role of the microRNA-200 Family in Breast Morphogenesis and Neoplasia." Genes **5**(3): 804-820.
Hilmarsdottir, B., E. Briem, V. Sigurdsson, S. R. Franzdottir, M. Ringner, A. J. Arason, J. T. Bergthorsson, M. K. Magnusson and T. Gudjonsson (2015). "MicroRNA-200c-141 and Np63 are required for breast epithelial differentiation and branching morphogenesis." Dev Biol **403**(2): 150-161.
Inoue, A., M. G. Seidel, W. Wu, S. Kamizono, A. A. Ferrando, R. T. Bronson, H. Iwasaki, K. Akashi, A. Morimoto, J. K. Hitzler, T. I. Pestina, C. W. Jackson, R. Tanaka, M. J. Chong, P. J. McKinnon, T. Inukai, G. C. Grosveld and A. T. Look (2002). "Slug, a highly conserved zinc finger transcriptional repressor, protects hematopoietic progenitor cells from radiation-induced apoptosis in vivo." Cancer Cell **2**(4): 279-288.
Javed, A. and A. Lteif (2013). "Development of the human breast." Semin Plast Surg **27**(1): 5-12.
Jayachandran, A., P. Prithviraj, P. H. Lo, M. Walkiewicz, M. Anaka, B. L. Woods, B. Tan, A. Behren, J. Cebon and S. J. McKeown (2016). "Identifying and targeting determinants of melanoma cellular invasion." Oncotarget **7**(27): 41186-41202.
Kal, A. J., A. J. van Zonneveld, V. Benes, M. van den Berg, M. G. Koerkamp, K. Albermann, N. Strack, J. M. Ruijter, A. Richter, B. Dujon, W. Ansorge and H. F. Tabak (1999). "Dynamics of gene expression

revealed by comparison of serial analysis of gene expression transcript profiles from yeast grown on two different carbon sources." Mol Biol Cell **10**(6): 1859-1872.
Khan, K., A. Rudkin, D. A. Parry, K. P. Burdon, M. McKibbin, C. V. Logan, Z. I. Abdelhamed, J. S. Muecke, N. Fernandez-Fuentes, K. J. Laurie, M. Shires, R. Fogarty, I. M. Carr, J. A. Poulter, J. E. Morgan, M. D. Mohamed, H. Jafri, Y. Raashid, N. Meng, H. Piseth, C. Toomes, R. J. Casson, G. R. Taylor, M. Hammerton, E. Sheridan, C. A. Johnson, C. F. Inglehearn, J. E. Craig and M. Ali (2011). "Homozygous mutations in PXDN cause congenital cataract, corneal opacity, and developmental glaucoma." Am J Hum Genet **89**(3): 464-473.
Lee, G. Y., P. A. Kenny, E. H. Lee and M. J. Bissell (2007). "Three-dimensional culture models of normal and malignant breast epithelial cells." Nat Methods **4**(4): 359-365.
Liu, Y., E. B. Carson-Walter, A. Cooper, B. N. Winans, M. D. Johnson and K. A. Walter (2010). "Vascular gene expression patterns are conserved in primary and metastatic brain tumors." J Neurooncol **99**(1): 13-24.
Mani, S. A., W. Guo, M. J. Liao, E. N. Eaton, A. Ayyanan, A. Y. Zhou, M. Brooks, F. Reinhard, C. C. Zhang, M. Shipitsin, L. L. Campbell, K. Polyak, C. Brisken, J. Yang and R. A. Weinberg (2008). "The epithelial-mesenchymal transition generates cells with properties of stem cells." Cell **133**(4): 704-715.
Moes, M., A. Le Bechec, I. Crespo, C. Laurini, A. Halavatyi, G. Vetter, A. del Sol and E. Friederich (2012). "A Novel Network Integrating a miRNA-203/SNAI1 Feedback Loop which Regulates Epithelial to Mesenchymal Transition." Plos One **7**(4): e35440.
Moustakas, A. and C. H. Heldin (2007). "Signaling networks guiding epithelial-mesenchymal transitions during embryogenesis and cancer progression." Cancer Sci **98**(10): 1512-1520.
Olson, P., J. Lu, H. Zhang, A. Shai, M. G. Chun, Y. Wang, S. K. Libutti, E. K. Nakakura, T. R. Golub and D. Hanahan (2009). "MicroRNA dynamics in the stages of tumorigenesis correlate with hallmark capabilities of cancer." Genes Dev **23**(18): 2152-2165.
Pechoux, C., T. Gudjonsson, L. Ronnov-Jessen, M. J. Bissell and O. W. Petersen (1999). "Human mammary luminal epithelial cells contain progenitors to myoepithelial cells." Dev Biol **206**(1): 88-99.
Peinado, H., D. Olmeda and A. Cano (2007). "Snail, ZEB and bHLH factors in tumour progression: an alliance against the epithelial phenotype?" Nature Reviews Cancer **7**(6): 415-428.
Peterfi, Z., A. Donko, A. Orient, A. Sum, A. Prokai, B. Molnar, Z. Vereb, E. Rajnavolgyi, K. J. Kovacs, V. Muller, A. J. Szabo and M. Geiszt (2009). "Peroxidasin is secreted and incorporated into the extracellular matrix of myofibroblasts and fibrotic kidney." Am J Pathol **175**(2): 725-735.
Petersen, O. W., H. Lind Nielsen, T. Gudjonsson, R. Villadsen, L. Ronnov-Jessen and M. J. Bissell (2001). "The plasticity of human breast carcinoma cells is more than epithelial to mesenchymal conversion." Breast Cancer Res **3**(4): 213-217.
Petersen, O. W. and K. Polyak (2010). "Stem cells in the human breast." Cold Spring Harb Perspect Biol **2**(5): a003160.
Sarrio, D., S. M. Rodriguez-Pinilla, D. Hardisson, A. Cano, G. Moreno-Bueno and J. Palacios (2008). "Epithelial-mesenchymal transition in breast cancer relates to the basal-like phenotype." Cancer Research **68**(4): 989-997.
Shimono, Y., M. Zabala, R. W. Cho, N. Lobo, P. Dalerba, D. Qian, M. Diehn, H. Liu, S. P. Panula, E. Chiao, F. M. Dirbas, G. Somlo, R. A. Pera, K. Lao and M. F. Clarke (2009). "Downregulation of miRNA-200c links breast cancer stem cells with normal stem cells." Cell **138**(3): 592-603.
Sigurdsson, V., A. J. Fridriksdottir, J. Kjartansson, J. G. Jonasson, M. Steinarsdottir, O. W. Petersen, H. M. Ogmundsdottir and T. Gudjonsson (2006). "Human breast microvascular endothelial cells retain phenotypic traits in long-term finite life span culture." In Vitro Cell Dev Biol Anim **42**(10): 332-340.

Sigurdsson, V., B. Hilmarsdottir, H. Sigmundsdottir, A. J. Fridriksdottir, M. Ringner, R. Villadsen, A. Borg, B. A. Agnarsson, O. W. Petersen, M. K. Magnusson and T. Gudjonsson (2011). "Endothelial induced EMT in breast epithelial cells with stem cell properties." PLoS One **6**(9): e23833.

Sitole, B. N. and D. Mavri-Damelin (2018). "Peroxidasin is regulated by the epithelial-mesenchymal transition master transcription factor Snai1." Gene **646**: 195-202.

Taube, J. H., G. G. Malouf, E. Lu, N. Sphyris, V. Vijay, P. P. Ramachandran, K. R. Ueno, S. Gaur, M. S. Nicoloso, S. Rossi, J. I. Herschkowitz, J. M. Rosen, J. P. Issa, G. A. Calin, J. T. Chang and S. A. Mani (2013). "Epigenetic silencing of microRNA-203 is required for EMT and cancer stem cell properties." Sci Rep **3**: 2687.

Tauber, S., A. Jais, M. Jeitler, S. Haider, J. Husa, J. Lindroos, M. Knofler, M. Mayerhofer, H. Pehamberger, O. Wagner and M. Bilban (2010). "Transcriptome analysis of human cancer reveals a functional role of heme oxygenase-1 in tumor cell adhesion." Mol Cancer **9**: 200.

Tindall, A. J., M. E. Pownall, I. D. Morris and H. V. Isaacs (2005). "Xenopus tropicalis peroxidasin gene is expressed within the developing neural tube and pronephric kidney." Dev Dyn **232**(2): 377-384.

Villadsen, R., A. J. Fridriksdottir, L. Ronnov-Jessen, T. Gudjonsson, F. Rank, M. A. LaBarge, M. J. Bissell and O. W. Petersen (2007). "Evidence for a stem cell hierarchy in the adult human breast." J Cell Biol **177**(1): 87-101.

Wellner, U., J. Schubert, U. C. Burk, O. Schmalhofer, F. Zhu, A. Sonntag, B. Waldvogel, C. Vannier, D. Darling, A. zur Hausen, V. G. Brunton, J. Morton, O. Sansom, J. Schuler, M. P. Stemmler, C. Herzberger, U. Hopt, T. Keck, S. Brabletz and T. Brabletz (2009). "The EMT-activator ZEB1 promotes tumorigenicity by repressing stemness-inhibiting microRNAs." Nat Cell Biol **11**(12): 1487-1495.

Yan, X., S. Sabrautzki, M. Horsch, H. Fuchs, V. Gailus-Durner, J. Beckers, M. Hrabe de Angelis and J. Graw (2014). "Peroxidasin is essential for eye development in the mouse." Hum Mol Genet **23**(21): 5597-5614.

Young, C. D., L. J. Zimmerman, D. Hoshino, L. Formisano, A. B. Hanker, M. L. Gatza, M. M. Morrison, P. D. Moore, C. A. Whitwell, B. Dave, T. Stricker, N. E. Bhola, G. O. Silva, P. Patel, D. M. Brantley-Sieders, M. Levin, M. Horiates, N. A. Palma, K. Wang, P. J. Stephens, C. M. Perou, A. M. Weaver, J. A. O'Shaughnessy, J. C. Chang, B. H. Park, D. C. Liebler, R. S. Cook and C. L. Arteaga (2015). "Activating PIK3CA Mutations Induce an Epidermal Growth Factor Receptor (EGFR)/Extracellular Signal-regulated Kinase (ERK) Paracrine Signaling Axis in Basal-like Breast Cancer." Mol Cell Proteomics **14**(7): 1959-1976.

Zhang, Z., B. Zhang, W. Li, L. Fu, L. Fu, Z. Zhu and J. T. Dong (2011). "Epigenetic Silencing of miR-203 Upregulates SNAI2 and Contributes to the Invasiveness of Malignant Breast Cancer Cells." Genes Cancer **2**(8): 782-791.

Figure legends

Fig. 1. Profiling miRNAs in the isogenic breast epithelial progenitor cell line D492 and its mesenchymal derivative D492M.

A) *Differentially expressed miRNAs between D492M and D492 in 3D culture based on small RNA sequencing.* Forty-seven miRNAs are differentially expressed between the mesenchymal (D492M) and epithelial (D492) state at day 14 in 3D culture. Twenty miRNAs are downregulated in D492M and among them are miRNAs that are important for epithelial integrity, such as the miR-200 family and miR-203a. Scale bar = 100 µm.

B) *Volcano plot showing differential expressed miRNAs in D492M and D492, depicting statistical significance and high fold change in expression of epithelial associated miRNAs.* Volcano plot constructed from small RNA sequencing data using fold change of expression values and p-values, enabling the visualization of the relationship between fold change and statistical significance. More extreme values on the x-axis show increased differential expression and higher values on the y-axis show increased statistical significance. The miR-200c-141 locus along with miR-205, miR-944, miR-584, miR-708 and miR-203 show the most fold change and statistical significance of the miRNAs downregulated in D492M.

Fig. 2. miRNA promoter methylation of D492 and D492M

A) Differential DNA methylation of D492 (red) and D492M (blue). CpG methylation in the promoter area of differentially expressed miRNAs was investigated using the HumanMethylation450 BeadChip. The yellow bar represents the pre-miRNA and differential methylation is determined by a beta value > 0.2. MiR-200c, miR-141 and miR-205 are differentially methylated with more methylation in D492M, while methylation of miRNA-203a is unchanged. The expression of miR-200c-141 and miR-205 is repressed through DNA methylation, while expression of miRNA-203a is not.

B) *Bisulfite sequencing of miRNA promoters in D492 and D492M.* The promoters of miR-200c-141, miR-205 and miR-203a are un-methylated in D492. In D492M, the promoter of miR-203a remains un-methylated, while the promoters of miR-200c-141 and miR-205 are methylated.

Fig. 3. MiR-203a is differentially expressed during branching morphogenesis in 3D culture.

A) *Heatmap showing differentially expressed miRNAs in D492 at different time points during branching morphogenesis.* Small RNA-sequencing of D492 at three different time points during branching morphogenesis at day 7, 14 and 21. miR-203a expression increases during branching of D492. Heatmap shows miRNAs with > 2-fold change in expression an FDR corrected p-values < 0.1.

B) *Expression of epithelial miRNAs in D492 at different time points during branching*. RT-qPCR showing that the expression of miR-203a and miR-141 significantly increases between time points during branching morphogenesis. Interestingly, expression of miR-203a increases markedly in late branching at day 21.

C) *Expression of miR-203a in breast primary cells and D492 EpCAM sorted cells.* In primary cells, miR-203a is expressed in the epithelial cells and is predominantly associated with the luminal cells but is absent in fibroblasts and endothelial cells. In D492 miR-203a expression is predominantly associated with the EpCAM High cells.

MiR-203a expression in breast cell lines. MiR-203a is expressed in breast cell lines with an epithelial phenotype but not with a mesenchymal phenotype. Expression of miR-203a in mesenchymal derivatives of D492 and HMLE, i.e. D492M and HMLEmes, is downregulated with little or no expression in the mesenchymal state. The normal like breast cell line MCF10A has high expression of miR-203a, while the triple negative mesenchymal breast cancer cell line MDA-MB-231 has no expression of miR-203a.

Fig. 4. Overexpression of miR-203a in D492M.

A) *Overexpression of miR-203a in D492M.* RT-qPCR showing 17,500-fold expression of miR-203a in D492M$^{miR\text{-}203a}$ compared to control.

B) Phase contrast images of monolayer cultures show that miR-203a overexpression in D492M causes cells to adhere more to each other compared to D492M^{Empty} control. Phase contrast images from 3D culture show that D492M$^{miR\text{-}203a}$ form more compact colonies, with some colonies showing protrusion of mesenchymal cells compared to control.

C) *MiR-203a reduces proliferation of D492M*. Reduced proliferation of D492M shown by staining with crystal violet from day 1 – 7 in monolayer culture.

D) *DAB staining of monolayer cultures from D492M$^{miR\text{-}203a}$*. Reduced expression of N-Cadherin but little change in expression of E-Cadherin in D492M$^{miR\text{-}203a}$.

E) *Western blot* of E- and N-Cadherin in D492M$^{miR\text{-}203a}$. There is slightly less protein expression of N-Cadherin (10 % reduction) but little change in expression of E-Cadherin in D492M$^{miR\text{-}203a}$ indicating reduced mesenchymal characteristics in D492M$^{miR\text{-}203a}$.

F) *Expression of SNAI2 is reduced in D492M$^{miR\text{-}203a}$*. D492M$^{miR\text{-}203a}$ has a known binding site in the 3´-UTR of SNAI2, which is an inhibitor of apoptosis.

G) *D492M$^{miR\text{-}203a}$ cells are more sensitive to chemically induced apoptosis.*

H) *Low attachment assay*. miR-203a reduces stem cell like properties in D492M. D492M$^{miR\text{-}203a}$ has reduced ability to generate colonies in low attachemtn assay than D492M^{Empty}.

I) *Transwell migration assay*. D492M$^{miR\text{-}203a}$ has less ability to migrate through trans-well filter than D492M^{Empty}.

Invasion assay. D492M$^{miR\text{-}203a}$ has reduced capability to invade through matrigel coated transwell filter. Data shown as average number of cells per field +SEM.

Fig. 5. Gene expression profiling of D492M overexpressing miR-203a.

A) Volcano plot showing differential expressed transcripts in D492M$^{miR\text{-}203a}$ and D492M, depicting statistical significance and high fold change in gene expression. Volcano plot was constructed from RNA sequencing data using beta and q-values from Seluth analysis (max FDR = 0.05), enabling the visualization of the relationship between differentially expressed transcripts and statistical significance. More extreme values on the x-axis show increased differential expression and higher values on the y-axis show increased statistical significance. PXDN is the most downregulated gene when miR-203a is overexpressed in D492M.

B) PXDN 3´-UTR has three potential binding sites for miR-203a
Bioinformatics analysis reveals three potential binding sites for miR-203 in the 3´-UTR of Peroxidasin a heme-containing peroxidase that is secreted into the extracellular matrix and is involved in extracellular matrix formation. One of the binding sites is conserved and two are poorly conserved.

C) D492M cells treated with miR-203a mimic have reduced expression of PXDN. D492M cells were transiently transfected with miR-203a mimic and expression of PXDN measured with qPCR.

D492M$^{miR\text{-}203a}$ cells treated with miR-203a inhibitor have increased expression of PXDN. D492M$^{miR\text{-}203a}$ cells were transiently transfected with miR-203a inhibitor and PXDN expression measured with qPCR.

D) Luciferase assay. HEK293T cells were transfected with plasmid containing the conserved binding site for miR-203a and the surrounding sequence from the PXDN 3'-UTR or a plasmid with only the miR-203a conserved binding site deleted. Cells transfected with the plasmid containing the miR-203a binding site had reduced luciferase activity compared to the empty plasmid control and the plasmid with the deleted miR-203a binding site, indicating binding of the miR-203a-3p mimic to the target sequence.

Fig. S1. Luciferase assay showing binding of miR-203a to P63 3'-UTR target sequence.

Luciferase assay. HEK293T cells were transfected with plasmid containing the conserved binding site for miR-203a and the surrounding sequence from the P63 3'-UTR or a plasmid with only the miR-203a conserved binding site deleted. Cells transfected with the plasmid containing the miR-203a binding site had reduced luciferase activity compared to the empty plasmid control and the plasmid with the deleted miR-203a binding site, indicating binding of the miR-203a-3p mimic to the target sequence.

A

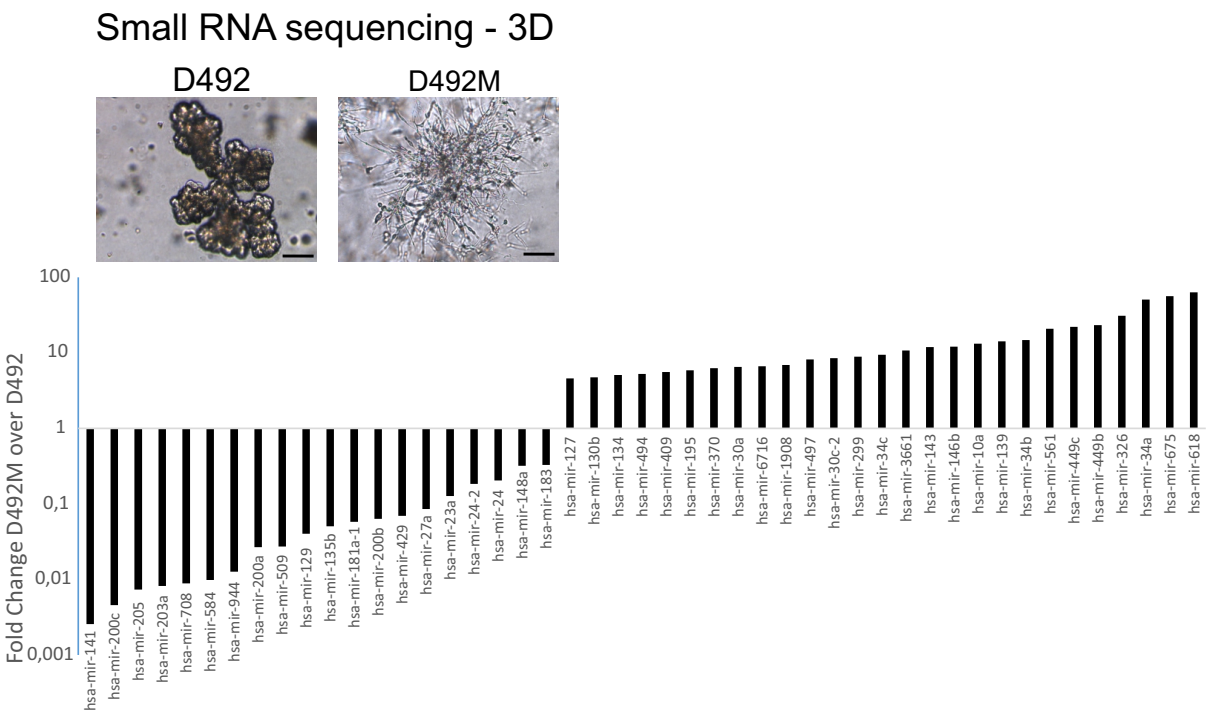
Small RNA sequencing - 3D
D492
D492M
Fold Change D492M over D492
100
10
1
0,1
0,01
0,001
hsa-mir-141
hsa-mir-200c
hsa-mir-205
hsa-mir-203a
hsa-mir-708
hsa-mir-584
hsa-mir-944
hsa-mir-200a
hsa-mir-509
hsa-mir-129
hsa-mir-135b
hsa-mir-181a-1
hsa-mir-200b
hsa-mir-429
hsa-mir-27a
hsa-mir-23a
hsa-mir-24-2
hsa-mir-24
hsa-mir-148a
hsa-mir-183
hsa-mir-127
hsa-mir-130b
hsa-mir-134
hsa-mir-494
hsa-mir-409
hsa-mir-195
hsa-mir-370
hsa-mir-30a
hsa-mir-6716
hsa-mir-1908
hsa-mir-497
hsa-mir-30c-2
hsa-mir-299
hsa-mir-34c
hsa-mir-3661
hsa-mir-143
hsa-mir-146b
hsa-mir-10a
hsa-mir-139
hsa-mir-34b
hsa-mir-561
hsa-mir-449c
hsa-mir-449b
hsa-mir-326
hsa-mir-34a
hsa-mir-675
hsa-mir-618

B

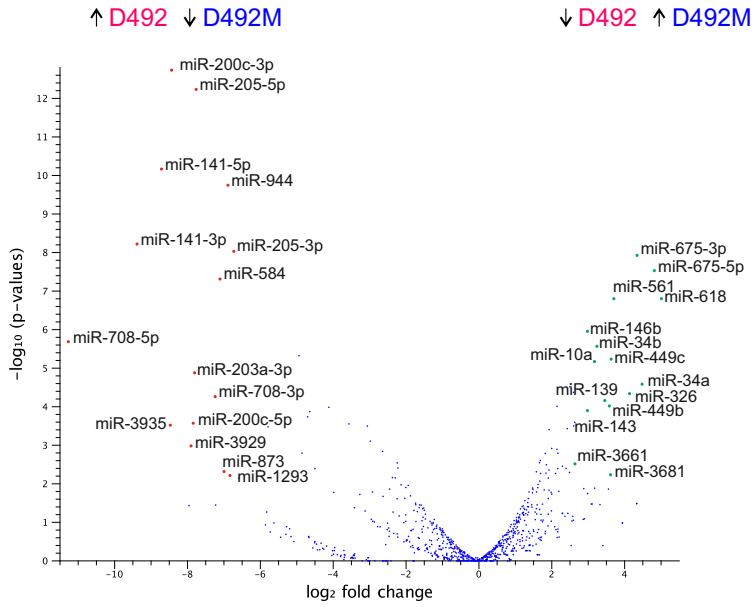
↑ D492 ↓ D492M
↓ D492 ↑ D492M
−log10 (p-values)
log2 fold change
miR-200c-3p
miR-205-5p
miR-141-5p
miR-944
miR-141-3p
miR-205-3p
miR-584
miR-708-5p
miR-203a-3p
miR-708-3p
miR-3935
miR-200c-5p
miR-3929
miR-873
miR-1293
miR-675-3p
miR-675-5p
miR-561
miR-618
miR-146b
miR-34b
miR-10a
miR-449c
miR-34a
miR-139
miR-326
miR-449b
miR-143
miR-3661
miR-3681

A miRNA promoter DNA methylation (HumanMethylation450 BeadChip)

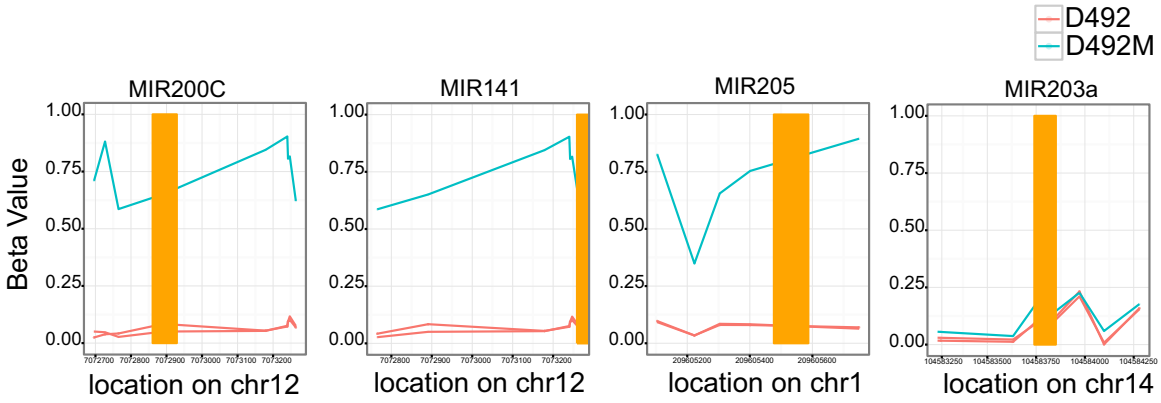

B MiR promoter DNA methylation (Bisulfite sequencing)

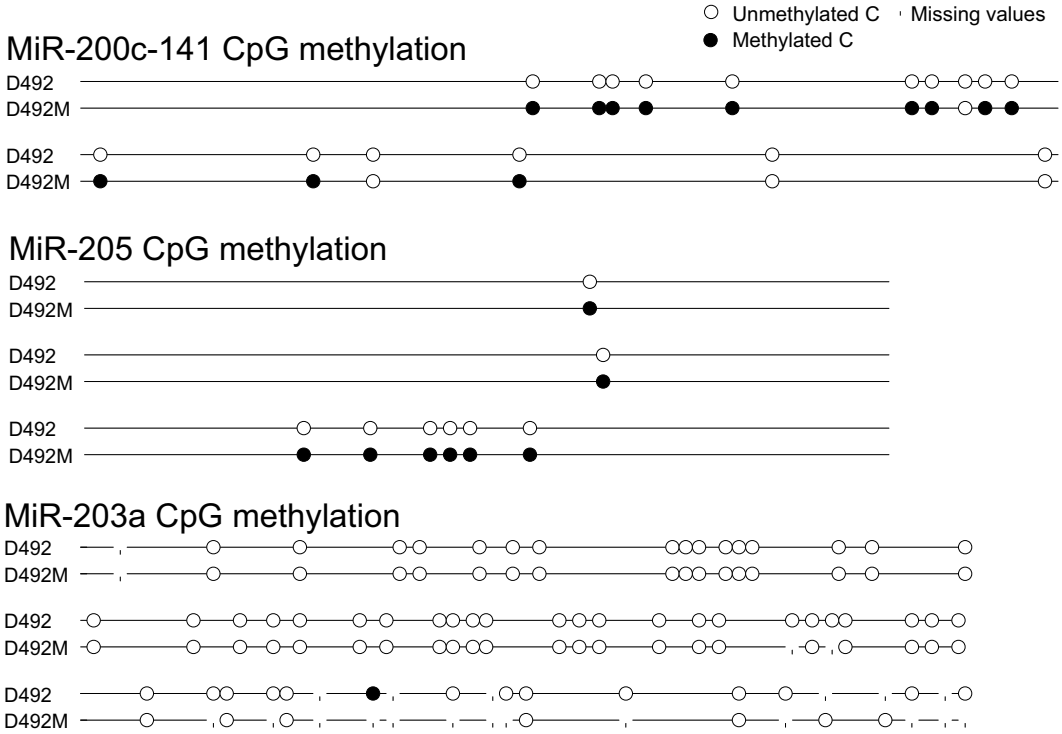

A

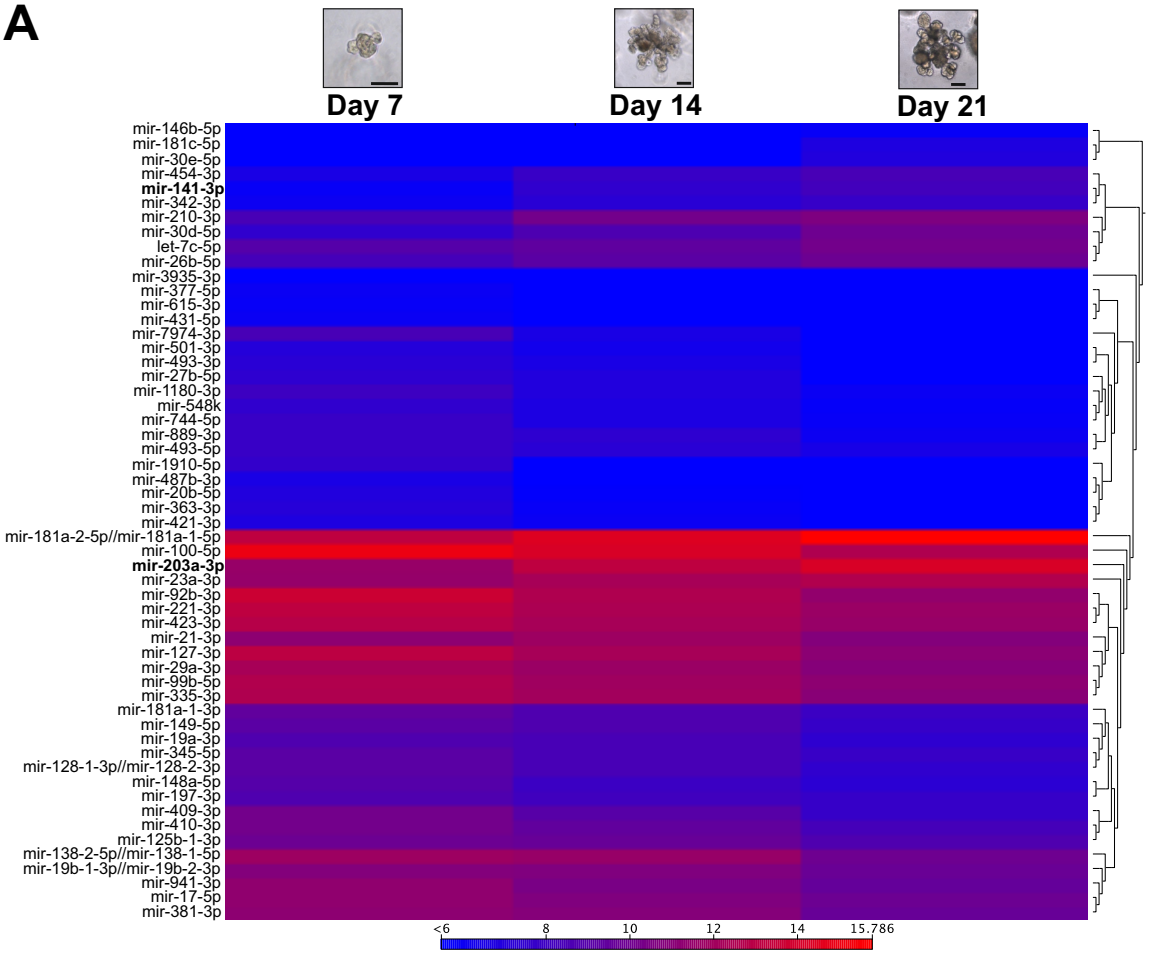
Day 7
Day 14
Day 21
mir-146b-5p
mir-181c-5p
mir-30e-5p
mir-454-3p
mir-141-3p
mir-342-3p
mir-210-3p
mir-30d-5p
let-7c-5p
mir-26b-5p
mir-3935-3p
mir-377-5p
mir-615-3p
mir-431-5p
mir-7974-3p
mir-501-3p
mir-493-3p
mir-27b-5p
mir-1180-3p
mir-548k
mir-744-5p
mir-889-3p
mir-493-5p
mir-1910-5p
mir-487b-3p
mir-20b-5p
mir-363-3p
mir-421-3p
mir-181a-2-5p//mir-181a-1-5p
mir-100-5p
mir-203a-3p
mir-23a-3p
mir-92b-3p
mir-221-3p
mir-423-3p
mir-21-3p
mir-127-3p
mir-29a-3p
mir-99b-5p
mir-335-3p
mir-181a-1-3p
mir-149-5p
mir-19a-3p
mir-345-5p
mir-128-1-3p//mir-128-2-3p
mir-148a-5p
mir-197-3p
mir-409-3p
mir-410-3p
mir-125b-1-3p
mir-138-2-5p//mir-138-1-5p
mir-19b-1-3p//mir-19b-2-3p
mir-941-3p
mir-17-5p
mir-381-3p
<6
8
10
12
14
15.786

B

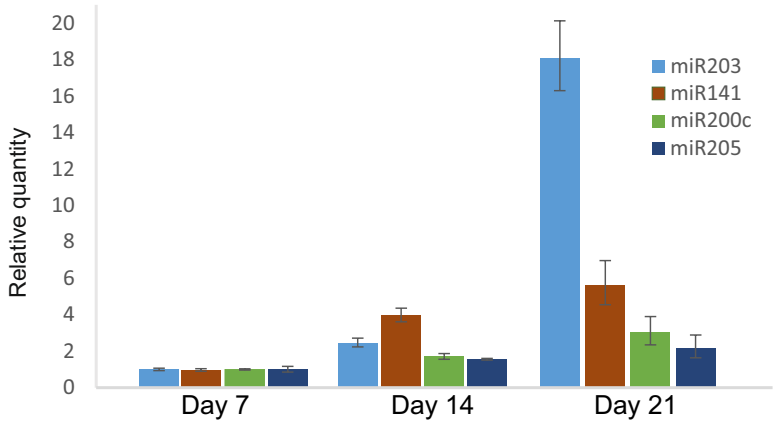

C

i) Primary cells (qPCR) ii) Cell lines (qPCR)

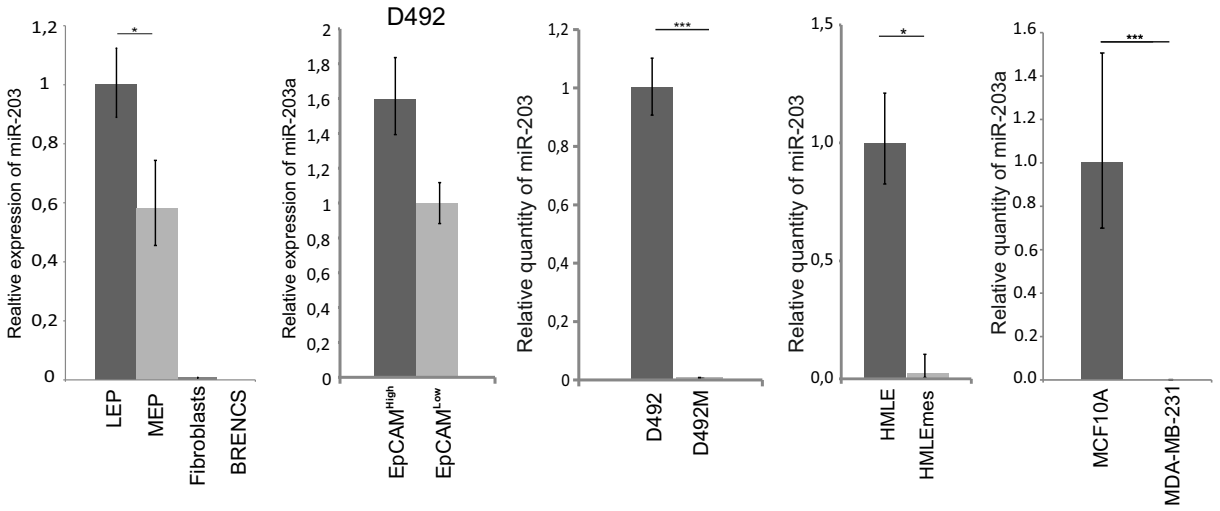

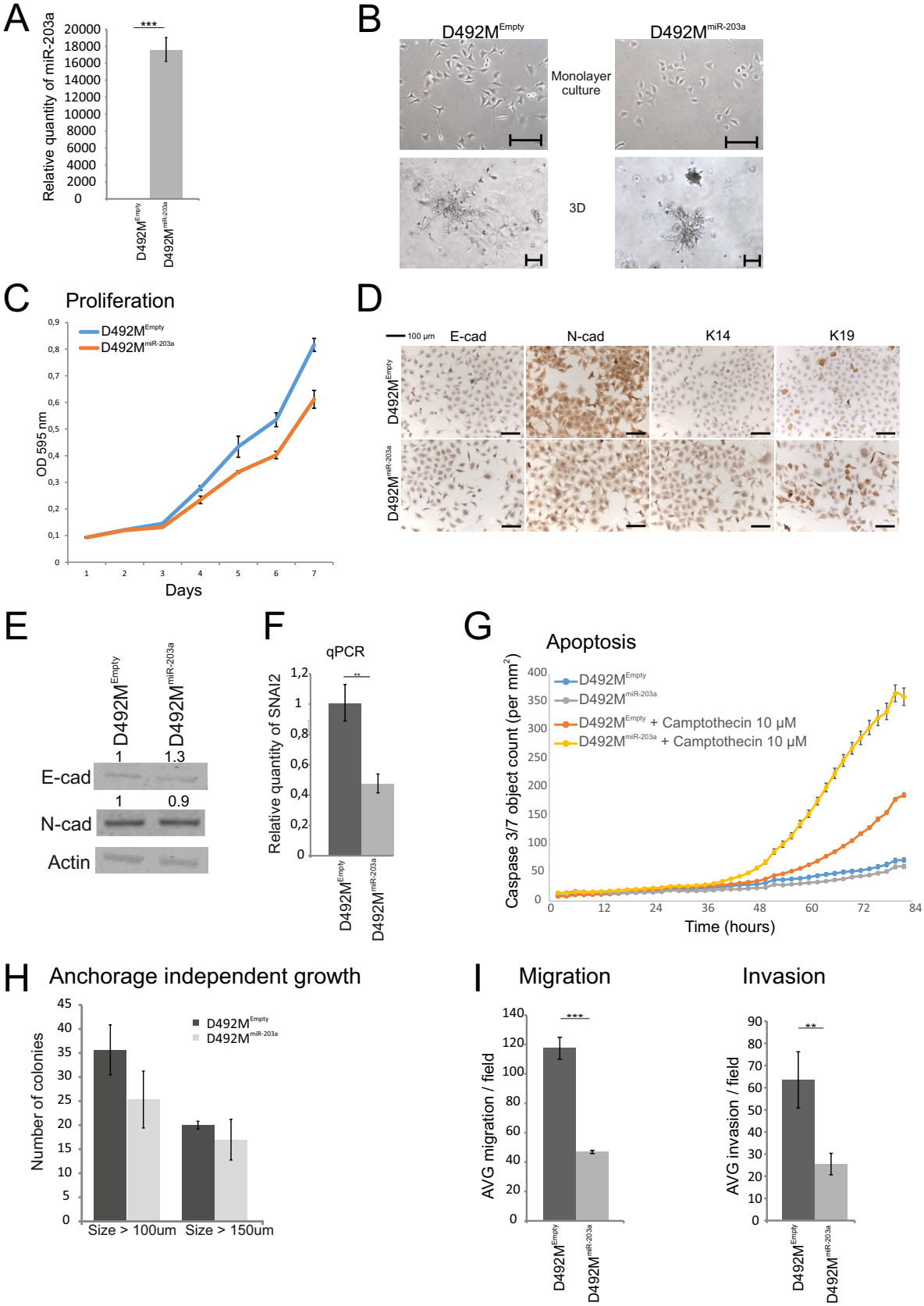
A
Relative quantity of miR-203a
***
D492M^Empty
D492M^miR-203a
B
D492M^Empty
D492M^miR-203a
Monolayer culture
3D
C
Proliferation
D492M^Empty
D492M^miR-203a
OD 595 nm
Days
D
100 µm
E-cad
N-cad
K14
K19
D492M^Empty
D492M^miR-203a
E
D492M^Empty
D492M^miR-203a
1
1.3
E-cad
1
0.9
N-cad
Actin
F
qPCR
Relative quantity of SNAI2
**
D492M^Empty
D492M^miR-203a
G
Apoptosis
Caspase 3/7 object count (per mm²)
D492M^Empty
D492M^miR-203a
D492M^Empty + Camptothecin 10 µM
D492M^miR-203a + Camptothecin 10 µM
Time (hours)
H
Anchorage independent growth
Number of colonies
D492M^Empty
D492M^miR-203a
Size > 100um
Size > 150um
I
Migration
AVG migration / field
***
D492M^Empty
D492M^miR-203a
Invasion
AVG invasion / field
**
D492M^Empty
D492M^miR-203a

A

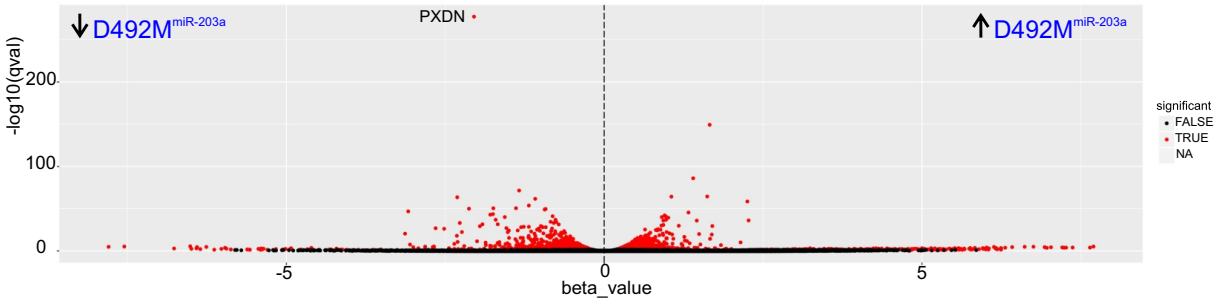

B PXDN 3´-UTR has three potential binding sites for miR-203a

Conserved

mRNA Position 106-113 of PXDN 3' UTR 5' ...CACCCAGAACUCGUGACAUUUCA...

miRNA miR-203a-3p 3' GAUCACCAGGAUUUGUAAAGUG

Poorly conserved

mRNA Position 638-645 of PXDN 3' UTR 5' ...UCUGGGCUCUCUGUAACAUUUCA...

miRNA miR-203a-3p 3' GAUCACCAGGAUUUGUAAAGUG

Poorly conserved

mRNA Position 1618-1624 of PXDN 3' UTR 5' ...CTGCGGCGGAGGCAGCAUUUCAG...

miRNA miR-203a-3p 3' GAUCACCAGGAUUUGUAAAGUG

C

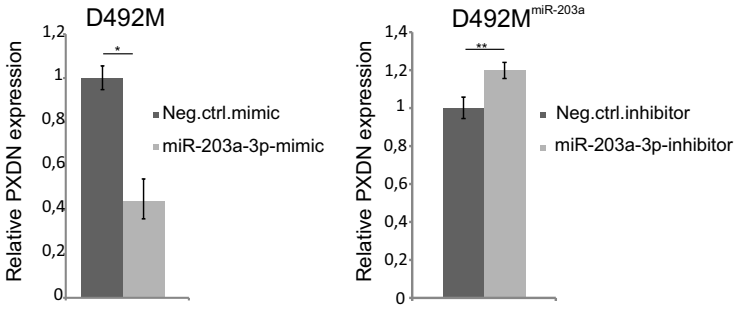

D

PXDN_miR-203a-3p target seq oligo

	PmeI		NotI internal site		miR-203-3p target site	XbaI	
5‘	AAAC	TA	GCGGCCGC	TAGT	CCCAGAACTCGTGACATTTCAT	T	3‘
3‘	TTTG	AT	CGCCGGCG	ATCA	GGGTCTTGAGCACTGTAAAGTA	AGATC	5‘

PXDN_miR-203a-3p target seq deleted oligo

	PmeI		NotI internal site		miR-203-3p target site	XbaI	
5‘	AAAC	TA	GCGGCCGC	TAGT	CCCAGAACTCGTGT	T	3‘
3‘	TTTG	AT	CGCCGGCG	ATCA	GGGTCTTGAGCACA	AGATC	5‘

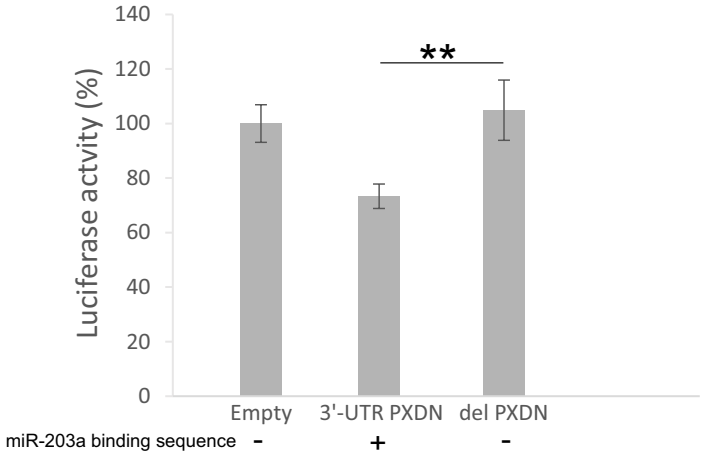

P63_miR-203a-3p target seq oligo

	PmeI		NotI internal site		miR-203-3p target site	XbaI	
5‘	AAAC	TA	GCGGCCGC	TAGT	GAATGAGTCCTTG ATTTCAA A	T	3‘
3‘	TTTG	AT	CGCCGGCG	ATCA	CTTACTCAGGAAC TAAAGTT T	AGATC	5‘

P63_miR-203a-3p target seq deleted oligo

	PmeI		NotI internal site		miR-203-3p target site	XbaI	
5‘	AAAC	TA	GCGGCCGC	TAGT	GAATGAGTCCTTGA	T	3‘
3‘	TTTG	AT	CGCCGGCG	ATCA	CTTACTCAGGAACT	AGATC	5‘

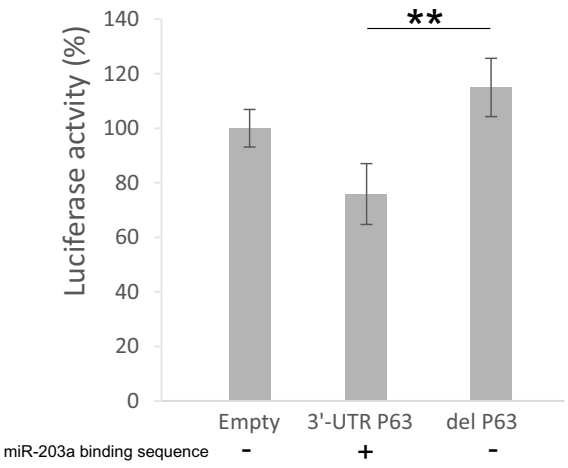

Table S1. Bisulfite genomic sequencing primers

miR-203 – *outer primers*

miR-203-1F - 5'-TTTTTTTTGAAGTGAGAGGGGT-3'
miR-203-1R – 5'- TAAAAACCACTAAACCCAAC-3'

miR-203 – *inner primers*

mir-203-2F – 5'-GAATTCGGGAGGTTAGGTG-3'
mir203-2R – 5'-ACCCCCTACCCTACTACAACC-3'

miR-205 – outer primers

miR-205-1F – 5'-TTTGTTTGTGTAGTAGGTGTAAGGA-3'
miR-205-1R – 5'- AAAAAAAATTAAAATTCCCATCTAC-3'

miR-205 – inner primers

miR205-2F – 5'-GTTTTTTTGGAGGATGTGATT-3'
miR205-2R - 5'-CACTCCAAATATCTCCTTCATTA-3'

mir-200c-141 – outer primers
miR-200c-141-1F – 5´-TTATTTTTTGGGGGTAGGTGGGTT-3´
miR-200c-141-1R – 5´-CAAAAACAAAAACCTCCATCATTACC-3´

mir-200c-141 – inner primers
miR-200c-141-2F – 5´-AAGGTTATTAGGGGAGAGGTTT-3´
miR-200c-141-2R – 5´-CTTCAAACCCAAAATCCCTA-3´

Inner miR-203 primers were obtained from (Bueno, Perez de Castro et al. 2008). Inner miR-200c-141 and inner miR-205 primers were obtained from (Wiklund, Bramsen et al. 2011).

Bueno, M. J., I. Perez de Castro, M. G. de Cedron, J. Santos, G. A. Calin, J. C. Cigudosa, C. M. Croce, J. Fernandez-Piqueras and M. Malumbres (2008). "Genetic and epigenetic silencing of microRNA-203 enhances ABL1 and BCR-ABL1 oncogene expression." Cancer Cell **13**(6): 496-506.

Wiklund, E. D., J. B. Bramsen, T. Hulf, L. Dyrskjot, R. Ramanathan, T. B. Hansen, S. B. Villadsen, S. Gao, M. S. Ostenfeld, M. Borre, M. E. Peter, T. F. Orntoft, J. Kjems and S. J. Clark (2011). "Coordinated epigenetic repression of the miR-200 family and miR-205 in invasive bladder cancer." Int J Cancer **128**(6): 1327-1334.

Paper III

OPEN

Citation: Cell Death and Disease (2017) 8, e2769; doi:10.1038/cddis.2017.177
Official journal of the Cell Death Differentiation Association

www.nature.com/cddis

Inhibition of PTP1B disrupts cell–cell adhesion and induces anoikis in breast epithelial cells

Bylgja Hilmarsdottir[1,2], Eirikur Briem[1,3], Skarphedinn Halldorsson[4], Jennifer Kricker[1,3], Sævar Ingthorsson[1,3], Sigrun Gustafsdottir[1,3], Gunhild M Mælandsmo[2], Magnus K Magnusson[1,3] and Thorarinn Gudjonsson*[,1,3]

Protein tyrosine phosphatase 1B (PTP1B) is a well-known inhibitor of insulin signaling pathways and inhibitors against PTP1B are being developed as promising drug candidates for treatment of obesity. PTP1B has also been linked to breast cancer both as a tumor suppressor and as an oncogene. Furthermore, PTP1B has been shown to be a regulator of cell adhesion and migration in normal and cancer cells. In this study, we analyzed the PTP1B expression in normal breast tissue, primary breast cells and the breast epithelial cell line D492. In normal breast tissue and primary breast cells, PTP1B is widely expressed in both epithelial and stromal cells, with highest expression in myoepithelial cells and fibroblasts. PTP1B is widely expressed in branching structures generated by D492 when cultured in 3D reconstituted basement membrane (3D rBM). Inhibition of PTP1B in D492 and another mammary epithelial cell line HMLE resulted in reduced cell proliferation and induction of anoikis. These changes were seen when cells were cultured both in monolayer and in 3D rBM. PTP1B inhibition affected cell attachment, expression of cell adhesion proteins and actin polymerization. Moreover, epithelial to mesenchymal transition (EMT) sensitized cells to PTP1B inhibition. A mesenchymal sublines of D492 and HMLE (D492M and HMLEmes) were more sensitive to PTP1B inhibition than D492 and HMLE. Reversion of D492M to an epithelial state using miR-200c-141 restored resistance to detachment induced by PTP1B inhibition. In conclusion, we have shown that PTP1B is widely expressed in the human breast gland with highest expression in myoepithelial cells and fibroblasts. Inhibition of PTP1B in D492 and HMLE affects cell–cell adhesion and induces anoikis-like effects. Finally, cells with an EMT phenotype are more sensitive to PTP1B inhibitors making PTP1B a potential candidate for further studies as a target for drug development in cancer involving the EMT phenotype.
Cell Death and Disease (2017) **8,** e2769; doi:10.1038/cddis.2017.177; published online 11 May 2017

Protein tyrosine phosphatases (PTPs) and tyrosine kinases modulate cellular levels of tyrosine phosphorylation and regulate many cellular events such as differentiation, cell growth, motility and proliferation.[1] Regulation of the balance between tyrosine phosphorylation and dephosphorylation within cells is important for many cellular processes and homeostasis and is implicated in a number of human diseases.[2]

Protein tyrosine phosphatase 1B (PTP1B) is a 50 kDa non-receptor phosphatase localized predominantly on the cytoplasmic surface of the endoplasmic reticulum, anchored via its C-terminal region.[3] PTP1B has a major role in downregulating insulin and leptin signaling[4] by dephosphorylating the insulin receptor and thus terminating its signals. PTP1B-deficient mice are hypersensitive to insulin and resistant to obesity induced by a calorie-rich diet.[5] For this reason, PTP1B has received attention over the last few years as a novel therapeutic target for the treatment of diabetes and obesity, and as such there are numerous inhibitors against PTP1B at various stages of development.[6]

In addition to insulin regulation, PTP1B also has a role in other signaling pathways, such as growth factor and integrin mediated processes, as well as cancer development.[7,8] PTP1B is a major activator of Src by dephosphorylating the inhibitory tyrosine phosphorylation site (Y529) on the COOH terminus of the kinase.[9] PTP1B has been shown to be a positive mediator of the ErbB2-induced signals that trigger breast tumorigenesis[10,11] and to be required for ErbB2 transformation in breast epithelial cells through Src activation.[12] Substrate trapping and biochemical studies have identified various substrates of PTP1B involved in cell adherence and matrix attachment. For example, PTP1B regulates the intracellular protein tyrosine kinases like focal adhesion kinase (FAK), Src and adaptor proteins like β-catenin and p130Cas.[13–15] PTP1B has also been shown to interact with integrin complexes and localize to early cell matrix adhesion sites.[3] Mouse fibroblasts, which expressed a dominant-negative form of PTP1B have small matrix sites, are impaired in cell spreading and show reduced Src activity. Similarly, cells derived from PTP1B KO mice also show defects in cell spreading.[16] These data suggest that PTP1B is an important regulator of integrin signaling pathways thereby indicating a role in adhesion, spreading and formation of focal adhesion.[17] Developmental events underlying branching morphogenesis in the breast are closely related to pathways important for cancer progression, that is, epithelial plasticity and epithelial–mesenchymal transition (EMT). EMT is a process where epithelial cells lose epithelial characteristics and gain mesenchymal traits. Although still debated, EMT is

[1]Stem Cell Research Unit, Department of Medical Faculty, Biomedical Center, School of Health Sciences, University of Iceland, Reykjavik, Iceland; [2]Department of Tumor Biology, Institute for Cancer Research, The Norwegian Radium Hospital, Oslo University Hospital Nydalen, Oslo, Norway; [3]Department of Laboratory Hematology Landspitali, University Hospital, Reykjavik, Iceland and [4]System Biology Center, University of Iceland, Reykjavik, Iceland
*Corresponding author: T Gudjonsson, Stem Cell Research Unit, Department of Medical Faculty, Biomedical Center, School of Health Sciences, University of Iceland, Vatnsmyrarvegi 16, Reykjavik 101, Iceland. Tel: +354 525 4827; Fax: +354 525 4884; E-mail: tgudjons@hi.is
Received 10.9.16; revised 21.3.17; accepted 22.3.17; Edited by A Stephanou

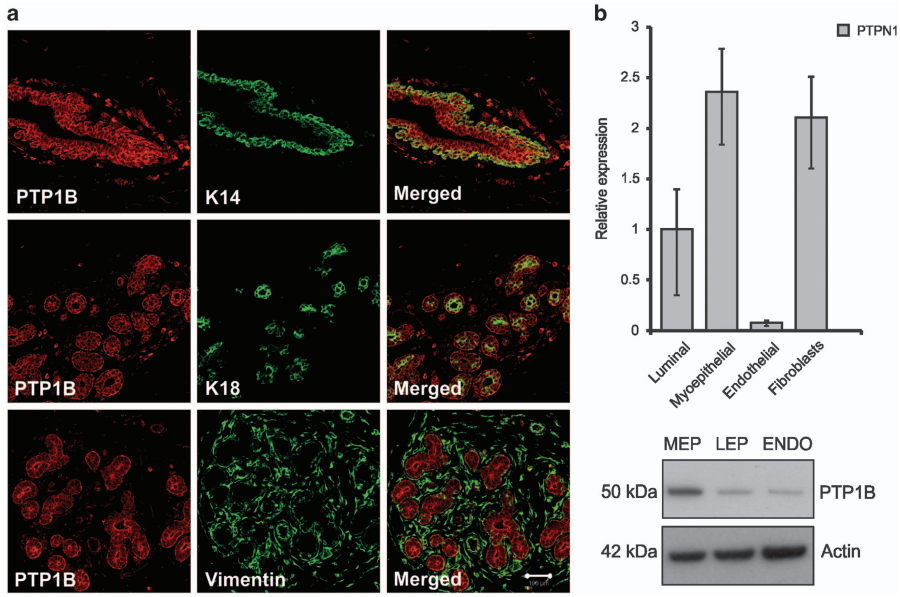

Figure 1 PTP1B is highly expressed in normal human breast tissue. (**a**) PTP1B is expressed both in the epithelial and stromal compartments of the breast. Immunohistochemical stainings show prominent co-expression of PTP1B (red) and K14 (green) in myoepithelial cells (top row), PTP1B (red) and K18 (green) in luminal epithelial cells (middle row), PTP1B (red) and vimentin (green) stains myoepithelial and fibroblasts (bottom row). Bar 100 μm. (**b**) PTP1B is predominantly expressed in myoepithelial cells and fibroblasts in the breast gland. qPCR mRNA analysis shows that PTP1B expression is higher in myoepithelial cells (MEP) and fibroblasts than in luminal epithelial cells (LEP) and endothelial cells (ENDO). Expression levels were normalized to GAPDH (upper). Western blot confirmed high expression of PTP1B in myoepithelial cells (lower). Actin was used as a loading control

widely considered to be a key process in metastatic breast cancer, which is the leading cause of cancer deaths.[18] During EMT, intracellular contacts change and during the transformation from a polarized epithelium to the mesenchymal state there is loss of tight junctions and adhesion molecules.[19] EMT is believed to have an important role in cancer progression, invasion, formation of metastasis and resistance to cancer treatment.[20] Thus, identification of drugs that specifically target cells with the EMT phenotype, could be a key event to improve cancer treatment.

In light of its central role in cell adhesion and Src regulation, as well as its potential role in cancer, we sought to investigate the impact of PTP1B inhibition on breast epithelial and mesenchymal cells. Inhibiting PTP1B in D492 and HMLE, breast epithelial cell lines, leads to apoptotic cell death with morphological characteristics of anoikis, cell death induced by loss of extracellular matrix attachment. PTP1B inhibition leads to downregulation of cell adhesion proteins and disrupted actin polymerization. In addition, we show that the transition from an epithelial to a mesenchymal state sensitizes mammary cells to PTP1B inhibition, suggesting the therapeutic potential of PTP1B inhibition in cancer treatment.

Results

PTP1B is ubiquitously expressed in normal human breast tissue. PTP1B has in recent years been linked to both tumorigenesis and tumor suppression[21,22] but less is known about its expression and function in the normal human breast gland. Histochemical analysis of paraffin-embedded breast tissue with antibodies against PTP1B and cell type-specific markers, K14 (myoepithelial), K18 (luminal epithelial) and vimentin (myoepithelial and fibroblasts), revealed that PTP1B is, at least partially, co-stained with each of these markers (Figure 1a). The expression intensity, however, varied between different cell populations. Isolated cell populations derived from reduction mammoplasty show that PTP1B expression is enriched in myoepithelial cells and fibroblasts (Figure 1b). Thus, PTP1B is ubiquitously expressed in epithelial cells in the breast, as well as in stroma.

PTP1B inhibition results in apoptosis of breast epithelial cells. Given the ubiquitous expression of PTP1B in the human breast gland, we examined if PTP1B had a role in proliferation and survival of breast epithelial cells. D492 is a breast epithelial cell line with stem cell properties that is able to generate luminal and myoepithelial cells and generates branching structures reminiscent of terminal duct lobular units (TDLUs) when cultured in 3D reconstituted basement membrane (3D rBM; Figure 3a). To test the effects of the inhibition of PTP1B in D492, a specific PTP1B inhibitor ($IC_{50} = 8\,\mu$M) against the catalytic domain of the protein was used. When cell growth and proliferation were analyzed, PTP1B inhibition had a major effect on the survival of D492. After 72 h of treatment with 16 μM of the PTP1B inhibitor, the

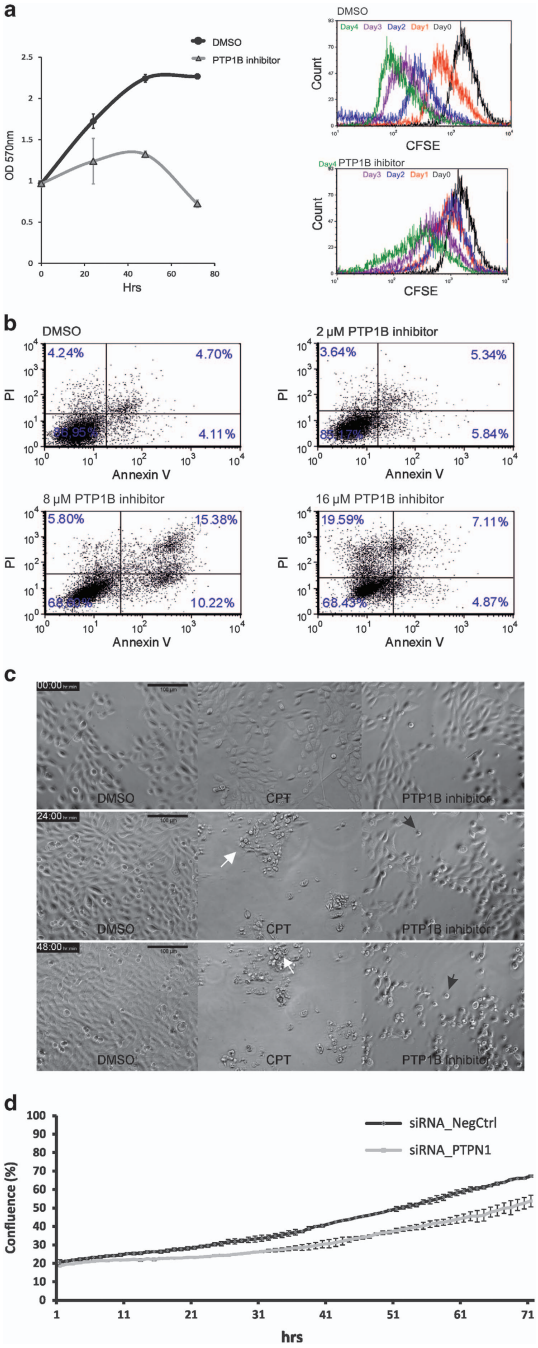

Figure 2 PTP1B is important for proliferation and survival of breast epithelial cells. (**a**) Inhibition of PTP1B reduces cell division and affects survival of D492 cells. Left cell survival assay reveals that PTP1B inhibitor causes reduction in proliferation and cell death in D492. D492 were treated with DMSO (control) or 16 μM of a specific PTP1B inhibitor for 3 days, stained with crystal violet and the optical density at 570 nm determined. All experiments were conducted in triplicate. Right, D492 cells were stained with CFSE fluorescent dye, treated with DMSO or 8 μM of PTP1B inhibitor and analyzed using flow cytometry over a period of 4 days. Note, reduced cell division in D492 after PTP1B inhibition. (**b**) Inhibition of PTP1B results in apoptosis of D492 cells. Annexin V and PI staining shows that PTP1B inhibitor induces apoptotic cell death in D492. D492 cells were treated with DMSO (control) and various concentrations of PTP1B inhibitor. (**c**) Cell death induced by the PTP1B inhibitor shows the characteristics of anoikis. CPT induces classical apoptosis of D492 cells over time in culture (middle column). D492 cells were treated with DMSO as a control (left column). Treatment with PTP1B inhibitor results in failure of cells to establish a confluent monolayer with a number of cells forming a rounded detached appearance as in cells undergoing anoikis. (**d**) Knockdown of PTPN1 reduces proliferation of D492 cells. D492 cells were transfected with siRNA PTPN1 s11507 or negative control no. 1 siRNA at 50 nM and cell confluence was monitored for 72 h using IncuCyte Zoom Live Cell Analysis System. Knockdown of PTPN1 resulted in an inhibition of confluency, whereby D492 cells treated with siRNA against PTPN1 demonstrated significantly less cell proliferation than cells treated with negative control siRNA. All experiments were done in triplicate

majority of D492 cells were dead (Figure 2a, left). To estimate the effect of PTP1B inhibition on the proliferation rate of D492 cells, we performed a cell tracing experiment using carboxyfluorescein succinimidyl ester (CFSE). CFSE is a fluorescent membrane dye that measures cell proliferation by flow cytometry. D492 cells were treated with either a DMSO control or 8 μM of the PTP1B inhibitor. Flow cytometry analysis of the CFSE-stained cells showed that 8 μM of PTP1B inhibitor substantially reduced cell division of D492 cells opposed to the DMSO-treated cells (Figure 2a, right). To further validate our findings, we tested the effect of PTP1B inhibition on two additional cell lines, MCF10a and HMLE (Supplementary Figures 1A and B). Treatment of both of these cell lines with the PTP1B inhibitor resulted in severe reduction of cellular growth and cell death, similar to what was observed in D492 cells.

Annexin V apoptosis assay demonstrates that PTP1B inhibition induces apoptosis in D492 (Figure 2b). In cells treated with DMSO or a low concentration of the PTP1B inhibitor (2 μM), only low levels of annexin V and propidium iodide (PI) were detected. In contrast, when D492 cells were treated with 8 μM of the PTP1B inhibitor, 26% of the cells were annexin V positive and 21% PI positive, of which 15% were stained for both markers. Annexin V/PI staining of cells with increasing PTP1B inhibitor concentration demonstrates several stages of programmed cell death, from early to late apoptosis. The highest level of cell death was observed when D492 cells were treated with 16 μM of the PTP1B inhibitor. Annexin V/PI staining indicates that the cells are in late apoptosis where 27% of cells stain positive for PI and only 12% are positive for annexin V. Interestingly, these apoptosis-inducing effects were not seen if experiments were done in medium containing serum or serum supplements (Supplementary Figure 3) indicating that this inhibitor is not effective in serum-containing media. To supplement our work with the inhibitor, we also knocked down PTP1B using siRNA (Figure 2d). This resulted in an inhibition of confluency, whereby D492 cells treated with siRNA against PTP1B demonstrated significantly less cell proliferation than cells treated with negative control siRNA. Moreover, addition of

serum did not rescue cell survival after PTP1B inhibition using siRNA (Supplementary Figure 3b). These results indicate that D492 cells are induced to undergo programmed cell death after inhibition of PTP1B, whether it is via a small molecule inhibitor or siRNA knockdown of PTP1B.

The classical morphology of a cell going through apoptosis is nuclear fragmentation, cell shrinkage and membrane blebbing.[23] The observed morphology of cells after treatment with the PTP1B inhibitor was not consistent with these hallmarks of apoptosis. To compare the morphology of cells undergoing classic apoptosis and cell death induced by PTP1B inhibition, D492 cells were treated with 10 μM camptothecin (CPT), an apoptosis inducer alongside the PTP1B inhibitor. Cells treated with CPT show typical apoptosis morphology (Figure 2c and Supplementary Video File 1), whereas cells treated with the PTP1B inhibitor appear round and surrounded by a halo as they detach from the surface. This morphology is consistent with cells undergoing anoikis, programmed cell death induced by detachment from the extracellular matrix.[24–26]

Inhibition of PTP1B in D492 cells results in disturbed morphogenesis suggesting anoikis. D492 cells generate *in vivo*-like branching structures in 3D cell culture (Figure 3a, top). Analysis of PTP1B expression in these branching structures revealed similar widespread expression as in the normal breast gland with increased intensity at the lobular ends (Figure 3a). F-actin is a cytoskeletal protein that is expressed equally throughout the structure, whereas β4-integrin is localized at the surface of the structure in contact with the basement membrane.

D492 branching structures were treated with the 32 μM of the PTP1B inhibitor, or 20 μM of CPT as control for 48 h. Figure 3b (see also Supplementary Video File 2) shows that while CPT induces cell blebbing, shrinkage and accumulation of cell debris surrounding the structure, the PTP1B inhibitor induces loss of cell–cell contact and the branching structure shows a 'grape-like' morphology where cells do not move synchronically within the structure (as in the control), but rather individually.

In-gel immunostaining of treated branching structures shows that only CPT treatment induces cleaved caspase-3 staining (Figure 3c). Staining for of F-actin is diminished in structures treated with PTP1B inhibitor compared with DMSO treatment.

Src activity in D492 cells is dependent on PTP1B. Src activity is regulated by phosphorylation of two distinct tyrosine residues, autophosphorylation of Tyr^{416} in the kinase domain activates Src whereas phosphorylation of Tyr^{529} in the C-terminal tail inactivates it. Consequently, activation of Src requires the removal of the C-terminal phosphate by specific PTPs. To assess the effect of PTP1B inhibition on Src phosphorylation in D492 cells, we treated the cells with various concentrations of the PTP1B inhibitor for 48 h followed by protein isolation for western blot analysis. The phosphorylation level at Tyr^{529} was determined using a phosphospecific antibody as shown in Figure 4. Treatment of D492 cells with the PTP1B inhibitor caused a significant increase in Tyr^{529} phosphorylation (Figure 4a). Phosphorylation on the inhibitory tyrosine increased gradually with increased concentration of the inhibitor. To support this finding, D492 cells were treated with DMSO or 16 μM of the PTP1B inhibitor for 3 h. The cells were then fixed with methanol and stained for PTP1B and pSrc Tyr^{529}. The phosphorylation status of Src had increased drastically and appeared to reside at the cell membrane (Figure 4a, right).

To confirm that the PTP1B inhibitor is working directly on PTP1B interactions with substrate proteins, we used proximity ligation assay (PLA), which detects localization of protein interactions within the cell. Using antibodies detecting EGFR and Src (known PTP1B substrates),[27,28] and PTP1B we observed a loss of signal when cells were treated with the inhibitor (Figure 4b, left). Each dot represents colocalization between PTP1B and Src and PTP1B and EGFR, respectively. The ImageJ (NIH, USA) program was used to quantify the number of dots in non-treated *versus* treated cells (Figure 4b, right).

PTP1B inhibitor induces loss of adhesion molecules in D492. To investigate how PTP1B inhibition affects cell adhesion, we used a cell detachment assay where cells were treated with 8 or 16 μM of the PTP1B inhibitor, 10 μM of CPT or DMSO as control for 24 h (Figure 5a). After treatment, cell attachment to the culture plate was measured as cells detached after 1 min of trypsinization compared with total number of cells. PTP1B-treated cells were much more sensitive to trypsinization than control cells. In contrast, induction of apoptosis with CPT did not facilitate detachment from the culture plate.

To further confirm our hypothesis that the PTP1B inhibitor is affecting cell adhesion, we treated D492 cells with different concentrations of the PTP1B inhibitor and tested the expression of selected adhesion molecules by western blot (Figure 5b). At the highest concentration of the inhibitor, cells lost the expression of claudin-1, FAK and E-cadherin, whereas occludin expression remained unchanged. Moreover, phalloidin staining shows that actin polymerization in D492 cells is completely abolished after treatment with the PTP1B inhibitor (Figure 5c), whereas total actin levels are unaffected (Figure 5b). To supplement this data, we treated HMLE cells with various concentration of the inhibitor for 48 h and tested the expression of E-cadherin, FAK and $pFAK^{Y925}$ (Supplementary Figure 4). Western blot analysis shows diminished expression of E-cadherin in HMLE cells treated with 16 μM of the PTP1B inhibitor, reduced expression of FAK and loss of FAK phosphorylation.

EMT sensitizes cells to loss of attachment caused by PTP1B inhibition. During EMT, epithelial cells loose cell–cell adhesion and gain increased migratory and invasive properties. To test the effect of the PTP1B inhibitor on less adherent cells than D492, we used D492M, a mesenchymal subline of D492. D492M is ideal to use as a comparison as it is directly derived from D492 and has all the characteristics of a cell line that has gone through EMT.[29]

D492M has a mesenchymal phenotype, is more mobile and has reduced attachment to the culture flask compared with D492. We compared the effects of the inhibitor on D492 and D492M using a crystal violet survival curve. Importantly, this

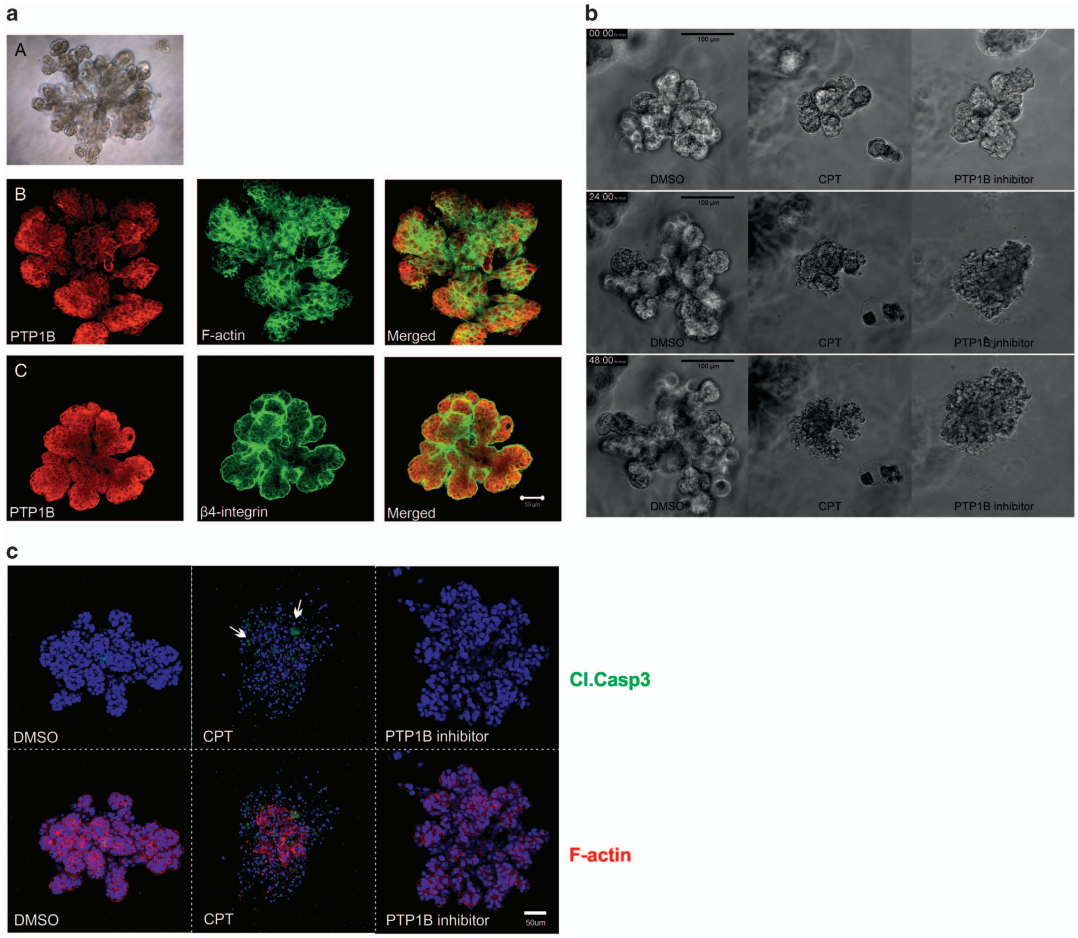

Figure 3 Inhibition of PTP1B affects branching morphogenesis and induces anoikis-like effects in D492 cells cultured in 3D. (**a**) Expression of PTP1B in TDLU-like structures generated by D492 cells in 3D culture. (A) D492 cells form branching structures when cultured in 3D rBM matrix. (B) Expression of F-actin (green), PTP1B (red) and (C) expression of β4-integrin (green) and PTP1B in D492 cells cultured in 3D rBM. Note, the strong expression of PTP1B at the lobular ends. Bar 50 μm. (**b**) Inhibition of PTP1B induces loss of cell adhesion in 3D structures. D492 cells cultured in 3D rBM were treated with 10 μM of CPT, 32 μM of the PTP1B inhibitor or DMSO as control for 48 h. (**c**) D492 cells treated with PTP1B inhibitor die by anoikis. D492 cells treated with the PTP1B inhibitor do not show staining for cleaved caspase 3 in 3D culture (green). CPT was used as a positive control for apoptosis, arrows point to cells positive for cleaved caspase 3. Phalloidin stains F-actin (red). DAPI was used for nuclear staining (blue)

assay does not assess cell death, but how many cells are attached to the culture flask surface in each measured time point. Figure 6a shows a significantly reduced cell count in D492M compared with D492, and thus, an increased effect of the PTP1B inhibitor. To show that the increased effects of PTP1B inhibition on mesenchymal cells are not cell line specific, we used the human mammary cell line HMLE[30] and its mesenchymal derivative HMLEmes. The mesenchymal-derived cells were made by sorting for the EpCAM-negative population of the HMLE cell line. HMLEmes show classical characteristics of EMT in gene expression and morphology (unpublished data). As with the D492 cell lines, HMLE and HMLEmes are not cultured in the presence of serum. Similar to D492/D492M, the mesenchymal cell line HMLEmes also proved to be more vulnerable to PTP1B inhibition than the epithelial HMLE cell line, indicating that cells with a mesenchymal phenotype and less expression of cell adhesion molecules are more sensitive to PTP1B inhibition (Figure 6b).

We have previously shown that overexpression of miR-200c-141 in D492M induces mesenchymal to epithelial transition (MET).[31] To analyze if MET makes cells more resistant to cell death after PTP1B inhibition, we used a cell detachment assay to compare the differences between $D492M^{Ctrl}$ and $D492M^{miR\text{-}200c\text{-}141}$ with regard to trypsinization. Figure 6c shows that $D492M^{Ctrl}$ is more sensitive to trypsinization after treatment with the PTP1B inhibitor than its epithelial subline, $D492M^{miR\text{-}200c\text{-}141}$.

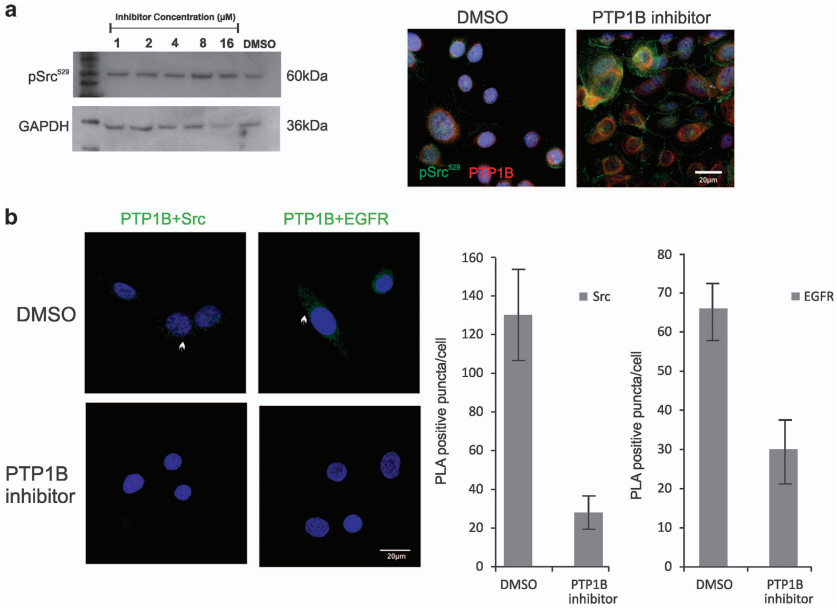

Figure 4 PTP1B inhibitor decreases Src activation in D492 cells. (**a**) Treatment with PTP1B inhibitor results in increased phosphorylation of the inhibitory Src^{Y529}. Left, western blot analysis of $pSrc^{Y529}$ shows that PTP1B inhibitor increases phosphorylation of $pSrc^{Y529}$. Protein extracts from D492 cells after treatment with DMSO and various concentrations of PTP1B inhibitor for 48 h. GAPDH as loading control. Right, Immunofluorescence staining of pSrc in D492 cells treated with the PTP1B inhibitor confirms increased phosphorylation of $pSrc^{Y529}$ after PTP1B inhibition. pSrc (green), PTP1B (red), TOPRO-3 nuclear staining (blue). Bar 20 μm. (**b**) Inhibition of PTP1B disrupts PTP1B protein interactions. PLA shows that PTP1B complexes with Src (left) and EGFR (right) (green arrows) are disassembled (left). DAPI nuclear stain (blue). Cell profiler was used to quantify frequency of positive puncta per cell (right)

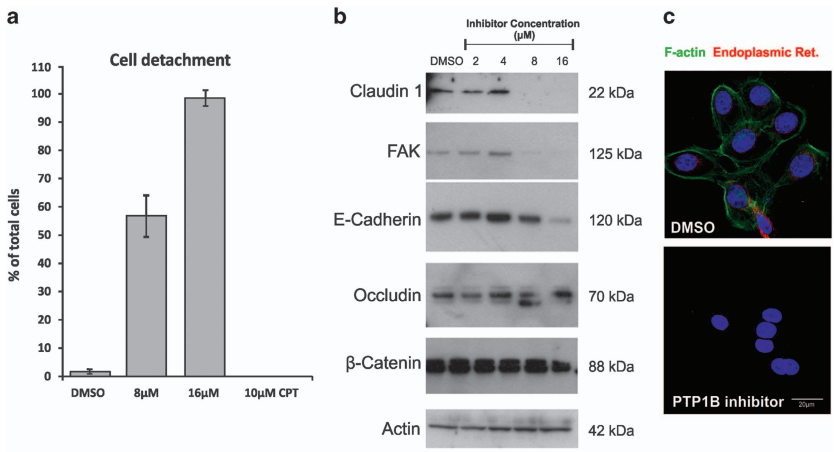

Figure 5 PTP1B inhibition affects expression of cell adhesion molecules and actin polymerization. (**a**) D492 cells treated with PTP1B inhibitor show loose surface attachment. D492 cells were treated with 8 or 16 μM of the PTP1B inhibitor, 10 μM of CPT or DMSO as control for 24 h, and assayed for sensitivity to trypsinization. (**b**) Expression of various cell adhesion molecules is reduced in D492 cells after PTP1B inhibition for 48 h. D492 cells were treated with various concentrations of the PTP1B inhibitor for 48 h followed by protein isolation. Claudin-1, FAK and E-cadherin expression is lost when treated with 16 μM of the inhibitor. PTP1B inhibition does not affect occludin, β-catenin and actin expression. (**c**) F-actin polymerization is lost in D492 cells treated with inhibitor for 5 h. Phalloidin stains F-actin (green), Concavalin A stains endoplasmic reticulum (red)

Collectively, we have shown that breast epithelial cells with a mesenchymal phenotype are more sensitive to PTP1B inhibition than their epithelial counterparts.

Discussion

In this work, we have studied the expression of PTP1B in human breast tissue and human breast epithelial progenitor cells. We have furthermore analyzed its role in cell proliferation and survival of breast epithelial cells in culture. PTP1B expression is abundant in primary human breast tissue with highest expression in primary basal/myoepithelial cells and fibroblasts. Expression of PTP1B is also high in D492 cells grown in 3D rBM where staining is increased at lobular ends of the branching structures. Inhibition of PTP1B via a specific PTP1B inhibitor or by siRNA knockdown of PTP1B resulted in marked effects on the survival of D492 cells by inducing cell death. Our data based on CFSE staining further indicates that the cell death in D492 is primarily in dividing cells. Furthermore, there were striking changes in the cell morphology during PTP1B inhibitor treatment; the cells were round with characteristics of reduced cell attachment and spreading. Collectively from these changes, we conclude that inhibition of PTP1B in D492 cells results in loss of cell attachment and cell death in the form of anoikis. In the current work, we have exclusively focused on *in vitro* models. Culturing cells in 3D rBM can capture morphogenesis seen *in vivo* but will never fully replace *in vivo* models. Therefore, it will be important to continue this work using *in vivo* models.

Our results in the breast gland are consistent with other publications where PTP1B inhibition resulted in apoptosis in non-small cell lung cancer cells[22] and susceptibility to anoikis in colorectal cancer cells.[32] We show here that the cell death induced by inhibition/knockdown of PTP1B and CPT-induced apoptosis demonstrates morphology representative of anoikis and classical apoptosis, respectively. We also provide evidence that PTP1B can activate Src, a well-known oncogene, which is known to have a role in anoikis.[33,34] Furthermore, PTP1B inhibition results in downregulation of the adhesion molecules claudin-1, E-cadherin and FAK and disrupted actin polymerization. Interestingly, mesenchymal derivatives of mammary epithelial cells (both D492M and HMLEmes) are more sensitive to PTP1B inhibition than the epithelial cell lines. Moreover, a MET cell line, $D492M^{miR\text{-}200c\text{-}141}$ is more resistant to PTP1B inhibition than the control cell line. These data are particularly interesting because cells that have undergone EMT, especially cancer cells, are in general more resistant against drug treatment. If inhibition of PTP1B renders these cells more vulnerable for induction of cell death, this could open up possibilities of using PTP1B inhibitors in therapy against a subset of breast cancer tumors, namely those enriched with cells showing an EMT phenotype.

Anoikis resistance of tumor cells constitutes an essential event in tumor progression to metastases in carcinomas.[35] The metastatic process involves the detachment of adherent cancer cells, invasion into the surrounding stroma and extravasation of the metastatic cells into vascular vessels. Anchorage-independent cells then travel to distant organs where they can colonize and form metastasis. Studies of anoikis and the characterization of the mechanisms mediating sensitivity to anoikis can provide important insights into epithelial homeostasis and metastasis. Src tyrosine kinase is one of the key molecules believed to have a critical role in the development of resistance against anoikis. Studies have shown that Src overexpression significantly contributes to resistance of epithelial cells to anoikis.[36,37] Src is a powerful oncogene but it is rarely mutated in human cancer, suggesting that it is involved in later stages of carcinogenesis and has a supporting, rather than an initiating role.[38] In human breast cancer, Src activity is often increased 4- to 30-fold compared with activity in normal breast tissue and it has also been reported that Src protein levels can be increased in breast cancer.[39] Numerous studies have shown that elevated catalytic activity of Src is required to confer resistance to cell death, thus identifying Src as a survival factor that protects cancer cells from apoptosis and anoikis.[40,41]

Studies indicate that PTP1B is the primary PTP capable of dephosphorylating c-Src in breast cancer cell lines and thus controlling its kinase activity.[42] Our findings suggest that when D492 cells are treated with the PTP1B inhibitor Src activity is diminished, identifying PTP1B as a positive regulator of Src. Western blotting showed that PTP1B inhibition enhanced phosphorylation on the tyrosine inhibitory phosphorylation site in Src. This finding was further confirmed by staining cells with a Src-phospho-specific (Y529) antibody, where D492 cells treated with PTP1B inhibitor showed increased Y529-phosphorylated Src at the cell membrane, as well as in the cytoplasm. This staining correlates with reported Src localization in other studies.[12]

In this study, we also show that inhibiting PTP1B downregulates adhesion signaling. Thus, PTP1B inhibition could interfere with the cancer cells abilities to reside in a secondary site. Importantly, the mesenchymal D492M cell line is more sensitive to PTP1B inhibition than D492. Mesenchymal cells are characteristically less sensitive to apoptosis and many chemotherapeutic agents.[43,44] Mesenchymal cells are furthermore less adhesive. We suggest that under these circumstances of low adhesion, the mesenchymal cells rely on Src activity to prevent anoikis. As PTP1B inhibition leads to reduced Src activity, this may explain the sensitivity of the mesenchymal cells to the inhibitor. These findings suggest a therapeutic role for PTP1B inhibition to target mesenchymal derivatives of cancer cells, cells that are usually less likely to be targeted by conventional chemotherapeutics.

Collectively, our data have relevance regarding PTP1B in normal cell biology and cancer biology. We have shown that PTP1B may have an important role in cell adhesion and anoikis. PTP1B has been studied intensively as a drug target for type-2 diabetes, and already there are several inhibitors in clinical trials. Our data suggest that these inhibitors could also have a therapeutic role in cancer, specifically targeting cells that rely on Src-mediated anchorage independence.

Materials and Methods

Cell culture. D492 and D492M were cultured in the chemically defined medium H14 (ref. 45) unless indicated otherwise. HMLE and HMLEmes cells were grown in DMEM/F-12 medium supplemented with 10 ng/ml EGF, 10 μg/ml insulin and 0.5 μg/ml hydrocortisone. HMLEmes cells were generated by sorting and collecting an EpCAM-negative population from HMLE cells. HMLE cells were used with the permission from Dr. Robert Weinberg. MCF10a were cultured in H14 medium. All cell lines were routinely authenticated with genotype profiling.

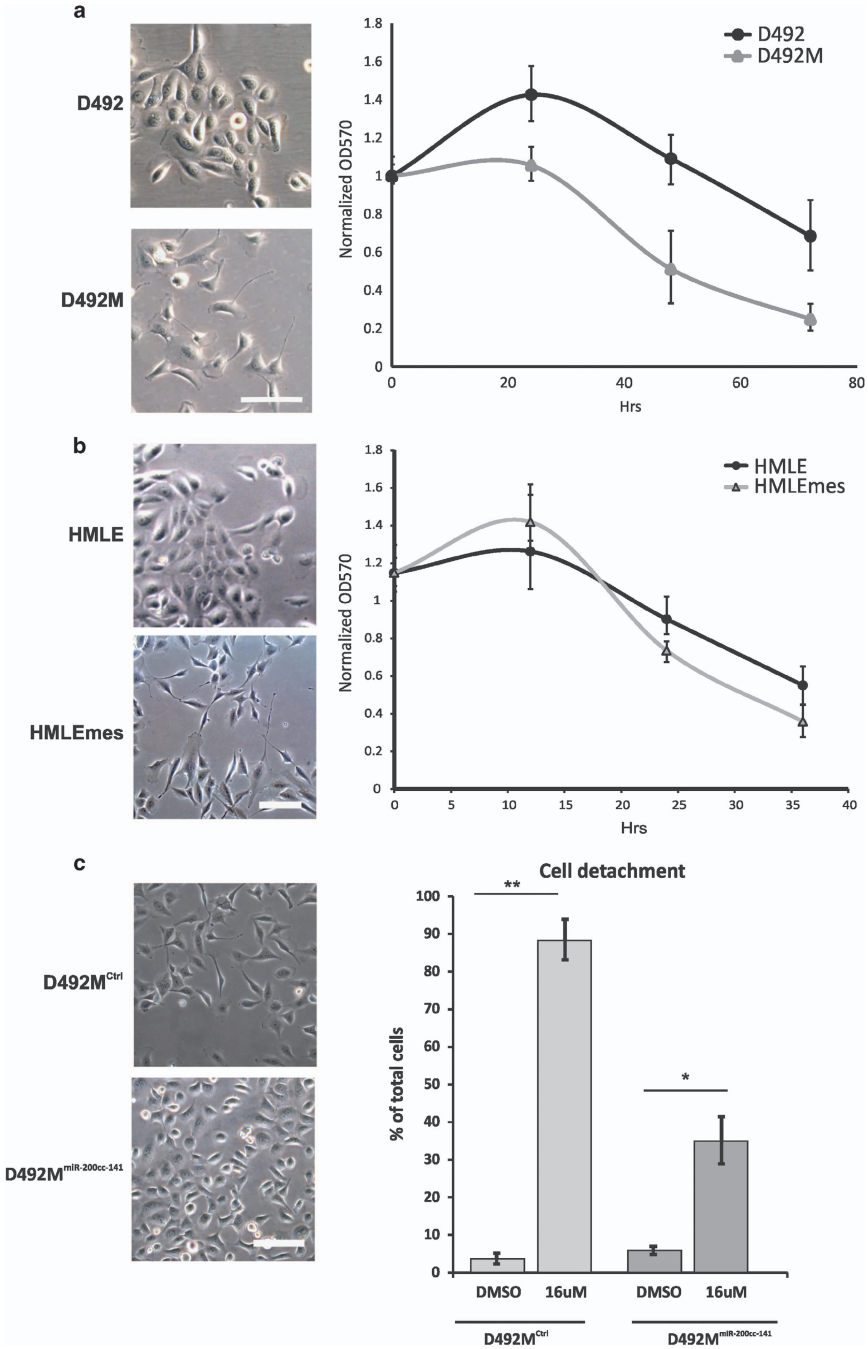

Primary endothelial cells were isolated as previously described[46] and cultured in EBM basal medium (Lonza, Walkersville, MD, USA), containing 50 IU/ml penicillin and 50 μg/ml streptomycin. The EBM medium was supplemented with 5% FBS. Primary luminal epithelial cells were cultured in the chemically defined medium CDM3.[47] Primary myoepithelial cells were cultured in the chemically defined medium CDM4.[48] For 3D cultures, 10 000 D492 cells were plated separately inside reconstituted basement membrane matrix, rBM (Matrigel, Becton Dickinson, Franklin Lakes, NJ, USA). Experiments were carried out in 24-well dishes (Falcon, Corning brand, NY, USA) using 300 μl Matrigel, in which single cells were suspended.

For staining of 3D structures, the Matrigel was dissolved with Matrigel lysis buffer on ice at mild rotation for 20–60 min. Branching structures were then spun down in a pre-cooled rotor at 1000 r.p.m. for 5 min at 2 °C. The structures were then resuspended in 30 μl PBS and left to dry on glass slides.[49]

Materials. PTP1B inhibitor[50] was purchased from Calbiochem; EMD Millipore brand, Billerica, MA, USA (#539741) and CPT from Sigma (St. Louis, MO, USA) (#C9911). PTP1B rabbit polyclonal antibody was purchased from R&D Systems (Minneapolis, MN, USA) and PTP1B mouse IgG1 antibody was purchased from BD Bioscience (Fisher Scientific brand, Waltham, MA, USA), Src (phospho Y529), actin, GAPDH and K14 antibodies were purchased from Abcam (Cambridge, UK). K18 and vimentin were purchased from DAKO (Agilent brand, Santa Clara, CA, USA) and β4-integrin was from Sigma-Aldrich (St. Louis, MO, USA). F-actin was stained with conjugated phalloidin (Invitrogen, Carlsbad, CA, USA). Isotype-specific secondary antibodies were from Invitrogen as well as TOPRO-3 nuclear counterstain. Specimens were visualized on a Zeiss LSM 5 Pascal laser-scanning microscope (Carl Zeiss, Germany) and Olympus FluoView 1200 (Japan).

qRT-PCR. Total RNA was extracted with Tri-Reagent (Ambion, Thermo Scientific brand, Waltham, MA, USA). The RNA was DNAase treated and reverse transcribed with hexanucleotide primers using Supercript II and Superscript IV (ThermoFisher, Waltham, MA, USA). Resulting cDNA was used as template for qPCR. Primer pairs and probes from Applied Biosystems (Foster City, CA, USA) (TaqMan) were used for PTPN1 (HS00182260_m1) and GAPDH (4326317E) as an endogenous reference gene.

PTPN1 knockdown. D492 cells were transfected with Silencer Select pre-designed siRNAs (Ambion, silencer select negative control no. 1 siRNA, silencer select validated siRNA PTPN1 s11506, silencer select validated siRNA PTPN1 s11507 and silencer select validated siRNA PTPN1 s11508). Transfections were done according to the manufacturer´s protocol using Lipofectamine RNAiMAX (Invitrogen, cat. 13778030) in 24-well plates (Corning, New York, USA, cat. 353047). RNA was extracted using Tri-Reagent solution (Ambion, cat. AM9738) according to the manufacturer's protocol. RNA was reverse transcribed using SuperScript IV Reverse Transcriptase (Invitrogen, cat. 18090050) and expression of PTP1B was assayed on Applied Biosystems 7500 Real-Time PCR System using TaqMan Gene Expression Assays Hs00942477 for PTPN1 and Hs99999905 for GAPDH as a control. Cell proliferation was assayed using IncuCyte Zoom Live Cell Analysis System, Essen Bioscience, Ann Arbor, MI, USA.

Western blot analysis. Protein lysates were acquired using RIPA lysis buffer supplemented with both phosphatase and protease inhibitor cocktails (Life Technologies, Thermo Fisher Scientific brand, Waltham, MA, USA). Equal amounts (5 μg) of proteins in RIPA buffer were separated on 10% NuPage Bis-Tris gels (Invitrogen) and transferred to a PVDF membrane (Invitrogen). Antibodies used are as follows: E-Cad (BD), PTP1B (BD, Fisher Scientific brand, Waltham, MA, USA), pSrc529 (Abcam), claudin-1 (Zymed, San Francisco, CA, USA), occludin (Zymed), β-catenin (Biolegend, San Diego, CA, USA), FAK (Cell Signaling, Danvers, MA, USA), pFAK (Cell Signaling) GAPDH (Abcam) and actin (Abcam) were used. In Figures 1,4 and 5, secondary antibodies were horsesadish peroxidase-conjugated anti-mouse or rabbit (BD Scientific; Fisher Scientific brand, Waltham, MA, USA) used at dilution 1:10 000. The protein bands were visualized using enhanced chemiluminescence (ECL) system (Thermo Scientific, Waltham, MA, USA). In Supplementary Figure 4, secondary antibodies were mouse or rabbit IRDye (Li-Cor, Lincoln, NE, USA) used at 1:10 000 and protein bands were detected using the Odyssey Infrared Imaging System (Li-Cor) and then fluorescent images were converted to gray scale.

All western blots are representative of three separate experiments.

Cell growth curve with PTP1B inhibitor. D492 cells were seeded at 70% confluency per well in a 24-well plate in growth media. One day after seeding, the medium was replaced with H14 medium and treated with either DMSO or the indicated concentration of inhibitor. For each time point, cells were fixed with 250 μl of crystal violet solution (0.25% crystal violet in 20% methanol). Fixed cells were then incubated in 500 μM lysis solution (33% acetic acid) for 10 min. To quantitate the amount of crystal violet in each sample, the optical density at 570 nm was determined using a spectrophotometer.

Apoptosis assay. Analysis of annexin V/PI binding was determined using an Annexin V-FITC apoptosis Detection Kit I (BD Pharmingen, Becton Dickinson brand, Franklin Lakes, NJ, USA). The D492 cell line was treated with DMSO or indicated concentrations of PTP1B inhibitor for 48 h. Cells were harvested and resuspended in binding buffer at a concentration 1×10^6 cells/ml. Later, 2.5 μl of Annexin V were added to 100 μl of suspension and incubated at RT in the dark for 15 min. In all, 400 μl of 1 × binding buffer were added to each tube and 2.5 μl of PI just before 10 000 cells from each tube were analyzed in a FACSCalibur, BD Bioscience. Data were processed using FCSexpress (*De novo* software, Los Angeles, CA, USA).

CFSE-based cell proliferation. Proliferation was assessed with a CellTrace CFSE Proliferation Kit – for flow cytometry (Invitrogen). D492 cells were resuspended in 1 ml PBS with 0.1% BSA at 1×10^6 cells/ml and CFSE dye added to the cells in a final concentration of 0.5 μM. The cells were incubated in a water bath at 37 °C for 10 min, 10 ml of FBS was added to stop the reaction and the cells resuspended in 1 ml of normal growth media and seeded in a 24-well plate. PTP1B inhibitor at a final concentration of 8 μM or equivalent amount of DMSO was added to the cells. The dilution of CFSE was measured by counting 10 000 viable cells with FACSCalibur (BD Bioscience) for 4 consecutive days.

***In situ* PLA.** Colocalization analysis of PTP1B interactions with substrate proteins was studied using a PLA using the Duolink(R) kit (Olink Bioscience, Sigma, St. Louis, MO, USA). D492 cells were treated with 32 μM of the PTP1B inhibitor for 5 h, fixed with 4% formaldehyde, blocked and incubated with primary antibodies in two different combinations: PTP1B mouse (BD, #610139) with Src rabbit (Cell Signaling, #2109) and PTP1B rabbit (R&D Systems, AF1366) with EGFR mouse (BD, #555996) overnight, followed by a standard PLA protocol according to the manufacturer's instruction. Nuclei were counterstained with DAPI and specimens were visualized on a Olympus FluoView 1200. For quantification of PLA signal, ImageJ was used to quantify the number and area of the Duolink puncta, and for all experiments quantifications were performed from at least three images.

Live cell imaging. D492 cells were seeded directly onto eight-well chamber slides, or embedded in Matrigel and seeded into eight-well chamber slides (BD) at densities of 3000 cells per well in 100 μl Matrigel. After 10 days in culture in a standard incubator, the chamber slide was removed from the incubator, treated with

Figure 6 Cells with mesenchymal phenotype are more sensitive to PTP1B inhibition than their isogenic epithelial counterparts. (**a**) D492M is more sensitive toward PTP1B inhibition than D492. The isogenic cell lines D492M and D492 that show mesenchymal and epithelial phenotype, respectively, were treated with DMSO (control) or 16 μM of a specific PTP1B inhibitor for 3 days. Cells were stained with crystal violet at different time points and optical density measured at 570 nm to evaluate the survival of cells. Note how D492M cells show lesser survival than D492. All experiments were conducted in triplicate. (**b**) HMLEmes is more sensitive to PTP1B inhibition than HMLE. HMLE and HMLEmes were treated with DMSO (control) or 16 μM of a specific PTP1B inhibitor for 3 days, stained with crystal violet and the optical density at 570 nm determined. (**c**) MET reverses sensitivity to PTP1B inhibition in D492M. $D492M^{Ctrl}$ (mesenchymal) and $D492M^{miR\text{-}200c\text{-}141}$ (epithelial) were treated with 16 μM of the PTP1B inhibitor or DMSO as control for 24 h and assayed for sensitivity to trypsinization

the relevant inhibitor and transferred to an automated inverted microscope (Leica DMI 6000B, Germany) equipped with an environmental chamber, temperature control module and CO_2 regulator (Pecon, Germany). Images were taken through a 20x objective with a CCD camera (Exi Blue, QImaging, Belmont, CA, USA) at 10 min intervals for 50 h. All microscope and camera controls were programmed through the μManager software package (UCSF, San Francisco, CA, USA).[51] Annotated time-laps videos were created with the Fiji software package (NIH) for ImageJ.[52]

Cell detachment assay. Cells were seeded in 24-well plates, grown to 90% confluency and treated with 8 or 16 μM of the PTP1B inhibitor, 10 μM of CPT or DMSO as control in H14 media. After 24-h incubation, the medium was removed and the cells were washed once with 1 × PBS and incubated with 0.25% trypsin at 37 °C for 1 min. In order to detach the cells from the culture plates, 1 × PBS with 10% FBS was added into the wells to inactivate the trypsin and the detached cells were collected into tubes. The remaining cells were incubated with 0.25% trypsin for 20 min to detach all the cells and collected into fresh tubes. The cells were counted and the data were presented as a percentage of cells detached after 1 min of trypsin incubation to total cells.

Statistical analysis. All growth curves were performed in triplicate for statistical accuracy. Graphs were created in Excel. Error bars represent the standard deviation of the sample (S.D.). *P*-values below 0.05 were considered significant ($^{**}P \leqslant 0.01$, $^{*}P \leqslant 0.05$).

Conflict of Interest

The authors declare no conflict of interest.

Acknowledgements. This work was supported by Grants from Landspitali University Hospital Science Fund, University of Iceland Research Fund, Icelandic Science and Technology Policy Council Research Fund no. 1103010061 and Icelandic Science and Technology Policy - Grant of Excellence: 152144051. 'Göngum saman', a supporting group for breast cancer research in Iceland (www.gongumsaman.is). The funders had no role in study design, data collection and analysis, decision to publish, or preparation of the manuscript.

1. Barr FA, Elliott PR, Gruneberg U. Protein phosphatases and the regulation of mitosis. *J Cell Sci* 2011; **124**(Pt 14): 2323–34.
2. Bartholomew PJ, Jones CW, Benware A, Chernoff J, LaFlamme SE. Regulation of the catalytic activity of PTP1B: roles for cell adhesion, tyrosine residue 66, and proline residues 309 and 310. *Exp Cell Res* 2005; **311**: 294–306.
3. Hernández MV, Sala MGD, Balsamo J, Lilien J, Arregui CO. ER-bound PTP1B is targeted to newly forming cell-matrix adhesions. *J Cell Sci* 2006; **119**(Pt 7): 1233–43.
4. Kenner KA, Anyanwu E, Olefsky JM, Kusari J. Protein-tyrosine phosphatase 1B is a negative regulator of insulin- and insulin-like growth factor-I-stimulated signaling. *J Biol Chem* 1996; **271**: 19810–6.
5. Tonks NK. PTP1B: from the sidelines to the front lines!. *FEBS Lett* 2003; **546**: 140–8.
6. Tamrakar AK, Maurya CK, Rai AK. PTP1B inhibitors for type 2 diabetes treatment: a patent review (2011 - 2014). *Expert Opin Ther Pat* 2014; **24**: 1101–15.
7. Lessard L, Stuible M, Tremblay ML. The two faces of PTP1B in cancer. *Biochim Biophys Acta* 2010; **1804**: 613–9.
8. Stuible M, Doody KM, Tremblay ML. PTP1B and TC-PTP: regulators of transformation and tumorigenesis. *Cancer Metastasis Rev* 2008; **27**: 215–30.
9. Bjorge JD, Pang A, Fujita DJ. Identification of protein-tyrosine phosphatase 1B as the major tyrosine phosphatase activity capable of dephosphorylating and activating c-Src in several human breast cancer cell lines. *J Biol Chem* 2000; **275**: 41439–46.
10. Bentires-Alj M, Neel BG. Protein-tyrosine phosphatase 1B is required for HER2/Neu-induced breast cancer. *Cancer Res* 2007; **67**: 2420–4.
11. Julien SG, Dubé N, Read M, Penney J, Paquet M, Han Y *et al.* Protein tyrosine phosphatase 1B deficiency or inhibition delays ErbB2-induced mammary tumorigenesis and protects from lung metastasis. *Nat Genet* 2007; **39**: 338–46.
12. Arias-Romero LE, Saha S, Villamar-Cruz O, Yip S-C, Ethier SP, Zhang Z-Y *et al.* Activation of Src by protein tyrosine phosphatase 1B is required for ErbB2 transformation of human breast epithelial cells. *Cancer Res* 2009; **69**: 4582–8.
13. Burdisso JE, González Á, Arregui CO. PTP1B promotes focal complex maturation, lamellar persistence and directional migration. *J Cell Sci* 2013; **126**(Pt 8): 1820–31.
14. Balsamo J, Leung T, Ernst H, Zanin MK, Hoffman S, Lilien J. Regulated binding of PTP1B-like phosphatase to N-cadherin: control of cadherin-mediated adhesion by dephosphorylation of beta-catenin. *J Cell Biol* 1996; **134**: 801–13.
15. Liu F, Hill DE, Chernoff J. Direct binding of the proline-rich region of protein tyrosine phosphatase 1B to the Src homology 3 domain of p130(Cas). *J Biol Chem* 1996; **271**: 31290–5.
16. Cheng A, Bal GS, Kennedy BP, Tremblay ML. Attenuation of adhesion-dependent signaling and cell spreading in transformed fibroblasts lacking protein tyrosine phosphatase-1B. *J Biol Chem* 2001; **276**: 25848–55.
17. Arregui CO, Balsamo J, Lilien J. Impaired integrin-mediated adhesion and signaling in fibroblasts expressing a dominant-negative mutant PTP1B. *J Cell Biol* 1998; **143**: 861–73.
18. Vanharanta S, Massagué J. Origins of metastatic traits. *Cancer Cell* 2013; **24**: 410–21.
19. Huang RY-J, Guilford P, Thiery JP. Early events in cell adhesion and polarity during epithelial-mesenchymal transition. *J Cell Sci* 2012; **125**(Pt 19): 4417–22.
20. Smith BN, Bhowmick NA. Role of EMT in metastasis and therapy resistance. *J Clin Med* 2016; **5**: E17.
21. Yip S-C, Saha S, Chernoff J. PTP1B: a double agent in metabolism and oncogenesis. *Trends Biochem Sci* 2010; **35**: 442–9.
22. Liu H, Wu Y, Zhu S, Liang W, Wang Z, Wang Y *et al.* PTP1B promotes cell proliferation and metastasis through activating src and ERK1/2 in non-small cell lung cancer. *Cancer Lett* 2015; **359**: 218–25.
23. Saraste A, Pulkki K. Morphologic and biochemical hallmarks of apoptosis. *Cardiovasc Res* 2000; **45**: 528–37.
24. Meredith JE, Fazeli B, Schwartz MA. The extracellular matrix as a cell survival factor. *Mol Biol Cell* 1993; **4**: 953–61.
25. Hanker AB, Healy KD, Nichols J, Der CJ. Romidepsin inhibits Ras-dependent growth transformation of NIH 3T3 fibroblasts and RIE-1 epithelial cells independently of Ras signaling inhibition. *J Mol Signal* 2009; **4**: 5.
26. Paoli P, Giannoni E, Chiarugi P. Anoikis molecular pathways and its role in cancer progression. *Biochim Biophys Acta* 2013; **1833**: 3481–98.
27. Zhang ZY, Walsh AB, Wu L, McNamara DJ, Dobrusin EM, Miller WT. Determinants of substrate recognition in the protein-tyrosine phosphatase, PTP1. *J Biol Chem* 1996; **271**: 5386–92.
28. Monteleone MC, González Wusener AE, Burdisso JE, Conde C, Cáceres A, Arregui CO. ER-bound protein tyrosine phosphatase PTP1B interacts with Src at the plasma membrane/substrate interface. *PLoS ONE* 2012; **7**: e38948.
29. Sigurdsson V, Hilmarsdottir B, Sigmundsdottir H, Fridriksdottir AJR, Ringnér M, Villadsen R *et al.* Endothelial induced EMT in breast epithelial cells with stem cell properties. *PLoS ONE* 2011; **6**: e23833.
30. Mani SA, Guo W, Liao M-J, Eaton EN, Ayyanan A, Zhou AY *et al.* The epithelial-mesenchymal transition generates cells with properties of stem cells. *Cell* 2008; **133**: 704–15.
31. Hilmarsdóttir B, Briem E, Sigurdsson V, Franzdóttir SR, Ringnér M, Arason AJ *et al.* MicroRNA-200c-141 and ΔNp63 are required for breast epithelial differentiation and branching morphogenesis. *Dev Biol* 2015; **403**: 150–61.
32. Hoekstra E, Das AM, Swets M, Cao W, van der Woude CJ, Bruno MJ *et al.* Increased PTP1B expression and phosphatase activity in colorectal cancer results in a more invasive phenotype and worse patient outcome. *Oncotarget* 2016; **7**: 21922–38.
33. Thapa N, Choi S, Hedman A, Tan X, Anderson RA. Phosphatidylinositol phosphate 5-kinase Iγi2 in association with Src controls anchorage-independent growth of tumor cells. *J Biol Chem* 2013; **288**: 34707–18.
34. Singh AB, Sharma A, Dhawan P. Claudin-1 expression confers resistance to anoikis in colon cancer cells in a Src-dependent manner. *Carcinogenesis* 2012; **33**: 2538–47.
35. Frisch SM, Screaton RA. Anoikis mechanisms. *Curr Opin Cell Biol* 2001; **13**: 555–62.
36. Ishizawar RC, Miyake T, Parsons SJ. c-Src modulates ErbB2 and ErbB3 heterocomplex formation and function. *Oncogene* 2007; **26**: 3503–10.
37. Zhao J, Zhang Y, Ithychanda SS, Tu Y, Chen K, Qin J *et al.* Migfilin interacts with Src and contributes to cell-matrix adhesion-mediated survival signaling. *J Biol Chem* 2009; **284**: 34308–20.
38. Ishizawar R, Parsons SJ. c-Src and cooperating partners in human cancer. *Cancer Cell* 2004; **6**: 209–14.
39. Verbeek BS, Vroom TM, Adriaansen-Slot SS, Ottenhoff-Kalff AE, Geertzema JG, Hennipman A *et al.* c-Src protein expression is increased in human breast cancer. An immunohistochemical and biochemical analysis. *J Pathol* 1996; **180**: 383–8.
40. Windham TC, Parikh NU, Siwak DR, Summy JM, McConkey DJ, Kraker AJ *et al.* Src activation regulates anoikis in human colon tumor cell lines. *Oncogene* 2002; **21**: 7797–807.
41. Golubovskaya VM, Gross S, Kaur AS, Wilson RI, Xu L-H, Yang XH *et al.* Simultaneous inhibition of focal adhesion kinase and SRC enhances detachment and apoptosis in colon cancer cell lines. *Mol Cancer Res* 2003; **1**: 755–64.
42. Liang F, Lee S-Y, Liang J, Lawrence DS, Zhang Z-Y. The role of protein-tyrosine phosphatase 1B in integrin signaling. *J Biol Chem* 2005; **280**: 24857–63.
43. Robson EJD, Khaled WT, Abell K, Watson CJ. Epithelial-to-mesenchymal transition confers resistance to apoptosis in three murine mammary epithelial cell lines. *Differ Res Biol Divers* 2006; **74**: 254–64.
44. Shang Y, Cai X, Fan D. Roles of epithelial-mesenchymal transition in cancer drug resistance. *Curr Cancer Drug Targets* 2013; **13**: 915–29.
45. Blaschke RJ, Howlett AR, Deprez P-Y, Petersen OW, Bissell MJ. Cell differentiation by extracellular matrix components *Meth Enzymol* 1994; **245**: 535–556.

46. Sigurdsson V, Fridriksdottir AJR, Kjartansson J, Jonasson JG, Steinarsdottir M, Petersen OW *et al.* Human breast microvascular endothelial cells retain phenotypic traits in long-term finite life span culture. *In Vitro Cell Dev Biol Anim* 2006; **42**: 332–40.
47. Petersen OW, van Deurs B. Preservation of defined phenotypic traits in short-term cultured human breast carcinoma derived epithelial cells. *Cancer Res* 1987; **47**: 856–66.
48. Petersen OW, van Deurs B. Growth factor control of myoepithelial-cell differentiation in cultures of human mammary gland. *Differ Res Biol Divers* 1988; **39**: 197–215.
49. Lee GY, Kenny PA, Lee EH, Bissell MJ. Three-dimensional culture models of normal and malignant breast epithelial cells. *Nat Methods* 2007; **4**: 359–65.
50. Wiesmann C, Barr KJ, Kung J, Zhu J, Erlanson DA, Shen W *et al.* Allosteric inhibition of protein tyrosine phosphatase 1B. *Nat Struct Mol Biol* 2004; **11**: 730–7.
51. Edelstein A, Amodaj N, Hoover K, Vale R, Stuurman N. Computer control of microscopes using μManager. *Curr Protoc Mol Biol Ed Frederick M Ausubel Al* 2010; **Chapter 14**: Unit14.20.
52. Schindelin J, Arganda-Carreras I, Frise E, Kaynig V, Longair M, Pietzsch T *et al.* Fiji: an open-source platform for biological-image analysis. *Nat Methods* 2012; **9**: 676–82.

Supplementary Information accompanies this paper on Cell Death and Disease website (http://www.nature.com/cddis)

Paper IV

Application of breast epithelial stem cells and 3D culture to explore branching morphogenesis, EMT and cancer progression

Eirikur Briem[1], Saevar Ingthorsson[1], Gunnhildur Asta Traustadottir[1], Bylgja Hilmarsdottir[3] and Thorarinn Gudjonsson[1,2]

[1]Stem Cell Research Unit, Biomedical Center, Department of Anatomy, Faculty of Medicine, School of Health Sciences, University of Iceland, Iceland

[2]Department of Laboratory Hematology, Landspitali - University Hospital, Iceland

[3]Department of Tumor Biology, The Norwegian Radium Hospital, Oslo, Norway

Correspondence: T Gudjonsson, Stem Cell Research Unit, Department of Medical Faculty, Biomedical Center, University of Iceland, Vatnsmyrarvegi 16, 101 Reykjavík, Iceland.

Tel: +354-5254827; Fax: +354-5254884. E-mail: tgudjons@hi.is

Abstract

The human female breast gland is composed of branching epithelial ducts that extend from the nipple towards the terminal duct lobular units (TDLUs), which are the functional, milk-producing units of the gland and the site of origin of most breast cancers. The epithelium of ducts and TDLUs is composed of an inner layer of polarized luminal epithelial cells and an outer layer of contractile myoepithelial cells, separated from the vascular-rich stroma by a basement membrane. The luminal- and myoepithelial cells share an origin and in recent years, there has been increasing understanding of how these cell types interact and how they contribute to breast cancer. Accumulating evidence link stem/or progenitor cells in the mammary/breast gland to breast cancer. In that regard much knowledge has been gained from studies in mice due to specific strains that have allowed for gene knock out/in studies and lineage tracing of cellular fates. However, there is a large histologic difference between the human female breast gland and the mouse mammary gland that necessitates that research needs to be done on human material where primary cultures are of most importance. However, due to difficulties of long-term cultures and lack of access to material, human cell lines are of great importance to bridge the gap between studies on mouse mammary gland and human primary breast cells. There is a number of outstanding breast epithelial cell lines available, which have been used for studies on normal breast morphogenesis and in breast cancer research. In this review, we describe D492, a suprabasal breast epithelial progenitor cell line that can generate both luminal- and myoepithelial cells in culture, and in 3D culture it forms branching ducts similar to TDLUs. We have applied D492 and its daughter cell lines to explore

cellular and molecular mechanisms of branching morphogenesis and cellular plasticity including EMT and MET. In addition to discussing the application of D492 in studying normal morphogenesis, we will also discuss how this cell line has been used to study breast cancer progression.

Introduction

The human breast gland is an evolutionary modification of an apocrine sweat gland that originates from the epidermis and through interactions with the mesenchyme forms branching ducts that terminate in terminal duct lobular units (TDLUs) (Ronnov-Jessen, Petersen et al. 1996, Javed and Lteif 2013) (Fig. 1a and b). From birth to puberty, the breast glands are essentially the same in males and females (Javed and Lteif 2013). At the onset of puberty in females, the breast gland develops further, grows into an increasingly elaborate ductoalveolar tree, embedded in collagen and adipose tissue. Periodic pulses in estrogen and progesterone production induce monthly cycles of branching morphogenesis of the glandular epithelium preparing for pregnancy and lactation. If pregnancy does not occur the epithelium partially involutes during menstruation preparing for a new round of branching morphogenesis. On the other hand, if pregnancy occurs the glandular epithelium progresses through to a more dramatic expansion, eventually reaching maximal differentiation during lactation (Arendt and Kuperwasser 2015). These changes are driven by sustained hormonal production and by heterotypic interactions between the glandular epithelium and the surrounding vascular rich stroma (Inman, Robertson et al. 2015). The ducts and TDLUs are composed of an inner layer of polarized luminal epithelial cells and an outer layer of contractile myoepithelial cells that share a common origin

(Gudjonsson, Villadsen et al. 2002, Villadsen, Fridriksdottir et al. 2007, Fridriksdottir, Villadsen et al. 2017) (Fig. 1b and c). Luminal- and myoepithelial cells are dependent on each other for correct form and function in the mammary gland (Gudjonsson, Ronnov-Jessen et al. 2002, Fridriksdottir, Villadsen et al. 2017, Miyano, Sayaman et al. 2017). During breast cancer initiation and progression, the histoarchitecture of the epithelium is disrupted. Initially, a localized lesion exhibiting an increase in proliferation and loss of polarization fills the ductal tree. Eventually, adhesion between cells is reduced, and in many cases phenotypic changes towards a more invasive, mesenchymal phenotype (Shibue and Weinberg 2017). Some of these changes are accompanied by increased stemness and metastatic ability and development of drug resistance (Hanahan and Weinberg 2011, Shibue and Weinberg 2017).

In vivo models have contributed enormously to our knowledge in breast biology and cancer (Asselin-Labat, Vaillant et al. 2008, Borowsky 2011, Arendt and Kuperwasser 2015). Knock-in and knock-out mutations have unraveled the functions of important tumor suppressor and or oncogenes and hundreds of mouse strains are available that capture phenotypes changes related to these gene interventions (Cardiff, Bern et al. 2002, Borowsky 2011). While all this knowledge in terms of mouse mammary gland biology exist, it is important to acknowledge, there are major differences between mammary glands in mouse and humans. This is due to histological differences between these two species. While both species' mammary glands are embedded in adipose tissue, the mouse gland presents with very limited amount of collagenous stroma. The human female breast gland on the other hand is embedded in cellular rich intralobular stroma surrounded by interlobular collagen rich stroma (Morsing, Klitgaard et al. 2016). Obviously the

species exhibit vast differences in life span (1 year compared to approx. 80 in humans), and therefore exhibit different sensitivity to cancerogenic insults (Cardiff and Wellings 1999, Dontu and Ince 2015). It is increasingly evident that breast cancer progression is an excellent example of Darwinian evolutionary principals, where cells that proliferate faster, survive better and adapt more proficiently to challenges in the environment. A one-year lifespan as is the case for the mouse is hardly a perfect model for recapitulating those parameters. Modeling breast morphogenesis and cancer progression *in-vitro* is therefore an important tool to explore molecular and cellular mechanisms that drive these phenotypic events. It is of great importance that we advance the understanding of how the human breast gland develops by improving cell culture models that recapture *in vivo* like morphogenesis. This will ultimately contribute to a better understanding of breast morphogenesis in normal conditions and in neoplasia.

There are a number of excellent breast epithelial cell lines that have been used through the years to unravel molecular and cellular mechanisms in breast epithelial differentiation and breast cancer research. In that regard, isogenic cell lines representing normal and malignant conditions are of high importance. Of these HMLE, MCF10, HMT3522 and their tumorigenic derivatives are probably the best known and their properties have been discussed in details in a number of papers (Tait, Soule et al. 1990, Weaver, Howlett et al. 1995, Mani, Guo et al. 2008). In this review, we will discuss a cell line referred to as D492, initially named subrabasal epithelial cell line (Gudjonsson, Villadsen et al. 2002). D492 has been shown to exhibit stem cell properties measured by its ability to generate both luminal- and myoepithelial cells and when cultured in three-dimensional reconstituted basement membrane matrix (3D-rBM) by the formation of

branching structures reminiscent of terminal duct lobular units in the breast (Gudjonsson, Villadsen et al. 2002, Villadsen, Fridriksdottir et al. 2007) (Fig. 1c). D492 shows a high degree of plasticity and in culture with endothelial cells undergoes epithelial to mesenchymal transition (EMT) (Sigurdsson, Hilmarsdottir et al. 2011). D492M was isolated from an D492-derived EMT colony and has a fixed mesenchymal phenotype. MicroRNA expression comparison between D492 and D492M showed a distinct profile with loss of number of epithelial associated miRNAs in D492M. Re-introduction of some these miRNAs into D492M resulted in mesenchymal to epithelial transition (MET) (Hilmarsdottir, Briem et al. 2015). Also in a recent paper, we demonstrated that overexpressing HER2 in D492 resulted in EMT and tumor progression in mouse models. This tumor formation was reduced if $D492^{HER2}$ cells were co-transduced with EGFR (Ingthorsson, Andersen et al. 2015).

Cellular origin of the D492 cell line

The search for the true human breast epithelial stem cells has been a long journey and open for discussion within the research field for many years and still is. We have witnessed great success in cell lineage tracing and hunt for stem cells in the mouse mammary gland, where numbers of papers have demonstrated the presence of stem and progenitor cells (dos Santos, Rebbeck et al. 2013, Visvader and Stingl 2014, Fu, Rios et al. 2017). For obvious reason the linage tracing of breast epithelial stem/progenitor cells *in vivo* in humans is not possible. Instead, studies on human breast tissue rely on tissue from biopsies such as reduction mammoplasties and on established cell lines. Reduction mammoplasties have been a great resource for cell biologists studying breast development and breast

cancer due to the large amount of material available from each biopsy and due to the normal histology of the tissue. This unique material is rich in cellular components both epithelial and stromal cells. Pioneering work by Mina Bissell, Ole William Petersen and others have paved the way for culture of human primary cells from tissue derived from reduction mammoplasty (Petersen, Ronnov-Jessen et al. 1992, Pechoux, Gudjonsson et al. 1999, Gudjonsson, Ronnov-Jessen et al. 2002). Isolation protocols for different cell types and subsequent improvements of cell culture conditions for the last two decades have accelerated search for breast epithelial stem cells and increased knowledge on how the microenvironment regulates cell fate decision (Fridriksdottir, Kim et al. 2015, Morsing, Klitgaard et al. 2016, Fridriksdottir, Villadsen et al. 2017). Initial separation of luminal epithelial- and myoepithelial cells and subsequent findings that subpopulation of luminal epithelial cells could give rise to myoepithelial cells was an important step (Pechoux, Gudjonsson et al. 1999). In a following paper, it was demonstrated that MUC1 negative and EpCAM positive suprabasal cells had stem cell properties. Isolated MUC1 negative and EpCAM positive suprabasal cells were immortalized using retroviral constructs containing the E6 and E7 oncogenes from the human papilloma virus 16. This cell line was initially referred to as suprabasal cell line (Gudjonsson, Villadsen et al. 2002, Villadsen, Fridriksdottir et al. 2007) and later renamed as D492 (Sigurdsson, Hilmarsdottir et al. 2011). D492 has stem cell properties as measured by its ability to form luminal- and myoepithelial cells in monolayer culture and to generate branching colonies akin to TDLUs when cultured in three-dimensional reconstituted basement membrane (3D-rBM) (Fig.1c). Interestingly, co-expression of both luminal and myoepithelial keratins (K14 and K19) is found in subpopulations of

D492 cells. Co-expression of these two keratins is also found in suprabasal cells of the breast gland *in situ* (Villadsen 2005, Villadsen, Fridriksdottir et al. 2007) and has been associated with stem cell properties. Although, D492 cells show stem cell properties by giving rise to both luminal- and myoepithelial cells they are not able to give rise to estrogen receptor (ER) positive luminal epithelial cells. It has been a major problem for decades to culture ER positive normal breast epithelial cells. The only ER positive cell lines available are derived from breast cancer such as MCF-7 and T47-D (Brooks, Locke et al. 1973, Holliday and Speirs 2011). Overcoming this problem is important due to the fact that 70% of breast cancers are ER positive and it is currently unknown if this type of breast cancer originates in ER positive cells or if its expression is turned on during cancer progression. Most recently, an important milestone was reached, when Fridriksdottir et al. succeeded in expanding ER positive primary cells in culture. This was achieved by inhibiting the TGFB receptor with two small molecule inhibitors and by adaption to specific cell culture media (Fridriksdottir, Kim et al. 2015). In a following paper, the same group succeeded in generating immortalized normal-derived ER positive cell line referred to as iHBEC^{ERpos} (Hopkinson, Klitgaard et al. 2017). Thus, the iHBEC^{ERpos} cell line and D492 are important normal-derived breast epithelial cell lines that can be highly useful to study normal breast morphogenesis and to contribute to better understanding of ER positive and ER negative breast cancer, respectively.

Application of D492 to explore EMT and branching morphogenesis

One of the greatest advantages of 3D culture is the recapitulation of morphogenesis *in vitro* through the ability of cells to interact with each other. One

important platform is to create co-culture conditions between epithelial and stromal cells. It has been shown in a number of studies that stroma confers instructive signals to epithelial cells (Ronnov-Jessen, Petersen et al. 1996, Hansen and Bissell 2000, Bissell, Radisky et al. 2002). Stroma is a broad term encompassing extracellular matrix and all the resident cell types that inhabit the stroma, including fibroblasts, immune cells and endothelial cells. Fibroblasts have been shown to be important instructors of morphogenesis in organogenesis, including the mammary gland (Medina 2004, Sadlonova, Novak et al. 2005). Morsing et al demonstrated recently that fibroblasts in stroma around TDLU in the breast differ greatly from fibroblasts around ducts. Based on marker expression using CD26 (ductal fibroblasts) and CD105 (TDLU associated fibroblasts) as surrogate markers the researchers were able to isolate and characterize these two distinct cell populations. TDLU associated fibroblasts expressed a fibrotic profile in contrast to more immunogenic profile in fibroblasts around ducts. Furthermore, TDLU associated fibroblasts were much more efficient in stimulating branching morphogenesis compared to their ductal counterpart (Morsing, Klitgaard et al. 2016). Immune cells have also been shown to contribute to breast morphogenesis (Gouon-Evans, Rothenberg et al. 2000, Plaks, Boldajipour et al. 2015). The vasculature in the breast has been thoroughly studied in terms of angiogenesis during cancer progression. However, less focus has been on the contribution of endothelial cells to mammary gland morphogenesis. Using the D492 cell line we have established a co-culture system where D492 cells were cultured with organotypic breast endothelial cells (BRENCs) derived from reduction mammoplasty (Sigurdsson, Fridriksdottir et al. 2006, Sigurdsson, Hilmarsdottir et al. 2011). It is worth mentioning that isolation

and expansion of endothelial cells from the breast gland is a time consuming and difficult task, reflected in the dearth of literature discussing primary breast endothelial cells. When plating endothelial cells on top of rBM they quickly form (within 4-10 hours) capillary like networks. This is, however, a very unstable structure that dissolves within 48-72 hours (Sigurdsson, Fridriksdottir et al. 2006, Ingthorsson, Sigurdsson et al. 2010). Interestingly, when embedded into 3D-rBM, BRENCs stay as single cells inside the gel and do not proliferate. They are, however, metabolically active as evidenced by their ability to take up acetylated low-density lipoprotein (Fig. 2a and b) (Sigurdsson, Fridriksdottir et al. 2006, Ingthorsson, Sigurdsson et al. 2010). In co-culture, BRENCs stimulate proliferation and branching morphogenesis of D492 cells. This is evident when D492 are seeded at clonal density. In 3D monoculture of D492 seeded at clonal density, no growth occurs. In contrast, in co-culture with BRENCs, large branching structures are seen that are remarkably reminiscent of the terminal duct lobular units (TDLUs) of the breast (Fig. 2c). In addition to enhanced branching BRENCS induced growth of spindle-like mesenchymal colonies in D492 cells (Fig. 2c). Cells isolated from a mesenchymal structure gave rise to a subline referred to as D492M. D492M has a mesenchymal phenotype, measured by a spindle like phenotype in culture and by marker expression. D492M has lost epithelial markers such as keratins, E-cadherin and transcription factors such as p63. In contrast, D492M gained mesenchymal markers including N-cadherin, Vimentin and alpha smooth muscle actin (Fig. 2d). D492M has acquired a cancer stem cell phenotype measured by increased CD44/CD24 ratio, anchorage independent growth, resistance to apoptosis and increased migration/invasion. However, when D492M cells are transplanted into nude mice, they are non-tumorigenic.

Using transwell filters where endothelial cells were cultured on top of filters and D492 in rBM below the filter we demonstrated that EMT was facilitated by soluble factors. Blocking hepatocyte growth factor in the culture media partially inhibited mesenchymal colony formation (Sigurdsson, Hilmarsdottir et al. 2011).

Functional role of microRNAs in EMT and MET

Noncoding RNAs (ncRNAs) have in recent years demonstrated the complexity of biological processes that previously were only considered to be regulated by coding genes. MicroRNAs (miRNAs) a well-known class of ncRNAs are involved in most biological processes both in health and diseases (Croce and Calin 2005, Ebert and Sharp 2012). Epithelial to mesenchymal transition (EMT) and its reverse process mesenchymal to epithelial transition (MET) are important processes involved in organ development but are hijacked in some forms of cancer (Shibue and Weinberg 2017). We have applied D492 and D492M to study the role of miRNAs in EMT and MET. Microarray analysis revealed profound changes in miRNA expression between D492 and D492M (Hilmarsdottir, Briem et al. 2015). The miR-200 family, miR-203a and miR-205 were among the most downregulated miRNAs in D492M. These miRNAs have been described being highly expressed in epithelial tissue and loss of expression has been shown to occur during EMT (Moes, Le Bechec et al. 2012, Tran, Choi et al. 2013, Hilmarsdottir, Briem et al. 2014). The miR-200 family is composed of five miRNAs (mir-200a, mir-200b, miR-200c, miR-141 and miR-429). MiR-200c and miR-141 are located on the same cluster on chromosome 12. They share a promoter but their seeding sequence is different. In D492M, overexpression of miR-200c-141 induced MET, but only towards the luminal epithelial phenotype. D492M$^{miR\text{-}200c\text{-}141}$ expresses the

epithelial marker E-cadherin and luminal epithelial markers such as EpCAM and K19. However, the expression of myoepithelial markers such as P-cadherin, K14, K5/6, K17 and the transcription factor p63 were not re-induced in the cell line. In 3D culture D492M$^{miR\text{-}200c\text{-}141}$ retains epithelial phenotype, but does not form branching colonies like D492. In addition, constitutive expression of miR-200c-141 in D492 does not affect its ability to form branching colonies in 3D culture, it does however, prevented endothelial induced EMT. This means that while miR-200c-141 governs epithelial phenotype in the cell line, its downregulation is not necessary for the cells to carry out branching morphogenesis, which involves partial EMT.

The miR-200 family has previously been linked to epithelial integrity and EMT and using the D492 model system we have shown that miR-200c-141 inhibits EMT in epithelial cells and enforces MET in mesenchymal cells to a luminal epithelial phenotype. In order to capture the full phenotype of D492 with both luminal and myoepithelial marker expression and branching morphogenesis we used p63, a well-known transcription factor expressed in myoepithelial cells in the breast. p63 expression did not reoccur when miR-200c-141 was introduced to D492M. Overexpression of p63 together with miR200c-141 in D492M resulted in reinvention of both the luminal- and myoepithelial phenotype and the ability of generating branching structures reminiscent of TDLU in 3D-rBM. These results highlight the importance of cells with both luminal and myoepithelial characteristics for a full branching morphogenesis to take place and underscore the importance of both lineage expression patterns in development (Fig. 3).

Collectively, the differences in expression of numbers of miRNAs between D492 and D492M makes these isogenic cell lines highly useful to explore miRNA functions in breast epithelial morphogenesis, EMT and MET. So far, we have only been looking into a small selection of miRNAs that are the most downregulated in D492M and we are currently working on other miRNAs in these cell lines.

Oncogene-induced EMT and tumor progression

As mentioned above, D492 has stem cell properties and can undergo EMT through interactions with stromal cells, as evidenced by the ability of endothelial cells to induce EMT in this cell line. Due to the stem cell properties including the ability to form branching structures reminiscent of TDLU when cultured in 3D-rBM we decided to analyze the effects of overexpressing oncogenes in D492 to see if this would push the cells towards increased tumorigenicity. We chose EGFR and EGFR2 (HER2) due to their common overexpression and/or amplification in breast cancers (Slamon, Clark et al. 1987) (Fig. 4a). D492 being a predominantly basal cell line, expresses high levels of endogenous EGFR. In contrast HER2 is not expressed in D492, consistent with the fact that HER2 is predominantly expressed in luminal epithelial cells in the breast (Ingthorsson, Andersen et al. 2015). When, EGFR was overexpressed in D492 we saw an increase in the basal/myoepithelial phenotype. Interestingly HER2 overexpressing D492 cells underwent EMT and formed disorganized spindle-shape or grape like colonies in 3D culture (Fig. 4b). In addition, overexpression of HER2 and the resulting EMT caused a downregulation of endogenous expression of EGFR. This could be partially reverted by ectopic expression of EGFR in the HER2 expressing cells (double expression). In monolayer, cells expressing HER2 exhibited an EMT phenotype,

with or without expression of EGFR. However, in 3D culture, E-cadherin expression could be seen in cultures of HER2/EGFR cells, indicating that EGFR expression was sufficient to revert the HER2 induced EMT under the correct culture conditions.

When transplanted into nude mice $D492^{HER2}$ cells formed large tumors. Interestingly $D492^{EGFR/HER2}$ were not as tumorigenic as $D492^{HER2}$. While all mice developed tumors, the growth was stunted compared to HER2 alone, indicating that EGFR has some growth suppressive properties (Fig 4c). Incidentally, we observed that the HER2/EGFR tumors had high levels of epithelial cells, consistent with the 3D culture observations. We therefore postulated that EGFR enabled the HER2 overexpressing cells to maintain an epithelial phenotype, resulting in slower tumor growth. Finally, we treated $D492^{HER2}$ tumor xenografted mice with either trastuzumab (monoclonal antibody against HER2), cetuximab (monoclonal antibody against EGFR) or combination of both for 20 days. As expected treatment with trasuzumab reduced the volume of the $D492^{HER2}$ tumors. Cetuximab resulted in growth arrest during treatment. Combination of tratuzumab and cetuximab also reduced the tumor volume initially but after end of treatment tumor growth resumed. Most interestingly, if the mice with the $D492^{HER2}$ tumors were treated with cetuximab and trastuzumab advanced growth was seen compared to treatment with trastuzimab alone, indicating that EGFR treatment in a HER2 driven environment could have detrimental effects (Fig. 4d). Although, considered negative for EGFR based on immunostaining, $D492^{HER2}$ cells were positive for phosphorylated EGFR when tested on western blot. Thus, these data indicate that EGFR expression may work as a tumor suppressor in the $D492^{HER2}$

cells and combination treatment with both trastuzimab and cetuzimab could actually override the effects achieved by treatment with trastuzimab alone.

Discussion

Cell culture models that capture morphogenic traits of human tissues and organs are warranted to facilitate researchers to explore development, cellular remodeling and disease progression such as cancer. Although animal studies, in particular mouse studies, have contributed significantly to research on the function of genes and signaling mechanisms, they have short comings due to several aforementioned biological and histological differences between mice and humans. Thus, it is necessary to validate data obtained from mice in human cell culture models. Using primary cultures is important because these cells are closer to *in vivo* conditions and have not been expanded or manipulated in culture prior to conducting experiments. It is, however, a major drawback when using primary cultures that these cells have a short life span that halts or prevents long term studies. Heterogeneity of cells from different individuals can also interfere with the conclusions drawn from studies with primary cells.

Using representative cell lines with extended lifespan or immortalized cell lines can contribute significantly to the understanding of tissue morphogenesis and cancer. This has probably been best acknowledged in the human breast were several excellent human cell culture models have been created. In this review we have discussed the application of D492 and its daughter cell lines in studies exploring breast morphogenesis and cellular plasticity and cancer progression. This cell line(s) has the potential to capture *in vivo* like branching morphogenesis in 3D culture reminiscent of TDLUs in the breast gland. Furthermore, D492 cells

show high degree of cellular plasticity as they respond to endothelial cells by undergoing EMT. D492M is highly mesenchymal and shows expression pattern close to myofibroblasts. D492M is non-tumorigenic and has provided a useful platform to study MET. Moreover, we have used the D492 cell lines to study cancer progression and the interaction between EGFR and HER2.

D492^{HER2} cells show mesenchymal traits, but not as prominent as D492M. It is possible that partial EMT in D492^{HER2} render the cells with increased cellular plasticity that further accelerates the tumor growth. In contrast D492M is more fixed in its mesenchymal phenotype that could explain its low tumorigenicity. Shibue et al discussed cellular plasticity and EMT in a recent review (Shibue and Weinberg 2017). Here they discussed that tumor cells were highly malignant if they were showing partial EMT but not if their phenotype was more into the mesenchymal differentiation (Shibue and Weinberg 2017). It is possible that partial EMT is reflecting cellular plasticity rather than true EMT and that these cells can change their phenotype in order to adapt better to new environments, which is necessary for cancer cell invasion and metastasis.

Concluding remarks and future perspectives

Although animals (mainly mice) have contributed significantly to research on mammary gland morphogenesis and cancer it is of importance to acknowledge that there is a histological and biological difference between the mouse mammary gland and the human female breast that cannot be ignored. Data are accumulating that in the human breast the TDLU-associated stroma has a dominant role on branching morphogenesis. TDLU in addition to its milk producing function during lactation is the place where most breast cancer take place. In mice, there are no

TDLUs, only terminal end buds and the stroma is mainly composed of fat tissue. If the stroma is dominant in bringing signals to the epithelium it is obvious that these signals are different between mice and humans. It is also important to acknowledge that cell culture is and will continue to be conducted in artificial environments. However, using breast cells, both epithelial and stromal cells and continuous improvement of cell culture environment will help to fill the gaps that exist between the mouse and the human mammary gland. It is no doubt that cell lines are important and will continue to be so in the near future. They are important tools but have their disadvantages that need to be taken into account when experiments are designed.

Arendt, L. M. and C. Kuperwasser (2015). "Form and function: how estrogen and progesterone regulate the mammary epithelial hierarchy." J Mammary Gland Biol Neoplasia **20**(1-2): 9-25.
Asselin-Labat, M. L., F. Vaillant, M. Shackleton, T. Bouras, G. J. Lindeman and J. E. Visvader (2008). "Delineating the epithelial hierarchy in the mouse mammary gland." Cold Spring Harb Symp Quant Biol **73**: 469-478.
Bissell, M. J., D. C. Radisky, A. Rizki, V. M. Weaver and O. W. Petersen (2002). "The organizing principle: microenvironmental influences in the normal and malignant breast." Differentiation **70**(9-10): 537-546.
Borowsky, A. D. (2011). "Choosing a mouse model: experimental biology in context--the utility and limitations of mouse models of breast cancer." Cold Spring Harb Perspect Biol **3**(9): a009670.
Brooks, S. C., E. R. Locke and H. D. Soule (1973). "Estrogen receptor in a human cell line (MCF-7) from breast carcinoma." J Biol Chem **248**(17): 6251-6253.
Cardiff, R. D., H. A. Bern, L. J. Faulkin, C. W. Daniel, G. H. Smith, L. J. Young, D. Medina, M. B. Gardner, S. R. Wellings, G. Shyamala, R. C. Guzman, L. Rajkumar, J. Yang, G. Thordarson, S. Nandi, C. L. MacLeod, R. G. Oshima, A. K. Man, E. T. Sawai, J. P. Gregg, A. T. Cheung and D. H. Lau (2002). "Contributions of mouse biology to breast cancer research." Comp Med **52**(1): 12-31.
Cardiff, R. D. and S. R. Wellings (1999). "The comparative pathology of human and mouse mammary glands." J Mammary Gland Biol Neoplasia **4**(1): 105-122.
Croce, C. M. and G. A. Calin (2005). "miRNAs, cancer, and stem cell division." Cell **122**(1): 6-7.

Dontu, G. and T. A. Ince (2015). "Of mice and women: a comparative tissue biology perspective of breast stem cells and differentiation." J Mammary Gland Biol Neoplasia **20**(1-2): 51-62.
dos Santos, C. O., C. Rebbeck, E. Rozhkova, A. Valentine, A. Samuels, L. R. Kadiri, P. Osten, E. Y. Harris, P. J. Uren, A. D. Smith and G. J. Hannon (2013). "Molecular hierarchy of mammary differentiation yields refined markers of mammary stem cells." Proc Natl Acad Sci U S A **110**(18): 7123-7130.
Ebert, M. S. and P. A. Sharp (2012). "Roles for microRNAs in conferring robustness to biological processes." Cell **149**(3): 515-524.
Fridriksdottir, A. J., J. Kim, R. Villadsen, M. C. Klitgaard, B. M. Hopkinson, O. W. Petersen and L. Ronnov-Jessen (2015). "Propagation of oestrogen receptor-positive and oestrogen-responsive normal human breast cells in culture." Nat Commun **6**: 8786.
Fridriksdottir, A. J., R. Villadsen, M. Morsing, M. C. Klitgaard, J. Kim, O. W. Petersen and L. Ronnov-Jessen (2017). "Proof of region-specific multipotent progenitors in human breast epithelia." Proc Natl Acad Sci U S A.
Fu, N. Y., A. C. Rios, B. Pal, C. W. Law, P. Jamieson, R. Liu, F. Vaillant, F. Jackling, K. H. Liu, G. K. Smyth, G. J. Lindeman, M. E. Ritchie and J. E. Visvader (2017). "Identification of quiescent and spatially restricted mammary stem cells that are hormone responsive." Nat Cell Biol **19**(3): 164-176.
Gouon-Evans, V., M. E. Rothenberg and J. W. Pollard (2000). "Postnatal mammary gland development requires macrophages and eosinophils." Development **127**(11): 2269-2282.
Gudjonsson, T., L. Ronnov-Jessen, R. Villadsen, F. Rank, M. J. Bissell and O. W. Petersen (2002). "Normal and tumor-derived myoepithelial cells differ in their ability to interact with luminal breast epithelial cells for polarity and basement membrane deposition." J Cell Sci **115**(Pt 1): 39-50.
Gudjonsson, T., R. Villadsen, H. L. Nielsen, L. Ronnov-Jessen, M. J. Bissell and O. W. Petersen (2002). "Isolation, immortalization, and characterization of a human breast epithelial cell line with stem cell properties." Genes Dev **16**(6): 693-706.
Hanahan, D. and R. A. Weinberg (2011). "Hallmarks of cancer: the next generation." Cell **144**(5): 646-674.
Hansen, R. K. and M. J. Bissell (2000). "Tissue architecture and breast cancer: the role of extracellular matrix and steroid hormones." Endocr Relat Cancer **7**(2): 95-113.
Hilmarsdottir, B., E. Briem, J. T. Bergthorsson, M. K. Magnusson and T. Gudjonsson (2014). "Functional Role of the microRNA-200 Family in Breast Morphogenesis and Neoplasia." Genes (Basel) **5**(3): 804-820.
Hilmarsdottir, B., E. Briem, V. Sigurdsson, S. R. Franzdottir, M. Ringner, A. J. Arason, J. T. Bergthorsson, M. K. Magnusson and T. Gudjonsson (2015). "MicroRNA-200c-141 and Np63 are required for breast epithelial differentiation and branching morphogenesis." Dev Biol **403**(2): 150-161.
Holliday, D. L. and V. Speirs (2011). "Choosing the right cell line for breast cancer research." Breast Cancer Res **13**(4): 215.
Hopkinson, B. M., M. C. Klitgaard, O. W. Petersen, R. Villadsen, L. Ronnov-Jessen and J. Kim (2017). "Establishment of a normal-derived estrogen receptor-positive cell line comparable to the prevailing human breast cancer subtype." Oncotarget **8**(6): 10580-10593.

Ingthorsson, S., K. Andersen, B. Hilmarsdottir, G. M. Maelandsmo, M. K. Magnusson and T. Gudjonsson (2015). "HER2 induced EMT and tumorigenicity in breast epithelial progenitor cells is inhibited by coexpression of EGFR." Oncogene.

Ingthorsson, S., V. Sigurdsson, A. J. Fridriksdottir, J. G. Jonasson, J. Kjartansson, M. K. Magnusson and T. Gudjonsson (2010). "Endothelial cells stimulate growth of normal and cancerous breast epithelial cells in 3D culture." BMC Res Notes **3**(1): 184.

Inman, J. L., C. Robertson, J. D. Mott and M. J. Bissell (2015). "Mammary gland development: cell fate specification, stem cells and the microenvironment." Development **142**(6): 1028-1042.

Javed, A. and A. Lteif (2013). "Development of the human breast." Semin Plast Surg **27**(1): 5-12.

Mani, S. A., W. Guo, M. J. Liao, E. N. Eaton, A. Ayyanan, A. Y. Zhou, M. Brooks, F. Reinhard, C. C. Zhang, M. Shipitsin, L. L. Campbell, K. Polyak, C. Brisken, J. Yang and R. A. Weinberg (2008). "The epithelial-mesenchymal transition generates cells with properties of stem cells." Cell **133**(4): 704-715.

Medina, D. (2004). "Stromal fibroblasts influence human mammary epithelial cell morphogenesis." Proc Natl Acad Sci U S A **101**(14): 4723-4724.

Miyano, M., R. W. Sayaman, M. H. Stoiber, C. H. Lin, M. R. Stampfer, J. B. Brown and M. A. LaBarge (2017). "Age-related gene expression in luminal epithelial cells is driven by a microenvironment made from myoepithelial cells." Aging (Albany NY) **9**(10): 2026-2051.

Moes, M., A. Le Bechec, I. Crespo, C. Laurini, A. Halavatyi, G. Vetter, A. del Sol and E. Friederich (2012). "A Novel Network Integrating a miRNA-203/SNAI1 Feedback Loop which Regulates Epithelial to Mesenchymal Transition." Plos One **7**(4).

Morsing, M., M. C. Klitgaard, A. Jafari, R. Villadsen, M. Kassem, O. W. Petersen and L. Ronnov-Jessen (2016). "Evidence of two distinct functionally specialized fibroblast lineages in breast stroma." Breast Cancer Res **18**(1): 108.

Pechoux, C., T. Gudjonsson, L. Ronnov-Jessen, M. J. Bissell and O. W. Petersen (1999). "Human mammary luminal epithelial cells contain progenitors to myoepithelial cells." Dev Biol **206**(1): 88-99.

Petersen, O. W., L. Ronnov-Jessen, A. R. Howlett and M. J. Bissell (1992). "Interaction with basement membrane serves to rapidly distinguish growth and differentiation pattern of normal and malignant human breast epithelial cells." Proc Natl Acad Sci U S A **89**(19): 9064-9068.

Plaks, V., B. Boldajipour, J. R. Linnemann, N. H. Nguyen, K. Kersten, Y. Wolf, A. J. Casbon, N. Kong, R. J. van den Bijgaart, D. Sheppard, A. C. Melton, M. F. Krummel and Z. Werb (2015). "Adaptive Immune Regulation of Mammary Postnatal Organogenesis." Dev Cell **34**(5): 493-504.

Ronnov-Jessen, L., O. W. Petersen and M. J. Bissell (1996). "Cellular changes involved in conversion of normal to malignant breast: importance of the stromal reaction." Physiol Rev **76**(1): 69-125.

Sadlonova, A., Z. Novak, M. R. Johnson, D. B. Bowe, S. R. Gault, G. P. Page, J. V. Thottassery, D. R. Welch and A. R. Frost (2005). "Breast fibroblasts modulate epithelial cell proliferation in three-dimensional in vitro co-culture." Breast Cancer Res **7**(1): R46 - 59.

Shibue, T. and R. A. Weinberg (2017). "EMT, CSCs, and drug resistance: the mechanistic link and clinical implications." Nat Rev Clin Oncol **14**(10): 611-629.

Sigurdsson, V., A. J. Fridriksdottir, J. Kjartansson, J. G. Jonasson, M. Steinarsdottir, O. W. Petersen, H. M. Ogmundsdottir and T. Gudjonsson (2006). "Human breast microvascular endothelial cells retain phenotypic traits in long-term finite life span culture." In Vitro Cell Dev Biol Anim **42**(10): 332-340.
Sigurdsson, V., B. Hilmarsdottir, H. Sigmundsdottir, A. J. Fridriksdottir, M. Ringner, R. Villadsen, A. Borg, B. A. Agnarsson, O. W. Petersen, M. K. Magnusson and T. Gudjonsson (2011). "Endothelial induced EMT in breast epithelial cells with stem cell properties." PLoS ONE **6**(9): e23833.
Slamon, D. J., G. M. Clark, S. G. Wong, W. J. Levin, A. Ullrich and W. L. McGuire (1987). "Human breast cancer: correlation of relapse and survival with amplification of the HER-2/neu oncogene." Science **235**(4785): 177-182.
Tait, L., H. Soule and J. Russo (1990). "Ultrastructural and immunocytochemical characterization of an immortalized human breast epithelial cell line MCF-10." Cancer Research **50**: 6087-6094.
Tran, M. N., W. Choi, M. F. Wszolek, N. Navai, I. L. Lee, G. Nitti, S. Wen, E. R. Flores, A. Siefker-Radtke, B. Czerniak, C. Dinney, M. Barton and D. J. McConkey (2013). "The p63 protein isoform DeltaNp63alpha inhibits epithelial-mesenchymal transition in human bladder cancer cells: role of MIR-205." J Biol Chem **288**(5): 3275-3288.
Villadsen, R. (2005). "In search of a stem cell hierarchy in the human breast and its relevance to breast cancer evolution." Apmis **113**(11-12): 903-921.
Villadsen, R., A. J. Fridriksdottir, L. Ronnov-Jessen, T. Gudjonsson, F. Rank, M. A. LaBarge, M. J. Bissell and O. W. Petersen (2007). "Evidence for a stem cell hierarchy in the adult human breast." J Cell Biol **177**(1): 87-101.
Visvader, J. E. and J. Stingl (2014). "Mammary stem cells and the differentiation hierarchy: current status and perspectives." Genes Dev **28**(11): 1143-1158.
Weaver, V. M., A. R. Howlett, B. Langton-Webster, O. W. Petersen and M. J. Bissell (1995). "The development of a functionally relevant cell culture model of progressive human breast cancer." Semin Cancer Biol **6**(3): 175-184.

Figure legends

Figure 1. Schematic figure of the human mammary gland and the spatial origin of the D492 cell line.

A) Schematic view of the branching mammary gland. B) Schematic view of terminal duct lobular unit (TDLU) which are composed of cluster of acini surrounded by cellular rich stroma. C) Schematic view of an acinus (top), which is composed of a bilayer of epithelial cells, an inner layer of luminal epithelial cells (red) surrounded by an outer layer of myoepithelial cells (yellow). Suprabasal cells are depicted as blue cells. (Bottom) D492 was established from isolated suprabasal cells. D492 generate luminal and myoepithelial cells in culture and in 3D-rBM they form structures reminiscent of TDLU.

Figure 2. Endothelial cells induce branching morphogenesis and EMT in D492.

A) Microvessels in TDLU. Immunostaining for CD31 shows the vascular rich stroma around the TDLU. Green, staining against CD31. Blue, nuclear staining. Insert, isolated breast endothelial cells (BRENCs) derived from reduction mammoplasty. Courtesy Sigurdsson et al. (Sigurdsson, Fridriksdottir et al. 2006). B) BRENCs cultivated on top of rBM (upper) or within (lower). On top of rBM BRENCs form capillary-like structures. In contrast, when cultivated within rBM cells appear as single nonproliferative cells. Courtesy Inthorsson et al. (Ingthorsson, Sigurdsson et al. 2010). C) Coculture of BRENCs and D492. BRENCs enhance the branching potential of D492 cells but also induce EMT in a subpopulation of D492 cells. Courtesy Sigurdsson et al. (Sigurdsson, Hilmarsdottir et al. 2011) . D) Comparison of the D492 and D492M cell lines. D492 express

epithelial markers such as E-cadherin and keratins (K14 and K19). In contrast, D492M lack epithelial markers but expresses N-cadherin an EMT marker. Scale bar 100µm. Courtesy Sigurdsson et al. (Sigurdsson, Hilmarsdottir et al. 2011).

Figure 3. Application of D492 and D492M to study EMT and MET.

D492 form branching TDLU like structures in 3D-rBM. When cocultured with BRENCs, the branching potential is enhanced but simultaneously a subpopulation of D492 cells undergoes EMT. D492M was established from mesenchymal colonies derived from endothelial induced EMT of D492. When overexpressed in D492M, microRNA-200c-141 was able to revert the EMT phenotype back to the epithelial, albeit only to the luminal epithelial phenotype. Overexpression of P63, an important transcription factor for myoepithelial cells, along with miR-200c-141 were sufficient to revert D492M back to the branching epithelial phenotype seen in D492.

Figure 4. Her2 overexpression in D492 induces tumorigenesis.

A) Overexpression of HER2 in D492 reduces the endogenous expression of EGFR. B) $D492^{Her2}$ generate grape-like or disorganized spindle-like colonies in 3D-rBM. C) $D492^{Her2}$ generate large tumors when transplanted into nude mice. Cotransfection of Her2 and EGFR in D492 ($D492^{Her2/EGFR}$) reduces the tumor growth. $D492^{EGFR}$ does not form tumors in mice. D) Treating $D492^{Her2}$ cells with combination of traztuzmab (Her2 antibody) and Cetuximab (EGFR antibody) results in poorer outcome than treated with traztuzumab alone. Courtesy Ingthorsson et al. (Ingthorsson, Andersen et al. 2015).

Figure 1

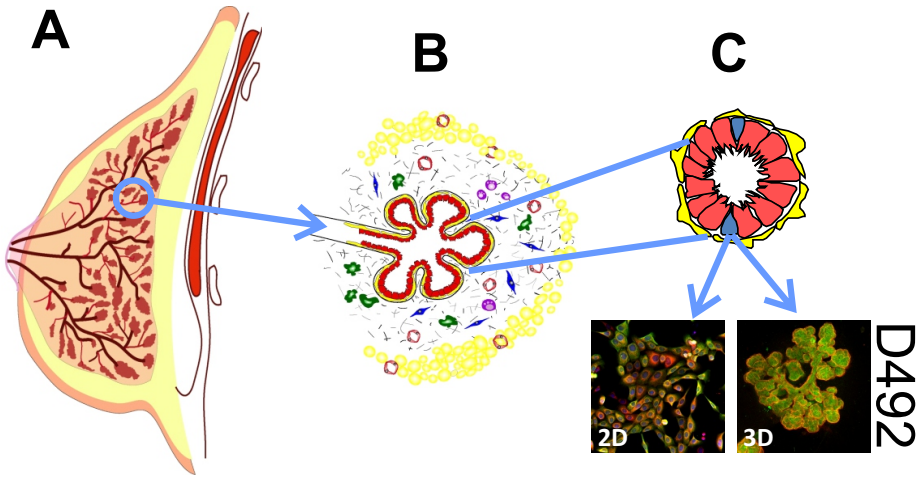

Figure 2

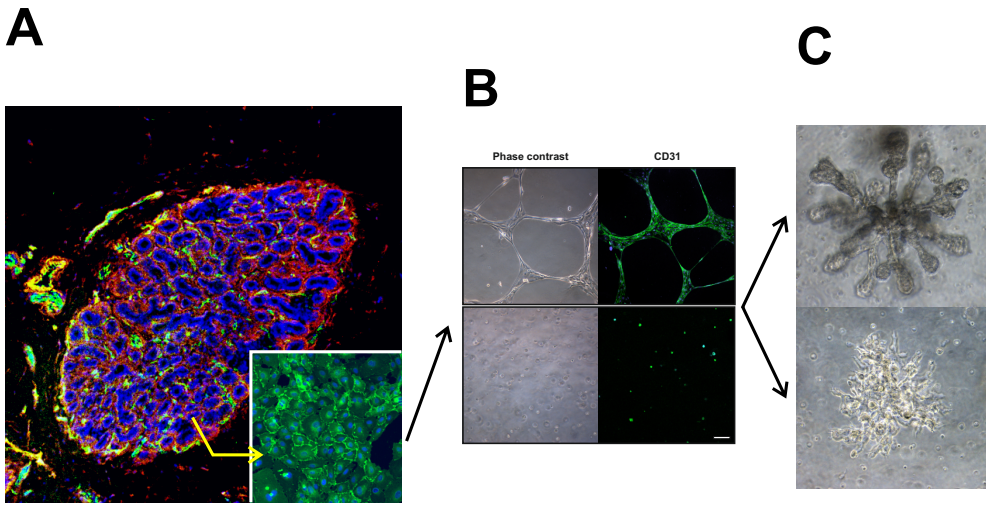
A
B
C
Phase contrast
CD31

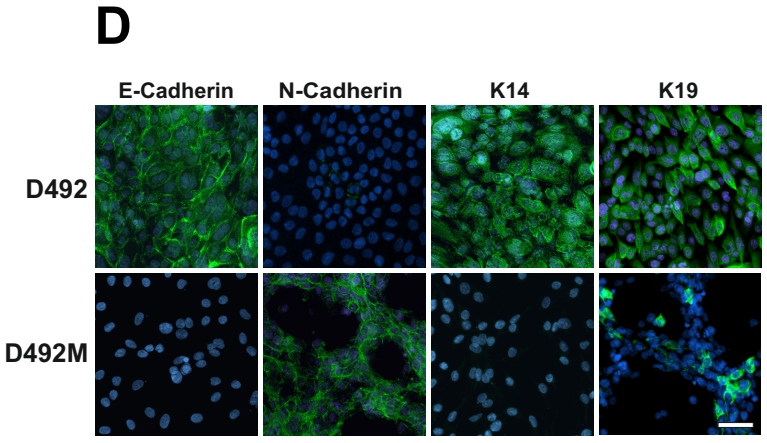
D
E-Cadherin
N-Cadherin
K14
K19
D492
D492M

Figure 3

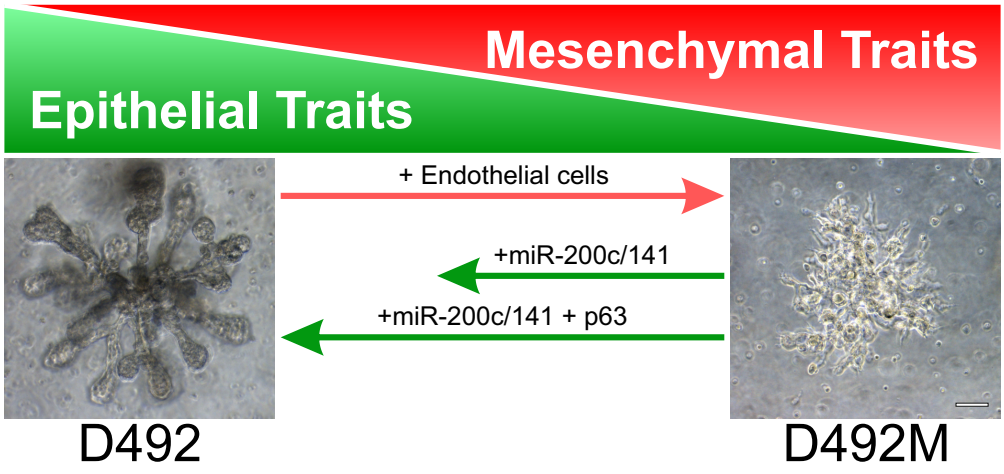
Mesenchymal Traits
Epithelial Traits
+ Endothelial cells
+miR-200c/141
+miR-200c/141 + p63
D492
D492M

Figure 4

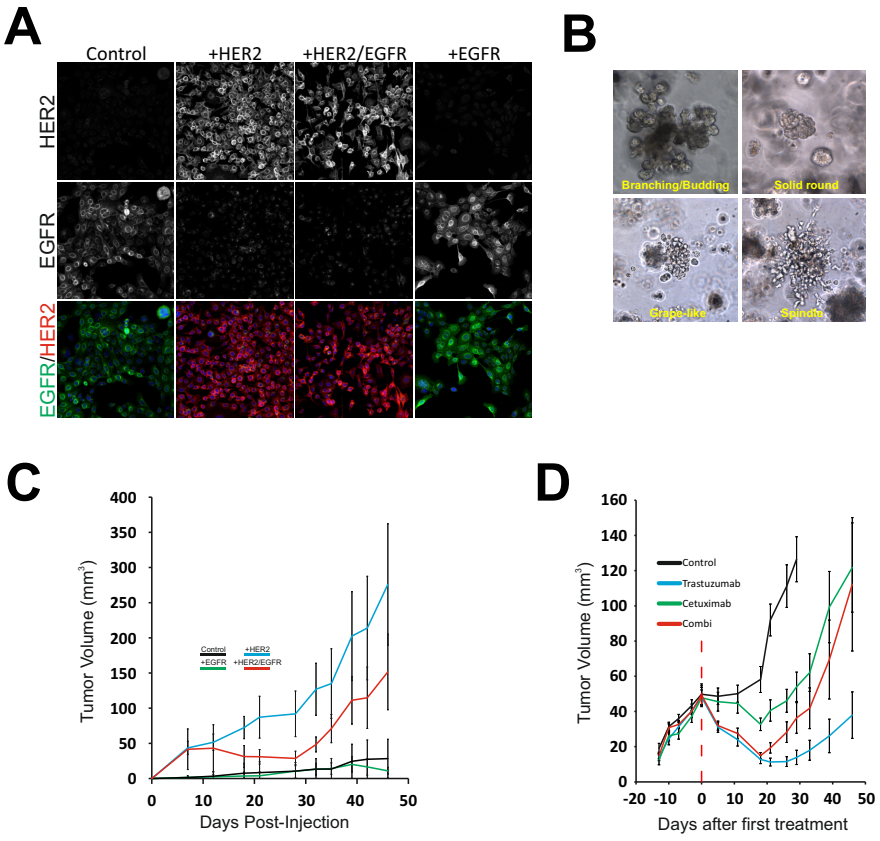
A
Control
+HER2
+HER2/EGFR
+EGFR
HER2
EGFR
EGFR/HER2
B
Branching/Budding
Solid round
Grape-like
Spindle
C
Tumor Volume (mm3)
Days Post-Injection
Control
+HER2
+EGFR
+HER2/EGFR
D
Tumor Volume (mm3)
Days after first treatment
Control
Trastuzumab
Cetuximab
Combi